Investigations into the molecular interactions between *Claviceps purpurea*, the causal agent of ergot, and cereal hosts

UNIVERSITY OF CAMBRIDGE

Eleni Tente

Downing College

National Institute of Agricultural Botany

University of Cambridge

This thesis is submitted for the degree of Doctor of Philosophy

September 2020

Declaration

This thesis is the result of my own work and includes nothing which is the outcome of work done in collaboration except as declared in the Preface and specified in the text. It is not substantially the same as any that I have submitted, or, is being concurrently submitted for a degree or diploma or other qualification at the University of Cambridge or any other University or similar institution except as declared in the Preface and specified in the text. I further state that no substantial part of my thesis has already been submitted, or, is being concurrently submitted for any such degree, diploma or other qualification at the University of Cambridge or any other University or similar institution except as declared in the Preface and specified in the text. It does not exceed the prescribed word limit for the relevant Degree Committee

Summary

Investigations into the molecular interactions between *Claviceps purpurea*, the causal agent of ergot, and cereal hosts

Eleni Tente

The fungus *Claviceps purpurea* infects female flowers of cereals and grasses, producing an ergot sclerotia (the overwintering structure of the pathogen) in place of a grain. *C. purpurea* can infect wheat, barley, rye, oats, triticale and millet, detrimentally affecting grain production and flour quality. Ergot also impacts human health directly through the ingestion of toxic alkaloids (found in very high levels in sclerotia), resulting in a condition known as ergotism. Currently, the content of ergot sclerotia in unprocessed cereal grains is set by the European Commission Regulation (EC) No. 1881/2006. In grain for human consumption the amount of sclerotia is restricted to a maximum of 0.05%. However, these limits are set to be reduced, and new regulations regarding the levels of alkaloids found in processed foods from cereals is about to be introduced through new EC regulations. The aim of this thesis was to obtain a better understanding of the genetic and molecular changes that occur in wheat ovaries following inoculation with *C. purpurea*, as well as to understand the routes by which cereal grains can become contaminated with ergot alkaloids.

The data from an extensive transcriptomics study indicated a substantial reprogramming of wheat hormonal pathways, with a high proportion of genes involved in GA, auxin, ethylene and cytokinin metabolism showing differential expression relative to ovary tissue-type and time after inoculation. The results suggest that *C. purpurea* is able to co-opt the host's hormonal pathways in order to facilitate infection. In addition, the host is able to activate several defence mechanisms during the early stages of infection, while the persistent up-regulation of certain categories of host defence-related genes in the later stages of infection is indicative for an ongoing basal defence response against *C. purpurea.* Of particular interest is evidence of a mobile signal sent from the inoculated stigma to the ovary base, differential expression of host genes being observed at the base of the ovary long before the arrival of *C. purpurea* hyphal tissue.

Currently, no complete resistance against the fungal pathogen *C. purpurea* is known. Partial resistance to ergot has been previously shown to co-locate with the wheat Reduced height (*Rht*) dwarfing gene alleles *Rht-B1b* and *Rht-D1b.* The wheat *Rht* loci encode DELLA proteins, *Rht-B1b* and *Rht-D1b* representing GA-insensitive mutations in DELLA. A linkage between *Rht-B1b* and *Rht-D1b* and ergot resistance could therefore indicate a role of GA in *C. purpurea* infection. Reduced honeydew production, along with a reduction in the size and weight of sclerotia were found in lines carrying the dwarf and semi-dwarf mutant alleles *Rht-D1b*, *Rht-D1c*, *Rht-B1c*. Furthermore, the levels of GA_4, auxin and dihydrozeatin-type (DHZ) cytokinins were found to be elevated during infection. Taken together, these results indicate in wild type wheat GA acts to increase susceptibility to *C. purpurea*. In addition, the profiles and levels of a range of other endogenous hormones were also are significantly altered in response to *C. purpurea* infection.

Re-emerging concerns over the potential health risks presented by the ergot alkaloids, produced during *C. purpurea* infection, has led to new legislation on ergot alkaloids being proposed by the EC. In this thesis we show that a significant risk of grain contamination by ergot alkaloids exists both pre-harvest, due to contamination of grain while in the ear, as well as post-harvest, as a result of physical contact between sclerotia and grain. Very low levels of ergot alkaloids were found in honeydew with all *C. purpurea* isolates tested. Levels increased in sphacelia tissues and reached levels as high as 3 million parts per billion (ppb; 3 million μg of ergot alkaloids per kg of sclerotia) in mature ergot sclerotia. In wheat and barley, ergot alkaloids were found to transfer to healthy grain that developed above and below flowers infected with the *C. purpurea* isolates 04-97.1, EI4 and Rye 20.1. In addition, significant levels of ergot alkaloids were found to be transferred to clean grain of wheat and barley as a result of direct physical contact with broken pieces of sclerotia, compared to intact sclerotia, with significant differences also seen between wheat and barley.

Acknowledgments

Thank you to my supervisor Dr. Anna Gordon for her continued support throughout my PhD. This entire project would not have been possible without your constant guidance. I would also like to show my gratitude to Dr. Lesley Boyd. Thank you for taking the time to teach me how to look at the bigger picture when it came to putting all this together. Your questions and edits greatly improved my research and this thesis. My thanks also to Dr. Nelzo Ereful for his significant contribution to the bioinformatics work and for always answering my questions.

This PhD journey would not have been as much fun without the support of my friends. To Benedetta and Marcella thank you for all the breaks, the laughs, the conversations, for not letting me work too hard and for keeping me sane. To Rowena thank you for showing me how a PhD is done. To Anastasia, simply, thank you for your friendship and for being with me, every step of the way, since we were 9 years old.

I am hugely grateful to my parents Aliki and Yiannis, and my brother Kriton for their unconditional love and support. Thank you for the Greek WE. WE carried out experiments, WE studied, WE read, WE wrote, WE did this. And lastly to my partner Melina, thank you for always believing in me and for always showing me what really matters. You have been with me through the highs and lows and helped me to achieve all my goals and more. You have made me a better person, and for that I am profoundly grateful.

Table of Contents

List of Tables

List of Figures

List of Abbreviations and Acronyms

Abbreviation	Full Name
ABA	Abscisic Acid
ACO	1-Aminocyclopropane-1-carboxylate oxidase
ACS	1-Aminocyclopropane-1-carboxylate synthase
AHDB	Agriculture and Horticulture Development Board
AOS	Allene Oxide Synthase
AUX/IAA	Auxin/indole-3-acetic acid
AzA	Azelaic Acid
BZR1	BRASSINAZOLE RESISTANT1
CDA	Cyclopropane-1,1-dicarboxylic acid
CKs	Cytokinins
CKX	cytokinin oxidase/dehydrogenase
CMS	Cytoplasmic Male Sterility
CNS	Central Nervous System
COI1	Coronatine-Insensitive 1
CPS	*ent*-copalyl diphosphate synthase
CRK	Cysteine-rich Receptor-like Kinases
DEG	Differentially Expressed Genes
DHZ	Dihydrozeatin
DIR1	Defective in Induced Resistance
EC	European Comission
ERF	Ethylene responsive transcription factors
ET	Ethylene
ETS	Effector Triggered Suppression

EU	European Union
FHB	Fusarium Head Blight
FSA	Food Standards Agency
G3P	Glycerol-3-phosphate
GA	Gibberellic Acid
GA2ox	Gibberellin 2-beta-oxidase
GGPP	*trans*-geranylgeranyl diphosphate
GID1	GIBBERELLIN-INSENSITIVE DWARF1
GH3	Glycoside Hydrolase 3
HIN1	Harpin Induced Protein 1
HSP40s	Heat-Shock Protein 40
IAA	Indole-3-acetic acid
IBMCP	Institute for Plant Molecular and Cell Biology
iP	N^6-(2-isopentenyl) adenine
IWGSC	International Wheat Genome Sequencing Consortium
JA	Jasmonic Acid
JAZ1	Jasmonate-zim-domain protein 1
KAO	*ent*-kaurenoic acid oxidase
KO	*ent*-kaurene oxidase
KS	*ent*-kaurene synthase
LecRK	Lectin Receptor Kinases
LOQ	Limits of Quantification
LPS	d-Lysergyl Peptide Synthetase
MAPK	Mitogen-Activated Protein Kinase
MeSA	Methyl Salicylate
NBS-LRR	Nucleotide-Binding Site Leucine-Rich Repeat
NCBI	National Centre of Biotechnology Information

NILs	Near-Isogenic Lines
NINJA	Novel INteractor of JAZ
NPR3	NON-EXPRESSOR OF PR3
NRPS	Nonribosomal Peptide Synthethase
ODDs	2-oxoglutarate-dependent dioxygenases
OPR	12-Oxophytodienoate reductase
ORF	Open Reading Frame
PAMPs	Pathogen-associated Molecular Patterns
PIFs	PHYTOCHROME INTERACTING FACTORS
PTI	PAMP-Triggered Immunity
QTL	Quantitative Trait Loci
Rht	Reduced Height genes
ROS	Reactive Oxygen Species
RPK	Receptor Protein Kinases
SA	Salicylic Acid
SAR	Systemic Acquired Resistance
SAURs	small Auxin-Up RNAs
SLP	Subtilisin-like Proteases
STK	Serine/Threonine Kinases
TDI	Tolerable Daily Intake
tZ	Trans-zeatin
UK	United Kingdom
US	United States

List of Appendices

Chapter 1: General Introduction

1.1 Global Food Security: Challenges and Impact of Plant Pathogens

In the past few years the world has seen the human population reach 7 billion, a number which has been projected to increase to over 9 billion by 2050 (FAO, 2015). With currently 800 million people being estimated to have limited access to adequate food, global food security is currently one of the most crucial issues in international politics (FAO, 2015). As it has been estimated that a staggering 200,000 billion calories per annum will have to be produced in order to meet the future global demand for food (Bebber & Gurr, 2015), it is not just the physical production of food that needs to increase. A balanced geographic spread of food production is needed to ensure food security, along with improvements in nutritional quality, transportation and long term storage (Flood, 2010).

Set against the need to increase global food production are the factors responsible for crop loss. It is estimated that between 30% - 50% (or 1.2-2 billion metric tonnes) of global crop production never reaches the consumers (Thornton & Wills, 2013). One of the leading factors impeding food production, accounting for global yield losses of up to 20% (Oerke, 2006), are plant pests and diseases; including diseases caused by insects, viruses, bacteria, fungi and oomycetes. Among plant pathogens, fungi and oomycetes represent the greatest threat to global food production (Fisher *et al*., 2012). Unless steps are taken towards the improvement of plant defences, plant pathogen attacks will be exacerbated with alarming implications for the sector of agriculture and the health of humans (Fisher *et al*., 2012).

1.2 Host Overview: Wheat

Wheat is the single most important global crop in terms of total harvested yield, reaching 705 million metric tonnes (mmt), and being used for both direct human and animal consumption (Fones & Gurr, 2015). Modern hexaploid wheat (*Triticum aestivum*) and tetraploid durum wheat (*Triticum durum*) cultivars account for 95% and 5% of the global wheat production, respectively (Peng *et al*., 2011). Tetraploid wheat resulted from the hybridization of two diploid grass genomes. The donor of the A genome, a wild diploid wheat (*T. urartu*), hybridized with the donor of the B genome, a close relative of *Aegilops speltoides*, to produce

the tetraploid wild emmer wheat (*T. dicoccoides*) (Haas *et al*., 2019; Venske *et al*., 2019; Peng *et al*., 2011). Human cultivation of wild emmer eventually created a cultivated emmer, and later durum wheat (Haas *et al*., 2019). Finally, around 8,000 years ago, in an area called the Fertile Crescent, a second hybridization between the cultivated emmer and the goat grass, *Ae. Tauschii*, resulted in the creation of the hexaploid, *T. aestivum*, which following domestication and years of selection gave rise to today's bread wheat (Venske *et al*., 2019). Some of the key early traits associated with the domestication of wheat, and which differentiate domestic wheat from wild species, include a non-brittle rachis, free-threshing grain and reduced seed dormancy (Haas *et al*., 2019; Faris, 2013).

While advances were made to wheat through farmer selection and early 19th century crossing efforts, it was the "Green Revolution" of the 60s that led to massive improvements and the modern cultivars we know today. These high yielding cultivars are characterised by their short stature and reduced flowering time, traits which were controlled by the inclusion of the *Reduced height* (*Rht-B1b* and *Rht-D1b*) and *Photoperiod* (*Ppd-D1a*) genes, respectively (Wilhelm *et al*., 2013). However, domestication and selection breeding have led to a reduction in the genetic variability within modern wheat cultivars (Fu & Somers, 2009). Several new techniques and technologies have been developed in order to increase the genetic diversity of wheat, including induced mutagenesis, introgression of new genetic diversity from wild relatives and targeted genome editing (Venske *et al*., 2019; Bedo & Lang, 2015).

Another strategy for exploiting wheat genetic diversity is through the cultivation of F1 hybrids with often display heterosis, or hybrid vigor (Martin *et al*., 2018). F1 hybrid production requires a male sterile female parent, which means the natural self-fertilisation process of wheat needs to be blocked, a process which can be achieved in a number of ways, including cytoplasmic male sterility (CMS) (Martin *et al*., 2018). However, CMS has proven difficult to obtain in wheat, while chemical hybridizing agents that induce male sterility have been associated with toxicity issues (Whitford *et al*., 2013). Furthermore, wheat hybrids have been found to exhibit changes in their floral architecture, namely open flowering phenotypes which can cause susceptibility issues against flower-infecting pathogens (Whitford *et al*., 2013).

Instrumental in the application of new technologies for wheat breeding and improvement has been the creation of a high-quality reference genome sequence for bread wheat (https://urgi.versailles.inra.fr/download/iwgsc/IWGSC_RefSeq_Assemblies/v2.0/). However, the assembly of such a reference genome sequence has been challenging due to the

complexity of the wheat genome (Appels *et al*., 2018). Hexaploid wheat contains three homeologous copies of seven chromosomes, a total of 42 chromosomes (Alonge *et al*., 2020). The resulting wheat genome is therefore very large (approximately 16Gbp), but is also made up of a high proportion of repeat sequences, including retrotransposon (approximately 85% of the hexaploid wheat genome is repetitive sequence) (Alonge *et al*., 2020; Appels *et al*., 2018). These features greatly contributed to the difficulties encountered during genome assembly. Nonetheless, an annotated reference genome for bread wheat (IWGSC CS v1.0, Chinese Spring) was made available in 2018 by the International Wheat Genome Sequencing Consortium (IWGSC) (Appels *et al*., 2018).

Currently, the EU produces 15% more wheat than China, 35% more than India, and 60% more than the US, thus making the EU the largest producer of wheat worldwide (Fones & Gurr, 2015). The EU currently exports approximately 20% of its annual wheat harvest, with one third of the remaining harvest being used for human consumption and two thirds for animal feed (FAO, 2016). In the EU wheat is also grown as a raw material for the production of biofuel (Fones & Gurr, 2015). These statistics demonstrate the substantial social and economic significance of wheat as a crop, and as a commodity for the EU. As wheat is more widely traded than all other crops combined (Curtis *et al*., 2002), it is certain that any perturbations in production, quality or market value of wheat will have implications that are felt across global markets.

The most globally important diseases for wheat are caused by a variety of biotrophic and necrotrophic fungi (Singh *et al*., 2016). While fungicides and resistant cultivars have significantly helped in reducing yield loses caused by disease, the evolution of more virulent pathogen races, the excessive use of fungicides leading to fungicide resistant pathogen isolates, as well as, the increasing global reach and aggressiveness of some diseases in recent years, only serves to demonstrate the importance of renewing and reinforcing our efforts of produce durable resistant and productive wheat cultivars (Singh *et al*., 2016).

1.3 Disease Overview: Ergot

Ergot is a disease of cereals and grasses, caused by the fungus *Claviceps purpurea*, which infects the female parts of the flower Ergot can result in devastating economic damage as the infection detrimentally affects the grain and flour quality. This is due to toxic alkaloids produced by the fungus; alkaloids that can cause severe health issues in mammals upon ingestion (Tudzynski *et al*., 2001). The health issues and symptoms associated with these alkaloids is known as ergotism and can manifest as two distinct types, namely convulsive or gangrenous (Hulvova *et al*., 2013). Convulsive ergotism is characterised by convulsions, fever, hallucinations and, in severe cases, death as the alkaloids have been found to affect the central nervous system (CNS) of mammals by activating serotonin receptors (Eadie, 2003). Gangrenous ergotism is characterised by acute burning sensations and shooting pains in the body's extremities, followed by gangrene in extreme cases of intoxication, the result of vasoconstriction caused by the alkaloids (Hulvova *et al*., 2013). Human history contains many cases where ergot has resulted in stories of plague, witchcraft and death. In the Middle Ages grains contaminated with alkaloid containing sclerotia (the overwintering structures of *C. purpurea*) resulted in epidemic outbreaks of ergotism, also known at the time as St. Antony's fire (De Costa, 2002). An example of an ergotism epidemic occurred in 944-945 AD in France and led to the deaths of approximately 10,000 people (Hulvova *et al*., 2013). There is also evidence to suggest that ergotism played a significant role in the famous, 17th century witch-trials in both Salem (Massachusetts, USA), as well as in Finnmark (Norway) (Spanos & Gottlieb, 1976; Alm, 2003).

On the other hand, the alkaloids produced by this fungus have also been biotechnologically exploited for their pharmaceutical value (Keller and Tudzynski, 2002). The first evidence of ergot being used for medicinal purposes originated in China in approximately 1100 BC (Schiff, 2006). Since then, ergot has been used throughout the years for various medical purposes, such as to initiate abortion during the 16th century, or to prevent excess bleeding during and post childbirth, and throughout the 19th century ergot scerotia were used to treat migraines (Haarmann *et al*., 2009). The roles of ergot alkaloids in modern medicine can be said to have emerged in 1918 along with the isolation of the first alkaloid, ergotamine, by Stoll (Haarmann *et al*., 2009). Currently, alkaloid-based substances are used for the treatment of various conditions, such as migraines, hypertension, as well as for degenerative diseases of the CNS like Parkinson's (Haarmann *et al*., 2009). This use of alkaloids can be

attributed to their biological activity, structurally resembling the neurotransmitters noradrenalin, dopamine and serotonin (Hulvova *et al*., 2013).

C. purpurea is a pervasive fungus that infects the ovaries of a number of economically important cereal crops, including wheat, barley, rye, oats, triticale and millet (Tudzynski & Scheffer, 2004). Since infection by *C. purpurea* initiates at the stigmatic tissue, the agronomic parameters that most affect susceptibility to *C. purpurea* are related to the host's fertility characteristics, such as floral architecture, flowering time, as well as pollen availability and pollen shedding (Miedaner & Geiger, 2015). These host characteristics are also highly affected by weather patterns, which therefore also contribute to susceptibility (Miedaner & Geiger, 2015). Generally cool temperatures, high humidity and rain increase host susceptibility the most, as temperature and humidity can negatively affect pollen availability and viability, while rain can decrease pollen shedding (Miedaner & Geiger, 2015). While few sources of wheat resistance to *C. purpurea* have been found (Gordon et al., 2015; Gordon et al., 2020), passive mechanisms of resistance, such as cleistogamy, do play a role in the avoidance of infection (Miedaner & Geiger, 2015). Cereals such as rye, that exhibit open flowering, are particularly at risk of being infected (Miedaner & Geiger, 2015). Wheat, on the other hand, represents a closed flowering cereal and its risk of infection is much lower. Nevertheless, wheat, barley and rye lines that are male sterile in response to environmental factors (e.g. drought), or produced for F1 hybrid breeding, display flowers that gap open, thereby increasing the risk of *C. purpurea* infection (Miedaner *et al*., 2010).

Currently, ergot sclerotia content in unprocessed cereal grains is set by the European Commission Regulation (EC) No. 1881/2006 (with the exception of corn and rice). In grain for human consumption the amount of ergot sclerotia is restricted to a maximum of 0.05%. Following a stakeholder consultation, the EC is proposing to introduce a maximum level of ergot alkaloids. For cereal milling products from wheat, spelt, barley and oats, a limit of 75–200 ppb will be set for alkaloids. For rye products, the limit will be higher c.250–500 ppb, while for cereal-based food for infants and young children it will be lower, < 50 ppb. The minimum levels of ergot sclerotia in unprocessed grain lots will also be reduced to 0.02% (0.2g/kg), instead of the current 0.05% (0.5g/kg) (FSA, 2019) (Further details provided in Chapter 4).

Several methods are employed in order to reduce the risk of *C. purpurea* infection. While there are currently no fungicides approved for controlling ergot in cereals (AHDB,

2020), certain agronomic measures can be taken to minimize risk. Firstly, rotation of a cereal crop with a crop that is resistant to *C. purpurea* can dramatically decrease risk of infection, as ergot sclerotia cannot survive in the soil indefinitely (Miedaner & Geiger, 2015). In addition, ploughing the soil to at least 5cm helps bury sclerotia, stopping the ascospores from being released into the air and thus infecting subsequent cereal crops (AHDB, 2020). Finally, grassweeds can also be infected by *C. purpurea* and can act as a source of inoculum for cereal crops (AHDB, 2020). Control of grass species includes the cutting of field boundaries prior to flowering, or to sow later-flowering species at the borders of the crop (Miedaner & Geiger, 2015). Grain that is contaminated with ergot sclerotia can also be cleaned, gravity separation and mechanical sieves being used to remove sclerotia (AHDB, 2020).

C. purpurea therefore remains a persistent threat to modern agriculture. Both the agronomic and biological aspects of this fungus have sustained scientific interest, such that an integrated understanding of cereal-*C. purpurea* interactions is needed, not only to develop novel defence strategies for susceptible crops, but also for the discovery of novel drugs for the treatment of CNS degenerative disorders. In this thesis, we set out to address three main aims. Firstly, we aimed to obtain a better understanding of the wheat-*C. purpurea* interaction through an examination of the genetic and molecular changes that occur in wheat female flowers following inoculation with *C. purpurea* through the use of RNASeq. Previous work had indicated that the wheat Reduced height, *Rht* genes may confer partial ergot resistance (Gordon *et al.,* 2015), implicating the DELLA proteins (encoded by *Rht*) and Gibberellic Acid (GA) pathways in the wheat-*C. purpurea* interaction. The potential role of GA was therefore further explored, along with an examination of the endogenous status of other hormones during *C. purpurea* infection. Finally, concerns have been raised at a European Commission policy level regarding possible contamination of healthy cereal grains by ergot alkaloids. Therefore, we addressed a number of questions regarding the ways in which ergot alkaloids might be able to contaminate grains of wheat, barley and rye, both *in planta* and during transportation of grain.

Chapter 2: Reprogramming of the wheat transcriptome in response to infection with *Claviceps purpurea*, the causal agent of ergot

2.1 Abstract

Ergot, caused by the fungal pathogen *Claviceps purpurea*, infects the female flowers of a number of economically important cereal crops, including wheat. *C. purpurea* is thought to exhibit a biotrophic lifestyle, keeping the floral tissues alive while it draws nutrients from the plant, and does not induce host tissue necrosis. We undertook an extensive examination of the transcriptomic reprogramming in wheat in response to *C. purpurea* across time and female floral tissues (i.e. the stigma, transmitting and base ovule tissues of the ovary). *C. purpurea* hyphae were observed to have grown into and down the stigma at 24 hours (H) after inoculation. By 48H hyphae had grown through the transmitting tissue and entered the base tissue, while by 72H hyphae had surrounded the ovule. By 5 days (D) the ovule had been replaced by fungal tissue. Of particular interest was the identification of significant differential expression of wheat genes in the base tissue well before the appearance of fungal infection in this part of the ovary, suggesting that a mobile signal, either pathogen or plant-derived, is delivered to the base tissue prior to its colonisation by the fungus. Significant differential gene expression was first observed at 1H in the stigma tissue. Many of the wheat genes differentially transcribed in response to *C. purpurea* infection were associated with plant hormones, and included the ethylene (ET), auxin, cytokinin, gibberellic acid (GA), salicylic acid (SA) and jasmonic acid (JA) biosynthetic and signaling pathways. Hormone-associated genes were first detected in the stigma and base tissues at 24H, but not in the transmitting tissue. Genes associated with GA and JA pathways were seen in the stigma tissue at 24H, while JA and ET-associated genes were identified in the base tissue at 24H. In addition, several defence-associated genes were differential expressed in response to *C. purpurea* infection, including genes belonging to the categories; antifungal proteins, endocytosis/exocytosis-related proteins, NBS-LRR class proteins, genes involved in programmed cell death, receptor protein kinases and transcription factors.

2.2 Introduction

Ergot, caused by the fungal pathogen *Claviceps purpurea*, is an ear disease of grasses and cereal, and infects a number of economically important cereal crops, including wheat, barley and rye (Tudzynski and Scheffer, 2004; Menzies and Turkington, 2015). Ergot can lead to significant economic loss, grain being rejected due to contamination with ergot sclerotia, the over-wintering fungal structure (Tudzynski *et al*., 2001). While sclerotia can generally be removed from grain by standard cleaning methods: colour sorting and gravity tables (Beuerle *et al*., 2012, Byrd *et al.,* 2017, MacDonald *et al*., 2017), sclerotia of a similar size to the seed are difficult to separate. Sclerotia contain a range of ergot alkaloids that are highly toxic to humans and animals (EFSA CONTAM report 2012; Shelby, 1999). These alkaloids are responsible for the condition ergotism, which during the Middle Ages was known as St Anthony's Fire. Symptoms of ergotism include gangrenous extremities, convulsions, psychosis and eventually death. Outbreaks were especially prevalent in the Middle Ages due to a diet high in rye (de Costa, 2002). In addition, recent findings suggest that ergot alkaloids, produced by the fungus and found at high concentrations in sclerotia, can find their way onto otherwise "healthy" grain (Gordon *et al*., 2019).

C. purpurea gains entry during anthesis, infecting the flower's female tissues and replacing the seed with an ergot sclerotia (Tudzynski & Scheffer, 2004). Cereals such as rye, that exhibit open flowering, are therefore particularly at risk of infection, as are hybrid cereal seed production systems, such as those developed for barley and wheat (Mette et al., 2015). *C. purpurea* is believed to exhibit a biotrophic lifestyle, keeping the floral tissues alive while it draws nutrients from the plant, and does not induce host tissue necrosis (Tudzynski & Scheffer, 2004). Spores germinate on stigma, penetrate stigmatic hairs and grow down the style to the transmitting tissue of the ovary (Figure 2.1). *C. purpurea* grows mainly intercellularly, although invasive hyphae, which are completely enclosed by the host plasma membrane, have been documented (Tenberge K, Tudzynski P, 1994). Within three days of spores landing on the stigma hyphae have completely overwhelmed the ovary and begin to branch. Between 5-7 days post-infection the fungus enters the sphacelial stage, manifesting itself as a soft white tissue that begins producing asexual conidiospores. The conidiospores are exuded from florets in a sugary liquid called honeydew (Tudzynski & Scheffer, 2004). The honeydew enables *C. purpurea* to disperse conidiospores to other receptive flowers, most likely with the help of insect vectors and rain splash (Tenberge, 1999; Swan & Mantle, 1991). After approximately 2

weeks a hardened, dark sclerotium is formed where a seed would have developed. These sclerotia, also known as ergots, produce the sexual reproduction structures that give rise to ascospores (Tenberge, 1999).

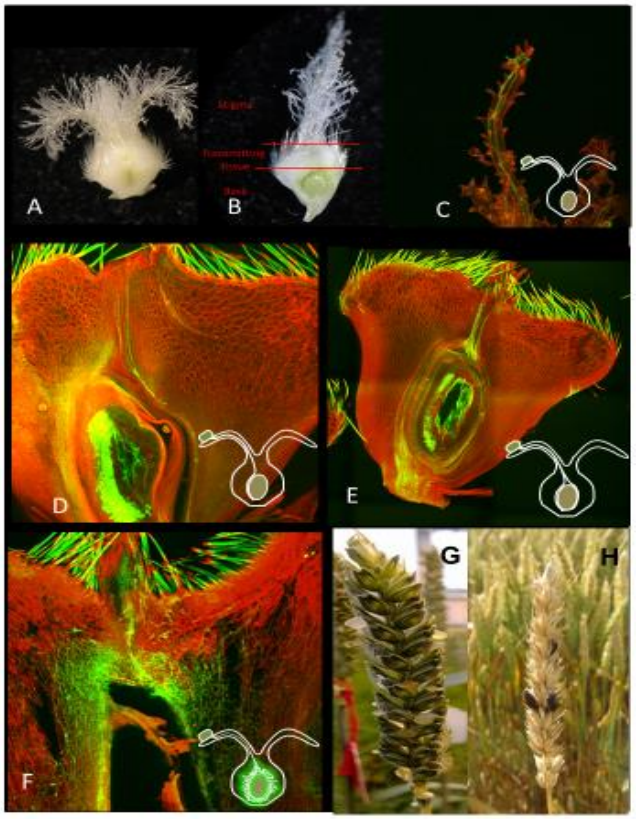

Figure 2.1 *Claviceps purpurea* infection of wheat.

(A) Wheat ovule. **(B)** Longitudinal section of ovule showing stigma, transmitting and base tissue. Confocal images of wheat ovaries infected with *C. purpurea* at **(C)** 24 hours, **(D)** 48 hours, **(E)** 72 hours and **(F)** 5 days after inoculation. Images stained with propidium iodide and aniline blue. At 24 hours *C. purpurea* conidia have germinated and grown down the stigma hairs (C). By 48 hours hyphae had grown down the transmitting tissue and entered the base tissue (D), while at 72 hours ovule surrounded by fungal hyphae (E). By 5 days after inoculation the ovule has been completely replaced by fungal tissue (F). (G) Wheat ear extruding honeydew. (H) Wheat ear with sclerotia.

The interaction between host plant and invading pathogen involves a continuous, two-way communication. Initial plant recognition of pathogen-associated molecular patterns (PAMPs) triggers PAMP-Triggered Immunity (PTI). A pathogen can suppress and/or avoid

PTI through the delivery of pathogen effectors (Effector Triggered Suppression – ETS). Effectors are thought to suppress PTI either by preventing detection of the PAMPs by the host (DeJonge *et al*., 2010), or by affecting downstream PTI-signaling pathways (Kazan and Lyons, 2014). However, it is becoming increasingly apparent that the role of effectors goes beyond suppression of plant defence, having a strategic role in modifying the plant environment to create conditions conducive for pathogen growth and reproduction. Therefore, many of the plant genes induced upon pathogen infection, once thought to be required for defence, are actually required for infection by the pathogen (Kazan and Lyons, 2014).

As a second line of defence plants have evolved an effector recognition system, mediated by host resistance (R-) genes that recognise effectors either directly or indirectly, leading to Effector Triggered Immunity (ETI; Jones & Dangl, 2006). Downstream responses often associated with PTI and ETI include a rapid influx of calcium ions, a burst of ROS (Dodds & Rathjen, 2010), deposition of callosic cell wall appositions at sites of attempted pathogen infection, as well as activation of a MAPK signaling cascade that triggers expression of WRKY-type transcription factors, key regulators of plant defence (Eulgem and Somssich, 2007). WRKY transcription factors elicit defence responses such as the generation of nitric oxide, production of antimicrobial compounds, and the hypersensitive or programmed cell death response (Eulgem and Somssich, 2007).

Plants have also established complex phytohormone-regulated signaling pathways to control defence responses (Kazan and Lyons, 2014). In return, the pathogen has developed strategies to manipulate phytohormone-regulated defense, delivering effectors that allow the pathogen to evade, hijack or disrupt hormone signaling pathways (Kazan & Lyons, 2014). The plant hormones salicylic acid (SA), jasmonic acid (JA) and ethylene (ET) have well established roles in the regulation of plant defence. SA is known for its role in the activation of defence responses against biotrophic pathogens and for the establishment of systemic acquired resistance (SAR) (Grant and Lamb, 2006). While JA and ET primarily activate defence responses against necrotrophic pathogens and herbivorous insects and have been found to operate in a mutually antagonistic manner with SA (Kunkel and Brooks 2002). Auxins and Giberellic Acid (GA) have also been shown to play a role in plant defence. Ding *et al*., 2008 demonstrated that the overexpression of the auxin conjugating protein GH3-8 in rice led to enhanced resistance to bacterial blight disease.

In *Arabidopsis* resistance to biotrophs and susceptibility to necrotrophs was regulated by a shift in the balance between JA and SA signaling, which in turn was dependent on GA-

dependent degradation of the DELLA proteins (Navarro *et al*., 2008). It has been suggested that DELLA proteins are able to bind to the JA suppressor JAZ1, preventing it from interacting with MYC2, a key transcriptional activator of JA responses, thereby leading to the activation of JA-responsive target genes (Hou *et al*., 2010). As the degradation of DELLA proteins is GA-dependent, GA was implemented in this control of JA-responsive target genes. Tanaka *et al*. (2006) found that the GA insensitive mutant *gid1,* which hyper-accumulates endogenous GA, displays enhanced susceptibility to rice blast, while rice plants compromised in GA biosynthesis (i.e. hypo-accumulation of GA) were found to exhibit increased resistance to *M. oryzae* (Qin *et al*., 2013).

RNA sequencing (RNASeq) has been successfully used to profile changes in the wheat transcriptome in response to a number of pathogens, including *Zymoseptoria tritici* (Yang et al., 2013; Rudd *et al*., 2015), *Fusarium graminearum* (Foroud et al., 2011), *Puccinia striiformis* and *Blumeria graminis* (Zhang *et al*., 2014).While the recent release of an annotated, hexaploid wheat reference genome sequence, RefSeq ((International Wheat Genome Sequencing Consortium (IWGSC), 2018)) means that resources are now available to support a detailed and global examination of changes in wheat gene expression in response to pathogen infection.

2.2.1 Aims

The aim of this study was to determine the genetic and molecular changes that occur in wheat female flowers following inoculation with *C. purpurea*. The female flowers of a male sterile wheat line were inoculated with an aggressive strain of *C. purpurea*. Female flowers were examined at specific time points after *C. purpurea* inoculation to follow the infection process through the stigma, the ovary transmitting tissue, to the ovule. Tissue samples were collected at the same times points from stigma, transmitting and ovule tissues for RNASeq analyses. Changes in wheat gene expression were then compared across time points and tissues in relation to the stages of *C. purpurea* development.

2.3 Materials and methods

2.3.1 Plant material, *Claviceps purpurea* inoculations and sampling

All inoculations and sampling were carried out by Dr. Anna Gordon. A cytoplasmic male sterile hexaploid wheat line, developed at NIAB by Steve Bentley (personal communication) was used in all *C. purpurea* inoculations. Plants were grown in the glasshouse at an18^{o}C/16 hour day and 15^{o}C/8 hour night cycle. The middle florets of each ear were inoculated with a single *C. purpurea* isolate when the stigma became receptive (i.e. fluffy in appearance), as described in Gordon et al (2015). *C. purpurea* inoculations were carried out using a 2 ml syringe and fine needle, delivering the conidia suspension between the lemma and palea of each floret. Twelve florets were inoculated on each ear. Each inoculated ear represented a single replicate, with five replicates being collected for each time point and tissue sampled. Mock-inoculated florets were injected with ultra-pure water. *C. purpurea (Cp)*- and Mock-inoculated samples were taken at 10 minutes, 1, 5, 24, 48 and 72 hours (H), and 5 and 7 days (D) after inoculation for both microscopy and RNASeq analyses (Table 2.1).

The *C. purpurea* UK isolate 04-97.1 (Gordon et al., 2020) were used in all inoculations. Isolate 04-97.1 was recovered from long-term glycerol stocks kept at -80^{o}C by inoculation onto the male sterile line two weeks prior to conidia being required. Fresh conidia, in the form of honeydew, were collected and diluted in ultrapure water to a concentration of 1 x 10^{-6} spores ml^{-1}. These conidia were used to inoculate plants over a 3-day period, being kept at 4^{o}C.

Additional fungal samples were collected including replicates of conidia from honeydew, and mycelia of *C. purpurea.* Conidia from a single inoculated ear was collected 10-12 days after inoculation and was resuspended in 1ml distilled water. Spores were centrifuged at 6000 rpm and then resuspended in 50 ml RNA*later*. Mycelial samples had been grown for 24h in liquid Mantle media at 20°C before collection by centrifugation and resuspension in 50 ml RNA*later* and stored at -80^{o}C. RNA was extracted for RNASeq analyses from both *C. purpurea* mycelia and conidia.

Table 2.1 Female floral tissues and time points sampled after *Claviceps purpurea* inoculation

Time points	Mock-inoculated	*Cp*-inoculated
$T_{10\ minutes}$	Stigma (2) TT (3) Base (3)	Stigma (3) TT (2) Base (3)
$T_{1\ H}$	Stigma (3) TT (3) Base (1)	Stigma (2) TT (3) Base (3)
T_{5H}	Stigma (2) TT (2) Base (2)	Stigma (3) TT (3) Base (3)
T_{24H}	Stigma (3) TT (3) Base (3)	Stigma (2) TT (3) Base (3)
T_{48H}	TT (3) Base (3)	TT (3) Base (3)
T_{72H}	TT (3) Base (3)	TT (3) Base (3)
T_{5D}	TT (2) Base (2)	TT (3) Base (3)
T_{7D}	TT (2) Base (3)	TT (3) Base (3)

TT - Transmitting ovary tissue, Base - Ovule tissue. Number in brackets is the number of replicate samples made into RNA libraries for RNASeq analysis. Stigma tissues could only be sampled up to 24H, as after 24 hours stigma began to degrade. H = hours after inoculation; D = days after inoculation.

2.3.2 Preparation of floral tissues for microscopy and RNA extraction

All floral tissue preparations were carried out by Dr. Anna Gordon. Whole ovaries were removed from each inoculated floret and sectioned using a double edge razor that had been wiped with RNAseZap. A longitudinal section was made along the dorsal groove of each ovary allowing for easy identification of the stigma, transmitting and base tissues (Figure 2.1). Half of the ovary was placed into formaldehyde for fixing and subsequent epifluorescent and confocal microscopy. The other half was placed into 30 µl of RNA*later* (Sigma) and left for 24 hours to allow full penetration of the liquid.

2.3.3 Microscopy procedures

All microscopy was carried out by Dr. Paul Grant. Ovule halves reserved for microscopy were stained with a solution of 0.05% aniline blue in potassium phosphate buffer, pH 9.0. Ovules were examined using epifluorescence microscopy and scored for the presence of stained hyphae in stigma, transmitting and base tissues, at each of the time points. For high resolution confocal microscopy ovule halves were fixed in 1M KOH for 24 hrs, rinsed in water, and then treated with 0.3mg/ml amylase for 36-48 hrs at 37^{o}C. Ovules were stained using the mPS-PI technique (Truernit et al., 2008). Ovules were treated with Schiff reagent (100mM sodium metabisulphite and 0.15M HCL) and 100µg/ml propidium iodide for 1-2 hrs at room temperature, rinsed in water, and then stained and cleared in a modified SCALE solution with aniline blue (Hama et al., 2011; 50mM K_2HPO_4, 4M Urea, 10% glycerol, 0.1% Triton X-100 and 0.05% aniline blue; pH 9.0). Ovules were mounted in staining solution and imaged with a Leica SP5 confocal microscope (Leica Microsystems UK Ltd). Aniline blue-stained tissues were visualised using an excitation of 370nm and detected at 509 nm and propidium iodide was visualised using an excitation of 561nm and detected at 580-660 nm.

2.3.4 RNA extraction, library construction and RNAseq

RNA extractions were carried out by Dr. Anna Gordon. The individual ovules (up to 12 ovules per ear) collected from each *Cp*-inoculated ear were pooled if the corresponding ovule half tested positive for *C. purpurea* infection (based on microscopy observations). The ovules from one ear formed an RNA replicate. Tissue disruption of plant and fungal tissues was carried out using 2 mm RNase-free steel balls (Spheric Transfer). RNA was prepared using the Trizol (Invitrogen) method. RNA was DNase treated (Qiagen) and then cleaned using RNeasy 96-well columns, before quantification using nanodrop. RNA integrity was assessed using a Shimadzu MultiNA in order to select 3 of the 5 replicates RNA samples for Illumina TruSeq library preparation.

Three replicate RNAseq libraries were made of the Mock- and *Cp*-inoculated wheat ovaries for each of the three tissues - stigma, transmitting and base tissues, at each time point. For stigma viable tissue was not available beyond 24H (Table 2.1). RNAseq libraries were also made from ungerminated *C. purpurea* conidia (two replicates) and *C. purpurea* mycelium grown *in vitro* (three replicates). RNAseq libraries were prepared and sequenced by Source Bioscience (www.sourcebioscience.com): mRNA was isolated using Illumina poly-T oligo-attached magnetic beads, undergoing two rounds of purification. The mRNAs were fragmented and primed with random hexamers for cDNA synthesis. Libraries were prepared in accordance with the Illumina TruSeq RNA sample preparation guide (November 2010, rev.A) for Illumina Single-End Multiplexed Sequencing. Libraries were pooled and run on two flow cells.

2.3.5 Bioinformatics pipeline: Pre-processing

The bioinformatics analyses, with the exception of annotation were carried out by Dr. Nelzo Ereful. Quality checking of fastq files was performed using FastQC (Andrews, 2010). Adapter sequences were removed using FASTX clipper (Gordon, 2009) (parameters: –M 15 –l 20 –a <adapter sequence>). Sequence ends with quality scores of less than 20 were trimmed and sequences shorter than 35 were removed (parameters: –t 20 –l 35) using FASTQ Quality Trimmer (Gordon, 2009).

2.3.6 Genome-guided assembly

The bread wheat variety Chinese Spring (IWGSC RefSeq v1; URGI INRA) cDNA version 1 and the *C. purpurea* cDNA (Ensembl release 35) were merged to form a transcriptome fasta reference sequence. Both Mock- and *Cp*-inoculated reads were aligned against this indexed reference sequence using bowtie2 with the default parameters (Langmead and Salzberg, 2012). Using SAMtools alignment files were converted in binary format (command: view –b) (Li et al., 2009), and reads with low mapping quality (option: view –b –q 5) and PCR duplicates (option: rmdup) were removed (Oeser et. al, 2017). Percentage alignment results are provided in Table 7.1 (Appendix A). The average proportion of reads removed across all libraries was 0.0093%.

2.3.7 Cross-mapping check

As the pipeline involved the merging of the wheat IWGSC RefSeq v1 and *C. purpurea* cDNA reference (Ensembl release 35) sequences we checked whether there was significant reciprocal mapping of reads between the wheat and *C. purpurea* transcriptomes. We mapped all Mock-inoculated wheat sample reads to the *C. purpurea* reference sequence. Likewise, we mapped *C. purpurea* reads (two reps of conidia-only and two reps of media-grown *C. purpurea* mycelium) to the wheat transcriptome reference sequence. Removal of low-quality reads and mapping were performed as described above. After removal of low-quality reads and PCR duplicates, we calculated the percentage alignment of wheat reads mapping to the *C. purpurea* transcriptome and the *C. purpurea* reads mapping to the wheat transcriptome reference sequences.

2.3.8 D*e novo* assembly of unmapped *Claviceps purpurea* reads

Results of percentage alignment dropped at 5D and 7D timepoint. We speculated an enormous number of *C. purpurea* reads were unmapped to the reference sequence. We therefore performed *de novo* assembly using Trinity. Reads from the ungerminated *C. purpurea* conidia (2 reps) and *C. purpurea* grown on artificial media (3 reps) libraries were mapped to the *C. purpurea* cDNA (Ensembl release 35) transcriptome references. Unmapped reads were

extracted using SAMtools (command: view -b -f 4). Read duplicates were tagged and removed using GATK (option: MarkDuplicates; McKenna et al. 2010) and PRINSEQ (option: derep) (Schmieder and Edwards, 2011) respectively. This aimed to reduce memory space and increase calculation speed. This resulted in 1.33 M reads in fastq format. Trinity was used to perform *de novo* assembly using the default kmer length equivalent to 25 (options: --bflyHeapSpaceMax –bflyHeapSpaceInit –bflyCalculateCPU). After assembly, contigs with no predicted open-reading frame (ORF) were dropped using a web-based ORF predictor (Min et al. 2005). *C. purpurea* cDNA (Ensembl release 35) and the *de novo* assembled references were merged to form a new *C. purpurea* reference transcriptome. Reads derived from the *C. purpurea* at 5D and 7D timepoints were remapped using this new *C. purpurea* reference.

2.3.9 Read count quantification and differential gene expression analysis

Quantification of read counts contained within the alignment bam files was performed using Salmon's alignment-based mode (parameters: --biasCorrect --useErrorModel) (Patro et al. 2017). The annotation name and the number of reads columns generated by Salmon were extracted and a count data matrix created using R (in Linux). Rows with low read counts (R command: rowSums(CD@data)> ncol(CD)) were removed to reduce object size and increase calculation speed. Histograms were created before and after the removal of near-zero read counts or low expressed isoforms to assess the distribution curve of the datasets.

To normalize datasets with respect to library size, library scaling factors were calculated using baySeq trimmed mean of M-values (TMM; Robinson and Oshlack, 2015). MA plots (where M is the difference in log expression values and A is the average; Dudoit et al. 2002) were created and used to determine if the normalization procedure was adequate with respect to library size. Loess regression curves (Cleveland et al. 1988) were plotted to determine whether the normalization step had "centered" the MA plots.

Pairwise, cross-conditional differential gene expression analysis between *Cp*- and Mock-inoculated samples was performed using baySeq (Hardcastle and Kelly (2010), Hardcastle, 2017a; Hardcastle 2017b). The average normalized read counts of all replicates of each tissue by time point sample were calculated, incremented by 1 to avoid 0 denominators in subsequent analyses. Expression ratios were obtained by dividing the average normalized counts of the *Cp*- over the Mock-inoculated samples (Treatment/Control or T/C), generating log (base 2)

ratio or fold changes (FC). Genes are considered to be differentially expressed between *Cp*- and Mock-inoculated treatments when they exhibit a $FC \geq 2$ (or $|\log_2 FC| \geq 1$) at a false discovery rate (FDR) p-value correction < 0.05 (Benjamini and Hochberg, 1995), and showed an absolute difference > 10, as previously implemented (Chandra et al. 2016).

Customised heatmaps and boxplots were produced using R to visualise gene expression across tissues and time points. Fitted regression lines were superimposed onto the boxplots to facilitate interpretation of gene expression patterns across time.

2.3.10 Annotation of differentially expressed genes

The genes that were found to be differentially expressed in the stigma, transmitting or base tissues, at one or more time points, were annotated using Blast2go (http://www.blast2go.com/b2ghome). For functional annotation the genes were aligned against the National Centre of Biotechnology Information (NCBI) nr protein database. The blastx function was used to search gene sequences against the Swiss-Prot protein database, with the e-value cut-off set at $1e^{-5}$. Gene names were assigned based on the top Blastx hit, having the highest similarity score. Genes related to hormonal pathways, defence and photosynthesis were further, manually explored based on the names that had been assigned to them during annotation. The functions of these potential genes of interest were investigated through manual searches of scientific literature databases.

2.4 Results

2.4.1 Microscopic examination of *Claviceps purpurea* infection of wheat

The percentage of ovules with *C. purpurea* hyphae in stigma, transmitting and base tissues were scored at each time point (Table 2.2). At 10 mins after inoculation conidia of *C. purpurea* were visible on the stigma, but no hyphal growth was observed at this early time point. Conidia were observed to have germinated with hyphae growing into and down the stigma at 24H (Figure 2.1C). By 48H hyphae had grown through the transmitting tissue and had entered the base tissue (Figure 2.1D). By 72H hyphae had surrounded the ovule and were occupying much of the base tissue especially close to the boundary of the ovule to rachis, where the vasculature enters the ovule. At 5D much of the wheat tissue of the ovule had been replaced by fungal tissue which takes on a very branched appearance (Figure 2.1F).

Table 2.2 The development of *Claviceps purpurea* infection in female floral tissues over time

Time after *Cp* inoculation	% of ovules with hyphae visible in stigma tissue	% of ovules with hyphae visible in transmitting tissue	% of ovules with hyphae visible in base tissue
10 min (n=12)	0%	0%	0%
1H (n=13)	7.7%	0%	0%
24H (n=2)*	100.0%	0%	0%
48H (n=41)	59%	59%	51%
72H (n=57)	87%	87%	87%
5D (n=60)	100%	100%	100%
7D (n=60)	100%	100%	100%

n = number of ovules observed; H = hours after inoculation; D = days after inoculation; *only 2 ovule samples were available for the 24H time point, therefore the value of 100% of ovules with hyphae visible in stigma tissue must be interpreted with caution.

2.4.2 Quality check of RNAseq libraries

To determine the response of wheat to infection with *C. purpurea* we undertook an RNASeq analysis of female floral tissues – stigma, transmitting and base tissues, at specific time points after *Cp*-inoculation, up until 7D (Table 2.1). Each tissue by time point interaction was represented by a minimum of two replicate libraries. Libraries with an average read

coverage of less than 5× were removed from the study. Consequently, the 5H *Cp*- and Mock-inoculated samples were removed from subsequent analyses. The average read coverage of the remaining libraries was 9×, the highest being 29×. Pearson's coefficient of correlations, using the normalized read counts, were used to compare replicate libraries of each tissue and time point. In general, correlations of 0.90–0.99 were found between replicate libraries. The Mock-inoculated transmitting tissue at 24H had the lowest correlations of 0.80 to 0.83.

MA plots with Loess curves were generated to determine whether the normalization procedure was adequate with respect to the library size (Figure 7.1; Figure 7.2, Appendix A). Samples at the early time points gave symmetrical MA plots with "centered" Loess curves, indicating that the normalization procedure was adequate. However, in the 5D and 7D samples we found bimodal distribution of points in the MA plots due to the presence of RNA transcripts from two biological organisms, wheat and *C. purpurea*. The apparent asymmetry in the MA plots is due to the contrasting transcriptional activities of wheat and *C. purpurea* at these later time points, *C. purpurea* genes being expressed at higher levels as the wheat ovary is replaced by fungal hyphae.

2.4.3 Establishment of a reference transcriptome for wheat and *Claviceps purpurea*

To check whether there was any significant reciprocal mapping of reads between the wheat and *C. purpurea* transcriptomes we calculated the percentage of wheat reads mapping to the *C. purpurea* reference transcriptome and vice-versa. Only 0.0016% of the wheat reads mapped to the *C. purpurea* transcriptome reference, while 0.037% of the *C. purpurea* reads aligned to the wheat transcriptome reference. These percentages demonstrate that there is a negligible number of reads cross-mapping between the reference sequences of these two species. The bread wheat variety Chinese Spring IWGSC RefSeq v1 and *C. purpurea* cDNA (Ensembl release 35) transcriptomes were therefore merged to create a single reference transcriptome that was used in the subsequent gene differential expression analysis.

Using this reference transcriptome 95 of the 114 libraries (83%) had read percentage alignment rates from 70 to 85%, particularly at the early timepoints. However, with libraries from 5D and 7D the alignment rates fell to values as low as 36% (Table 7.1, Appendix A). The low read alignments were found to be due to a high percentage of *C. purpurea* reads present at these later time points, and a significant number of the *C. purpurea* transcripts not being

represented in the *C. purpurea* cDNA reference transcriptome (Ensembl release 35). Reads from the ungerminated *C. purpurea* conidia and *C. purpurea* hyphae grown on artificial media libraries were mapped to the *C. purpurea* cDNA (Ensembl release 35) transcriptomes. Unmapped reads from the two *C. purpurea* libraries were extracted, pooled and *de novo* assembled to provide a new *Cp*-reference transcriptome. Alignment of the 5D and 7D *Cp*-inoculated libraries to this new wheat-*C. purpurea* transcriptome reference now gave percentage alignments in the range of 85% – 90%, a big improvement from the original 36% – 39%. This indicates that a large percentage of the unmapped reads at the latter time-points are derived from *C. purpurea* transcripts that are not represented in the *C. purpurea* transcriptome assembly (Ensembl release 35).

2.4.4 Differential expression of wheat genes in response to *Claviceps purpurea* infection

To understand the changes that occur in wheat female flowers upon infection with *C. purpurea* we undertook a time course experiment looking at changes in the wheat transcriptome in stigma, transmitting and base tissues of ovaries at 10 min, 1, 24, 48 and 72H, and 5 and 7D after inoculation with a single isolate of *C. purpurea* (Table 2.1). A pairwise, cross-conditional differential expression analysis was performed, comparing *Cp*- to Mock-inoculated samples in each tissue and at each time point.

Overall, a large number of wheat genes were observed to be differentially expressed in the three ovary tissues across the 7 day period of *C. purpurea* infection. Annotation of these DEG indicated enrichment for a number of functional categories. These included classical defence-related genes and wheat genes associated with hormonal pathways. Other functional categories included genes associated with photosynthesis, genes involved in oxidation/reduction processes and genes involved in protein phosphorylation.

No significant changes in the wheat transcriptome were seen at 10 minutes after inoculation with *C. purpurea*. At 1H seven DEG were detected in the stigma, but no DEG were found in the transmitting or base tissues at this time point. Of the seven stigma DEG one was up-regulated, being annotated as a chlorophyll a-b binding protein. Chlorophyll a-b binding protein forms part of the plant's light harvesting complex, located in the chloroplast, which captures and delivers excitation energy to photosystems I and II. However, it is unclear why this gene should be up-regulated in stigma.

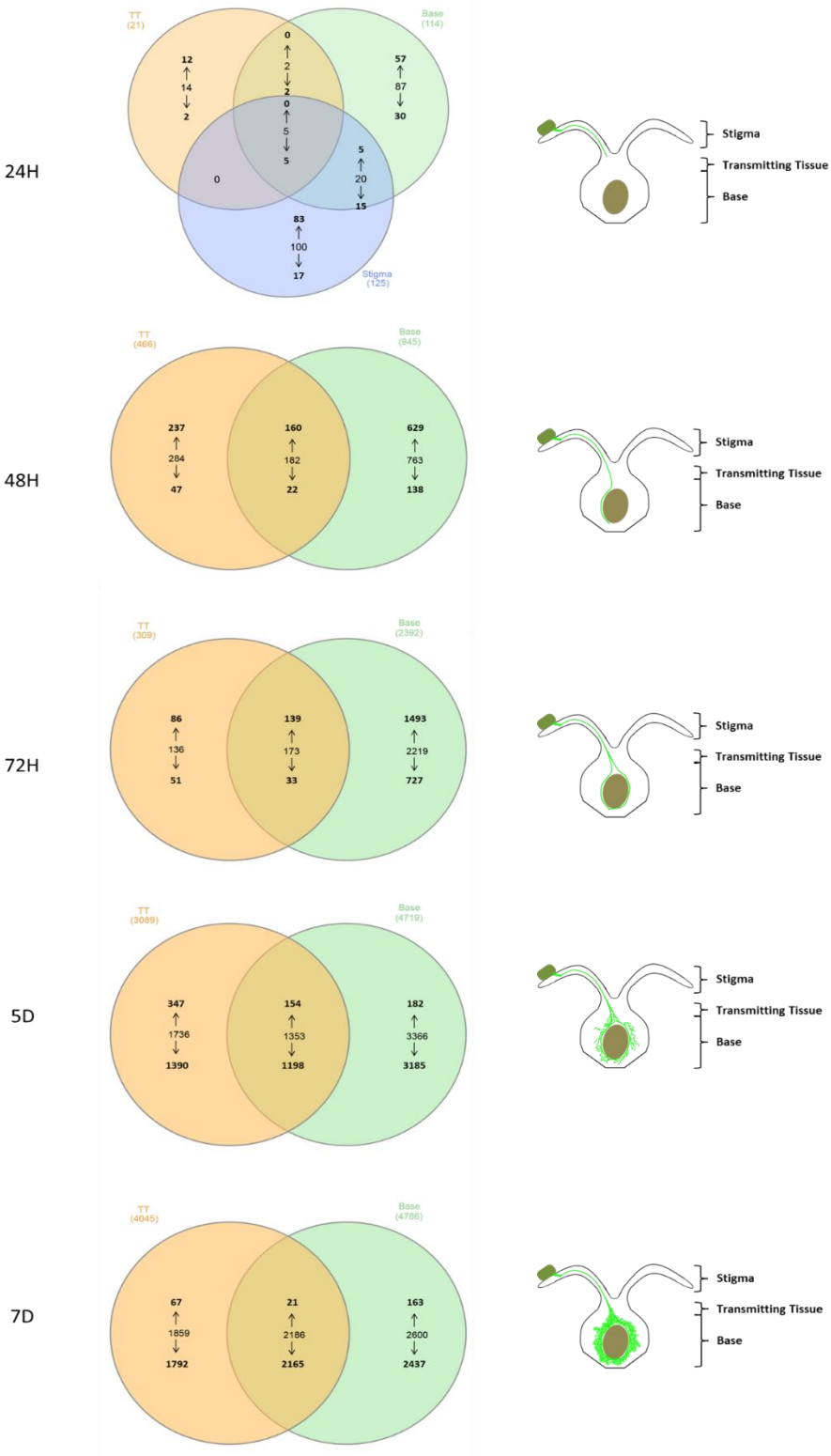

Figure 2.2 Venn diagram showing the numbers of wheat differentially expressed genes within stigma, transmitting and base ovule tissues at 24H, 48H, 72H, 5D and 7D after inoculation with a single isolate of Claviceps purpurea. The arrows pointing up and down designate the numbers of genes that are up- or down-regulated respectively. A schematic representation of the stage of fungal development in the wheat ovule at each time point is shown to the right of each Venn diagram. H = hours; D = days.

Two of the six down-regulated genes in the stigma at 1H were DNA binding transcription factors (TFs). While transcription factors are an important element of the complex regulatory network of signaling that allows plants to respond to infection, the generic annotation of these TFs makes it difficult to identify the pathways in which they operate, and therefore their potential downstream targets. Also, down-regulated in the stigma at 1H were a myosin protein, known for its role in cytoplasmic streaming (Tominaga & Ito, 2015), a Kelch-like protein, a DnaJ protein and a sucrose synthase. Kelch proteins contain repeat motifs forming β-propeller domains that mediate protein-protein interactions and are involved in a wide array of cellular activities (Adams et al., 2000). DnaJ proteins, otherwise known as HSP40s (heat-shock protein 40), are a family of conserved co-chaperones for HSP70s and are known to play diverse roles in stress responses and developmental processes such as flowering time (Liu & Whitham, 2013). Sucrose synthase has a role in the rapid mobilisation of carbohydrates during defence (Essmann *et al*., 2008), so may indicate an early attempt by *C. purpurea* to alter the carbohydrate profiles within the floral tissues in support of fungal growth.

At subsequent time points most of the wheat DEG were tissue specific, especially at the early time points (Figure 2.2). At 24H significantly more genes were transcribed in the stigma (125 DEG) and base (114 DEG) tissues than in the transmitting tissue (21 DEG). Five DEG were found in common between the stigma, transmitting and base tissues, all being down-regulated. Twenty DEG were shared between the stigma and base tissues, two DEG between the transmitting and base tissues, while no DEG were shared between the stigma and transmitting tissues. At 24H *C. purpuea* was observed to have grown into the stigma, however no *C. purpurea* hyphal growth was ever observed in the base tissue at this early time point (Figure 2.1). Therefore, changes in gene expression in the base tissue preceded the arrival of fungal tissue. This would suggest the presence of a potential mobile signal, either pathogen or plant-derived, that is delivered to the base tissue prior to its colonisation by the fungus.

The five down-regulated DEG found in all three tissues at 24H included a glycosyl hydrolase (xylanase), a F-box family protein, a myosin and a vesicle-associated membrane protein. As xylanases; involved in hemicellulose breakdown, myosin; involved in ATP-dependent actin-based motility, F-box proteins; involved in ubiquitination of proteins and vesicle-associate membrane proteins, can all be inked to the plant raising defence responses to pathogen attach, global down-regulation of these genes, in all three ovule tissues, would fit with an early attempt of *C. purpurea* to suppress plant defence.

Of the 20 DEG in common between the stigma and base tissues at 24H, 5 were up-regulated and 15 down-regulated (Figure 2.2). The up-regulated genes included an acid phosphatase, a cell wall invertase, a glutaredoxin, a Ras-like protein and a VQ motif family protein. The 15 down-regulated genes encoded for proteins having a wide variety of functions, including a cinnamoyl-CoA reductase, an E3 ubiquitin-protein ligase, F-box family proteins, a vesicle-associated membrane protein, a histone deacetylase, and a galactosyltransferase family protein. The transmitting and base tissues shared only two genes (both down-regulated) which encoded for a replication protein A 32 kDa subunit and a signal recognition particle receptor alpha subunit family protein.

At 48H and 72H significantly more wheat genes were up-regulated in the transmitting (48H - 397 up/69 down and 72H - 225 up/84 down) and base tissues (48H - 789 up/160 down and 72H - 1637 up/760 down) than there were down-regulated (Figure 2.2). The number of DEG increased further at 5D and 7D in both the transmitting (5D – 3089 and 7D – 4045) and base tissues (5D – 4719 and 7D – 4786) (Figure 2.2), although the ratio of up- to down-regulated genes observed at 48H and 72H was reversed at these later time points, with far more DEG being down-regulated. Interestingly, while the wheat ovary becomes overwhelmed by *C. purpurea* hyphal tissue at 5D and 7D, wheat genes were detected that remained up-regulated. Specifically, 501 and 88 DEG were up-regulated in the transmitting tissue at 5D and 7D, respectively, while 336 and 184 genes were up-regulated in the base tissue at 5D and 7D. A large percentage of these up-regulated genes belonged to functional categories related to defence and hormonal pathways. In particular, in the transmitting tissue at 5D, 24.75% of the up-regulated genes were defence-related and 6.19% were hormone-related. At 7D 38.64% of the up-regulated genes were defence related, while 3.41% were hormone related. In the base tissue at 5D 23.51% of the up-regulated genes were defence-related and 4.46% were hormone-related. At 7D 40.76% of the up-regulated genes were defence-related, while 3.80% were hormone-related. With regards to specific categories, up-regulated genes at 5D and 7D belonged to the auxin, ET and cytokinin pathways, as well as in defence-related gene categories such as antifungal proteins, NBS-LRR class proteins, receptor protein kinases, and genes involved in the regulation and signaling of reactive oxygen species (ROS).

2.4.5 Reprogramming of the hormonal status of wheat ovary tissues

Many of the wheat genes differentially transcribed in response to *C. purpurea* infection were those known to be involved in biosynthesis and signaling pathways of plant hormones, and included the ET, auxin, cytokinin, gibberellic acid (GA), salicylic acid (SA) and jasmonic acid (JA) biosynthetic and signaling pathways (Figure 2.3). A list of all hormone related genes that were found to be differentially expressed are shown in Tables 7.2, 7.3 and 7.4 (Appendix A). Hormone associated genes were first detected in the stigma and base tissues at 24H, but not in the transmitting tissue. DEG associated with GA and JA pathways were seen in stigma tissue and JA and ET pathways in base tissue at 24H, indicating not only a very rapid response of hormone-associate gene expression to *C. purpurea* infection, but a long-distance triggering of hormone-associated gene expression in the base tissue, prior to arrival of fungal hyphae. By 48H DEG were seen in both transmitting and base tissues associated with most major groups of plant hormones. Genes were increasingly up-regulated with time, generally reaching a peak between 48H and 72H, followed by down-regulation at 5D and 7D, in transmitting and base tissues. The exception being JA-associated genes, which were not detected as significantly differentially expressed in transmitting tissue until 5D.

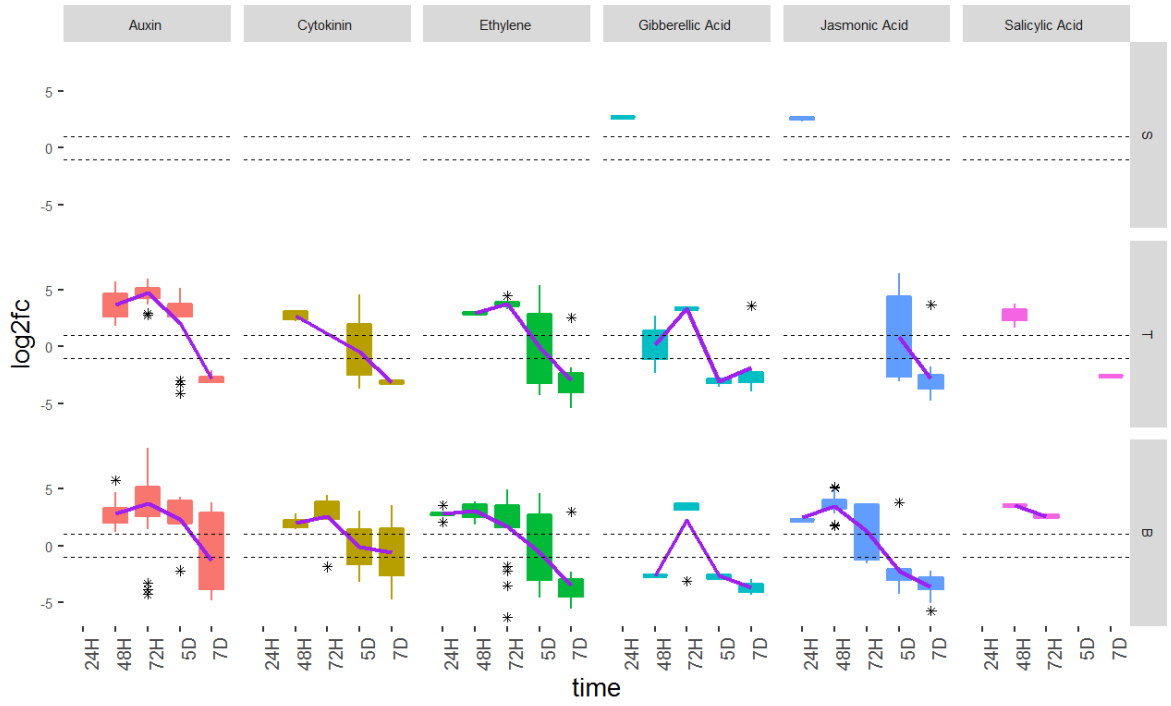

Figure 2.3: Hormone-associated differentially expressed genes (DEG) identified across time points and female floral tissues. Each box shows the number of DEG belonging to each hormonal group expressed in stigma (S), transmitting (T) and base (B) tissues at 24H, 48H, 72H, 5D and 7D after inoculation with *Claviceps purpurea*, H = hours. D = days. The asterisks show the outliers beyond the

upper and lower quantiles. The solid line is a regression line fitted to the data. The dotted line represents the fold change at -1 and +1, with genes considered not to be significantly differentially expressed if their fold change values fall between the dotted lines.

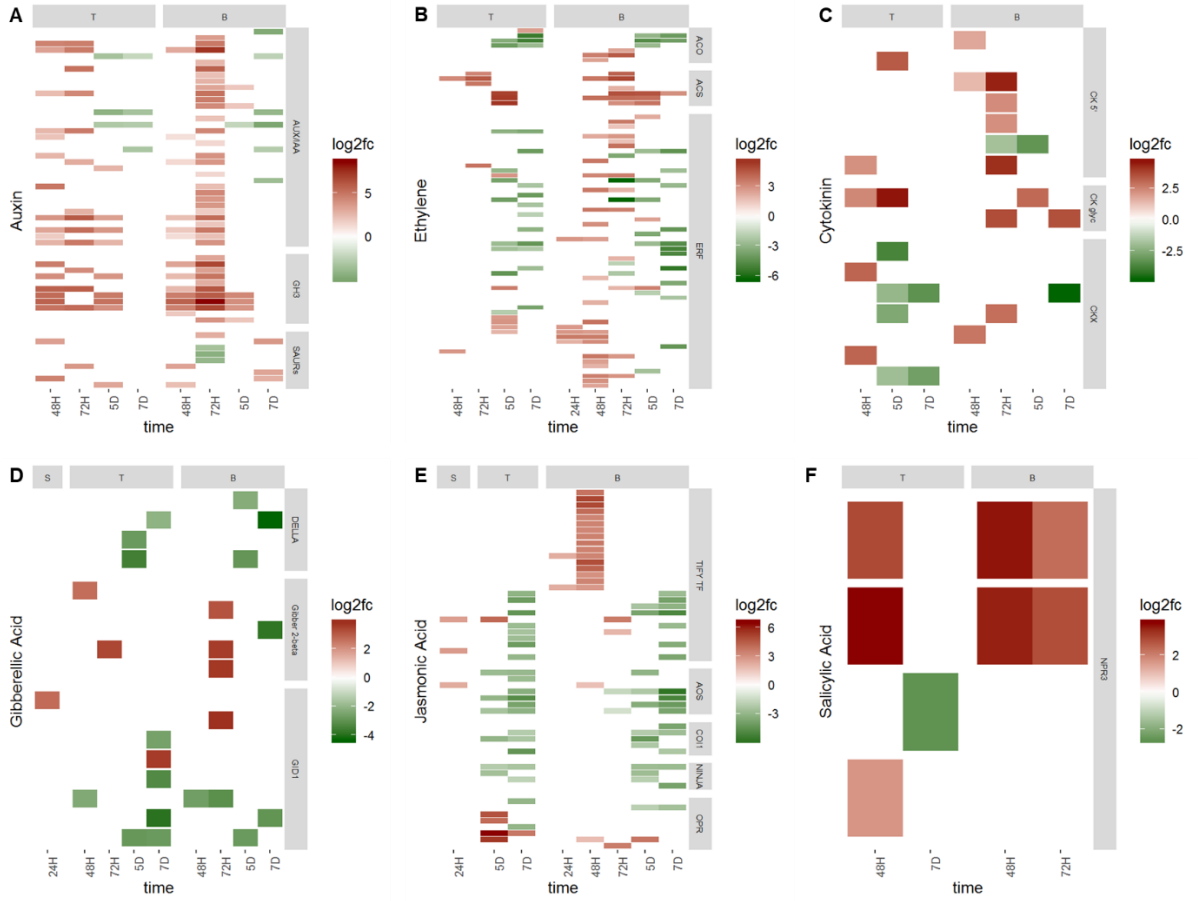

Figure 2.4: Heatmaps of hormonal-associated differentially expressed genes (DEG) across time points and tissues. DEG are defined by functional categories. **(A)** Auxin-related genes ((Categories from top to bottom: Auxin/indole-3-acetic acid (AUX/IAA), Glycoside Hydrolase 3 (GH3), small Auxin-Up RNAs (SAURs)**)**; **(B)** Ethylene-related genes ((Categories from top to bottom: 1-Aminocyclopropane-1-carboxylate oxidase (ACO), 1-Aminocyclopropane-1-carboxylate synthase (ACS), Ethylene responsive transcription factors (ERF)); **(C)** Cytokinin-related genes ((Categories from top to bottom: cytokinin riboside 5′-monophosphate phosphoribohydrolase (CK 5'), cytokinin specific glycosyltransferases (CK glyc), cytokinin oxidase/dehydrogenase (CKX)); **(D)** Gibberellic acid-related genes ((Categories from top to bottom: DELLA, gibberellin 2-beta-oxidase (Gibber 2-beta), GA-INSENSITIVE DWARF1 (GID1)); **(E)** Jasmonic acid-related genes ((Categories from top to bottom: TIFY transcription factors (TIFY TF), allene oxide synthase (AOS), coronatine-insensitive 1 (COI1), Novel INteractor of JAZ (NINJA), 12-oxophytodienoate reductase (OPR)); and **(F)** Salicylic acid-related genes ((Categories: NON-EXPRESSOR OF PR3 (NPR3)).

Within each hormone class certain gene functional categories were of particular interest, exhibiting significant up-regulation during *C. purpurea* infection. At 48H and 72H, when fungal hyphae have reached the ovule and surrounded the ovule, respectively, a

significant up-regulation of auxin genes was observed in both the transmitting and base tissues (Figure 2.4A). These genes primarily belonged to the AUX/IAA and IAA-amido synthetase (GH3) gene families, with GH3s showing particularly prolonged up-regulation in some cases, even at the 5D timepoint. AUX/IAA genes encode known transcriptional repressors of auxin response genes, while the GH3 family of genes encode auxin-conjugating enzymes that regulate the auxin pool through negative feedback. Both AUX/IAAs and GH3s are early auxin response genes, with auxin modulating their levels to re-equilibrate the system at different steady states, depending on the auxin concentration (Leyser, 2018). The up-regulation of these genes therefore points towards the presence of elevated levels of auxin in the floral tissues during *C. purpurea* infection, as well as a potential increase in auxin signaling. The up-regulation of the NPR3 receptor of auxin's mutually antagonistic hormone SA was also seen in transmitting and base tissues at 48H and 72H (Figure 2.4F).

Among the ET genes the two categories that showed the highest up-regulation were 1-Aminocyclopropane-1-carboxylate synthase (ACS) and 1-Aminocyclopropane-1-carboxylate oxidase (ACO) (Figure 2.4B). These form multi-gene families and encode ET biosynthesis enzymes, forming the final steps in the biosynthetic pathway (Yang & Hoffman, 1984). Up-regulation was observed in both the transmitting and base tissues. ACS genes remained up-regulated at 5D, with one gene in the base tissue remaining up-regulated at the 7D. ET responsive transcription factors (ERF), which drive many of the signaling cascades in response to ET (Stepanova & Alonso, 2005), were also found to be significantly up-regulated across the transmitting and base tissues. The majority of these ERF sustained up-regulation across early time-points in the base tissue, with down-regulation occurring only at 5D and 7D. The up-regulation of genes found in both the biosynthetic and signaling pathways of ET suggest the activation of ET dependent responses during *C. purpurea* infection.

Another hormonal group that responded to *C. purpurea* infection were the cytokinins (Figure 2.4C). Three functional gene categories involved in cytokinin homeostasis were of interest. Firstly, cytokinin specific glycosyltransferases were observed to be significantly up-regulated in the transmitting and base tissues throughout infection, with the up-regulation persisting even in the later time-points (5D and 7D) when the fungal hyphae have overwhelmed the ovule. These glycosyltransferases operate by deactivating cytokinin through conjugation with a sugar moiety (Wang et al., 2011). A second gene category, also involved in cytokinin deactivation, were the cytokinin oxidase/dehydrogenase (CKX) which catalyse the irreversible degradation of cytokinins (Wang et al., 2011). However, contrary to cytokinin

glycosyltransferase, CKX were not up-regulated across all time-points, being up-regulated at 48H in the transmitting tissue, and at 48H and 72H at the base tissue. Finally, the LOG genes, encoding for cytokinin riboside 5′-monophosphate phosphoribohydrolase (CK 5'), which are responsible for the single step activation of cytokinins were, in most cases, up-regulated early on during *C. purpurea* infection (48H and 72H), with the majority of up-regulated genes being detected in base tissue. The differential expression of genes involved in cytokinin homeostasis therefore suggests a significant alteration in cytokinin levels of *C. purpurea* infected female floral tissues.

Differential gene expression analyses also indicated that GA pathways were induced during infection (Figure 2.4D). The gibberellin 2-beta-oxidase (GA2ox) gene was found to be up-regulated very early during infection, being found at 24H in the stigma, at 48 and 72H in the transmitting, and at 72H in base tissue. GA2ox is involved in GA catabolism and inactivation of GAs and is up-regulated in response to elevated GA signaling and GA treatment (Fleet & Sun, 2005). The GA receptor GID1 (GA-INSENSITIVE DWARF1) gene was also up-regulated at 24H in stigma tissue, then down-regulated in transmitting and base tissues at 48H and 72H. GID1 has previously been found to be up-regulated under conditions of GA deficiency, or DELLA accumulation (Hirano *et al.,* 2008). Take together these findings could indicate a response by wheat to remove GA from the floral tissues.

A number of genes involved in the biosynthesis and signaling pathways of JA were also differentially expressed (Figure 2.4E). With regards to the biosynthetic pathway, 12-oxophytodienoate reductase (OPR) and allene oxide synthase (AOS), which catalyses the first step in JA biosynthesis, were both found to be differentially expressed in response to *C. purpurea* infection. While OPR was up-regulated between 48H and 7D in the transmitting and base tissues, only in the case of one AOS gene was up-regulation observed at 24H in stigma and 48H in base tissue, the remaining AOS encoding genes being down-regulated. With respect to JA signaling two functional gene categories were of interest. Firstly, the F-box protein coronatine-insensitive 1 (COI1) was found to be down-regulated across the transmitting and base tissues during the last two time-points. In the presence of JA COI1 binds to jasmonate ZIM domain (JAZ) proteins leading to their ubiquitin-dependent degradation (Katsir *et al*., 2008). JAZ proteins repress transcription of JA-responsive genes, so removal of COI1 would potentially limit JAZ protein degradation and allow continued suppression of transcription of JA-responsive genes. The second signaling component affected by *C. purpurea* infection were transcription factors containing the TIFY domain. TIFY transcription factors are found in the

JAZ family (Bai *et al*., 2011). TIFY transcription factors were found that were up-regulated at 24H in the stigma, as well as in the base tissue. Furthermore, these transcription factors were significantly up-regulated at 48H and 72H in base tissue. These observations suggest the possible repression of JA signaling in response to *C. purpurea* infection.

2.4.6 Differential expression of defence-associated genes

Several defence-associated genes were among the genes differentially expressed in response to *C. purpurea* infection. A list of all defence related genes that were found to be differentially expressed are shown in Tables 7.5, 7.6 and 7.7 (Appendix A). The predicted functions of these DEG were quite varied, ranging from transport and signaling, to genes involved in a wide array of metabolic reactions. Out of all the functional categories that were identified, six categories; antifungal proteins, endocytosis/exocytosis-related proteins, NBS-LRR class proteins, genes involved in programmed cell death, receptor protein kinases and transcription factors were selected as the most biologically relevant, as well as those exhibiting the most significant patterns of differential expression. Defence-associated DEG were first detected at 24H and in all three ovary tissues (Figure 2.5). Thus, similar to hormone-related genes, defence-associated genes were observed to be differentially expressed in base tissues prior to the colonisation of these tissues by the fungus. In general, a significant up-regulation of DEG in all functional categories was seen between 24H and 72H in all tissues, followed by down-regulation at 5D and 7D.

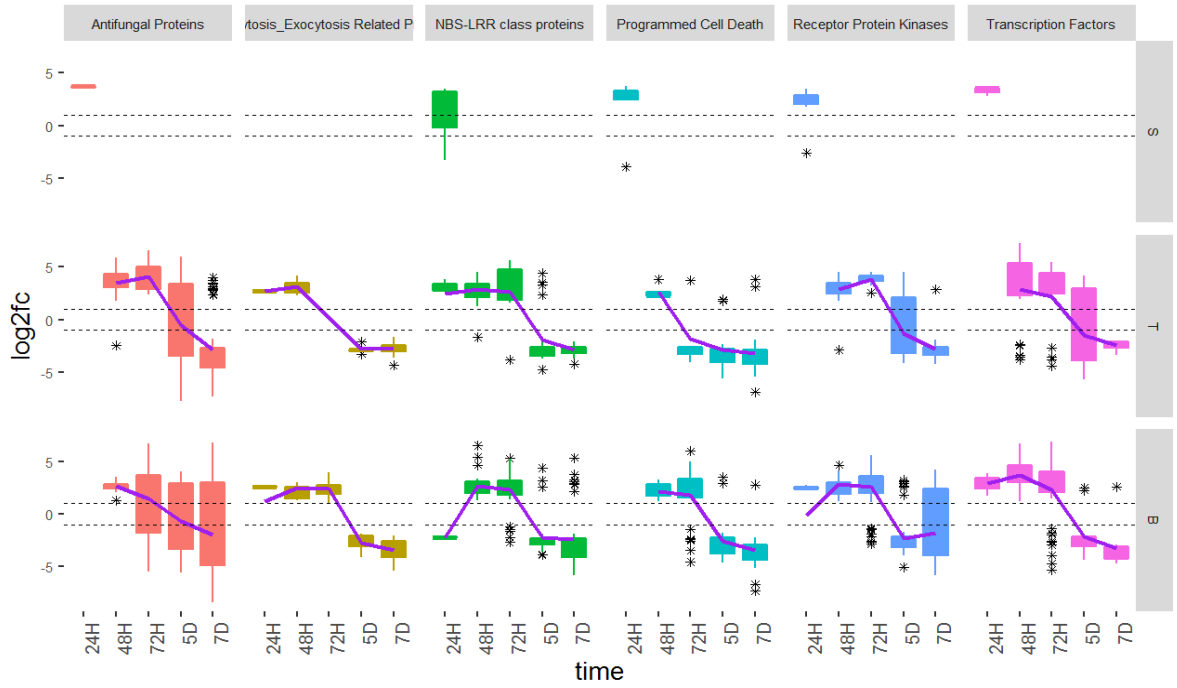

Figure 2.5: Defence-associated differentially expressed genes (DEG) identified across time points and female floral tissues. Each box shows the number of DEG belonging to each defence-associated functional category expressed in stigma (S), transmitting (T) and base (B) tissues at 24H, 48H, 72H, 5D and 7D after inoculation with *Claviceps purpurea*, H = hours. D = days. The asterisks show the outliers beyond the upper and lower quantiles. The solid line is a regression line fitted to the data. The dotted line represents the fold change at -1 and +1, with genes considered not to be significantly differentially expressed if their fold change values fall between the dotted lines

Within the functional category NBS-LRR genes, most genes exhibited similar patterns of differential expression (Figure 2.6A). Interestingly, at 24H in the base tissue NBS-LRR genes were down-regulated. These genes were then up-regulated at 48H in the transmitting and base tissues, maintaining that status until 72H, after which down-regulation was observed. However, some NBS-LRR genes exhibited LogFC values of up-regulation much higher than the rest. These genes were identified as being members of the RPM1 and RGA3 gene classes which have been found to play important roles in hypersensitive resistance (Grant *et al.*, 2001).

Other receptor protein kinases (RPK), grouped separately from the NBS-LRR class of proteins, showed a significant up-regulation in response to *C. purpuerea* infection (Figure 2.6B). Genes resembling RPK were first up-regulated at 24H in the stigma and base tissues, being continuously up-regulated in the transmitting and base tissues until 72H. While the most abundant genes in this category were serine/threonine kinases (STK), the two groups of RPK that showed the highest levels of up-regulation were the cysteine-rich receptor-like kinases (CRK) and lectin receptor kinases (LecRK). Their up-regulation was sustained until 5D, with

certain members in each category maintaining up-regulation at 7D within the base tissue. These two classes of RPK play a variety of roles in plants, including roles in down-stream signaling during pathogen recognition (Afzal *et al*., 2008).

Genes associated with antifungal activity were induced during *C. purpurea* infection, first showing up-regulation at 24H in stigma tissue (Figure 2.6C). Most genes were up-regulated in the transmitting and base tissues at the 48H and 72H timepoints. The antifungal gene classes that showed the most significant up-regulation were cytochrome P450s and chitinases. Cytochrome P450s represent one of the largest super-families of proteins in plants and are responsible for catalysing the oxygenation of many fatty acids (Pinot & Beisson, 2010). Many of the compounds resulting from these reactions have been found to have antifungal properties. The chitinase encoding genes displayed the most sustained up-regulation throughout *C. purpurea* infection, across all three tissues. Chitinases are responsible for catalysis of the hydrolytic cleavage of specific bonds found in chitin, and thus play a significant role in plant defence against a range of pathogens (Kasprzewska, 2003).

A particularly interesting functional category of defence-associated DEG were those involved in endocytosis/exocytosis processes, showing an early induction in the transmitting and base tissues (Figure 2.6D). DEG in this category included SNARE proteins, syntaxins and a homologue of the exocyst complex component EXO70B1, all of which have been found to have a role in cell wall apposition formation (Pecenkova *et al*., 2011). Of these, the group that showed the highest levels of up-regulation were those of the exocyst complex component EXO70B1.

The category transcription factors contained WRKY and MYB transcription factors that were significantly up-regulated by *C. purpurea* between 24H and 72H in all three tissues (Figure 2.6E). The genes identified as WRKY-type transcription factors in particular showed high levels of up-regulation. The WRKY and MYB transcription factor families have both been implicated in transcriptional reprogramming associated with plant defence responses (Eulgem & Somssich, 2007).

Genes classified as involved in programmed cell death were up-regulated early, being seen in stigma tissue at 24H, peaking in transmitting tissue at 48H, and base tissue between 48h and 72H, after which these genes were down-regulated (Figure 2.6F). Genes in this category included the harpin induced protein 1 (HIN1) and subtilisin-like proteases (SLP) (Kim *et al*., 2003; Figueiredo *et al*., 2014). HIN1 has been found to be highly induced during

proteasome-mediated programmed cell death (Kim *et al*., 2003), while subtilisin-like proteases have been implemented in pathogen recognition and in triggering the hypersensitive response (Vartapetian *et al*., 2011).

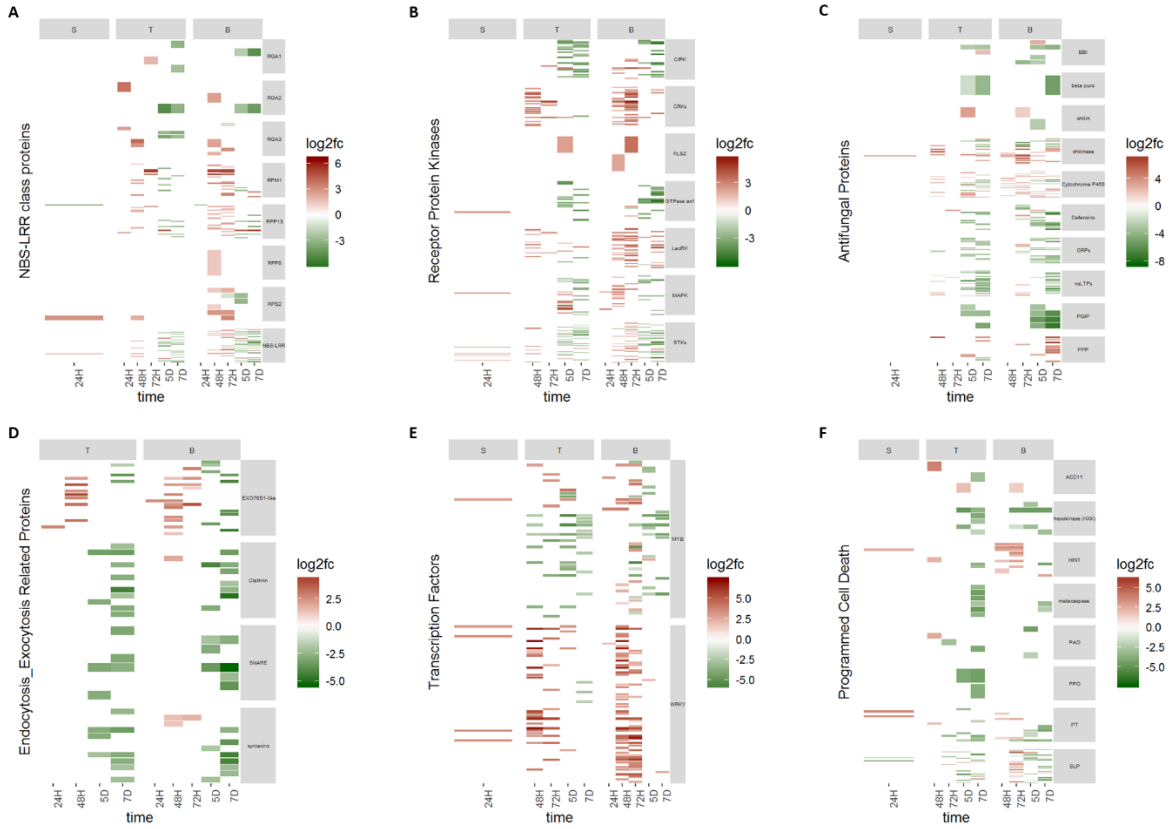

Figure 2.6: Heatmaps of defence-associated differentially expressed genes (DEG) across time points and tissues. DEG are defined by functional categories. **(A)** NBS-LRR class proteins (functional categories from top to bottom: RGA1, RGA2, RGA3, RPM1, RPP13, RPP8, RPS2, NBS-LRR); **(B)** Receptor protein kinases ()functional categories from top to bottom: CBL-interacting protein kinases (CIPK), Cysteine-rich receptor-like kinases (CRKs), Flagellin-sensing 2 (FLS2), GTPase activating 1, Lectin receptor kinases (LecRK), Mitogen-activated kinase (MAPK), serine/threonine kinases (STKs)); **(C)** Antifungal proteins ((functional categories from top to bottom: Bowman-Birk type trypsin inhibitor (BBI), beta purothionins, chitin elicitor-binding, chitinase, Cytochrome P450, Defensins, Glycine-rich proteins (GRPs), non-specific lipid transfer proteins (nsLTPs), polygalacturonase inhibiting protein (PGIP), plant-pathogenesis proteins (PPP)); **(D)** Endocytosis/Exocytosis related proteins; **(E)** Transcription factors; **(F)** Programmed cell death related genes ((functional categories from top to bottom: Accellerated Cell Death 11 (ACD11), hexokinase (HXK), Harpin induced protein (HIN1), metacaspase, polyamine oxidase (PAO), polyphenol oxidase (PPO), Potassium transporter (PT), subtilisin-like proteases (SLP)).

2.5 Discussion

Ergot has serious consequences for cereal grain quality and yield, but also directly impacts on human health due to the high levels of toxic alkaloids found in sclerotia. During the Middle Ages ergot alkaloids were responsible for the human disease known as St Anthony's fire. While sclerotia can now be removed from contaminated grain loads by physical cleaning methods: colour sorting and gravity tables (Beuerle *et al*., 2012, Byrd *et al.*, 2017, MacDonald *et al*., 2017), we know very little about the interactions that occur between wheat and *C. purpurea* at a cellular and molecular genetic level. Using an RNASeq approach we report the first examination of the reprogramming of the wheat transcriptome in response to *C. purpurea* infection in defined tissues of the ovary, i.e. the stigma, transmitting and base tissues (Figure 2.1).

Infection with *C. purpurea* resulted in major changes in expression of wheat genes associated with hormonal metabolism and signaling, as well as a wide range of genes related to defence. There is considerable evidence which indicates the crucial role plant hormones play in the regulation of immune responses to pathogens (Pieterse *et al*., 2012). Complex synergistic and antagonistic interactions provide the plant with the regulatory potential to activate, and fine-tune defences (Pieterse *et al*., 2012). Our results suggest that *C. purpurea* is also able to rapidly alter hormone levels *in planta*, co-opting the host's hormonal homeostasis and/or signaling mechanisms in order to facilitate infection.

Auxin-related genes were particularly abundant among the hormone-associated genes differentially expressed in this study. Specifically, genes belonging to the AUX/IAA and IAA-amido synthetase (GH3) gene families were up-regulated during the early stages of *C. purpurea* infection. Oeser *et al*. (2017) also observed the up-regulation of these families of auxin-related genes in rye ovules infected with *C. purpurea*. As *C. purpurea* is able to produce and secrete significant amounts of auxin (Kind *et al*., 2018), it has been suggested that the pathogen co-opts its host's auxin homeostasis in order to facilitate infection (Oeser *et al*., 2017). It is therefore possible that the repression of auxin signaling, through the up-regulation of AUX/IAA gene expression, and the conjugation of excessive auxin by GH3 proteins, is a direct response of the host to the elevated auxin levels produced by *C. purpurea*. Over-expression of GH3 has also been shown to result in elevated accumulation of SA (Zhang et al., 2007). While the observed up-regulation of the SA receptor NPR3, a low affinity SA receptor which requires high levels of SA to be induced (Fu *et al*., 2012), would support the elevation of SA within the

wheat ovaries. This would tie-in with the increased levels of SA observed in wheat varieties Mercia and Maris Huntsman upon *C. purpurea* infection in Chapter 3.

SA plays a crucial role in the activation of defence responses against biotrophic and hemi-biotrophic pathogens, with SA insensitive mutants showing increased susceptibility to both groups of pathogens (Bari & Jones, 2009). It has also been suggested that SA acts in an opposing manner to auxin. SA can inhibit pathogen growth through the stabilisation of AUX/IAA auxin repressors, achieved by limiting the auxin receptors required for their degradation (Wang *et al*., 2007). Indeed, our data show the down-regulation of an auxin binding protein (probably an auxin receptor) within the transmitting and base tissues, which coincides with the up-regulation of the AUX/IAA genes.

The ET and JA biosynthetic genes, *ACS* and *ACO*, and *OPR* and *AOS*, respectively, were significantly up-regulated in transmitting and base ovary tissues upon infection by *C. purpurea*, while the JA signaling gene *COI1* was down-regulated. Infection of wheat ears with *Fusarium graminearum*, the causal agent of Fusarium Head Blight, also resulted in up-regulation of the JA biosynthetic genes AOS and OPR in the FHB resistant variety Wangshuibai, while the JA signaling gene *COI1* was down-regulated in the susceptible wheat upon infection with *F. graminearum* (Xiao *et al*., 2013). Xiao *et al*. (2013) also observed similar patterns in the expression of ET genes, namely the up-regulation of the ET biosynthetic genes ACS and ACO. Ding *et al.* (2011) also found similar JA and ET genes being induced in response to FHB infection. Iwai *et al*. (2006) observed up-regulation of ACS and ACO genes in rice (*Oryza sativa*), accompanied by the enhanced emission of ET, in response to infection with the hemi-biotroph fungus *M. grisea.* ET responsive transcription factors (ERFs) were also up-regulated during the early stages of infection. ERFs play a significant role in the regulation of defence, and changes in their expression have been shown to lead to changes in resistance to different types of fungi (Catinot *et al*., 2015). For instance, in *Arabidopsis*, while the constitutive expression of ERF1 enhances tolerance to *Botrytis cinereal* infection (Berrocal-Lobo *et al*., 2002), the over-expression of ERF4 leads to an increased susceptibility to *Fusarium oxysporum* (Catinot *et al*., 2015).

Our data showed that the induction of ET biosynthesis genes *ACS* and *ACO* coincided with the induction of two genes involved in JA biosynthesis. Studies have suggested that ET signaling operates in a synergistic way with JA signaling to activate defence reactions, and in particular defence reactions against necrotrophic pathogens (Glazebrook, 2005). It has also

long been considered that JA/ET signaling pathways act in a mutually antagonistic way to SA, however, other studies have shown that ET and JA can also function in a mutually synergistic manner, depending on the nature of the pathogen (Mur *et al*., 2006).

Cytokinins were also implicated in *C. purpurea* infection of wheat with the up-regulation of CKX and cytokinin glycosyltransferase in transmitting and base tissues. These two cytokinin inducible genes are both involved in cytokinin homeostasis, and function by degrading and conjugating cytokinin (Bari & Jones, 2009). The cytokinin glycosyltransferase deactivates cytokinin through conjugation with a sugar moiety, while CKX catalyzes the irreversible degradation of cytokinins in a single enzymatic step (Schmülling *et al*., 2003). *C. purpurea* is able to secrete significant amounts of cytokinins *in planta*, in order to facilitate infection (Hinsch *et al*., 2015), and *M. oryzae*, the rice blast pathogen (Chanclud *et al*., 2016) also secretes cytokinins, being required for full pathogenicity. The up-regulation of these cytokinin degrading wheat genes maybe therefore be in response to elevated levels of *C. purpurea* cytokinins, and a defence response of the host.

The early induction of the GA receptor GID1 in wheat stigma tissue, as well as the subsequent up-regulation of key GA catabolic enzymes, such as GA2ox, in transmitting and base tissues, suggests that GA accumulates in response to *C. purpurea* infection. The accumulation of GA likely leads to the degradation of the negative regulators of GA signaling, the DELLA proteins. This observation is in accordance with a study by Navarro *et al.* (2008) in which the *Arabidopsis* loss of function quadruple-*della* mutant was resistant to the biotrophic pathogens *Pst*DC3000 and *Hyaloperonospora arabidopsidis*. Furthermore, a recent study by Gordon *et al*. (2015) identified a partial resistance to *C. purpurea* associated with the DELLA mutant, semi-dwarfing alleles, *Rht-1Bb* and *Rht-1Db.*

The complexity of plant immunity was evident from the variety of genes, with known roles in plant defence that were differentially expressed in response to *C. purpurea* infection. All classes of defence genes, except endocytosis/exocytosis related genes, were up-regulated in stigma tissue at 24H. Many RPK and NBS-LRR class proteins, which are known to be involved in PAMP and effector recognition, were up-regulated early in *C. purpurea* infection (DeYoung & Innes, 2007).

Many NBS-LRR proteins detect effector molecules produced by the pathogen, either directly, by binding with the effector protein, or indirectly through the modifications these effectors have on host target proteins (DeYoung & Innes, 2006). The indirect mechanisms tend

to operate by the NBS-LRR proteins' binding to key host targets of the pathogen, and trigger defence when those targets are altered in response to infection (DeYoung & Innes, 2006). The up-regulation of these NBS-LRR proteins at 24H in the transmitting and base tissues, before the arrival of fungal hyphae in these tissues, suggests that these genes are induced in response to a pathogen, or plant-derived, mobile signal. The up-regulation of a wide variety of NBS-LRR proteins early during *C. purpurea* infection could indicate an attempt by the host plant to increase its recognition capacity to *C. purpurea* effectors. The *Arabidopsis* R-gene, *RPP13,* has been shown to confer resistance to five different isolates of the biotrophic oomycete, *Hyaloperonospora arabidopsidis* (Allen *et al*., 2004). These NBS-LRR proteins could then activate specific defence reactions, such as cell wall modification, secondary metabolite production, and even programmed cell death, in order to counteract pathogen attack. Homologues of known NBS-LRR resistance (R-) genes were identified, including *RGA2* and *RGA3*, which are required for resistance to leaf rust (*Puccinia triticina*) in tetraploid and hexaploid wheat (Loutre *et al*., 2009). Homologues of the R-genes *RPM1* and *RPS2* were both found to be significantly induced in response to the biotrophic fungus *Exobasidium vexans* that causes blister blight in tea (Jayaswall *et al*., 2016).

In addition to the specific NBS-LRR class of RPK proteins, other RPK, namely serine/threonine kinases (STK) and cysteine-rich receptor-like protein kinases (CRK), were found to be strongly induced throughout *C. purpurea* infection. Contrary to the NBS-LRR proteins, these RPKs exhibited up-regulated that were sustained at the late time-points of *C. purpurea* infection. STK are membrane proteins that form a first line of defence, recognising pathogen-associated molecular patterns (PAMP), which can then lead to the activation of the MAPK signaling cascade and ultimately other defence-related genes (Afzal *et al*., 2008). Ma *et al*. (2018) similarly observed strong up-regulation of genes encoding receptor-like kinases and pathogenesis-related proteins during the early, asymptomatic phase of *Septoria tritici* blotch (STB) infection on wheat. CRK are a sub-member of receptor-like kinases and many genes belonging to this family of proteins have been found to be induced by a variety of pathogens. One such CRK was found to be induced in barley in response to the biotrophic fungus *Blumeria graminis f. sp. hordei*, which causes barley powdery mildew (Collinge *et al*., 2002). Taken together, these results would suggest that wheat recognises *C. purpurea* through the activation of multiple receptor proteins, and is then able to discharge an array of defence responses.

A common, early response upon pathogen recognition is cell wall modification. Cell wall defensive appositions called papillae are formed beneath the attempted pathogen penetration sites of many biotrophic and hemi-biotrophic pathogens (Pecenkova *et al*., 2011). This process has been shown to be facilitated through the actions of genes such as SNARE proteins, syntaxins and the exocyst complex component EXO70B. Genetic screenings for mutants which allowed increased penetration by *B. graminis* identified the crucial role of syntaxins and SNARE proteins in cell wall modification in response to attempted fungal penetration (Collins *et al*., 2003). Homologues of these genes were up-regulated in wheat during the early stages of *C. purpurea* infection, although to the best of our knowledge papillae have not been observed in cereal- *C. purpurea* interactions.

The observed induction of WRKY and MYB transcription factors during the early stages of *C. purpurea* infection further points towards the reprogramming of the wheat transcriptome. WRKY transcription factors participate in regulating defence gene expression at various levels, activating the production of antimicrobial compounds and triggering cell death, while MYB transcription factors have also been found to be involved in the induction of the hypersensitive cell death program (Pandey & Somssich, 2009; Ambawat *et al*., 2013). The effects of these transcription factors were evident within our dataset from the induction of genes with antifungal action, roles in cell wall modification and programmed cell death, and the generation of secondary metabolites. The observed early induction of antifungal compounds, such as chitinases and defensins, known inhibiters of fungal growth (De Coninck *et al*., 2013; Collinge *et al*., 1993), has also been observed during infection of rye by *C. purpurea* (Oeser *et al*., 2017).

Overall, our data suggests that upon infection by *C. purpurea* the host wheat plant activates several defence mechanisms at early stages of infection. In addition to well characterised defence-related genes, genes involved in wheat hormonal homeostasis and signaling pathways were induced. These hormone-associated genes may be up-regulated as part of a defence response on the part of the host, but equally could be induced by *C. purpurea* to create an environment suitable for *C. purpurea* colonisation and reproduction, and to disrupt the host's defence responses. The evidence for a long-distance mobile signal triggering differential genes expression at the base of the ovary, long before the arrival of the pathogen, again could be derived from *C. purpurea*, sent to prepare the basal tissue for arrival of fungal hyphae, or be plant-derived and sent from the infected stigma to trigger a systemic defence reaction.

2.6 Further work

Further research would be required to clarify the individual expression patterns of prominent DEG, relate these changes in gene expression to hormonal levels, and to the stage of *C. purpurea* development in wheat ovaries. A qRT-PCR analysis of key hormonal and defence-related genes should be carried out in order to verify the observed differential genes expression patterns seen in this study. A number of hormones have been quantified during *C. purpurea* infection in Chapter 3. However, the hormone quantification in Chapter 3 was that of the endogenous hormone levels at 3 days after inoculation. In order to gain a better insight into the relationship between hormone levels and gene expression a time-course experiment should be carried out, relating endogenous hormone levels as the stages of *C. purpurea* infection.

Chapter 3: Gibberellic Acid (GA) and its Role in *Claviceps purpurea* Infection of Wheat

3.1 Abstract

Currently, no complete resistance against the fungal pathogen *Claviceps purpurea* is known. Partial resistance to ergot has previously been shown to co-locate with the wheat dwarfing genes *Rht-B1b* and *Rht-D1b*, implicating a potential role of GA in *C. purpurea* infection. In this chapter we explore the role of GA, along with the status of other endogenous hormones, during *C. purpurea* infection. For the purposes of this study, a number of near-isogenic lines (NILs) of the wheat (*Triticum aestivum*) varieties Mercia and Maris Huntsman that differed in alleles present at the Reduced height (*Rht*) loci on chromosome 4B and 4D were inoculated with the fungus. Honeydew and sclerotia measurements were taken to assess infection success.

In general, more honeydew was produced by the wild-type (WT), parental wheat varieties Mercia and Maris Huntsman than the NILs carrying the mutant alleles at the *Rht* loci *Rht-B1* and *Rht-D1*. Sclerotia produced on Maris Huntsman were found to be significantly bigger than the sclerotia produced on the NILs carrying *Rht-B1c* or *Rht-D1b*, however a consistent, statistically significant reduction in sclerotia size was not seen in the Mercia NILs.

Inoculation with *C. purpurea* resulted in elevated levels of the bioactive gibberellic acid (GA_4), the auxin indole-3-acetic acid (IAA) and the cytokinin dihydrozeatin (DHZ). GA_4, IAA and DHZ showed very similar induction patterns across the Mercia NILs as a result of infection with *C. purpurea*, with levels of all three hormones being particularly high in Mercia WT, and *Rht-B1b* and *Rht-D1b* NILs. GA_4 and IAA also displayed near identical patterns of induction in the Maris Huntsman NILs. While *C. purpurea* infection resulted in lower levels of jasmonic acid (JA) in Mercia and Maris Huntsman WT, no consistent effect of infection on JA levels was seen across the *Rht*-mutant NILs. Inoculation with *C. purpurea* did not significantly alter salicylic acid (SA) levels, or the levels of the cytokinin types trans-zeatin (tZ) or N^6-(2-isopentenyl) adenine (iP).

Taken together, these results would indicate that GA acts to increase susceptibility of wheat to the fungus *C. purpurea* through degrading the DELLA proteins.

3.2 Introduction

Gibberellins, also known as Gibberellic acid (GA), are considered phytohormones but were first identified in the rice fungal pathogen *Gibberella fujikuroi* (formally known as *Fusarium fujikuroi*) which causes supra-optimal elongation of seedlings and reduced grain yield. While GAs were originally thought to be unique to fungi, it is now known that they are found in plants, where they form a group that encompasses more than 136 structurally similar compounds (Sponsel, 2018). Out of all these compounds only a small number are considered to be bioactive, and therefore able to play a role in aspects of plant growth and development. Nevertheless, other GAs carryout significant functions, acting as precursors of the bioactive GAs, or as their inactivation factors or metabolites (Sponsel, 2018). Overall, plant GAs have been found to stimulate organ growth by increasing cell elongation and, in certain circumstances, cell division (Hedden & Thomas, 2012). In addition, GAs play important roles in several developmental switches, including seed dormancy and germination, juvenile and adult growth phases, and vegetative and reproductive development (Hedden & Thomas, 2012). Furthermore, GAs are important for fertility, being required for the release and germination of pollen, as well as, for pollen tube growth (Hedden & Thomas, 2012).

3.2.1 GA biosynthesis and inactivation in higher plants

GA biosynthesis occurs via the methylerythritol phosphate pathway (Kasahara *et al*., 2002) which is summarized in Figure 3.1. The biosynthetic pathway is initiated when *ent*-kaurene is produced from *trans*-geranylgeranyl diphosphate (GGPP) in proplastids (Aach *et al*,. 1997) via a two-step process (the intermediate being *ent*-copalyl diphosphate) which is catalyzed by the enzymes *ent*-copalyl diphosphate synthase (CPS) and *ent*-kaurene synthase (KS) (MacMillan, 1999). While *ent*-kaurene is the first product of the pathway it has been found not to play a major role in the final amount of bioactive GAs, as the regulation of their biosynthesis occurs at later stages of the biosynthetic pathway (Fleet *et al*., 2003). Overall, the conversion of *ent*-kaurene into the final, bioactive GAs involves multiple steps that depend on the functions of membrane-associated cytochrome P450 mono-oxygenases (P450s) and soluble (2-oxoglutarate-dependent dioxygenases (ODDs) (Hedden & Thomas, 2012). Specifically, *ent*-kaurene gets transformed into *ent*-kaurenoic acid in three steps of repeated hydroxylations

mediated by the mono-oxygenase *ent*-kaurene oxidase (KO; Morrone *et al*., 2010). Subsequently, the other mono-oxygenase *ent*-kaurenoic acid oxidase (KAO) facilitates the three-steps that lead to the oxidation of *ent*-kaurenoic acid to GA_{12} (Hedden, 1997) which has been found to be the common precursor of all plant GAs (Hedden & Phillips, 2000). The next step in the biosynthetic pathway represents a branching point wherein GA_{12} either undergoes oxidation on C-13 via the enzymatic activity of ODD 13-hydroxylase to produce GA_{53} (Sponsel & Hedden, 2010). Finally, through the activities of the two ODDs GA 20-oxidase (GA20ox) and GA 3-oxidase (GA3ox), GA_{12} and GA_{53} are converted in a parallel manner to the bioactive GA_4 and $GA_{1,}$ respectively (Hedden, 2018). These are multi-step processes where GA20ox acts first to oxidise GA_{12} and GA_{53} into GA_9 and GA_{20} respectively. GA3ox is then responsible for the final step of 3,β-hydroxylation of GA_9 and GA_{20} to the bioactive GA_4 and GA_1 respectively (Hedden, 1997).

The amounts of bioactive GAs are tightly regulated in plants, which have the ability to alter their GA content rapidly in response to biotic and abiotic stimuli (Hedden & Thomas, 2012). Similarly to other hormones, a number inactivation processes have been identified for GAs in order for plants to maintain homeostasis, or when a reduction of GA concentration is needed. The most common of these mechanisms is the 2β-hydroxylation of bioactive GAs via the enzymatic activity of GA 2-oxidases (GA2oxs; Thomas *et al*., 1999). Another example of a GA inactivation mechanism is that of epoxidation. It was found in rice that GAs are converted into their 16α, 17-epoxides by a cytochrome P450 mono-oxygenase (CYP714D1) causing them to become inactive (Zhu *et al*., 2006).

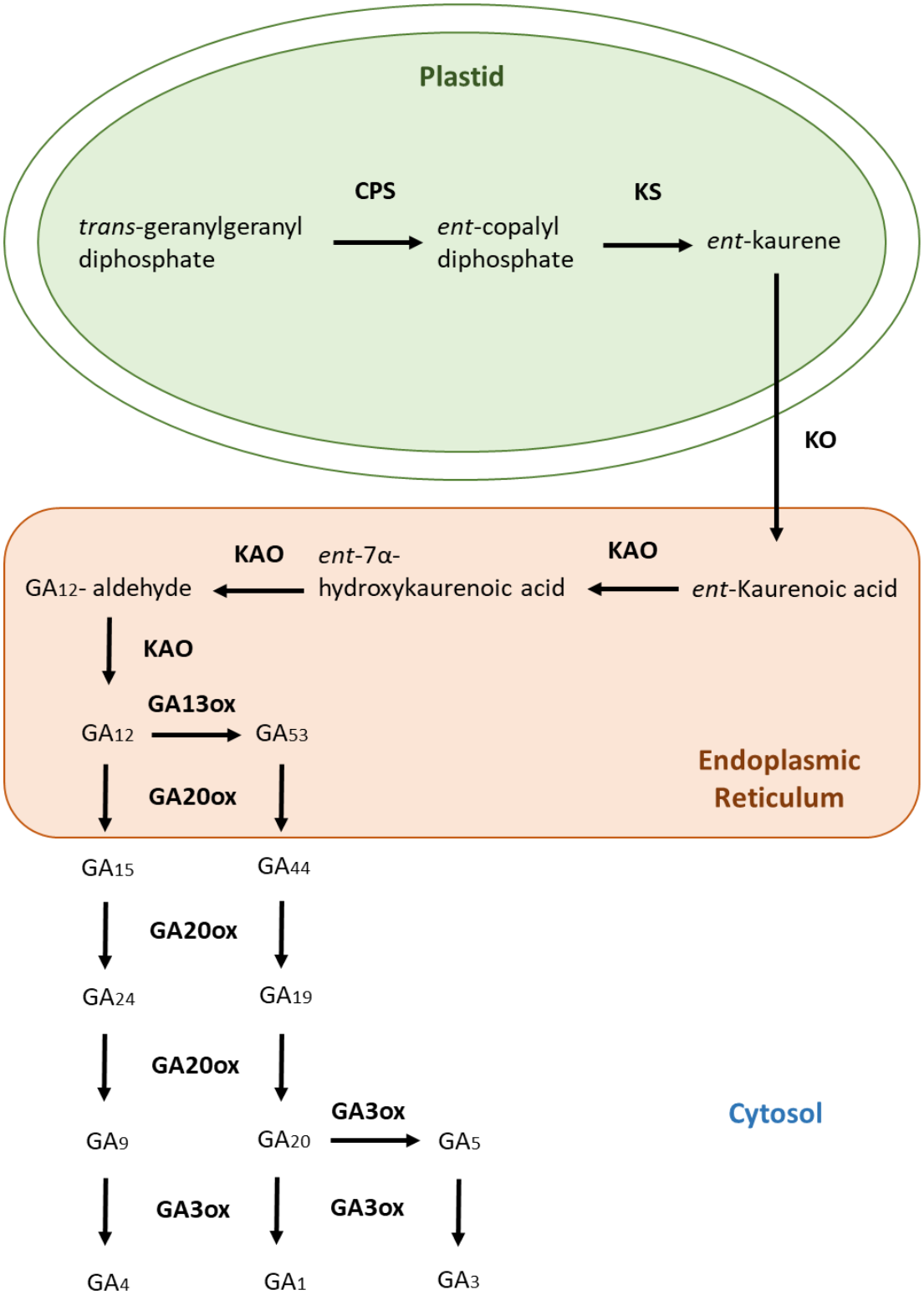

Figure 3.1: The GA-biosynthetic pathway in higher plants from *trans*-geranylgeranyl diphosphate to GA_1, GA_3 and GA_4.

3.2.2 GA biosynthesis in fungi

As was previously mentioned, GAs were first identified in the fungus *G. fujikuroi*. Since then, GAs have been identified in many fungi and bacteria (Salazar-Cerezo *et al*., 2018). Despite the fact that plants and fungi produce structurally identical GAs, major differences with regards to their biosynthesis suggest that their biosynthetic pathways evolved independently (Tudzynski, 2005). Specifically, the first two steps of the biosynthetic pathway that result in the formation of *ent*-kaurene from GGDP require two separate enzymes (CPS and KS) in higher plants but only one bifunctional terpene cyclase (CPS/KS) in fungi (Kawaide *et al*., 1997; Tudzynski et al., 1998). The steps of GA biosynthesis involving the sequential oxidations of *ent*-kaurene, leading ultimately to the formation of the GA_{12}-aldehyde are identical between plants and fungi (Tudzynski, 2005). However, after GA_{12}-aldehyde, at the stage where hydroxyl groups are added, the pathways between plants and fungi diverge. In fungi, GA_{12}-aldehyde is 3β-hydroxylated to GA_{14}-aldehyde and 13-hydroxylation occurs only in the final step to form GA_3 from GA_7, whereas in plants the final step is the 3β-hydroxylation of GA_9 and GA_{20} to GA_4 and GA_1 (Salazar-Cerezo *et al*., 2018; Tudzynski, 2005).

In addition to the biochemical reactions taking place during GA biosynthesis, the genes encoding the enzymes facilitating these reactions also differ significantly between plants and fungi. In fungi the genes for GA biosynthesis can be found in a cluster of 7 genes which include a pathway-specific geranyl-geranyl diphosphate synthase gene (ggs2), the bifunctional *ent*-copalyl diphosphate synthase/*ent*-kaurene synthase (*cps/ks*), a desaturase (2-oxoglutarate-dependent dioxygenase or DES) that converts GA_4 to GA_7 (Bhattacharya *et al*., 2012) and three cytochrome P450 monooxygenases (P450-1, P450-2 y P450-3) (Tudzynski, 2005).

3.2.3 GA signalling

During the past decade, most of the components of the GA signalling pathway have been identified. According to the current signalling model the DELLA proteins act by repressing plant growth while GA promotes it, GA being required for DELLA protein ubiquitin-mediated degradation (Achard & Genschik, 2009). In the presence of GA the GA receptor gibberellin insensitive dwarf1 (GID1) is able to bind to the DELLA proteins (a class of nuclear growth-repressing proteins) resulting in the ubiquitination and degradation of the

DELLAs through the 26S proteasome SCF complex (Gao *et al*., 2011). The DELLA proteins also appear to be primarily responsible for most of the GA-signalling dependent processes that take place in plants (Gao *et al*., 2011).

DELLAs are able to regulate gene expression by interacting with a great number of regulatory proteins (Daviere & Achard, 2013). For instance, DELLAs can regulate hypocotyl elongation by interacting with transcription factors such as PHYTOCHROME INTERACTING FACTORS (PIFs) (de Lucas *et al*., 2008) and BRASSINAZOLE RESISTANT1 (BZR1) (Gallego-Bartolomé *et al*., 2012), blocking their DNA-binding capacity (de Lucas *et al*., 2008). Furthermore, DELLAs have been found to act as coactivators, interacting with other transcription factors to activate the expression of downstream genes (Daviere & Achard, 2013).

3.2.4 GA role in plant infection

GAs have been found to play particularly complex roles in relation to plant defence by acting as both positive and negative regulators of disease resistance through intervention at multiple levels (De Bruyne *et al*., 2014). In some cases GAs have been found to promote the development of disease symptoms, while in others they are required for the induction of defence responses and plant immunity. Navarro *et al*. (2008) observed in *Arabidopsis* a role for DELLAs in resistance to the necrotrophic fungus *Alternaria brassicola*, but in susceptibility to the hemibiotrophic pathogen *P. syringae*. They suggested that GAs promote resistance to biotrophs and susceptibility to necrotrophs through the degradation of DELLAs, thereby changing the balance of SA/JA signaling during plant immunity. It is hypothesised that DELLAs bind to the JA suppressor JAZ1 preventing it from interacting with MYC2, a key transcriptional activator of JA responses, allowing MYC2 activation of JA-responsive target genes (Hou *et al*., 2010). The introduction of GA degrades DELLA, freeing JAZ1 to interact with and inhibit MYC2, leading to suppression of JA signaling and enhancement of resistance to fungi with a biotrophic growth phase. Similar observation were reported in wheat and barley (Saville *et al*., 2012). In wheat the *Rht* semi-dwarfing alleles encode for mutant DELLA proteins that are not degraded by GA, but continue to suppress plant growth producing the semi-dwarf phenotypes. Saville et al. (2012) observed that the wheat *Rht* (*Rht-B1b*, *Rht-D1b*, *Rht-B1c* and *Rht-D1c*) and the barley *Sln1* gain of function (GoF) mutants conferred increased

susceptibility to biotrophic pathogens and increased resistance to necrotrophic pathogens. They also found that the increased susceptibility to biotrophs was buffered in single *Rht* mutants in wheat due to polyploidy. The constant presence of Rht DELLA would therefore be hypothesized to prevent inhibition of JA-signaling through the *TaJAZ1* pathway, enhancing JA pathways and susceptibility to biotrophs such as *C. purpurea*. In contrast, Gordon *et al*., 2015 observed that resistance to the biotrophic fungus *C. purpurea* co-located with semi-dwarfing alleles at the *Rht* loci- *Rht-1B* and *Rht-1D.* Therefore, it could be hypothesized that the *Rht* della mutant proteins may also be unable to bind to TaJAZ1, resulting in constitutive suppression of TaMYC2 and JA signaling. In addition, GAs have also been found to lower resistance (not increase resistance as hypothesized in Arabidopsis) to the hemibiotrophic pathogens *Magnaporthe oryzae* and *Xanthomonas oryzae pv. oryzae* in rice (Yang et al., 2008; Qin et al., 2013).

GAs and DELLAs are potentially able to influence plant immunity through many different mechanisms. In addition to changing the balance of SA/JA signaling during plant immunity, Achard *et al*., 2008 showed that DELLAs are able to modulate ROS production by inducing genes involved in ROS detoxification, and thereby reduce ROS levels and inhibit cell death. This DELLA-mediated inhibition of cell death contributed to resistance towards necrotrophic pathogens such as *Botrytis cinerea* which derive nutrients from dead cell tissues (Achard *et al*., 2008). Furthermore, the interaction that exists between SA and ROS suggests that the DELLA-mediated repression of SA signaling results partially from the decrease in ROS levels (Grant & Jones, 2009).

3.2.5 GA levels and other hormones

GAs rarely act alone, but form part of a complex system that includes interactions between multiple hormones. These interactions can involve changes in hormone biosynthesis or in hormone signalling transduction (Joss *et al*., 2018).With regards to interactions that effect the levels of GAs, each hormone is specific. For example, auxin has been found to strongly induce the synthesis of bioactive GAs in a range of plant species, including barley (Wolbang *et al*., 2004), Arabidopsis (Frigerio *et al*., 2006) and rice, (Yin *et al*., 2007) by degrading Aux/IAA proteins and, in turn, leading to the up-regulation of GA biosynthesis genes GA 20-oxidases and GA 3-oxidases, and the down-regulation of deactivating genes GA 2-oxidases

(Joss *et al*., 2018). In contrast, ethylene signalling has been found to negatively affect GA biosynthesis (Joss *et al*., 2018) while, mutualistically, GA has been found to inhibit ethylene production. Ferguson *et al*., 2011 observed elevated ethylene production in a GA-deficient mutant of pea. Cytokinins have also been implicated in the negative regulation of GA levels, stimulating the expression of the GA deactivating genes encoding GA 2-oxidases (Jasinski *et al*., 2005).

3.2.6 The reduced height alleles of wheat

The introduction of the *Reduced height* (*Rht*) mutant genes into wheat varieties played a significant role in breeding for higher wheat yields iduring the Green Revolution (Hedden, 2003). These dwarfing alleles result in higher yields by preventing stem elongation, thereby improving lodging resistance, as well as by increasing the partitioning of photosynthate in the grain and increasing the number of grains (Youssefian *et al*., 1992). In wheat, the most widely used *Rht* alleles are the *Rht-B1b* and *Rht-D1b* semi-dwarfing alleles, found on chromosomes 4B and 4D respectively, and are now found in the majority of varieties cultivated worldwide (Evans, 1998). Both of these alleles carry mutations in the *Rht-1* coding region that result in the addition of stop codons within the N-terminal 'DELLA' domain (Phillips, 2018), and in both alleles produce truncated DELLA proteins that are unable to interact with GID1 in the presence or absence of GA (Pearce *et al.*, 2011).

In addition to *Rht-B1b* and *Rht-D1b*, other *Rht* alleles have been identified that affect height, including *Rht-B1c* and *Rht-D1c*. However, these alleles have not been used in breeding as they negatively affect yield (Flintham *et al.*, 1997). *Rht-B1c* and *Rht-D1c* confer a severe dwarf phenotype but differ in their mutations (Phillips, 2018). *Rht-D1c* carries the same stop codon as *Rht-D1b* but has been found to have a higher expression due to a higher copy number, and thus results in a more severe dwarfing phenotype (Pearce *et al.*, 2011). *Rht-B1c* contains the novel mutation of a 2-kbp retrotransposon insertion that results in an in-frame, 90-bp insertion in the region encoding the 'DELLA' domain (Pearce *et al.*, 2011). The translation product is similarly unable to interact with the GID1 protein (Pearce *et al.*, 2011). These *Rht* mutant alleles are all dominant, GA-insensitive alleles which have been suggested to accumulate DELLA proteins at much higher levels than their wild-type counterparts (Peng *et al*., 1999). In addition, it has been shown that the *Rht-B1c* severe dwarf allele has highly

elevated levels of bioactive GAs, and that both *Rht-B1c* dwarf, and *Rht-B1b* and *Rht-D1b* semi-dwarf lines exhibit reduced responses to exogenous GA (Phillips, 2018).

Other dwarfing genes identified include *Rht8* and *Rht12. Rht8* represents a semi-dwarfing gene, found on the short arm of chromosome 2D (Korzun *et al*.,1998), which unlike the others is not defective in GA biosynthesis or signaling, but rather exhibits reduced sensitivity to brassinosteroids (Gasperini *et al*., 2012). The phenotype produced by *Rht8* is the result of reduced cell elongation (Gasperini *et al*., 2012). *Rht12* has been found to be located on the long arm of chromosome 5A, however its role, if any, in GA biosynthesis or signaling remains unknown (Chen *et al*., 2013).

3.2.7 Aims

The findings of Gordon *et al*. (2015) that *C. purpurea* resistance co-located with the semi-dwarfing alleles *Rht-1B* and *Rht-1D,* as well as the results presented in Chapter 2, where significant changes in wheat GA biosynthesis gene transcription were observed in response to infection with *C. purpurea,* suggested a potential role of GAs and DELLAs in the interaction between wheat and *C. purpurea*. The main aim of this chapter was to further explore the relationship between GAs and DELLAs in the infection of wheat with *C. purpurea*. Specifically, the results presented here address two aims:

Firstly, to determine whether alterations to GA signaling contribute to resistance (or susceptibility) of wheat to *C. purpurea,* we assessed *C. purpurea* infection (i.e. the level of honeydew production and size of sclerotia) in wheat lines with mutations in GA signaling pathways. Near-isogenic lines (NILs) of wheat (*Triticum aestivum*) varieties Mercia and Maris Huntsman differing in alleles at the Reduced height (*Rht*) loci on chromosome 4B and 4D were used (Table 3.1). Specifically, the semi-dwarf alleles *Rht-B1b* and *Rht-D1b,* and the severe dwarf alleles *Rht-B1c* and *Rht-D1c* were used. Furthermore, two additional reduced-height NILs of Mercia carrying the GA-sensitive alleles *Rht8* (chromosome 2D) and *Rht12* (chromosome 5A) were also included. Finally, the wild-type (*rht-tall*) parental lines carrying GA-sensitive alleles at all three homoeologous loci (Flintham *et al*., 1997) were used as controls.

While the involvement of GA during *C. purpurea* infection was suggested by the differential expression analysis in Chapter 2, the genes that were found to be up- and down-regulated during infection provided an incomplete picture of events. Therefore, the second aim of this chapter was to determine whether GA levels were altered in ovule tissue by *C. purpurea* infection. We quantified the levels of bioactive GAs, along with those of auxin, SA, JA, and cytokinins, in *C. purpurea* infected and control materials.

3.3 Materials and methods

3.3.1 Plant material

C. purpurea infection was examined in NILs of the wheat varieties Mercia and Maris Huntsman differing in alleles at the *Rht* loci on chromosome 4B and 4D (Table 3.1). Specifically, the semi-dwarf alleles *Rht-B1b* and *Rht-D1b,* and the severe dwarf alleles *Rht-B1c* and *Rht-D1c* were used. Furthermore, the NILs of wheat variety Mercia carrying the GA-sensitive alleles *Rht8* (chromosome 2D) and *Rht12* (chromosome 5A) were also included.

Table 3.1: List of near-isogenic lines of wheat (*Triticum aestivum*) carrying *Rht* alleles.

***Rht* alleles in Wheat NILs**	**Background**	**Phenotype**	**GA Sensitivity**
rht-tall	Mercia	wild-type	sensitive
	Maris Huntsman	wild-type	sensitive
Rht -B1b	Mercia	Semi-dwarf	insensitive
Rht -B1c	Mercia	Severe dwarf	insensitive
	Maris Huntsman	Severe dwarf	insensitive
Rht -D1b	Mercia	Semi-dwarf	insensitive
	Maris Huntsman	Semi-dwarf	insensitive
Rht -D1c	Mercia	Severe dwarf	insensitive
Rht12	Mercia	Semi-dwarf	sensitive
Rht8	Mercia	Semi-dwarf	sensitive

3.3.2 *Claviceps purpurea* inoculations and infection assessments

3.3.2.1 Inoculations

C. purpurea inoculations were undertaken as described in Chapter 2. Conidia were collected from fresh honeydew and diluted with water to a concentration of 6×10^6 conidia/ml. Ten florets per ear, on 10 primary tillers (i.e. the first tiller formed on 10 plants), of each wheat line, were hand-inoculated with the conidia suspension using a hypodermic syringe as described in Gordon et al. (2015). The florets were inoculated just before anthesis, when the stigmas were fluffy but no pollen had been released (Zadoks Growth Stage 59; Gordon et al., 2015).

3.3.2.2 Honeydew measurements

NIL honeydew measurements were taken at 14dpi in order to determine whether infection has been successful and to assess the severity of the infection, as measured by the quantity of honeydew produced. The levels of honeydew production were scored following the stages outlined in Figure 3.2.

Figure 3.2: Honeydew scores are recorded 14 days after inoculation and follow a scale of 1 to 4. (1) No honeydew is produced; (2) Honeydew is confined within the glumes; (3) Small droplets of honeydew are exuded from the floret; (4) Large droplets of honeydew are exuded from the florets, often running down the stem.

3.3.2.3 Sclerotia and grain measurements

In order to examine the level of resistance or susceptibility to *C. pupurea*, the size of sclerotia formed within the inoculated florets of each NIL were measured. The size of the seed produced by each NIL was also measured in order to determine whether previous observations, showing differences in grain size produced by these lines, could be replicated, and whether there was a relationship between the size of wheat seed and the size of sclerotia. Seed was collected from the primary tillers of control, uninfected plants, which had been covered prior to flowering in order to avoid any cross fertilization between lines. The size of ergot sclerotia were analysed using the NIAB ergot size 0–7 scale (Figure 3.3). Sclerotia size (i.e. length and width) and grain size, as well as their weights were also determined using a Marvin digital seed analyser (GTA Sensorik GmbH, Lindenstraße 63 D-17033 Neubrandenburg, Germany).

Sclerotia Sizing Scale for *Claviceps purpurea*

Scale	0	1	2	3	4	5	6	7
Example sclerotia								
Length range / mm	0	≥ 1.5	1.5 - 3	3 – 4.5	4.5 – 7	7 – 9	9 - 11	≥ 11
Width range / mm	0	≥ 1.5	1.5 - 2	≥ 2.5	≥ 2.5	≥ 3	≥ 4	> 4
Further comments	Infection but no sclerotia formed. No seed set	Sclerotia that are the size of an ovary – usually round	Sclerotia that are larger than the size of an ovary – usually oblong	Sclerotia that are smaller than a seed	Sclerotia that are approx the size of a wheat seed	Sclerotia that completely fill the seed cavity	Sclerotia visible before extracting from ear	Massive. More than half is extending from the glumes

Figure 3.3: The NIAB ergot sclerotia sizing scale.

3.3.3 Hormone quantification

For the quantification of endogenous GA, IAA, JA, SA and cytokinin (CKs) levels, wheat ovules from three biological replicates (each replicate was made up of three wheat ears of inoculated or non-inoculated control florets), were harvested for each of the mutant and wild type lines at 3dai. Each ovule sample was lyophilized and then ground-up using a Geno/Grinder- automated high-throughput plant & animal tissue homogenizer and cell lyser, in order to stabilise the samples for storage and transportation. Each of the samples (50 mg dry weight) were sent to the Institute for Plant Molecular and Cell Biology (IBMCP) in Valencia for analysis of hormone levels.

The ground tissue (about 50 mg dry weight) was suspended in 80% methanol-1% acetic acid containing internal standards and mixed by shaking for one hour at 4ºC. The extract was kept a -20ºC overnight, centrifuged and the supernatant dried in a vacuum evaporator. The dry pellet residue was dissolved in 1% acetic acid and passed through a reverse phase column (HLB Oasis 30 mg, Waters), as described in Seo et al. (2011). For CKs, the extracts were additionally passed through an Oasis MCX (cationic exchange) cartridge and eluted with 60% methanol-5% NH4OH to obtain the basic fraction containing CKs. To recover the acid fraction, the MCX cartridge was further eluted with methanol. The final residues were dried and dissolved in 5% acetonitrile-1% acetic acid. Hormones were separated by UHPLC using a reverse Accucore C18 column (2.6 µm, 100 mm length; Thermo Fisher Scientific) with an acetonitrile gradient containing 0.05% acetic acid, at 400 µL/min. For CKs, the acetonitrile gradient was 2 to 25% over 13 min. For GAs, IAA, SA and JA the gradient was 2 to 55% acetonitrile over 21 min. The hormones were analyzed with a Q-Exactive mass spectrometer (Orbitrap detector; ThermoFisher Scientific) by targeted Selected Ion Monitoring (tSIM; capillary temperature 300ºC, S-lens RF level 70, resolution 70.000) and electrospray ionization (spray voltage 3.0 kV, heater temperature 150ºC, sheath gas flow rate 40 µL/min, auxiliary gas flow rate 10 µL/min) in negative mode for acidic hormones or positive mode for CKs. The concentration of hormones in the extracts were determined using embedded calibration curves and the Xcalibur 4.0 and TraceFinder 4.1 SP1 programs. The internal standards for quantification of each of the different plant hormones were the deuterium-labelled hormones, except for JA, for which the compound dhJA was used (purchased from OlChemim Ltd, Olomouc, Czech Republic).

3.3.4 Statistical analyses

All statistical analyses were performed using Genstat v.16. For the data relating to honeydew and sclerotia measurements, significant variation between lines was examined used a one way-ANOVA approach, followed by a post-hoc Tukey's test where appropriate. The data relating to grain were examined using a modified ANOVA approach, General Linear Regression. The model applied was replicates + genotype. For the measurements of JA, SA, DHZ and tZ, variation between lines and treatment (inoculated or un-inoculated) were examined using a two way-ANOVA approach, followed by a post-hoc Tukey's test where appropriate. The data relating to GA_1, GA_4, auxin (IAA) and iP did not satisfy the normality test and were therefore examined using a modified ANOVA approach, General Linear Regression.

3.4 Results

3.4.1 Variation in honeydew production between different *Rht*-NILs.

Honeydew measurements were taken at 14dai on the *Rht*-NILs of Mercia and Maris Huntsman (Figures 3.4 and 3.5, respectively). In the Mercia lines honeydew production differed significantly between *Rht*-NILs ($F = 6.05$, $p < 0.001$) in the 2017 expts. Specifically, the *Rht8* line produced significantly more honeydew than the *Rht12*, *Rht-D1c* and *Rht-D1b* lines. No other lines were detected as being significantly different from one another in terms of their honeydew production in 2017. However, in the 2018 expt no significant differences in honeydew production were detected between any of the *Rht*-NILs ($F = 1.43$, $p = 0.237$).

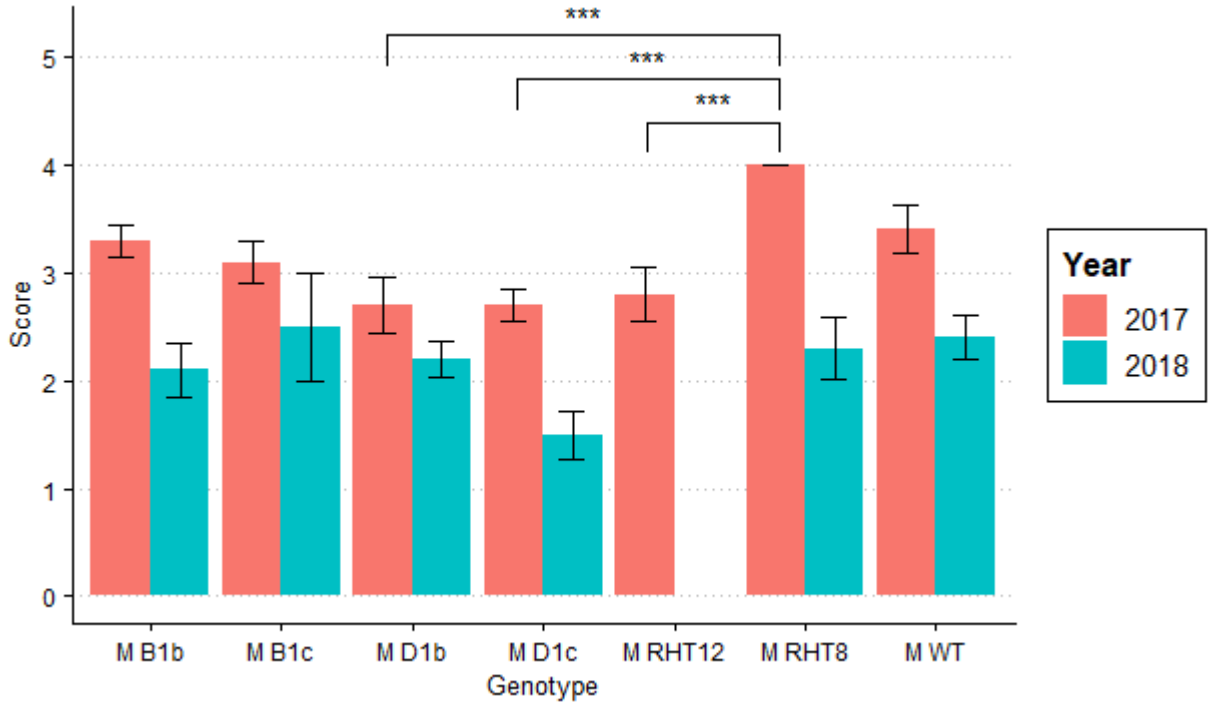

Figure 3.4: Levels of honeydew production in 7 different Rht-NILS of the wheat (*Triticum aestivum*) variety Mercia. Measurements taken in two different expts (2017 and 2018) are shown. The error bars show standard errors. The asterisks indicate significant differences between NILs pairs at a $p < 0.001$. The pairs exhibiting a significant difference (indicated by the brackets) were: *Rht-D1b-Rht8, Rht-D1c-Rht8, Rht12-Rht8.*

The Maris Huntsman NIL for the year 2017 exhibited significant differences in honeydew production between *Rht*-NILs ($F = 24.85$, $p < 0.001$; Figure 3.5). Specifically, *Rht-B1c* was found to produce significantly less honeydew than the *Rht-D1b* and *Rht*-tall (WT) lines. Despite the fact that the WT was observed to have the highest levels of honeydew production, they weren't significantly higher than the levels produced by *Rht-D1b*. Contrary to 2017, and similarly to Mercia, the Maris Huntsman NIL did not exhibit any significant differences in the levels of honeydew produced in the 2018 expt ($F = 2.02$, $p = 0.159$). Moreover in 2018, the *Rht-D1b* line was found to produce slightly lower levels of honeydew than *Rht-B1c*. However, although not statistically significant, the highest honeydew levels were again observed in the WT.

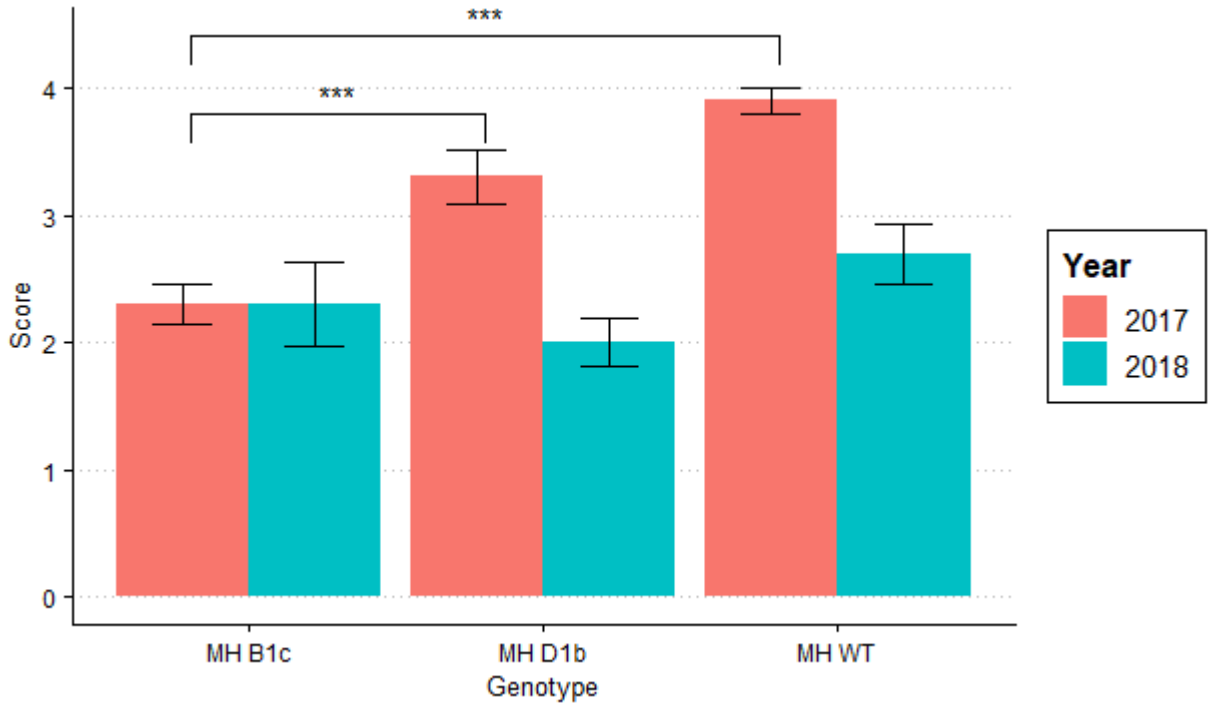

Figure 3.5: Levels of honeydew production in 7 different Rht-NILS of the wheat (*Triticum aestivum*) variety Maris Huntsman. Measurements taken at two different years (2017 and 2018) are shown. The error bars show standard errors. The asterisks indicate significant differences between NILs pairs at a $p < 0.001$. The pairs exhibiting a significant difference (indicated by the brackets) were: *Rht-D1b*-*Rht-B1c*, *Rht-B1c*-WT.

3.4.2 Variation in sclerotia size and weight between different *Rht*-NILs.

In order to determine whether disruption in the GA-DELLA signaling pathway contributes to resistance or susceptibility in wheat to *C. purpurea* the size and weight of sclerotia were measured in inoculated *Rht*-mutant NILs. The size of sclerotia serves as a good indicator of the level of resistance and/or susceptibility to the fungal pathogen *C. pupurea*. After honeydew was collected, sclerotia were allowed to develop in the 7 Merica *Rht*-NILs and in 3 Maris Huntsman *Rht*-NILs. The experiment was conducted twice, once in 2017, and again in 2018. In 2018 sample collection from the Mercia *Rht12* NIL was not possible and therefore no results are reported for this line. No statistical significant differences in sclerotia weight were found between any of the Mercia *Rht*-NILs ($F = 3.06$, $p = 0.011$) in 2017, however statistically significant differences were detected in sclerotia size ($F = 4.22$, $p = 0.001$) (Figure 3.6). While the WT line did not produce significantly larger sclerotia than the mutant lines, it did exhibit larger variations in terms of both weight and size compared to the other lines. *Rht-B1b* was found to produce significantly larger sclerotia than *Rht-D1c*.

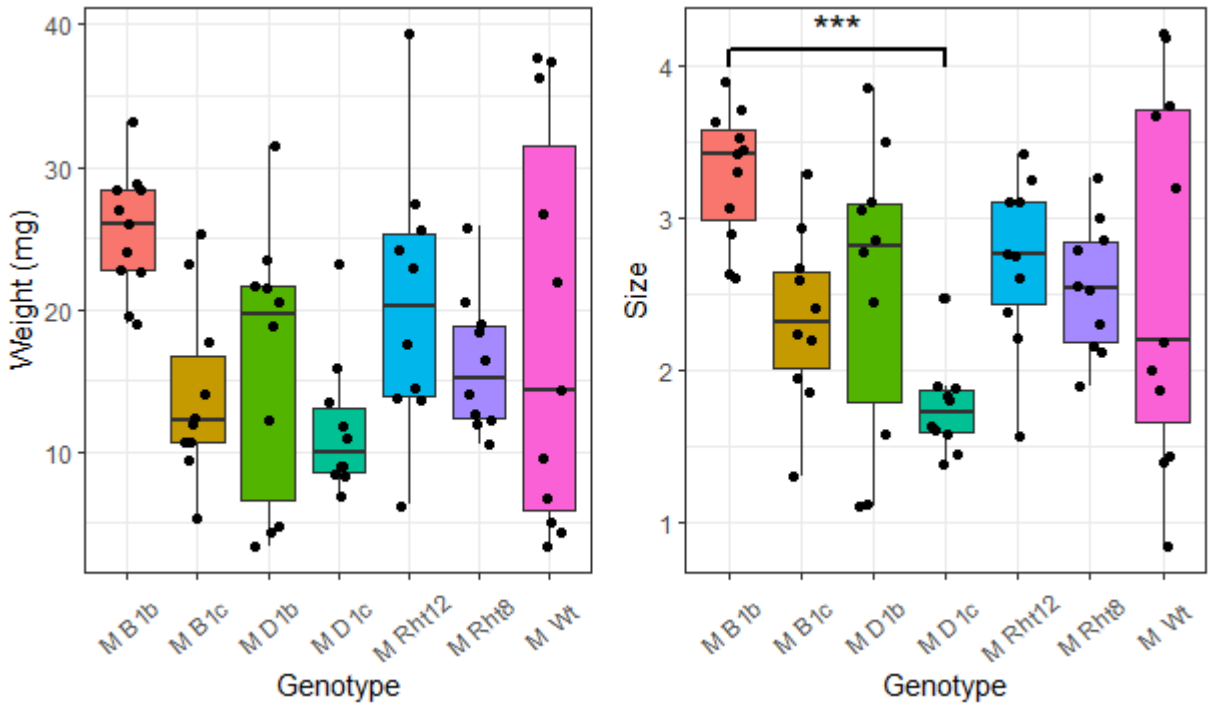

Figure 3.6: Box and whisker plots of mature ergot sclerotia size and weight developed in the wheat (*Triticum aestivum*) variety Mercia on the year 2017. Each data point represents the mean size or weight of sclerotia collected from a single ear. The box defines the upper and lower quartile and shows the median values. The asterisks indicate significant differences between NILs at a $p < 0.001$. The pairs exhibiting a significant difference (indicated by the brackets) were: *Rht-B1b-Rht-D1c*.

In 2017 statistically significant differences between the Maris Huntsman *Rht*-NILs were detected for both sclerotia weight ($F = 21.91$, $p < 0.001$) and size ($F = 26.01$, $p < 0.001$; Figure 3.7). The WT was found to produce significantly heavier sclerotia than both *Rht-D1b* and *Rht-B1c*, and significantly larger sclerotia than *Rht-B1c* (Figure 3.7). While WT sclerotia were not significantly larger than sclerotia produced on *Rht-D1b*, *Rht-D1b* did not produce significantly larger sclerotia than produced on *Rht-1Bc*.

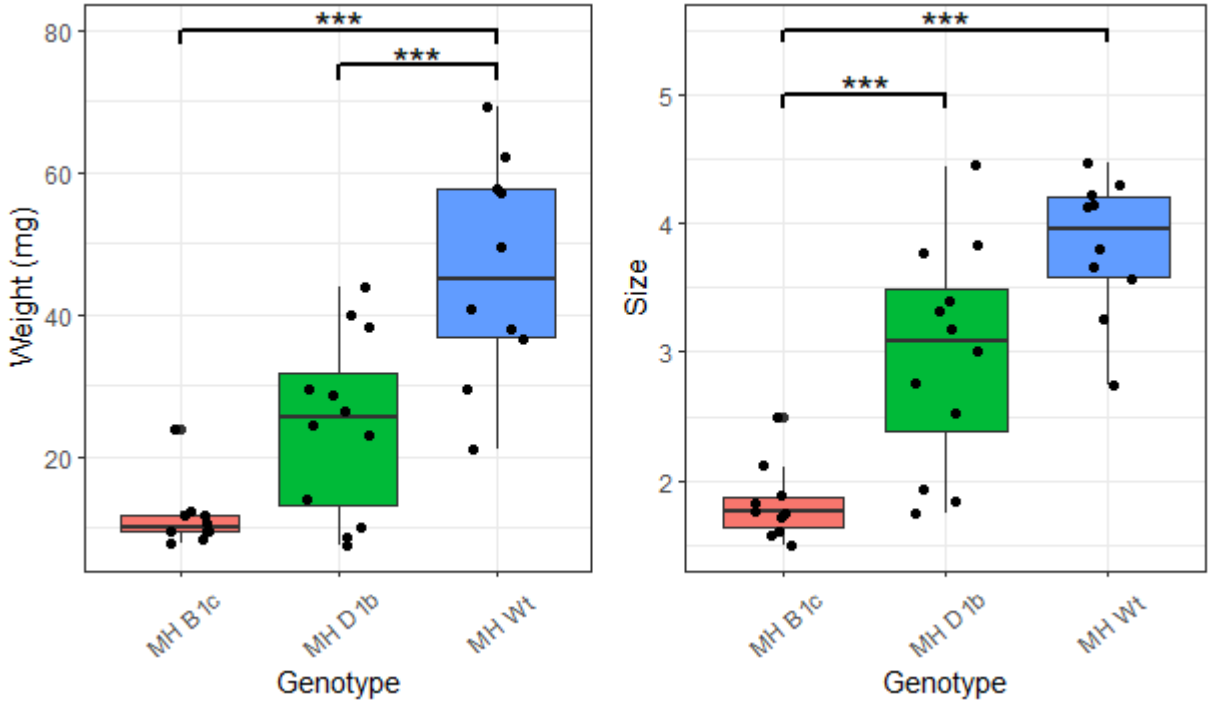

Figure 3.7: Box and whisker plots of mature ergot sclerotia size and weight developed in the wheat (*Triticum aestivum*) variety Maris Huntsman on the year 2017. Each data point represents the mean size or weight of sclerotia collected from a single ear. The box defines the upper and lower quartile and shows the median values. The asterisks indicate significant differences between NILs pairs at a $p < 0.001$. The pairs exhibiting a significant difference (indicated by the brackets) were: For weight: *Rht-D1b*-WT, *Rht-B1c*-WT; For size: *Rht-D1b*-*Rht-B1c*, *Rht-B1c*-WT.

Similar to the previous year, in 2018 the Mercia *Rht*-NILs did not exhibit any significant differences in terms of sclerotia weight ($F = 3.93$, $p = 0.005$) (Figure 3.8), but were found to produce significantly different sclerotia in terms of size ($F = 7.80$, $p < 0.001$; Figure 3.8). Specifically, the tall WT line was found to produce significantly larger sclerotia than the severe-dwarf *Rht-B1c* and *Rht-D1c* lines. In the Maris Huntsman NILs the three lines differed significantly in terms of both sclerotia weight ($F = 16.70$, $p < 0.001$) and size ($F = 13.95$, $p < 0.001$; Figure 3.9). Specifically, *Rht-D1b* and *Rht-B1c* produced significantly lighter sclerotia

compared to WT, but only *Rht-D1b* was significantly smaller to WT. The dwarf lines *Rht-D1b* and *Rht-B1c* did not differ significantly from each other in terms of the weight and size of the sclerotia.

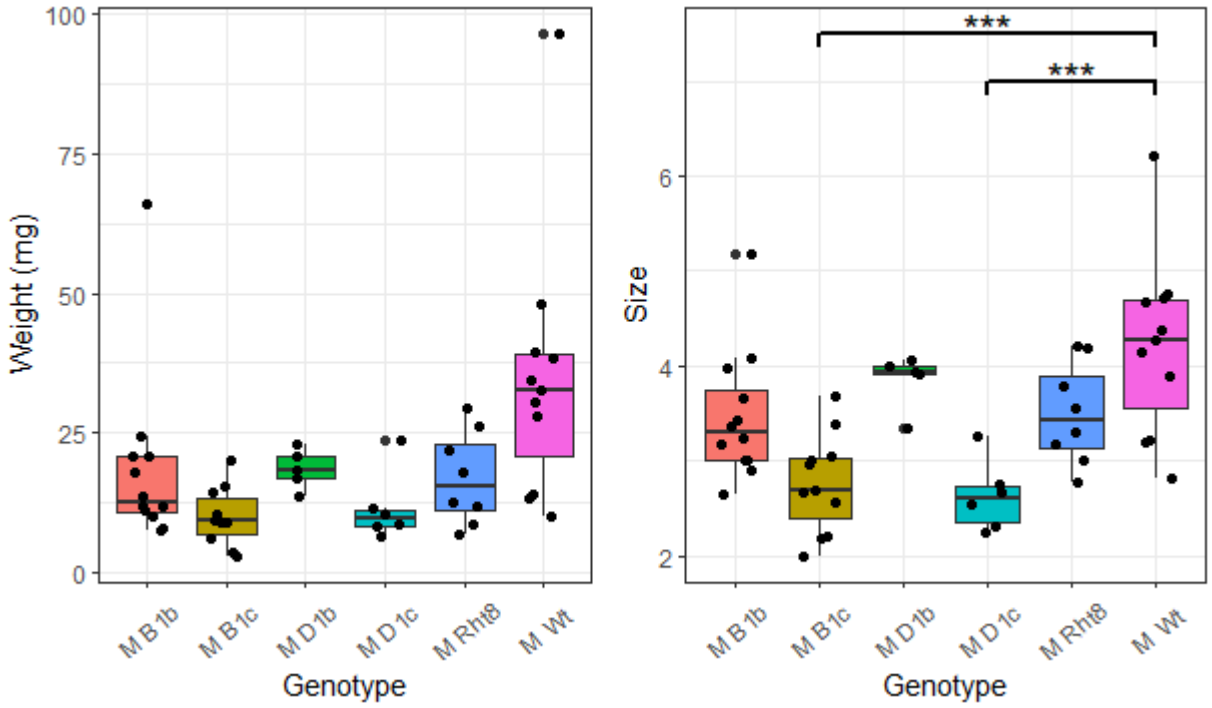

Figure 3.8: Box and whisker plots of mature ergot sclerotia size and weight developed in the wheat (*Triticum aestivum*) variety Mercia on the year 2018. Each data point represents the mean size or weight of sclerotia collected from a single ear. The box defines the upper and lower quartile and shows the median values. The asterisks indicate significant differences between NILs pairs at a $p < 0.001$. The pairs exhibiting a significant difference (indicated by the brackets) were: For size: *Rht-B1c*-WT, *Rht-D1c*-WT. No samples were taken for the *Rht12* line in 2018 as the wheat ears released their pollen before inoculation took place.

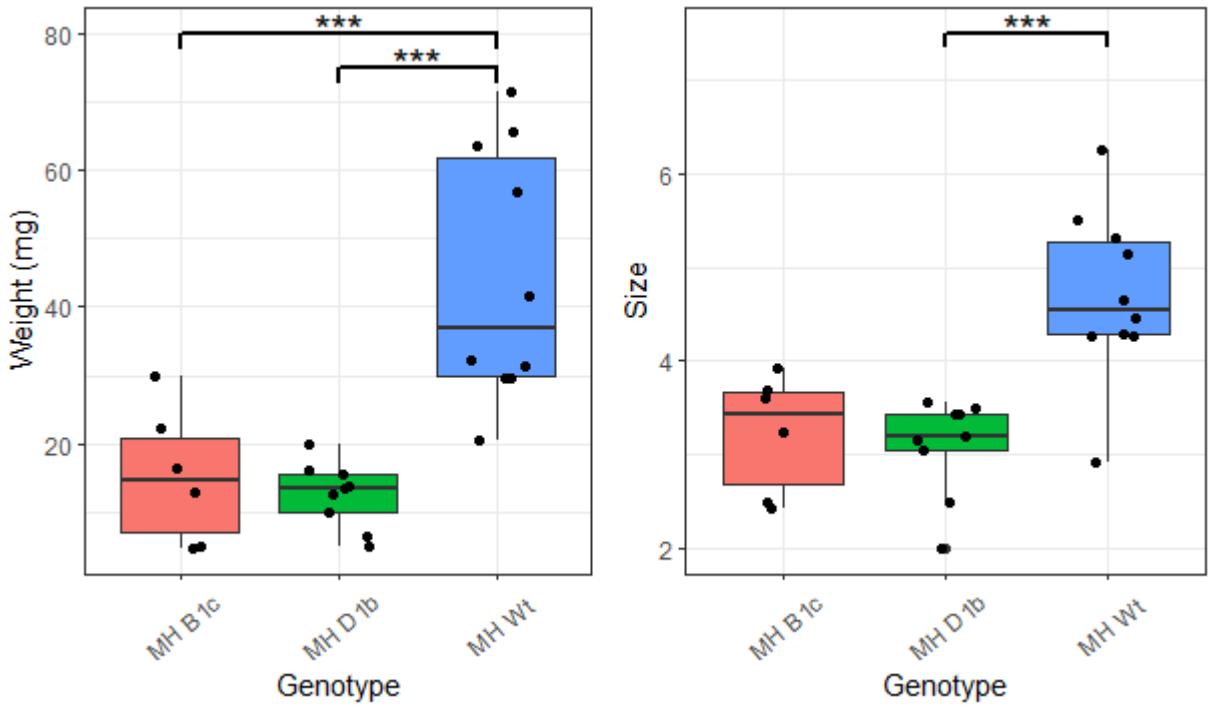

Figure 3.9: Box and whisker plots of mature ergot sclerotia size and weight developed in the wheat (*Triticum aestivum*) variety Maris Huntsman on the year 2018. Each data point represents the mean size or weight of sclerotia collected from a single ear. The box defines the upper and lower quartile and shows the median values. The asterisks indicate significant differences between NILs pairs at a $p < 0.001$. The pairs exhibiting a significant difference (indicated by the brackets) were: For weight: *Rht-D1b*-WT, *Rht-B1c*-WT; For size: *Rht-D1b*-WT.

3.4.3 Variation in seed size between the different *Rht*-NILs.

In order to determine whether previous observations (A. Gordon personal communication, 2017) showing differences in grain size produced by these lines could be replicated, and whether there was a relationship between the size of wheat seed and the size of sclerotia, the size of the seed produced by each of the respective lines were measured. Significant differences between 7 *Rht*-NILs regarding the length ($F = 37.12$, $p < 0.001$), width ($F = 19.58$, $p < 0.001$), and area ($F = 38.79$, $p < 0.001$) of the seed produced were detected in the Mercia NIL in 2017 (Figure 3.10). Comparing the WT line to the *Rht*-mutant lines, it was observed that the WT produced seed that had significantly longer lengths and greater areas than seed produced by the *Rht-D1c* line, and greater areas than seed produced by the *Rht-D1b* NIL. Interestingly, seed produced on the NIL Mercia *Rht12* was longer, wider and had a greater area than WT seed, and in general produced seed with significantly larger areas than all the other *Rht*-mutant lines measured. Mutant lines were also found to significantly differ from each

other, with *Rht-D1c* producing seed exhibiting significantly lower lengths and greater areas than the seed produced by *Rht8*, *Rht12* and *Rht-B1c* lines. With regards to width, *Rht-D1c* only produced significantly thinner seed than *Rht12*. In addition, *Rht-D1b* was found to produce seed with significantly shorter lengths and widths than *Rht8*, *Rht12* and *Rht-B1c*, as well as seed with smaller areas than *Rht8*, *Rht12* and *Rht-B1c*. Finally, the *Rht-B1b* line produced seed with significantly shorter lengths and width than *Rht12*, as well as significantly smaller areas than *Rht12* and *Rht-B1c*.

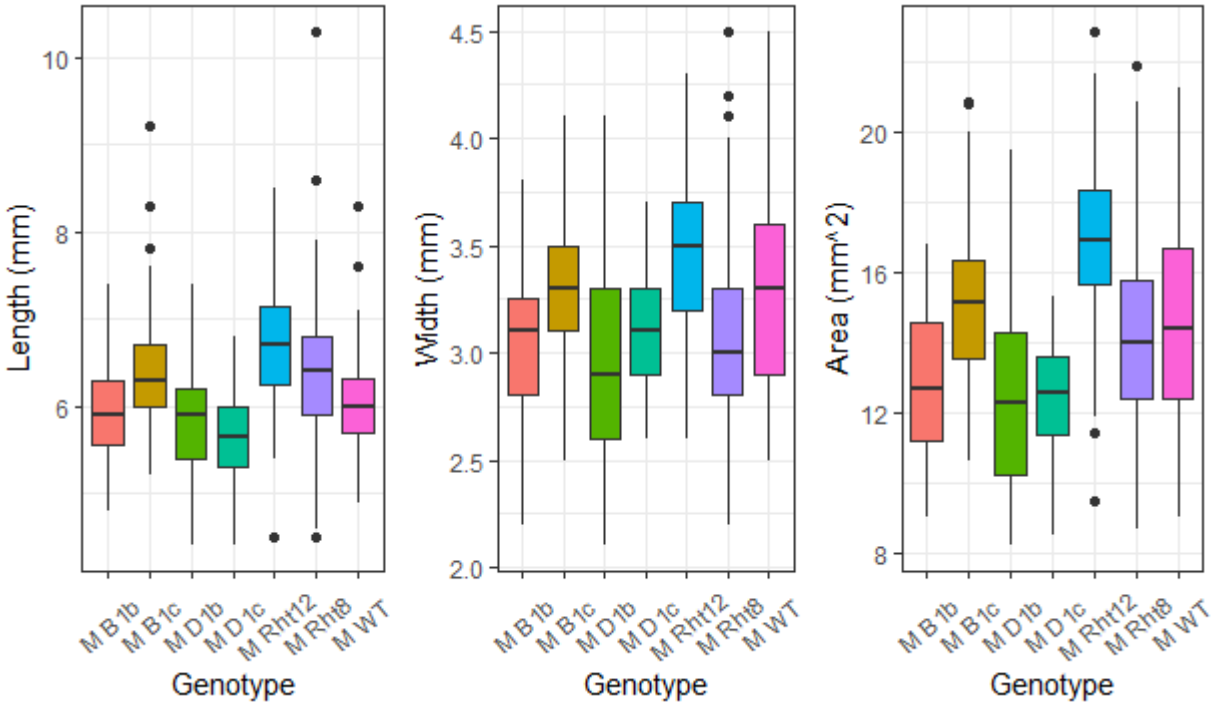

Figure 3.10: Box and whisker plots of seed length (mm), width (mm) and area (mm2) developed in the wheat (*Triticum aestivum*) variety Mercia Rht-mutant NILs in the year 2017. The box defines the upper and lower quartile, and shows the median values. The dots represent outlier data points.

In 2018 the seven Mercia *Rht*-NILs (Figure 3.11) again differed significantly in terms of seed length ($F = 69.76$, $p < 0.001$), width ($F = 58.23$, $p < 0.001$) and area ($F = 60.39$, $p < 0.001$. As in 2017 the WT line produced significantly bigger seed (length, width and area) than the *Rht-D1c* and *Rht-D1b* mutant lines. In 2018 WT seed was also found to be significantly larger than that produced by *Rht-B1c*. The alleles *Rht-D1c*, *Rht-D1b* and *Rht-B1c* also produced seed that differed in size from the seed produced by the other NILs. The *Rht-D1c* line produced the smallest seed. Specifically, *Rht-D1c* produced seed that had significantly shorter lengths than seed produced by all other lines, except *Rht-B1c*. *Rht-D1c* seed also had significantly shorter width than seed produce on all other lines apart from *Rht-D1b* and *Rht-B1b*, as well as

significantly smaller areas than the seed of all other lines, apart from *Rht-D1b*. In addition, *Rht-D1b* was found to produce seed with significantly shorter lengths than all other lines, except *Rht-B1c* and *Rht-D1c*, seed with significantly shorter widths than the *Rht-B1c* and *Rht12* lines, and seed with significantly smaller areas than the *Rht8* and *Rht12* lines. Finally, the line *Rht-B1c* produced seed with significantly shorter lengths than all other lines except *Rht-D1c* and *Rht-D1b*, as well as seed with significantly smaller areas than *Rht8*.

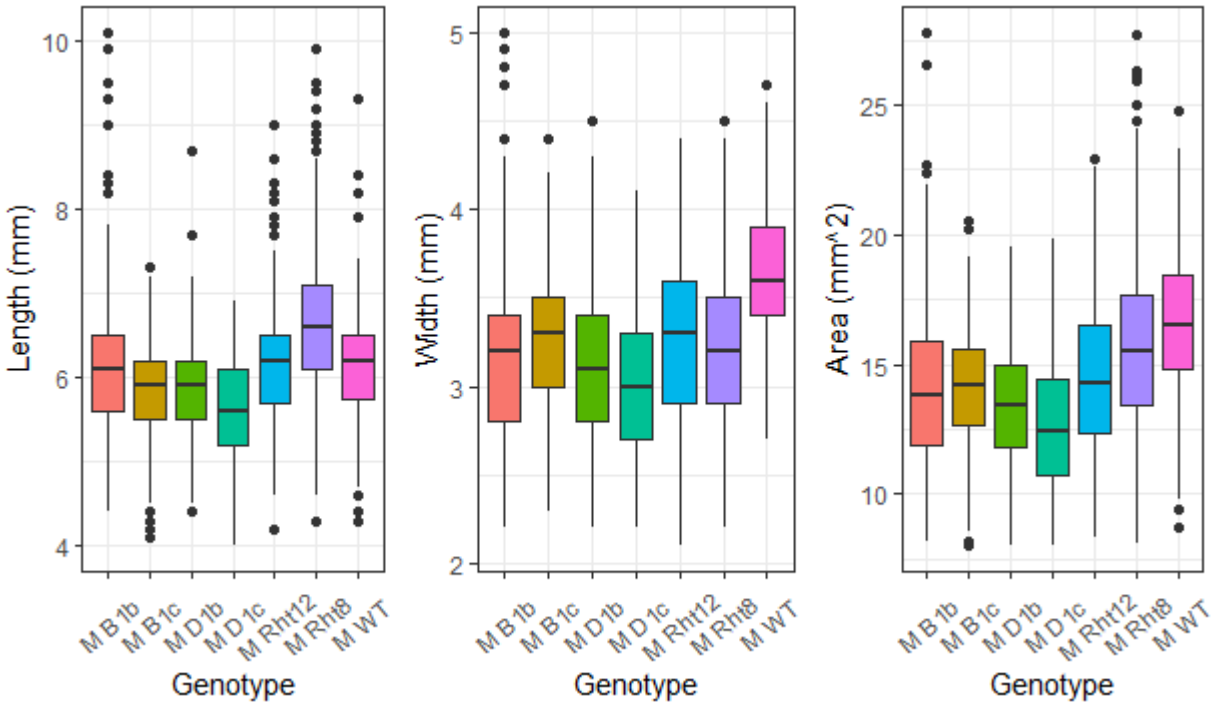

Figure 3.11: Box and whisker plots of seed length (mm), width (mm), and area (mm2) developed in the wheat (*Triticum aestivum*) variety Mercia Rht-mutant NILs in the year 2018. The box defines the upper and lower quartile and shows the median values. The dots represent outlier data points.

Contrary to the Mercia NILs, the three Maris Huntsman *Rht*-NILs in 2017 (Figure 3.12) did no exhibit any significant differences between seed length ($F = 4.11$, $p = 0.019$), width ($F = 1.34$, $p = 0.266$), or area ($F = 1.25$, $p = 0.290$). Similar in 2018 (Figure 3.13) no significant differences with regards to seed width ($F = 5.31$, $p = 0.005$) and area ($F = 4.91$, $p = 0.008$) were found. The length of seed did however differ significantly between the three *Rht*-NILs ($F = 47.75$, $p < 0.001$), with the WT producing longer seed than the seed produced by the Maris Huntsman NILs carrying alleles *Rht-D1b* and *Rht-B1c*.

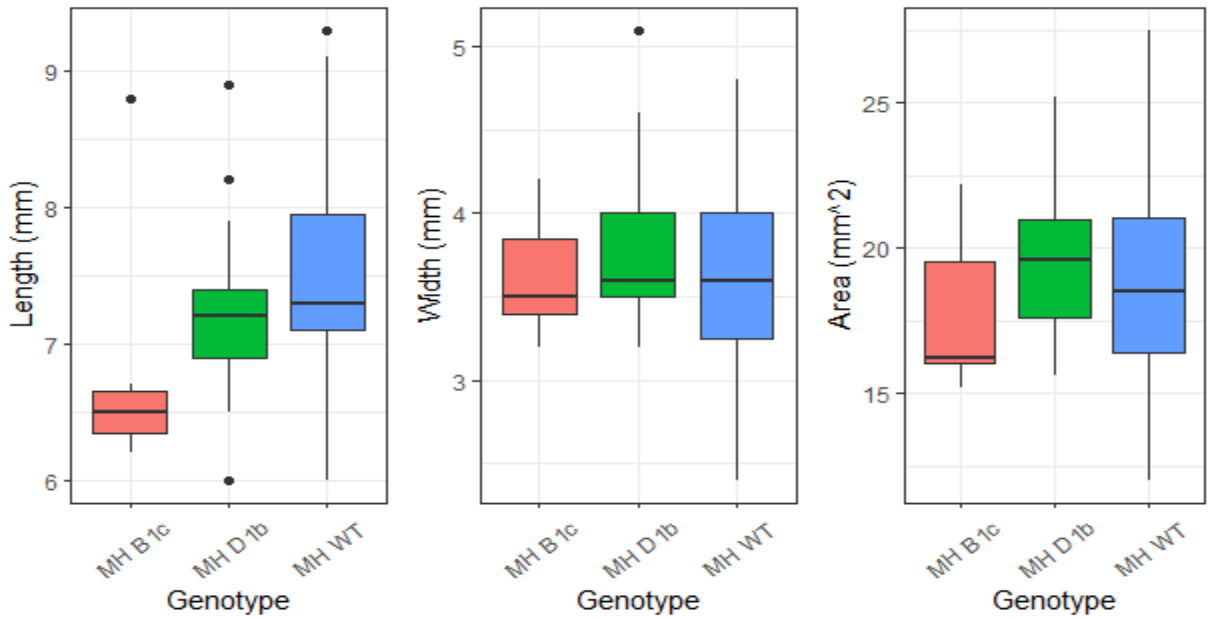

Figure 3.12: Box and whisker plots of grain length (mm), width (mm), and area (mm2) developed in the wheat (*Triticum aestivum*) variety Maris Huntsman Rht-mutant NILs in the year 2017. The box defines the upper and lower quartile and shows the median values. The dots represent outlier data points.

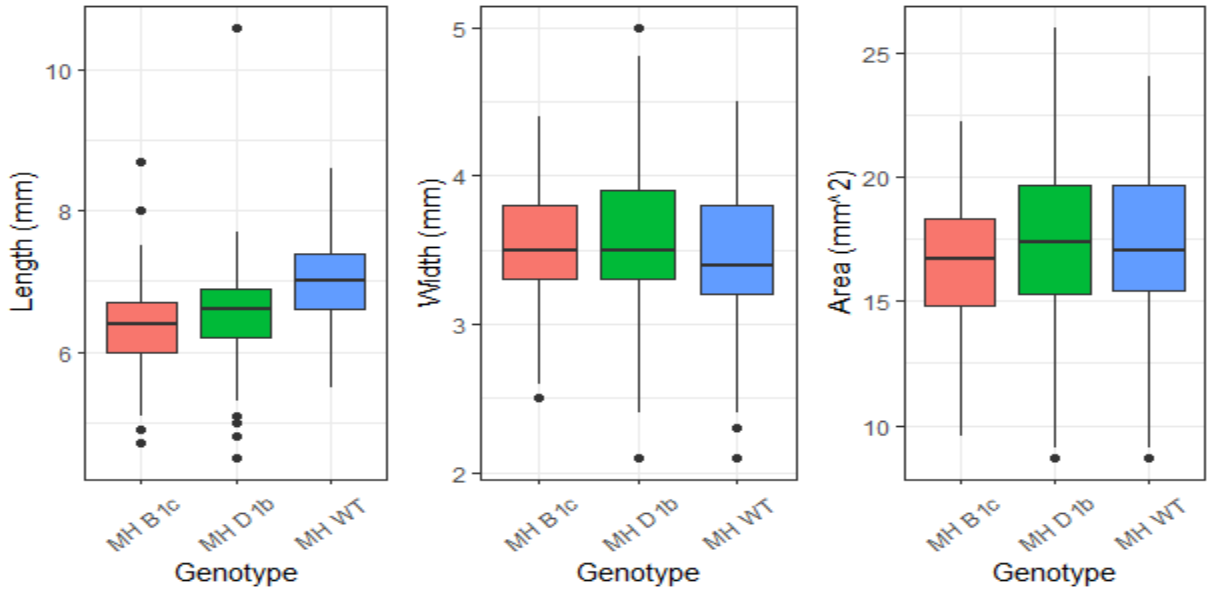

Figure 3.13: Box and whisker plots of grain length (mm), width (mm), and area (mm2) developed in the wheat (*Triticum aestivum*) variety Maris Huntsman Rht-mutant NILs in the year 2018. The box defines the upper and lower quartile and shows the median values. The dots represent outlier data points.

3.4.4 Variation in hormonal levels between inoculated and non-inoculated *Rht*-NILs.

In order to determine whether hormonal levels are altered in response to infection, and whether GA signalling plays a role in *C. purpurea* development, the levels of bioactive GAs, auxin (IAA), JA, SA and CKs were measured 3 days after *C. purpurea* inoculation in parental and *Rht*-NILs from the 2018 experiment. While variation was observed between the three biological replications this was not statistically significant for any of the hormones measured.

The bioactive gibberellin GA_1 was only detected at measurable levels in the parental line Mercia (Figure 3.14) and the Maris Huntsman *Rht*-mutant NIL *Rht-D1b* (Figure 3.15). The GA_1 levels where either 0.0 (detectable levels, but below the values of the calibration curve) or N/F (not found; below detectable levels). Statistical analyses therefore revealed no significant treatment (non-inoculated vs inoculated; $F = 0.08$, $p = 0.780$) or genotype ($F = 1.36$, $p = 0.320$) differences for GA_1 in the Mercia NILs, while no statistical analyses were conducted in the Maris Huntsman NILs.

The bioactive gibberellin GA_4 was detected in both the Mercia and Maris Huntsman NILs (Figures 3.14 and 3.15). Inoculation with *C. purpurea* resulted in elevated levels of GA_4 in Mercia and all the Mercia *Rht*-mutants, except *Rht-D1c* ($F = 34.08$, $p < 0.001$). A significant genotype ($F = 2.54$, $p = 0.039$) effect could be seen at the 5% level. In the Maris Huntsman NILs *C. purpurea* infection ($F = 69.09$, $p < 0.001$) also resulted in elevated levels of GA_4, but no effect of genotype ($F = 1.36$, $p = 0.294$), or a significant genotype/treatment interaction ($F = 3.03$, $p = 0.086$) was observed.

IAA levels in the Mercia NILs differed significantly between genotypes ($F = 10.45$, $p < 0.001$) and treatments ($F = 150.57$, $p < 0.001$), as well as showing a genotype/treatment interaction ($F = 11.03$, $p < 0.001$; Figure 3.14). Specifically, the impact of *C. purpurea* infection was genotype dependent, with the *Rht-B1b*, *Rht-D1b* and WT lines exhibiting significantly higher levels of IAA after inoculation than the other NILs, with *Rht-D1c* and *Rht8* lines having significantly lower levels of IAA than the *Rht-B1b*, *Rht-D1b* and WT lines. The *Rht12* NIL exhibited significantly lower IAA levels than *Rht-B1b* and *Rht-D1b*, and the *Rht-B1c* line exhibited significantly lower levels of IAA than *Rht-D1b*. While similar levels of IAA were observed in the Maris Huntsman NILs (Figure 3.15), only the treatment effect ($F = 102.60$, $p < 0.001$) was found to be statistically significant, with inoculated samples exhibiting significantly higher levels of IAA than non-inoculated. A significant genotype effect was seen

at the 5% level (F = 8.40, p = 0.005), as well as a significant genotype/treatment interaction (F = 10.63, p < 0.002). Upon inoculation, *Rht-B1c* exhibited significantly lower IAA levels than the WT line.

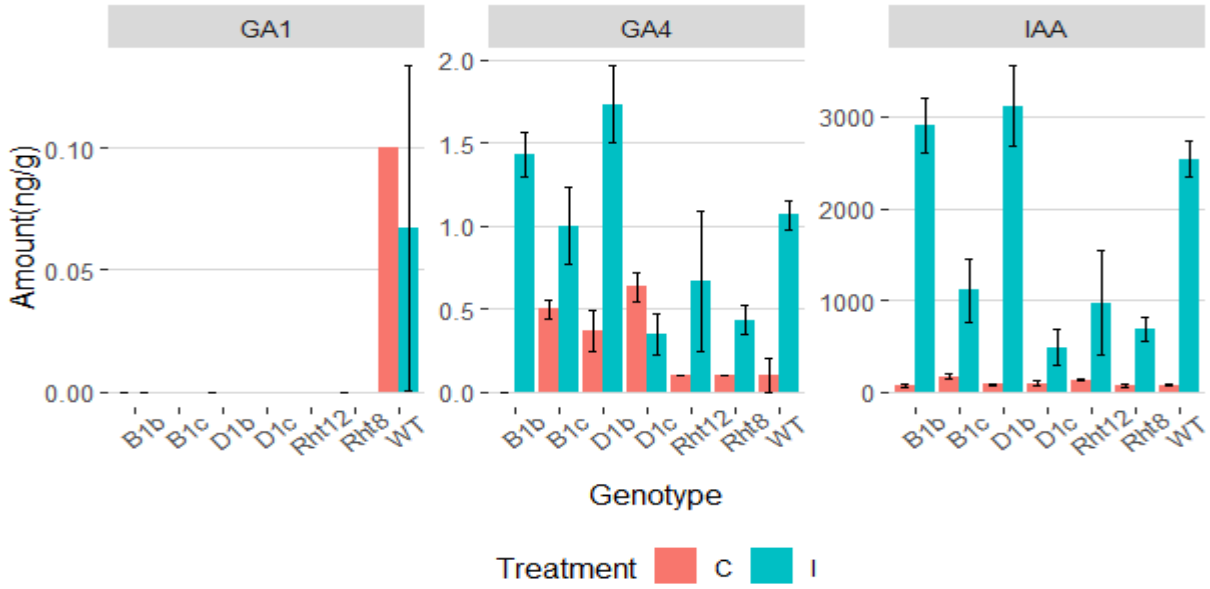

Figure 3.14: Mean levels of Gibberellins (GA1 & GA4) and auxin (IAA) (ng/g) found in non-inoculated (C) and *Claviceps purpurea* inoculated (I) *Rht*-NILs of the wheat variety Mercia. The error bars show standard errors. The standard error for the WT control of GA_1 could not be calculated as only one of the replicates showed a quantifiable amount.

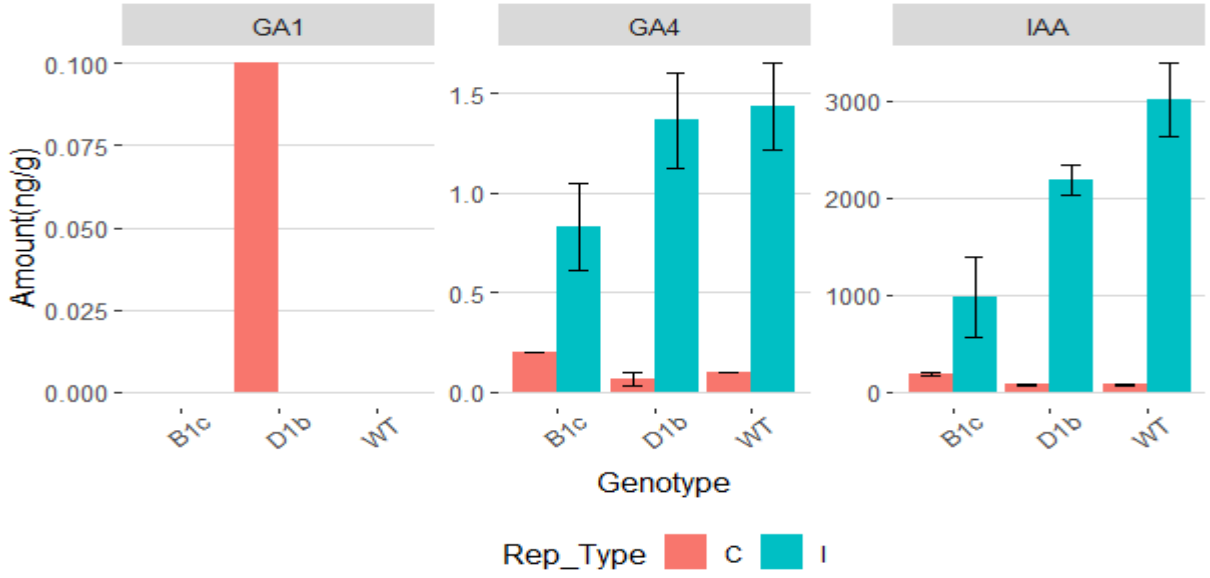

Figure 3.15: Mean amounts of Gibberellins (GA1 & GA4) and auxin (IAA) (ng/g) found in non-inoculated (C) and *Claviceps purpurea* inoculated (I) *Rht*-NILs of the wheat variety Maris Huntsman. The error bars show standard errors. The standard error for the *Rht-D1b* control of GA_1 could not be calculated as only one of the replicates showed a quantifiable amount.

In the Mercia NILs no significant effect of *C. purpurea* infection on JA levels was found ($F = 4.74$, $p = 0.038$; Figure 3.16), or a significant genotype/treatment interaction ($F = 3.29$, $p = 0.014$). A significant genotype effect ($F = 14.99$, $p < 0.001$) was recorded, with the *Rht-D1c* NIL exhibiting significantly higher levels of JA than *Rht-B1b*, *Rht-D1b* and *Rht8*. In addition, *Rht12* was found to exhibit significantly higher levels of JA than those found in *Rht8*. Similar patterns of JA levels were observed for the Maris Huntsman *Rht*-NILs (Figure 3.17), with *C. purpurea* infection having no statistically significant effect on JA levels ($F = 0.04$, $p = 0.847$). However, a significant genotype/treatment interaction ($F = 17.14$, $p < 0.001$), as well as a significant genotype ($F = 10.34$, $p = 0.002$) effect was found at the 5% level, each line appearing to be affected differently by the fungal inoculation and *Rht-D1b* exhibiting significantly lower JA levels than the WT. It was also observed, that in both Mercia and Maris Huntsman WT, inoculation with *C. purpurea* resulted in lower levels of JA.

In the Mercia NILs a significant genotype effect ($F = 6.42$, $p < 0.001$), as well as a significant genotype/treatment interaction ($F = 8.25$, $p < 0.001$) was seen for SA levels, but no significant effect of *C. purpura* infection was observed ($F = 0.01$ $p = 0.920$; Figure 3.16). *C. purpurea* infection affected different lines in different ways, as some *Rht*-NILs exhibited higher levels of SA when they were inoculated with *C. purpura*, while others did not. In the non-inoculated samples, *Rht12* exhibited significantly higher SA levels than *Rht-B1b*, *Rht-D1c* and WT. *Rht-B1c* had the second highest levels of SA, but they were only significantly higher than those seen in *Rht-B1b*. In the Maris Huntsman NILs (Figure 3.17), no significant differences were detected in terms of treatment ($F = 0.21$, $p = 0.659$), genotype ($F = 3.50$, $p = 0.063$), or genotype/treatment interaction ($F = 0.35$, $p = 0.710$).

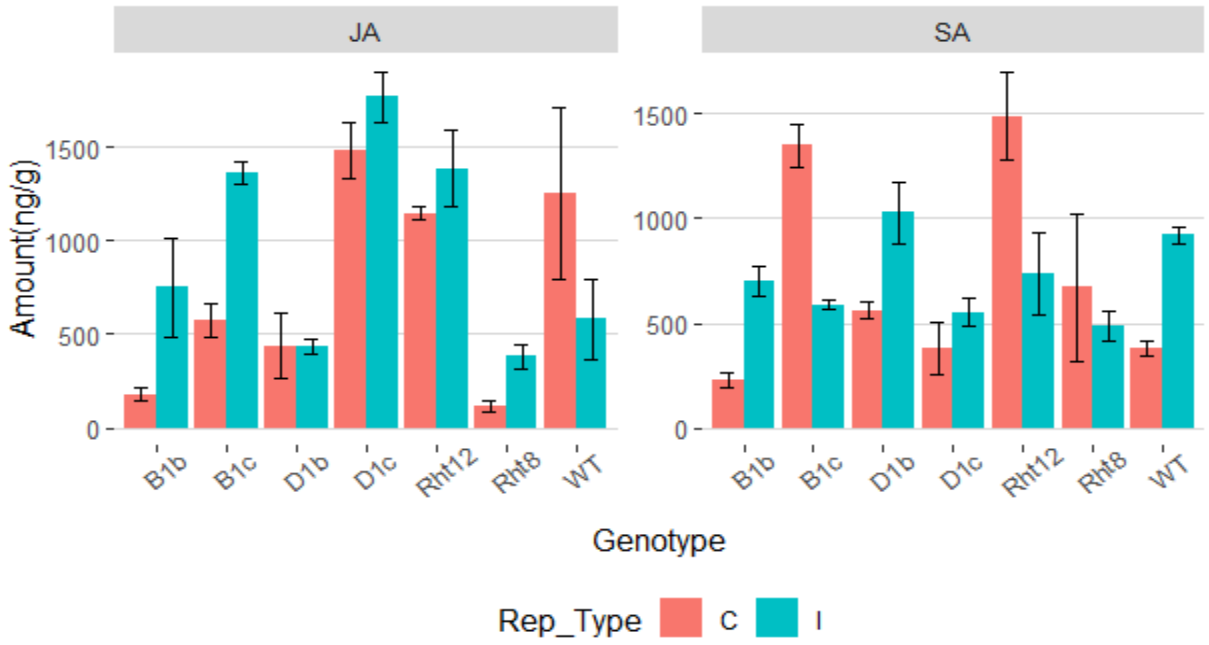

Figure 3.16: Mean amounts of Jasmonic acid (JA) and Salicylic acid (SA) (ng/g) found in non-inoculated (C) and *Claviceps purpurea* inoculated (I) *Rht*-NILs of the wheat variety Mercia. The error bars show standard errors**.**

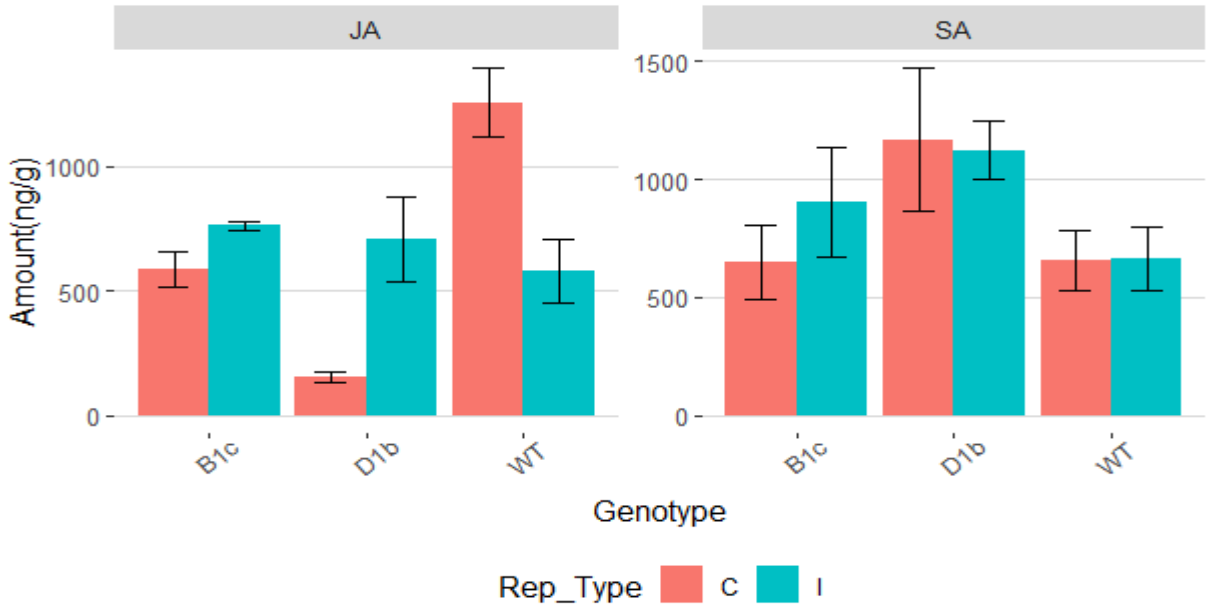

Figure 3.17: Mean amounts of Jasmonic acid (JA) and Salicylic acid (SA) (ng/g) found in non-inoculated (C) and *Claviceps purpurea* inoculated (I) *Rht*-NILs of the wheat variety Maris Huntsman. The error bars show standard errors.

Three cytokinins were measured, dihydrozeatin-type (DHZ), N^6-(2-isopentenyl)adenine-type (iP) and trans-zeatin-type (tZ). The cytokinin tZ was present in far higher levels than DHZ and iP, and in both the Mercia and Maris Huntsman NILs.

In the Mercia NILs (Figure 3.18) DHZ levels were significantly affected by genotype ($F = 14.46$, $p < 0.001$) and treatment ($F = 27.85$, $p < 0.001$), but no significant genotype/treatment interaction was detected ($F = 3.31$, $p = 0.014$). Overall, *C. purpurea* inoculated NILs exhibited significantly higher levels of DHZ than non-inoculated. Although no significant genotype/treatment interaction was detected *C. purpurea* infection had a bigger effect on DHZ levels in Mercia WT, and *Rht*-mutant allele NILs carrying *Rht-B1b*, *B1c* and *D1b*. In addition, NILs carrying *Rht-D1c* and *Rht8* had significantly lower levels of DHZ than WT, *Rht-D1c* lower DHZ levels than the *Rht-B1b* and *Rht-D1b* NILs, and *Rht8* lower levels of DHZ than *Rht-B1b*. These effects where not however observed in the Maris Huntsman NILs where no significant genotype ($F = 5.11$, $p = 0.025$), treatment ($F = 1.57$, $p = 0.234$), or a genotype/treatment interaction ($F = 0.36$, $p = 0.704$; Figure 3.19) were found.

The levels of iP type cytokinins in the Mercia NILs were found to be significantly affected by genotype ($F = 6.09$, $p < 0.001$), but not by treatment ($F = 0.44$, $p = 0.513$; Figure 3.18). Specifically, the *Rht-D1c* line was found to contain higher levels of iP type than *Rht-B1b*, *Rht-B1c*, and *Rht12*. However, no significant genotype ($F = 2.12$, $p = 0.157$) or treatment ($F = 4.07$, $p = 0.063$) effects were detected in the Maris Huntsman NILs (Figure 3.19).

Similarly, a significant genotype effect ($F = 17.78$, $p < 0.001$) but no significant treatment effect ($F = 2.19$, $p = 0.150$), or a significant genotype/treatment interaction ($F = 2.72$, $p = 0.033$) were detected for the tZ type of cytokinins in the Mercia NILs (Figure 3.18). Specifically, the *Rht8* line was found to have significantly lower levels of tZ type cytokinins than all other lines, except for *Rht-D1c*, which also exhibited significantly lower tZ levels than all lines, except *Rht8* and *Rht-B1c*. In addition, no significant genotype effect ($F = 3.76$, $p = 0.054$), treatment effect ($F = 0.28$, $p = 0.606$), or genotype/treatment interactions ($F = 8.32$, $p = 0.005$) were found for the tZ type cytokinins in the Maris Huntsman NILs.

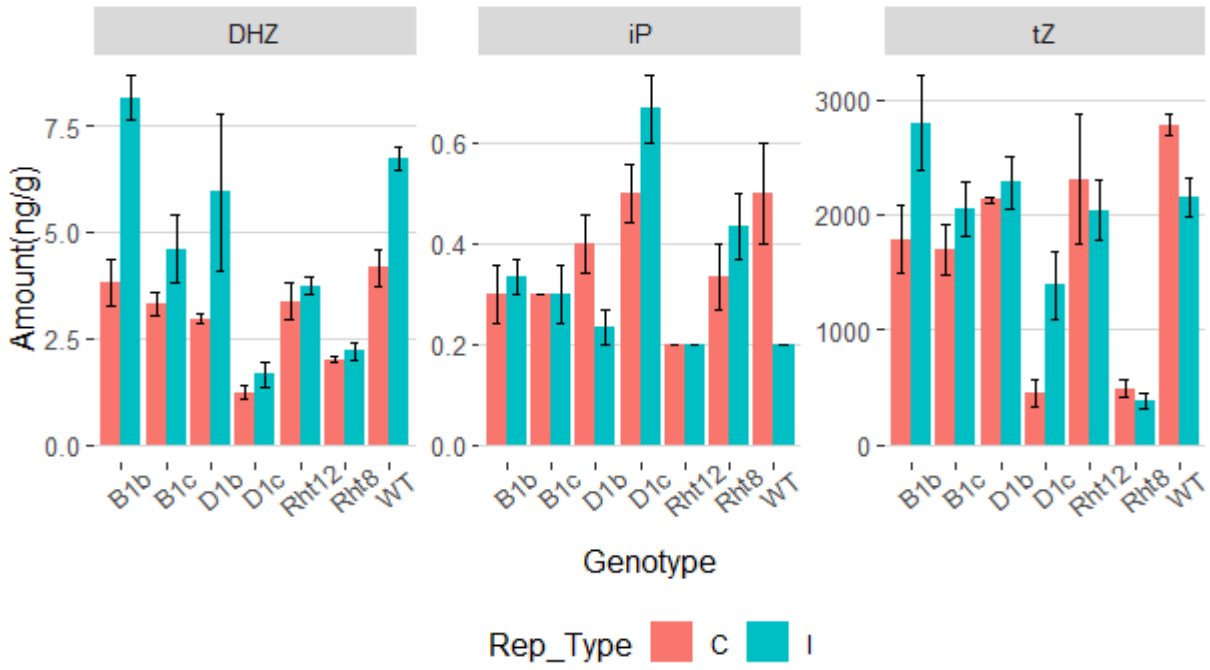

Figure 3.18: Mean amounts of dihydrozeatin-type (DHZ), N^6-(2-isopentenyl)adenine-type (iP), and trans-zeatin-type (tZ) cytokinins (ng/g) found in non-inoculated (C) and *Claviceps purpurea* inoculated (I) *Rht*-NILs of the wheat variety Mercia. The error bars show standard errors.

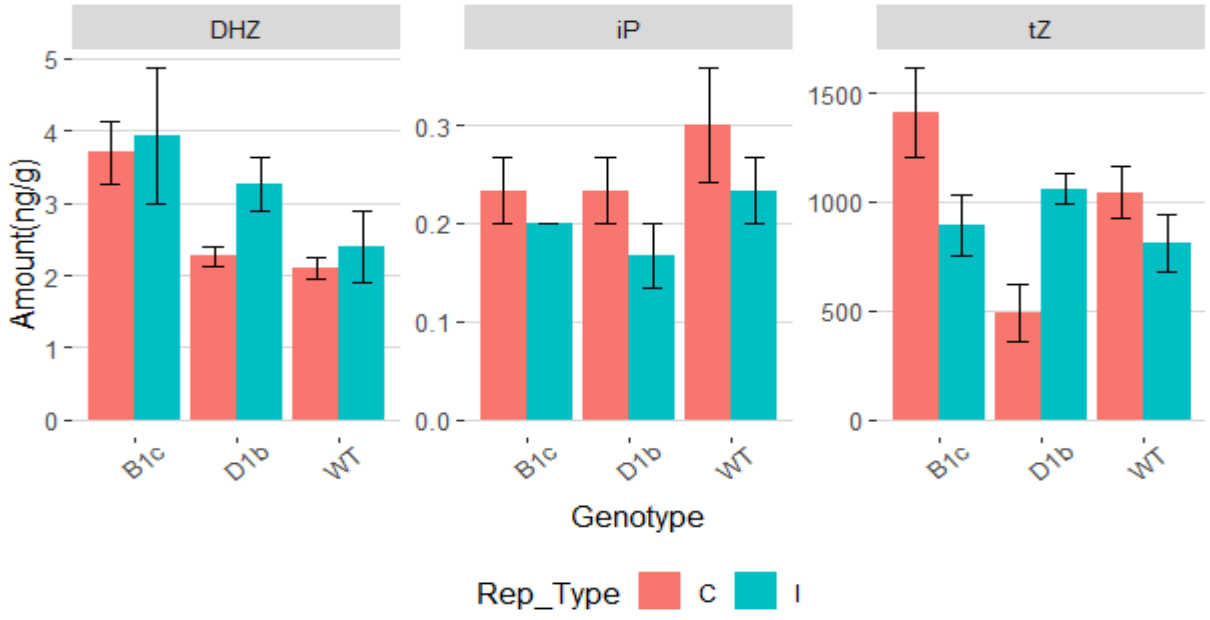

Figure 3.19: Mean amounts of dihydrozeatin-type (DHZ), N^6-(2-isopentenyl)adenine-type (iP), and trans-zeatin-type (tZ) cytokinins (ng/g) found in non-inoculated (C) and *Claviceps purpurea* inoculated (I) *Rht*-NILs of the wheat variety Maris Huntsman. The error bars show standard errors.

3.5 Discussion

C. purpurea is a biotrophic fungal pathogen that infects the ovaries of a number of economically important cereal crops, including wheat, barley, rye, oats, triticale and millet (Tudzynski & Scheffer, 2004). The disease can result in devastating economic damage as the infection detrimentally affects grain and flour quality due to the toxic alkaloids produced by the fungus (Tudzynski *et al*., 2001). Further aggravating the problem is the lack of active genetic resistance to *C. purpurea* in these cereal crops. As we have previously shown, a number of genetic pathways, including those of hormones, have been identified in wheat that have been shown to be active during infection. An improved understanding of the role hormones play in the establishment of *C. purpurea* in wheat could have a direct effect on crop improvement strategies for sustainable agricultural systems.

Multiple studies have implicated GAs in plant-pathogen interactions. In some studies it has been suggested that GA is required for pathogenicity, while others suggest that it has a role in resistance. Saville *et al*. (2012) showed that the combination of the dwarf and semi-dwarf DELLA mutant alleles *Rht-B1c and Rht-D1b* conferred increased susceptibility to biotrophic pathogens and increased resistance to necrotrophic pathogens. Their work was in agreement with studies by Achard *et al*. (2008) who demonstrated that DELLAs can delay ROS-induced cell death and Navarro *et al*. (2008) who reported that DELLAs suppress the accumulation of SA and cell death in response to infection by *Pseudomonas syringae* pv. tomato. Saville *et al*. (2012) proposed that the increased susceptibility to the biotroph *Blumeria graminis* results from the accumulation of the mutant DELLA proteins in these lines, which delayed ROS-accumulation and lead to a reduction in the effectiveness of the hypersensitive response. The observations in this chapter indicate that infection of wheat by *C. purpurea* is reduced in the GA-insensitive severe dwarf and semi-dwarf *Rht*-mutant NILs. This would suggest that mutations in the DELLA domains are conferring partial resistance to this fungus, and not susceptibility as found in biotrophic fungal pathogens by Saville at al. (2012). In general, more honeydew was produced by, and the sclerotia were larger on the WT parental wheat varieties Mercia and Maris Huntsman than the NILs carrying the mutant alleles *Rht-B1* and *Rht-D1*. The role of DELLAs in wheat in partial resistance to *C. purpurea* has also been indicated by Gordon *et al*. (2015), where resistance co-located with the *Rht* loci on chromosomes 4B and 4D.

Various possibilities to explain the observed results are considered. Firstly, in the WT Mercia and Maris Huntsman JA levels fell following infection by *C. purpurea*. Removal of the DELLA proteins in the WT parents, linked to elevated GA_4 levels following *C. purpurea* infection, would therefore appear to suppress the JA-mediated defense response. In the GA-insensitive *Rht*-mutant lines DELLA proteins would accumulate, despite elevated levels of GA_4. Hou *et al*. (2010) suggested that DELLAs can lead to the activation of JA-responsive target genes by binding to the JA suppressor JAZ1. The enhanced resistance to *C. purpurea* afforded by the *Rht*-mutant alleles could therefore be through JA-mediated defence mechanisms. Walters et al. (2002) also demonstrated that increased resistance to the biotroph *Blumeria graminis f. sp. hordei* was bought about through JA-mediated defence in barley.

Secondly, while ROS homeostasis is complex, it is possible that the observed partial resistance associated with the *Rht*-mutants could be due to an altered ROS balance. Indeed, it has been found that *C. purpurea* significantly contributes to the accumulation of ROS in plants during infection, and that NADPH oxidase mediated production of ROS is essential for the full pathogenicity of the fungus (Giesbert *et al*., 2008). As the accumulation of DELLAs can lead to a reduction of ROS through increasing the expression of genes encoding ROS-scavenging enzymes (Achard *et al*., 2008), the optimal ROS balance required for full pathogenicity of *C. purpurea* may be potentially altered in the mutant lines *Rht-B1c*, *Rht-D1b* and *Rht-D1c*.

It has been observed that the *Rht-B1b* and *Rht-D1b* alleles are able to positively affect yield through an increase in seed number per ear, despite reducing individual seed weights (Flintham *et al.*, 1997; Rebetzke & Richards, 2000). While more extreme dwarf alleles such as *Rht-B1c* and *Rht-D1c* generally have a negative effect on grain yield (Flintham *et al.*, 1997). It is therefore conceivable that DELLAs might also be affecting seed size. However, measurement of seed parameters produced on Mercia and Maris Huntsman, and their corresponding NILs did not provide clear support for these observations. In addition, no definitive pattern existed between the size of sclerotia and the size of healthy seed produced on *C. purpurea* infected ears. The two exceptions being the severe dwarf *Rht-D1c* and the semi-dwarf *Rht-D1b* in the Mercia background (Figure 3.10; Figure 3.11), these lines producing both smaller seed, as well as smaller sclerotia.

This study supports the theory that GAs are required for the successful infection of wheat by *C. purpurea*, acting to enhance susceptibility to the fungus, potentially via the degradation of WT DELLAs. The observed increase in endogenous GA_4 could be linked to an

auxin mediated induction of the GA biosynthetic pathway, as auxin has been known to strongly induce the synthesis of bioactive GAs (Wolbang *et al*., 2004). Indeed, Mercia and Maris Huntsman, and the *Rht*-NILs exhibited an almost mirror image of increased endogenous GA4 and IAA levels in response to *C. purpurea* infection, although IAA levels were much higher than those found for GA_4. It is known that *C. purpurea* can produce substantial quantities of auxins (P. Galuszka, unpubl. data). Therefore the elevated auxin levels observed during *C. purpurea* infection could actually be products of the fungus. However, as plant and fungal auxins are structurally identical, there was no way of determining, through the hormone assays undertaken in this study, whether the auxin found during infection was a fungal or a plant product.

Hinsch *et al*. (2015) showed that *C. purpurea* is also able to produce a variety of cytokinins, and that mutation in *C. purpurea* cytokinin biosynthesis genes, specifically genes that abolished cis-zeatin (cZ) -type cytokinins, resulted in a decrease in pathogenicity (Hinsch et al., 2015; Kind et al., 2018). In this study, similar to the *in planta* measurements of CKs of Kind et al., (2018), dihydrozeatin (DHZ) was found here to significantly increase upon *C. purpurea* infection. Their observations of an increase in the iP and tZ type CKs could not be replicated, however that could due to differences in the time of sampling as Hinsch *et al*., 2015 did note that the alterations in CKs levels were time dependent. The genotype effects observed in this chapter indicate that CK biosynthesis is potentially affected by the altered GA signaling that would be expected in the *Rht*-NILs.

Overall, GAs and GA signaling were found to play a role in the infection of wheat by *C. purpurea*. Specifically, a perturbation in GA signaling, potentially through disruption of the DELLA-GA degradation system, appears to reduce infection by *C. purpurea*. Through the quantification results, other hormones, namely auxin and DHZ-type cytokinins, were also found to play a significant role in the successful infection of wheat. While it is not known whether the observed patterns of the endogenous hormones are the result of fungal or plant biosynthesis, it is highly likely that successful infection depends on the interactions of these hormones.

3.6 Further work

Honeydew production, as well as sclerotia and seed size in the *Rht*-NILs were found to be quite variable between years. The genotype effect on honeydew production seen in 2017 in particular could not be replicated in 2018. It would be extremely beneficial for additional, replicated experiments to be conducted in order for these observations to be substantiated. In addition, the potential correlation between plant height and *C. purpurea* resistance should be further explored. An immediate step in this investigation could be the inclusion of lines containing a combination of dwarf and semi-dwarf mutant alleles (*Rht-B1c+Rht-D1b*), as well as the taking of accurate plant height measurements in further experiments.

Honeydew and sclerotia measurements alone do not reveal whether fungal colonisation of the mutants is accompanied by developmental defects and/or a delay in the formation of fungal structures within the ovules, prior to the emergence of sclerotia. In order to further characterise the effects the mutations might have on the successful colonisation of wheat ovules by *C. purpurea* a time-course experiment should be carried out, and the progression of infection inspected via confocal microscopy. Ovule samples for these particular experiments were taken. However, the staining protocol tried compromised the structural integrity of the ovules. A re-sampling was not possible due to time constraints.

A qRT-PCR analysis of key GA biosynthesis genes was planned. However, the molecular analysis of the Mercia and Maris Huntsman *Rht*-NILs was not possible as no efficient primer pairs could be identified. Furthermore, time-constraints imposed, due to the COVID-19 pandemic, did not allow for further experiments to be conducted. Evaluating the GA responses during infection in the Mercia and Maris Huntsman *Rht*-NILs, via the expression patterns of key biosynthetic and signaling GA genes *in planta* could shed further light on the results obtained in this study.

Chapter 4: Determining the Movement of Ergot Alkaloids in Cereal Grains

4.1 Abstract

The fungus *Claviceps purpurea* infects cereals and grasses at anthesis, producing an ergot sclerotia (the overwintering structure of the pathogen) in place of a grain. Ergot sclerotia contain a cocktail of ergot alkaloids that are highly toxic to humans and animals. There is evidence to suggest that ergot alkaloids are able to contaminate cereal grains, as alkaloids have been detected in cereal products for human consumption. Reemerging concerns over the potential health risks presented by ergot alkaloids have led to new legislation on ergot alkaloids being proposed by the European Commission. This chapter addresses a number of questions regarding the ways in which ergot alkaloids are able to contaminate grains of wheat, barley and rye through a series of repeat experiments conducted over two years. It was shown that a significant risk of grain contamination by ergot alkaloids exists both pre-harvest, due to contamination while in the ear, as well as post-harvest, as a result of contact between sclerotia and grain. Significant differences between isolates and cereal species were found in the size and weight of mature ergot sclerotia, with larger, heavier sclerotia being produced by wheat. Very low levels of ergot alkaloids were found in honeydew with all *C. purpurea* isolates tested. Levels increased in sphacelia tissues and reached levels as high as 3 million parts per billion (ppb; 3 million μg of ergot alkaloids per kg of sclerotia) in mature ergot sclerotia. In wheat and barley, ergot alkaloids were found to transfer to healthy grain that developed above and below flowers infected with the *C. purpurea* isolates 04-97.1, EI4 and Rye 20.1. The profiles of ergot alkaloids found on grain were very different from the profiles found in mature ergot sclerotia. Significantly more ergot alkaloids were transferred to clean grain of wheat and barley as a result of direct physical contact with broken pieces of sclerotia, compared to intact sclerotia, with significant differences also seen between wheat and barley.

4.2 Introduction

4.2.1 Alkaloid Biosynthesis

C. purpurea produces a range of toxic ergot alkaloids during its infection of cereal and grass flowers. Ergot alkaloids can be divided into three groups according to their structure: clavines, lysergic acid amides and peptides (ergopeptines) and they are characterized by the tetracyclic ergoline ring system (Wallwey & Li, 2011). Over the past several decades the biosynthetic steps necessary for the production of these alkaloids have been elucidated (Figure 4.1). The first biosynthetic steps, which result in the formation of argoclavine with its' tetracyclic ergoline ring system, are shared between all three groups of ergot alkaloids (Schardl *et al*., 2006). The process starts with the *C*4-prenylation of l-tryptophan with dimethylallyl diphosphate (DMAPP) as the prenyl donor, a reaction which is catalyzed by the prenyltransferase 4-dimethylallyltryptophan synthase (DMATS) and results in the formation of 4-L-dimethylallyltryptophan (4-L-DMAT) (Lee *et al*., 1976). 4-L-DMAT then undergoes *N*-methylation in the presence of S-adenosylmethionine (SAM), resulting in the formation of 4-dimethylallyl-l-abrine (4-DMA-l-abrine). This reaction is catalyzed by the enzyme 4-dimethylallyltryptophan *N*-methyltransferase (EasF) (Gerhards *et al*., 2014). The next intermediate in the pathway is chanoclavine-I which is converted from 4-DMA-l-abrine in one decarboxylation and two oxidation steps (Schardl *et al*., 2006) through the enzymatic actions of FAD-dependent oxidoreductase (EasE), and catalase (EasC) (Lorenz *et al*., 2010; Goetz *et al*., 2011). In the next reaction, the formation of chanoclavine-I aldehyde is catalyzed by the short-chain dehydrogenase/reductase (SDR) EasD (Gerhards *et al*., 2014). Finally, EasG is able to catalyze the formation of the final product agroclavine via an non-enzymatic reaction between chanoclavine and reduced glutathione (Matuschek *et al*., 2012).

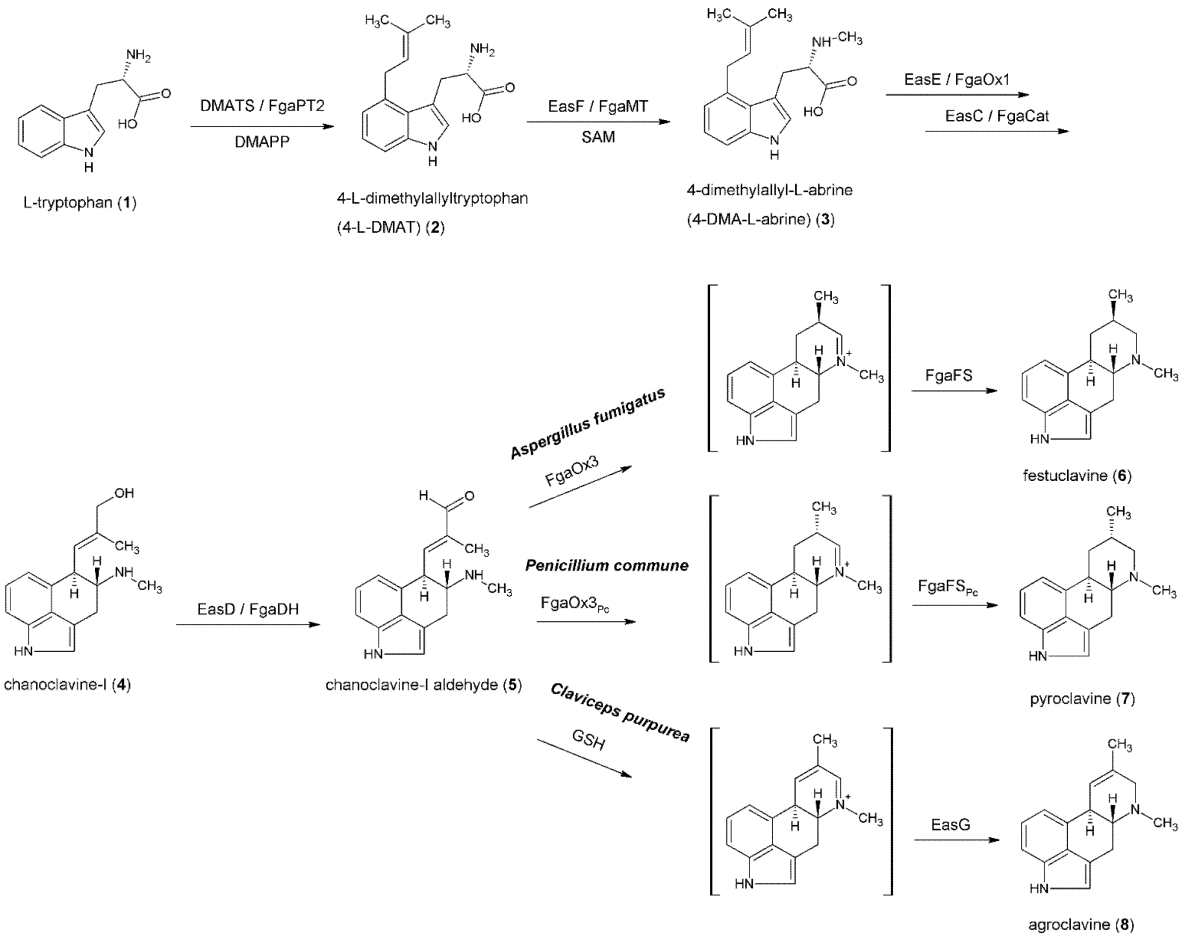

Figure 4.1: Formation of the ergoline scaffold-biosynthetic pathway (Gerhards *et al*., 2014).

In *C. purpurea*, the ergoline scaffold, in the form of agroclavine described above, undergoes a series of modifications by specific enzymes to produce the final ergot alkaloids. The first series of steps involve the transformation of agroclavine to lysergic acid, with elymoclavine and paspalic acid serving as the intermediate structures (Gerhards *et al*., 2014). Cytochrome P-450 monooxygenases and clavinet oxidase have been identified as the enzymes catalyzing the transformation of agroclavine to elymoclavine and elymoclavine to paspalic acid, respectively (Haarmann *et al*., 2006).

The steps involved in the production of the ergopeptines include the attachment of a tripeptide chain to activated lysergic acid, the tripeptide forming a bicyclic structure including a lactam ring and an oxazolidinone ring (e.g., ergotamine) (Gerhards *et al*., 2014). Ergopeptines are formed by an nonribosomal peptide synthethase (NRPS) enzyme complex containing two separable activities, d-Lysergyl peptide synthetases 1 and 2 (LPS1 and LPS2; Walzel *et al*., 1997; Figure 4.2), and result in the synthesis of the 6 most common ergot alkaloids, ergocornine, ergocristine, ergocryptine, ergometrine, ergosine and ergotamine.

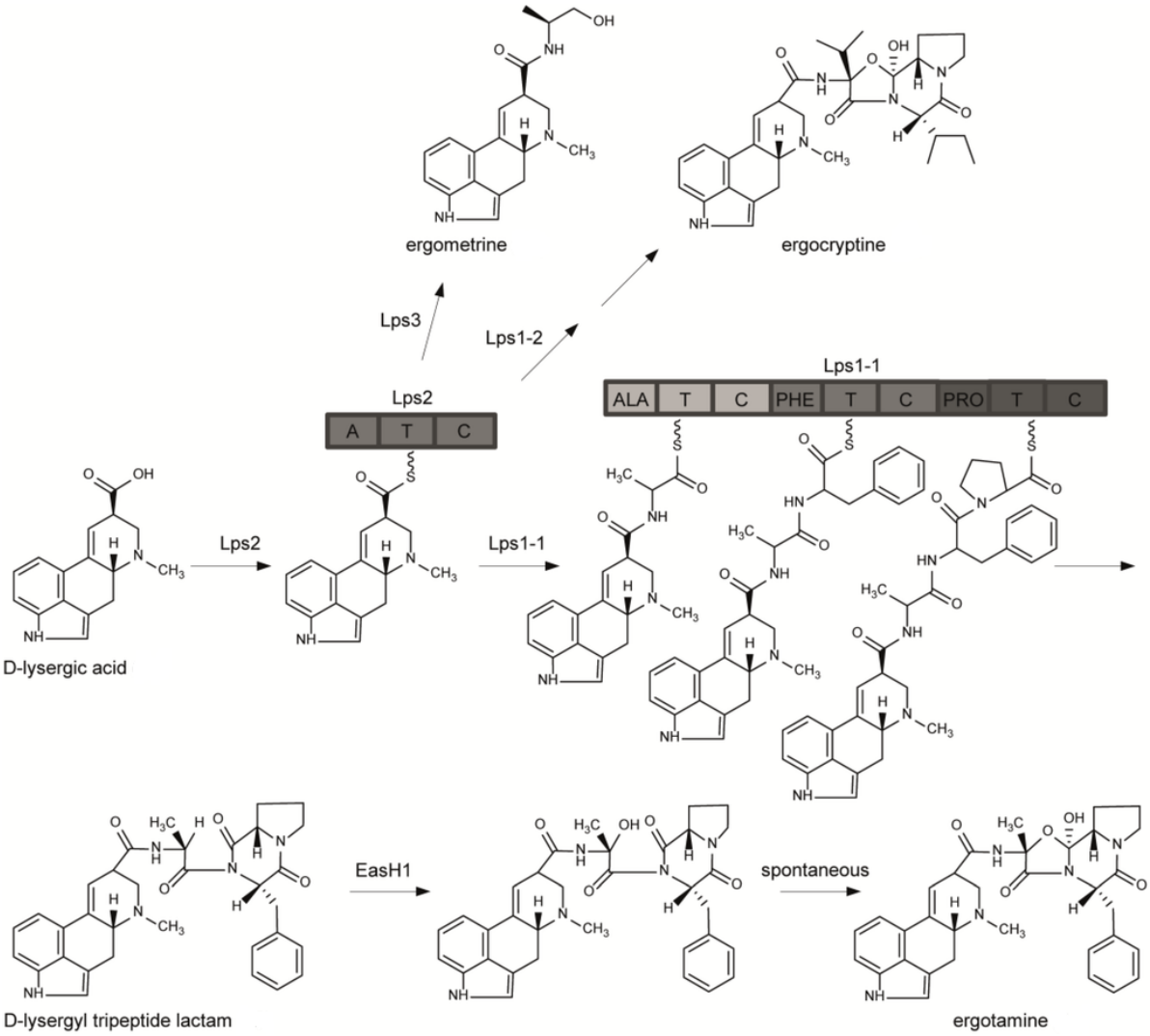

Figure 4.2: Formation of ergopeptines in *C. purpurea* (Adapted from Gerhards *et al*., 2014).

A gene cluster containing the genes responsible for this biosynthetic pathway has been identified (Figure 4.3). The NRPS complex, encoded by genes of this cluster, represents a unique natural combinatorial system that allows the formation of the various known ergopeptines. D-lysergic acid is activated by LPS2 and then used as substrate for the three different NRPSs, including LPS1 isoforms encoded by *lpsA*1 and *lpsA*2, and the monomodular NRPS-reductase encoded by *lpsC*. Variations in LPS1 can account for the variation of ergopeptines produced by *C. purpurea* (Gerhards *et al*., 2014).

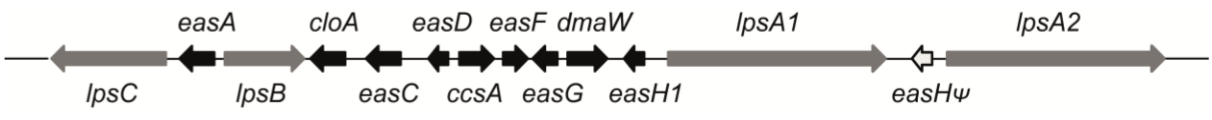

Figure 4.3: Ergot alkaloid gene cluster in *C. purpurea* (modified after Haarmann *et al*., 2005).

4.2.2 Grain Contamination

While the biosynthetic pathways of ergot alkaloids are relatively well characterised, very little is known about when and where in the *C. purpurea* infection process these alkaloids are produced, and whether the profile of alkaloids differs between fungal tissues (e.g. sphacelial, honeydew and sclerotia), between *C. purpurea* isolates and in different *C. purpurea*-host infections (e.g. with wheat, barley and rye). It is known that mycotoxins, including deoxynivalenol (DON) produced by *Fusarium culmorum* are able to travel in the ear via the xylem vessels and phloem sieve tubes (Kang, 1999). Therefore both honeydew and sphacelial tissue (which surrounds the phloem and xylem tissues that enter the ovule) could be routes for alkaloid transfer within the ear, resulting in contamination of healthy grain. Although a previous study in three wheat varieties, using a mixture of five UK and three Canadian *C. purpurea* isolates, indicated that alkaloid levels were low in honeydew (16 to 5,459 µg/kg; Tittlemier et al., 2016), the possibility of differences between *C. purpurea* isolates cannot be discounted.

Despite post-harvest removal of sclerotia by standard cleaning methods: colour sorting and gravity tables, ergot alkaloids have been detected in 'clean' grain samples (Beuerle et al., 2012; Byrd et al., 2017; MacDonald et al., 2017). Recent findings have suggested that alkaloids are localised towards the edge of the sclerotia and within the sclerotia groove (Nielen et al., 2014), such that even intact sclerotia can transfer alkaloids to otherwise healthy grain. In addition, sclerotia are brittle and can be broken during transport and indeed certain *C. purpurea* isolates have been observed to be more brittle than others (A. Gordon personal communication).

Due to our limited knowledge of alkaloid contamination of grain, as well as the lack of cereal varieties with good resistance to *C. purpurea* or approved fungicides to control ergot infection, grass weed management and good husbandry measures still remain the most effective methods of reducing ergot infection and therefore alkaloid contamination.

4.2.3 Policy Regulations of Alkaloid Levels

The European Union (EU) has certain principles for regulating contaminants in feed and food which apply to all stages of the production, processing and distribution chains. In addition, food law provides for the free movement within the EU of feed and food compliant with EU legislation. The main objectives of EU food law include a high level of protection of human health, protection of consumers' interests, and protection of animal health and welfare, plant health and the environment (Verstraete, 2008). Feed and food placed on the market has to be safe, while contaminant levels need to be kept as low as can reasonably be achieved following good practices at all stages of production and processing (Verstraete, 2008). In order for the EU to achieve these objectives legislation is based on risk analysis, a three-component process consisting of risk assessment, risk management and risk communication. While risk assessment is based on the available scientific evidence and undertaken in an independent, objective and transparent manner, risk management takes in to account the results of the risk assessment as well as the other factors that relate to the matter under consideration (Verstraete, 2008).

With regards to ergot alkaloids, the European Food Safety Authority, prompted by a European Commission request, submitted a scientific opinion where the establishment of a group acute reference dose (ARfD) of 1 µg/kg body weight (bw) and a group tolerable daily intake (TDI) of 0.6 µg/kg bw per day for the sum of the ergot alkaloids were reported (Beuerle *et al*., 2012). This led the Directorate General for Health and Food safety to propose introducing changes to the limits of sclerotia found in cereal grain and, unprecedentedly, to impose a threshold of total ergot alkaloids in processed grain, including milled products. Currently, ergot sclerotia content is set by the Commission Regulation (EC) No. 1881/2006 in unprocessed cereals (with the exception of corn and rice) used for humans, the amount of ergot sclerotia in food being restricted to a maximum of 0.05%. After years of debate and further data gathering by the industry, the measures will be voted on by the EC, and likely to be implemented from July 2021. For cereal milling products from wheat, spelt, barley and oats, a limit of 75–200 ppb will be set for alkaloids. For rye products, the limit will be higher c.250–500 ppb, while for cereal-based food for infants and young children it will be lower, < 50 ppb. The minimum levels of ergot sclerotia in unprocessed grain lots will be reduced to 0.02% (0.2g/kg), instead of the current 0.05% (0.5g/kg).

These new measures proposed by the EU will have effects on farmers, as well as the milling industry. While many mills already operate to a lower limit for ergot (0.01% or zero tolerance), more mills will be expected to operate to these stricter levels as evidence indicates that even a 0.02% sclerotia content of the grain would be too high to ensure compliance with processed product levels (Brennan, 2020). Therefore, farmers would also need to consider ergot as a serious compliance issue and would aim to clean grain prior to delivery to a mill in order to avoid the risk of rejection (Brennan, 2020).

4.2.4 Aims

Keeping in mind the serious implications of these policy changes on regulatory measures, as well as the gaps in our knowledge, the experiments in this chapter set out to determine to what extent ergot alkaloids may contaminate otherwise clean lots of grain, pre-harvest - within the ear, and post-harvest - during processing and transportation of grain. Specifically, the experiments presented here sought to address four main aims. Firstly, to determine whether ergot alkaloids are transferred from *C. purpurea* infected flowers to healthy grain developing in uninfected flowers on the same ear. Secondly, to determine whether the potential transfer of ergot alkaloids from *C. purpurea* infected flowers to healthy grain differs between cereal species, comparing wheat, barley and rye, and between pathogen isolates. Thirdly, to determine whether *C. purpurea* produces differing levels of ergot alkaloids in different fungal structures, comparing honeydew, sphacelia and sclerotia. Finally, to determine to what extent ergot alkaloids are transferred to clean grain during direct, physical contact with whole, partial and sclerotia dust.

4.3 Materials and methods

4.3.1 *Claviceps purpurea* inoculations and sample collection

4.3.1.1 Plant material

C. purpurea infection and alkaloid production were examined in three cereal species; wheat, barley and rye. The 2017 AHDB Recommended List wheat variety Mulika (Blackman Agriculture via Senova, spring wheat, nabim Group 1) and barley variety Concerto (Limagrain, spring barley, malting), and the descriptive list rye variety Mephisto (Saaten-Union, hybrid) were used. Plants were grown in a John Innes compost, with additional fertiliser, in 11cm pots in the glasshouse (16 hour day/8 hour night cycle, 10,000 lux sodium lights). Mephisto seedlings were vernalised for 8 weeks at 4^{o}C before transferring to the glasshouse.

4.3.1.2 *Claviceps purpurea* isolates

NIAB holds a collection of single-spore purified *C. purpurea* isolates collected from a range of cereal and grass species, from the UK, Germany and Canada. Seven single spore isolates of *C. purpurea* were used in this study (Table 4.1). Spores (conidia) of each isolate were revived from -80^{o}C storage and honeydew bulked on the spring wheat variety Mulika. The honeydew, containing conidia, was collected (10 to 14 days after inoculation; dai) and diluted in sterile water to a concentration of 1 x 10^{5} conidia/ml. The conidia were inoculated into flowers just before anthesis using a hypodermic syringe as described in Gordon et al. (2015).

Table 4.1: *Claviceps purpurea* isolates

***C. purpurea* isolates**	**Original host and location of origin**	**Year of collection**	**Additional info**
04-97.1	Black-grass (*Alopecurus myosuroides*); UK	2004	Strain used to ergot resistance study (Gordon et al., 2015)
04-41.1	Black-grass (*A. myosuroides*); UK	2004	UK isolate used in LINK study to identify resistance in UK winter wheat, 2008 (Bayles *et al*., 2009)
03-20.1	Wheat (*Triticum aestivum*); UK	2003	UK isolate used in LINK study to identify resistance in UK winter wheat, 2008
03-48.1	Wheat (*T. aestivum*); UK	2003	UK isolate used in LINK study to identify resistance in UK winter wheat, 2008
Rye 20.1	Rye (Secale cereale); Germany	unknown	The strain of *C. purpurea* - genome sequenced (https://fungi.ensembl.org/Claviceps_purpurea_20_1_gca_000347355/Info/Index)
EI2	Wheat (*T. aestivum*); Manitoba, Canada	1996	Canadian isolate used to identify resistance in durum wheat (Menzies, 2004)
EI4	Ergot sclerotia taken from seed cleaning plant; Manitoba, Canada	1996	Canadian isolate used to identify resistance in durum wheat (Menzies, 2004)

4.3.1.3 Pathogen inoculations and sampling

Experiments were undertaken to determine whether alkaloids produced by *C. purpurea* are able to transfer to "healthy" grain: The middle flowers on ears of the spring wheat variety Mulika, the barley variety Concerto and the rye variety Mephisto were inoculated with the *C. purpurea* isolate 04-97.1 (Figure 4.4). Isolate 04-97.1 is highly aggressive and results in high infection rates (Gordon et al., 2015). The central flowers of the 1st and 2nd ears of approximately 10 plants of each variety were inoculated just before anthesis, when the stigmas are fluffy but no pollen has been released (Zadoks Growth Stage 59), as described in Gordon et al. (2015). For wheat and rye the eight central flowers were inoculated, while for barley four central flowers were inoculated. Honeydew was collected into an Eppendorf tube from all inoculated flowers as soon as it appeared (approx. 10-14 dai) and stored at 4^{o}C. Fourteen dai

whole ears were harvested and sphacelia extracted and stored at -20°C. Other ears were left to allow ergot sclerotia and healthy grain to mature (approx. 6 weeks after inoculation). Each replicate honeydew, sphacelia and ergot sclerotia sample was made up of inoculated flowers from approximately 10 ears.

Mature grain was carefully dissected away from the ergot sclerotia that had formed in the middle flowers. Mature grain that had formed above and below the *C. purpurea* inoculated flowers was first removed from the ear, either by hand or using tweezers sterilised in 70% ethanol. For wheat 12-14 grains were harvested above and below the ergot per ear, for barley 8-10 grains were harvested, while 4-8 rye grains were harvested above and below as there were more blind florets due to lower pollination efficiency. Great care was taken not to allow the grain to come into physical contact with sclerotia that had formed in the middle, inoculated flowers. The grains that had developed below and above the *C. purpurea* inoculated flowers were kept as separate samples for alkaloid testing. Grain from uninoculated plants was used as a control. Once all grain had been removed from ears, the sclerotia, where formed, were collected from the middle, *C. purpurea* inoculated flowers. All sampling was carried out by one person to minimise variation introduced by human error.

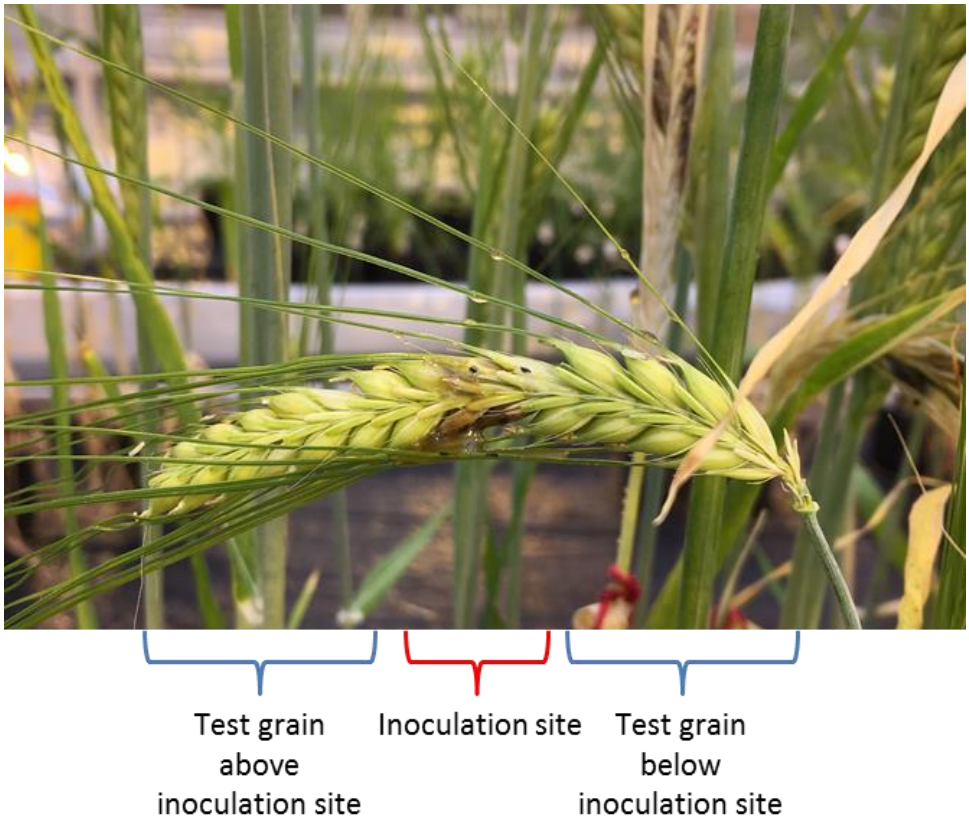

Figure 4.4: Experimental *Claviceps purpurea* inoculation procedure (barley ear pictured)

Experiments were undertaken to determine whether different isolates of *C. purpurea* produced different ergot alkaloid profiles. We inoculated the wheat variety Mulika with one of seven different single spore isolates (Table 4.1). Inoculation of middle flowers was carried out as for Expt.1. Honeydew, sphacelia, sclerotia were all collected for ergot alkaloid analysis.

The size of ergot sclerotia were analysed using the NIAB ergot size scale, 0–7 (Figure 3.3). Sclerotia from a single ear were analysed using a MARVIN seed analyser to determine the mean weight and means size or ergot sclerotia.

4.3.2 Ergot alkaloid assays

Sclerotia used to assess ergot alkaloid levels were selected in the size range 5–6 NIAB scale (7–11 mm in length Figure 3.5), with sclerotia from approximately 2–3 ears being pooled to make one replicate sample of 1g. To provide 1g of replicate sphacelial tissue approximately three infected ears were required. Honeydew was pooled from 8 to 12 ears to provide over 1ml per replicate. All *C. purpurea* samples were transported to Campden BRI on dry ice. On average, 2 to 3 inoculated ears were required to obtain the 1g of above or below grain required for each replicate ergot alkaloid assay. Three replicate samples of all test tissues were sent to Campden BRI for ergot alkaloid analyses.

The six major ergot alkaloids; ergocornine, ergocristine, ergocryptine, ergometrine, ergosine, ergotamine, and their respective –inine epimers were analysed by a LC-ECI-MS/MS procedure based on a published method (Krska and Crews, 2007). The ergot sclerotia and grain samples (0.5g) were ground and extracted into acetonitrile/ammonium carbonate buffer. The sphacelium samples were directly blended into the solvent/buffer mixture, while honeydew samples were resuspended in the buffer prior to extraction in the solvent/buffer solution. The extracted samples were finally cleaned-up by dispersive solid phase extraction (SPE), prior to LC-ESI-MS/MS determination with a limit of quantification for each ergot alkaloid and epimer of 4 µg/kg. This work was undertaken as a service by Camden BRI, Station Rd, Chipping Campden GL55 6LD, United Kingdom.

4.3.3 Physical transfer of ergot alkaloids to healthy grain

To determine to what extent ergot alkaloids could be transferred to clean grain during transportation and processing, when either whole or fragments of ergot sclerotia can come into physical contact with grain, we undertook "tumbling" experiments, as described below. Ergot sclerotia from the *C. purpurea* isolate 04-97.1 were produced as described above. Sclerotia were used whole or broken into fragments of approximately 0.5 to 5 mm in diameter in tumbling experiments with either wheat or barley grain. Two dose rates were used, one rate to match the current EU guidelines for allowable levels of ergot in grain (Regulation (EC) No 1881/2006: 0.5 g/kg in unprocessed cereals) and a higher rate (5 g/kg) to represent a worst-case scenario. Whole ergot sclerotia or sclerotia particles were added to 200g of Mulika spring wheat and Concerto spring barley grain. The samples were tumbled for 20 min in a Kek-Gardner blender, then spread onto a tray and visually screened for the presence of ergot sclerotia particles and sieved to remove dust. Sclerotia were removed and weighed to ensure full recovery. The grains were ground into wholegrain flour using a laboratory mill (LM 3100, Perten, Sweden) and the ergot alkaloid levels and profiles determined. The pipeline for these tumbling experiments is shown in Figure 4.5.

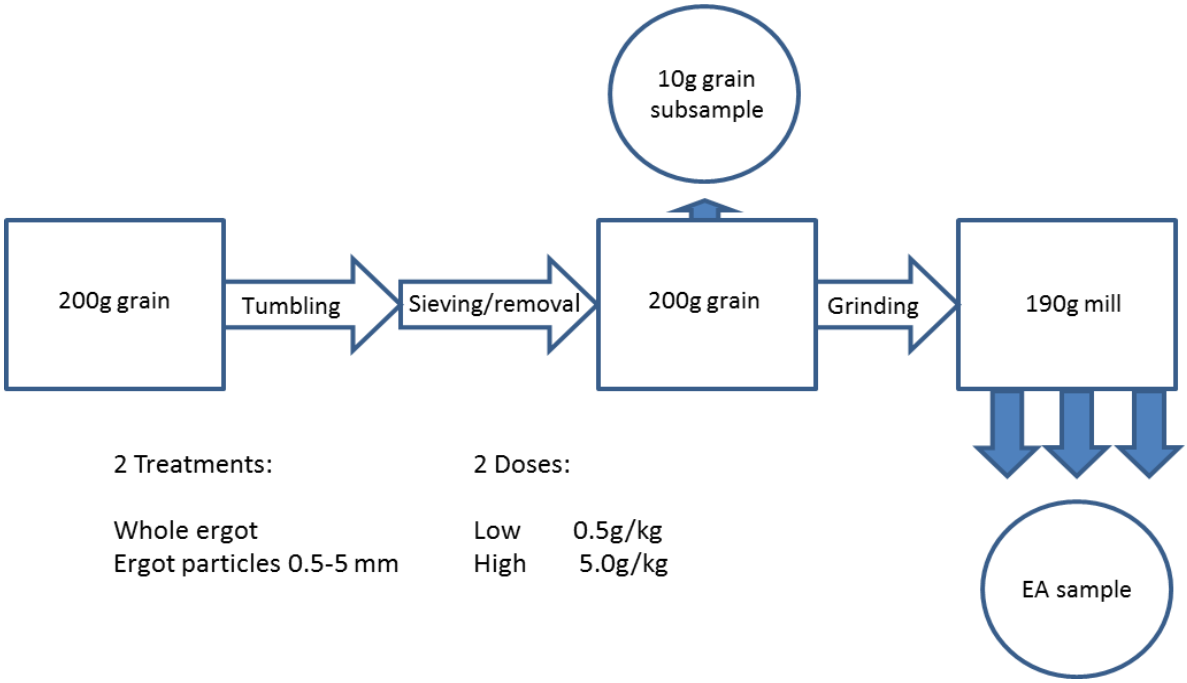

Figure 4.5: Experimental outline of tumbling experiments.

4.3.4 Statistical analyses

Significant variation between data sets was examined using a modified ANOVA approach, General Linear Regression, in Genstat v.16. The model applied was replicates + treatments. Significant differences, expressed as t-test values, were calculated for ergot sclerotia size, ergot sclerotia weight, and for total and individual ergot alkaloid content. No significant differences were detected between replicates in any of the analyses.

4.4 Results

4.4.1 Comparison of ergot infection and ergot alkaloid profiles on wheat between seven *Claviceps purpurea* isolates

In order to determine whether there are significant differences between different *C. purpurea* isolates in terms of sclerotia size and weight, as well as in terms of alkaloid levels across fungal tissues, the wheat variety Mulika was inoculated with one of seven isolates of *C. purpurea* (Table 4.1). Honeydew, sphacelia and mature ergot sclerotia were collected from three replicate experiments. The ergot alkaloid profiles found in each of the three fungal tissues were measured using LC-ECI-MS/MS for 12 different alkaloids. Mature ergot sclerotia collected from each ear were weighed and the size determined using the NIAB ergot size 0-7 scale (Figure 3.5).

4.4.1.1 Variation in ergot sclerotia size and weight between seven isolates of *Claviceps purpurea*

Statistical analyses revealed that ergot sclerotia produced by different *C. purpurea* isolates on wheat were significantly different in terms of their mean size (recorded as a mean sclerotia size per ear; $F = 5.56$, $p < 0.001$) and mean weight (recorded as a mean sclerotia weight per ear; $F = 14.44$, $p < 0.001$) (Figure 4.6). Isolate 04-97.1 produced the largest sclerotia, and significantly larger sclerotia than isolates EI4 and Rye 20.1 ($t < 0.001$), but not significantly larger than the other four isolates. More variation was observed in the weight of mature sclerotia, with isolates 04-97.1 and 03-20.1 producing significantly heavier sclerotia than EI4, EI2, Rye 20.1, 03-48.1 and 04-41.1 (all at $t < 0.001$). No significant differences in terms of sclerotia weight were detected between the isolates 04-97.1 and 03-20.1 ($t = 0.856$). Significant differences ($F = 4.39$, $p < 0.001$) in the total number of sclerotia produced per ear were found, the isolates 03-48.1, 04-41.1, EI2 and EI4 producing fewer sclerotia than the other three isolates.

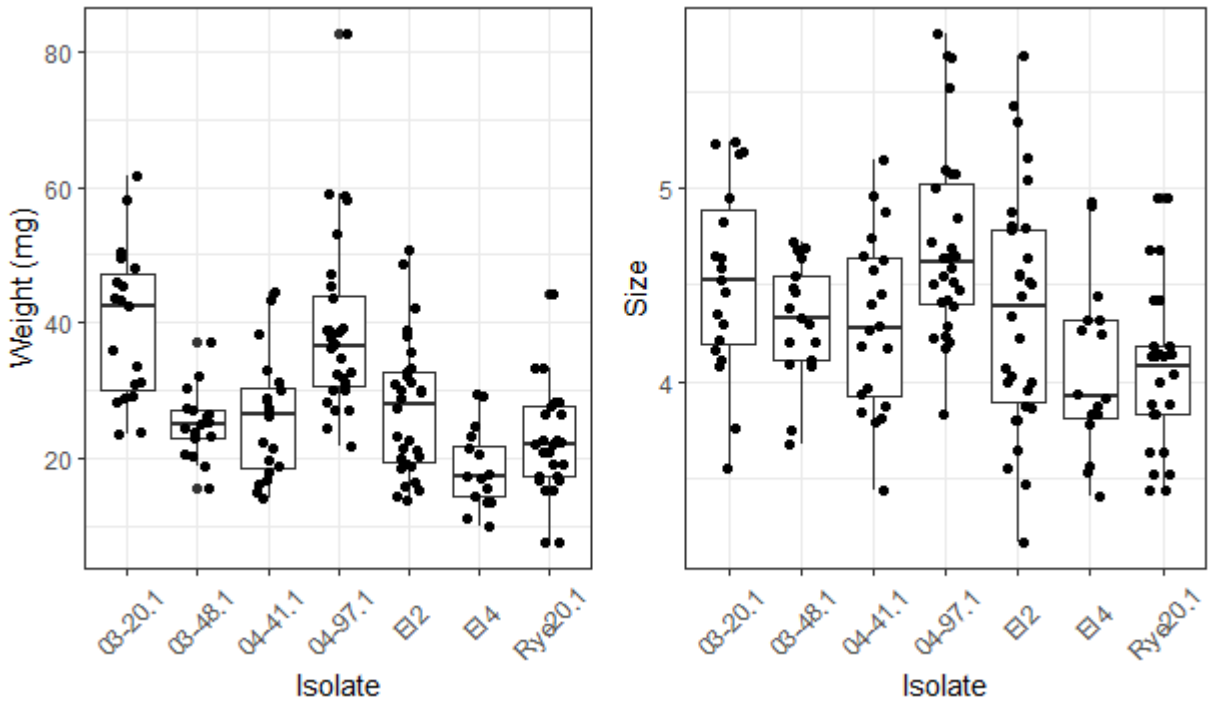

Figure 4.6: Box and whisker plots of mature ergot sclerotia size and weight data. Each data point represents the mean size or weight of sclerotia collected from a single ear. The box defines the upper and lower quartile and shows the median values.

4.4.1.2 Variation in ergot alkaloids in fungal tissues from seven isolates of *Claviceps purpurea*

The total ergot alkaloid levels (the sum of the 12 individual ergot alkaloids measured) (Figure 4.7), as well as the proportions of the 12 individual ergot alkaloids (Figure 4.8) in honeydew, sphacelia and mature ergot sclerotia of seven *C. purpurea* isolates grown on the wheat variety Mulika were determined. No significant differences were detected between replicates in any of the analyses. Big significant differences were found in the total alkaloid levels found in each fungal tissue, with low levels being found in honeydew, accumulating in sphacelia, and finally reaching their highest levels in the mature sclerotia. The proportions of individual alkaloids differed between isolates, but were generally similar across the three fungal tissues, the exceptions being isolates EI2, EI4 and Rye 20.1 where higher levels of ergometrine and lower levels of ergocryptine where observed in honeydew compared to sphacelia or mature sclerotia (Figure 4.8). Overall, the most prevalent alkaloid in isolates 03-20.1, 04-41.1 and 04-97.1 was ergocristine, followed by ergocristinine, ergotamine or ergocristinine and finally ergotaminine. Compared to these isolates, isolate 03-48.1 exhibited

higher levels of ergosine and ergosinine (Figure 4.8). Furthermore, isolates EI4 and Rye 20.1 contained high levels of ergocryptine and ergocryptinine; alkaloids that were not observed in the other five isolates (Figure 4.8).

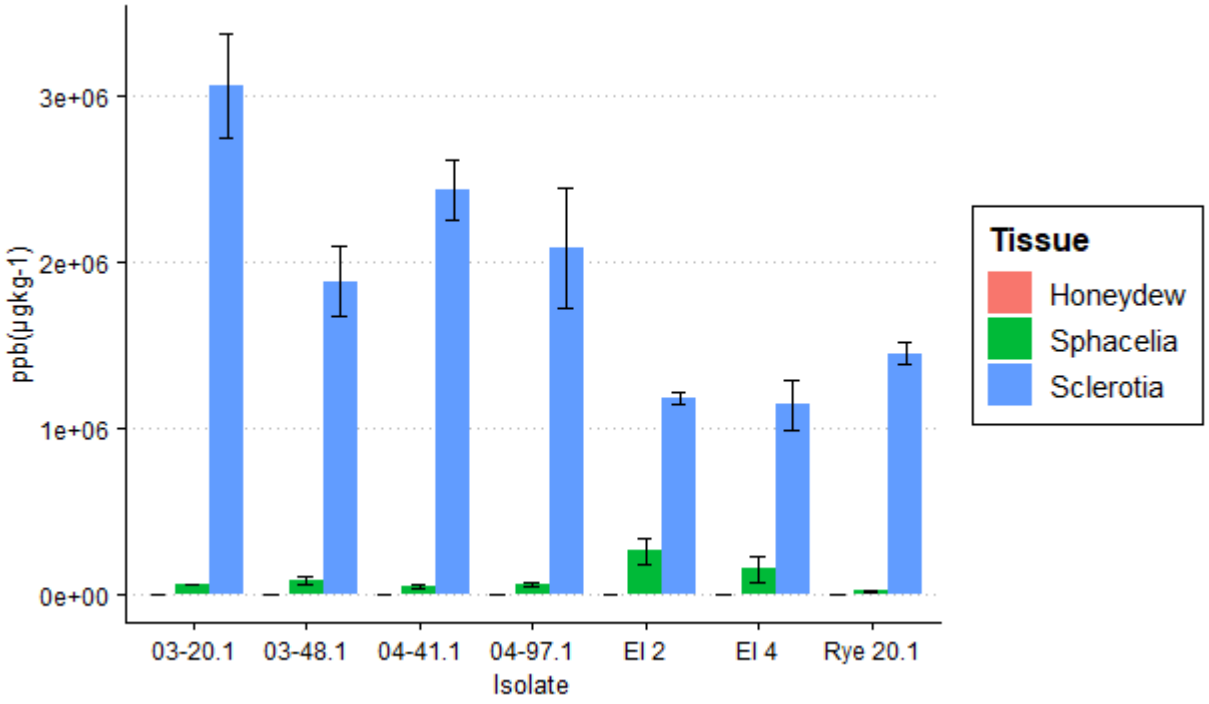

Figure 4.7: Levels of total ergot alkaloids in *Claviceps purpurea* tissues (mean values). The total ergot alkaloid levels (parts per billion) in honeydew, sphacelia and sclerotia of seven *C. purpurea* isolates grown on the wheat variety Mulika. The error bars show standard errors.

In honeydew, isolates did not differ significantly ($F = 5.02$, $p = 0.009$) with regards to their total alkaloid levels, but did differ significantly with regards to the levels of each of the 12 individual ergot alkaloids. Specifically, ergosine was found to be significantly different between the various isolates ($F = 45.85$, $p < 0.001$).

No significant differences were found between the isolates with regards to total ergot alkaloid levels found in sphacelia ($F = 3.82$, $p = 0.023$). Nevertheless, individual alkaloid levels did exhibit significant differences between isolates. These differences were observed for ergocornine ($F = 26.27$, $p < 0.001$), ergocorninine ($F = 9.50$, $p = 0.001$), ergocristine ($F = 38.08$, $p < 0.001$), ergocristinine ($F = 21.47$, $p < 0.001$), ergocryptinine ($F = 15.37$, $p < 0.001$), ergosine ($F = 18.73$, $p < 0.001$), ergotamine ($F = 9.01$, $p < 0.001$), and ergotaminine ($F = 7.99$, $p = 0.001$).

Unlike honeydew and sphacelia, mature sclerotia were found to have significant differences between isolates for total ergot alkaloid levels ($F = 9.15$, $p < 0.001$). The highest alkaloid levels were observed in isolate 03-20.1 which reached a total level of 3 million ppb. Furthermore, all 12 alkaloids exhibited significant differences between the 7 isolates at a $p < 0.001$ and with F values ranging between 16.22 (ergocristinine) and 364.00 (ergocryptinine).

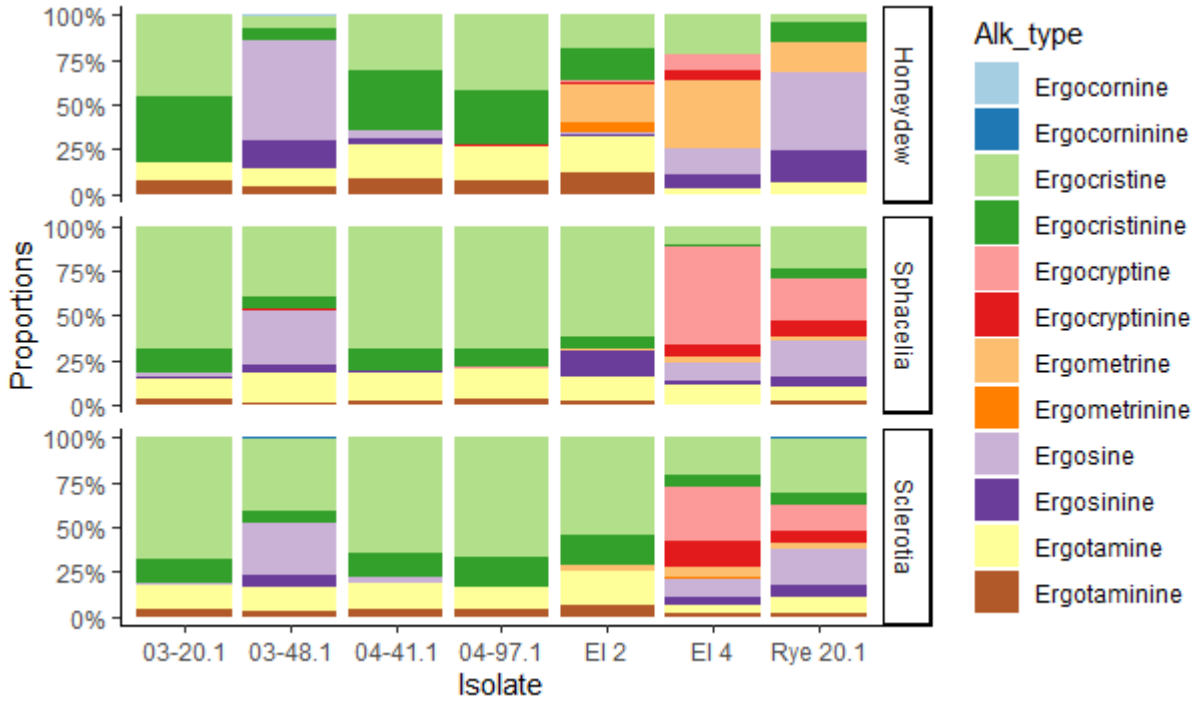

Figure 4.8: Proportions of 12 ergot alkaloids (Alk_type) found in honeydew, sphacelia and sclerotia of seven *Claviceps purpurea* isolates grown on the wheat variety Mulika.

4.4.2 Comparison of *Claviceps purpurea* inoculations on wheat, barley and rye

In order to determine whether there are significant differences in *C. purpurea* development, in terms of sclerotia size and weight, as well as alkaloid level in different fungal tissues, when grown on different host cereals the wheat variety Mulika, the barley variety Concerto and the rye variety Mephisto were all inoculated with the *C. purpurea* isolate 04-97.1. Collection of fungal tissues and measurements of alkaloid levels were conducted as described in section 4.1.

4.4.2.1 Variation in ergot sclerotia size and weight of *Claviceps purpurea* grown on different cereal species

Statistical analyses revealed that the *C purpurea* isolate 04-97.1 produced significantly heavier sclerotia (recorded as a mean sclerotia weight per ear) on the wheat variety Mulika than the barley variety Concerto or the rye variety Mephisto ($F = 12.83$, $p < 0.001$; Figure 4.9). Barley and rye did not produce sclerotia that differed significantly from each other in terms of weight ($t = 0.373$). Significant differences were also found for sclerotia mean size per ear (recorded as mean size per ear; $F = 9.08$, $p < 0.001$). However, sclerotia were only significantly bigger on barley compared to rye ($t < 0.001$), no significant differences in sclerotia size were found between wheat and barley, or between wheat and rye (Figure 4.9). This would suggest that the sclerotia produced on the barley variety Concerto were less dense than those produced on wheat, with a potential lower fungal biomass. Alternatively, sclerotia produced on barley could potentially be narrower as the criterion for size in the MARVIN seed analyser was length and the ergots from wheat were observed to visually be broader compared to barley.

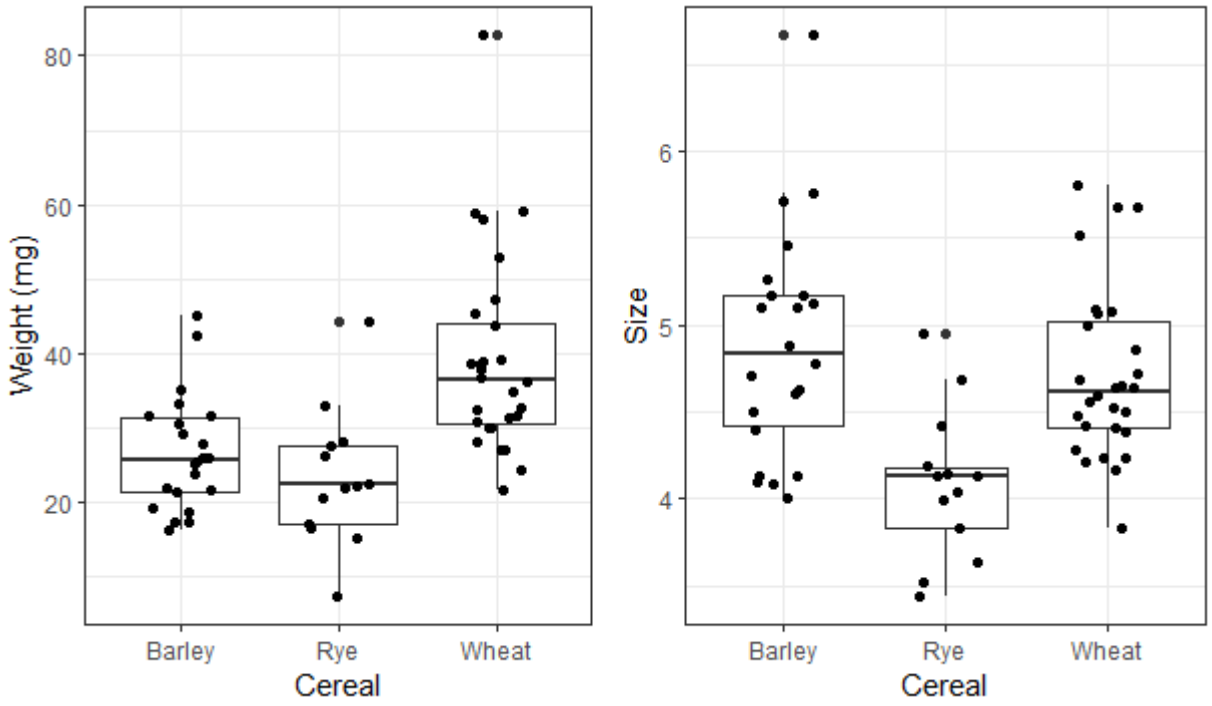

Figure 4.9: Box and whisker plots of mature ergot sclerotia size and weight data from *C. purpurea* isolate 04-97.1 grown on three cereal hosts. Each data point represents the mean size (length) or weight of sclerotia collected from a single ear. The box defines the upper and lower quartile and shows the median values.

4.4.2.2 Variation in ergot alkaloid profiles produced by *C. purpurea* isolate 04-97.1 grown on different cereal species

Honeydew and sphacelia of *C. purpurea* isolate 04-97.1 grown on wheat and barley were collected, while mature ergot sclerotia were collected from wheat, barley and rye. Total ergot alkaloids (Figure 4.10) were examined in each fungal tissue. Total alkaloid levels were significantly different between the three fungal tissues, with honeydew exhibiting only low levels, levels rising in sphacelia and the highest levels of alkaloids being seen in mature sclerotia. Detection of alkaloids in honeydew and sphacelia shows that alkaloids are synthesized in the early stages of infection (>14 days).

In honeydew and sphacelia wheat had a higher concentration of total ergot alkaloids than barley, although this was not statistically significant; honeydew ($F = 3.74$, $p = 0.193$) and sphacelia ($F = 13.44$, $p = 0.067$). While in mature sclerotia rye exhibited the highest ergot alkaloid concentration, but again this was not statistically significant ($F = 2.36$, $p = 0.210$).

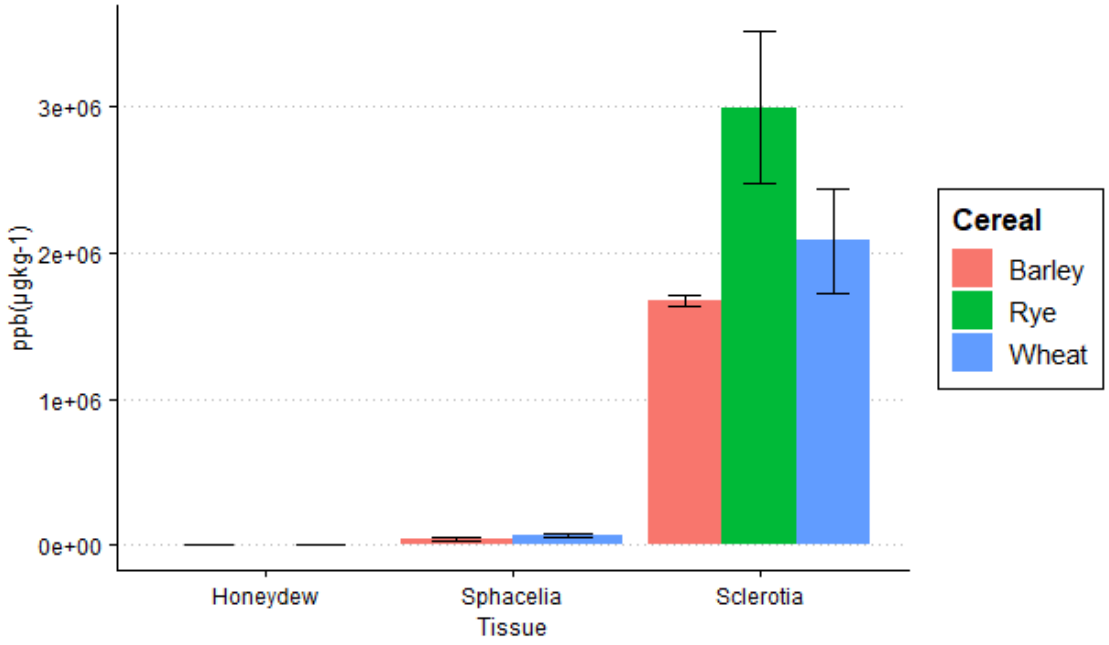

Figure 4.10: Mean levels of total ergot alkaloids in *Claviceps purpurea* tissues. The total ergot alkaloid levels (parts per billion) in honeydew, sphacelia and sclerotia of the *C. purpurea* isolate 04-97.1 grown on the wheat variety Mulika, barley variety Concerto and rye variety Mephisto. The error bars show standard errors.

The profiles of the 12 ergot alkaloids in honeydew, sphacelia or mature ergot sclerotia produced by *C. purpurea* isolate 04-97.1 (Figure 4.11) showed no significant differences between wheat, barley and rye at an F-probability of < 0.001, indicating that the host did not influence ergot alkaloid profiles. Across cereal species, the most prevalent alkaloid found within sphacelia and sclerotia was ergocristine followed, in most cases, by ergotamine, ergocristinine and finally by ergotaminine (Figure 4.11). In honeydew, the increased levels of ergocristinine compared to ergocristine could be attributed to the fact that these two compounds are epimers of each other and have the ability to interconvert under differing environmental conditions such as light, and is therefore unlikely to be as a result of any underlying biological differences.

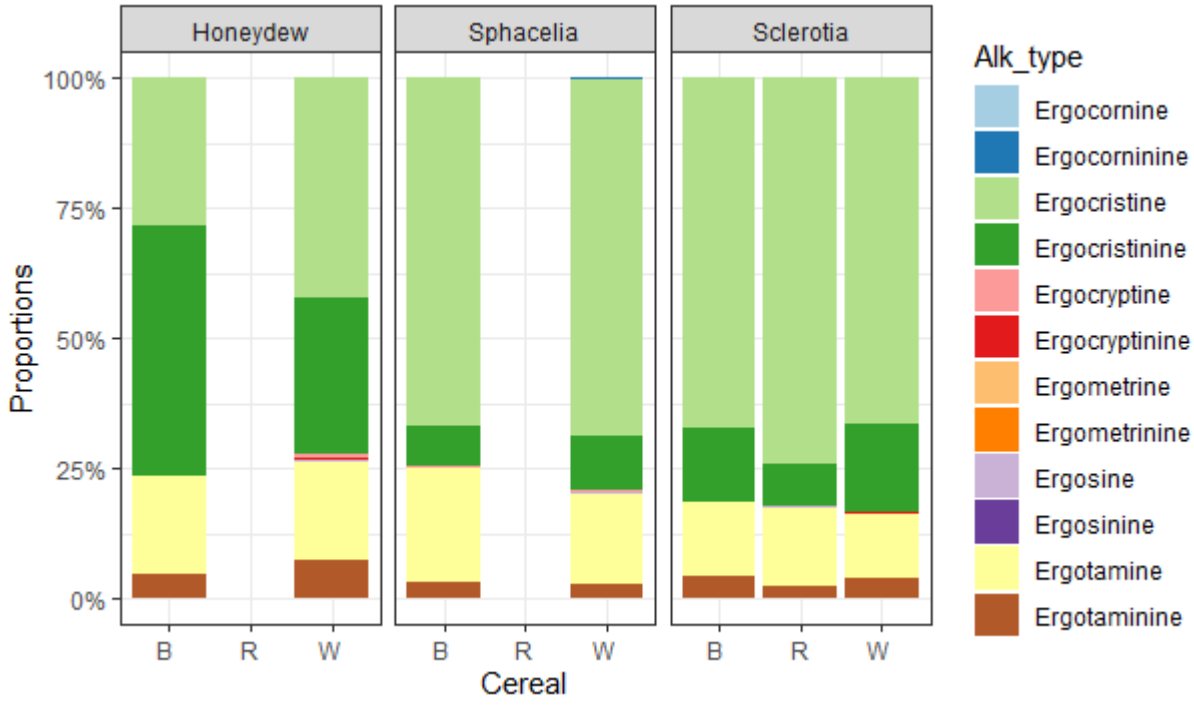

Figure 4.11: Proportions of ergot alkaloids in *Claviceps purpurea* fungal tissues grown on different cereal hosts. The proportion of 12 ergot alkaloids (%) found in honeydew, sphacelia and sclerotia of *C. purpurea* isolate 04-97.1 grown on the wheat variety Mulika (W), the barley variety Concerto (B) and the rye variety Mephisto (R).

4.4.3 Ergot alkaloid profiles on healthy grain formed above and below flowers infected with *Claviceps purpurea*

In order to determine whether ergot alkaloids can transfer from *C. purpurea* infected flowers onto or into healthy grain within the same ear, middle flowers of wheat, barley and rye were inoculated with isolate 04-97.1. Healthy grain that developed above and below the infection flowers were harvested and tested for the presence of ergot alkaloids (Figure 4.12).

Ergot alkaloids were detected in the healthy grain samples collected from above and below the infected flowers in all three cereal species (Figure 4.12). Total alkaloid levels ranged from 162,792 ppb found in one replicate of wheat grain above the infection site, to 5 ppb found in one replicate of rye grain above the infection site. While large differences in total alkaloid levels were observed between replicates, no statistically significant differences were found (F-probability = 0.065). Furthermore, neither the cereal species (F-probability = 0.197) nor the position of healthy grain (above and below the infection site) (F-probability = 0.298) were found to have a significant effect on the total level of alkaloids.

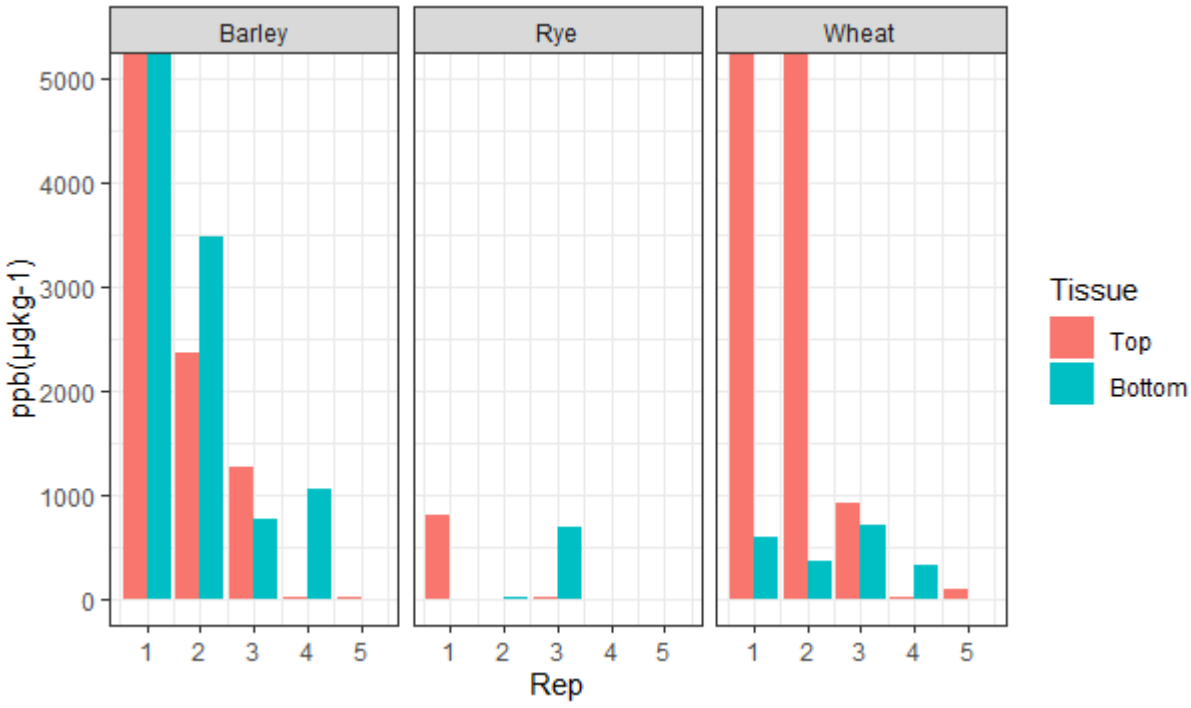

Figure 4.12: The total ergot alkaloid levels (parts per billion) in grain that developed above (top) and below (bottom) flowers inoculated with the *C. purpurea* isolate 04-97.1 grown on the wheat variety Mulika, barley variety Concerto and rye variety Mephisto. The total ergot alkaloid levels of individual replicate tests are shown. (Axis capped at 5000 ppb).

Despite the fact that the levels of individual alkaloids were not found to be significantly different between grain positions and cereal species (probably due to the very large difference between replicates), it is apparent (Figure 4.12) that in rye healthy grain is less contaminated.

A comparison of the 12 ergot alkaloids indicated similarities in the profiles of each alkaloid in healthy grain that developed above and below the infection site in wheat, barley and rye (Figure 4.13, Figure 4.14). However, the profiles of ergot alkaloids found in grain were, in many cases, different to those found in fungal tissue (Figure 4.11). Alkaloid profiles in healthy grain were far more diverse than those detected in mature sclerotia. Notably, in the healthy grain formed below the inoculation poin in barley and wheat, alkaloids such as ergocornine, ergocorninine, ergocryptine, ergocryptinine, ergometrine, ergometrinine, ergosine and ergosinine were detected (Figure 4.13, Figure 4.14). These alkaloid types were absent from mature sclerotia, which mainly contained ergocristine, ergocristinine, ergotamine and ergotaminine (Figure 4.11). This would indicate the ability of *C. purpurea* isolate 04-97.1 to produce a wide range of ergot alkaloids, but a preference to accumulate a subset of these alkaloids in sclerotia, specifically on wheat and barley. On rye grain the profiles of ergot alkaloids were less diverse.

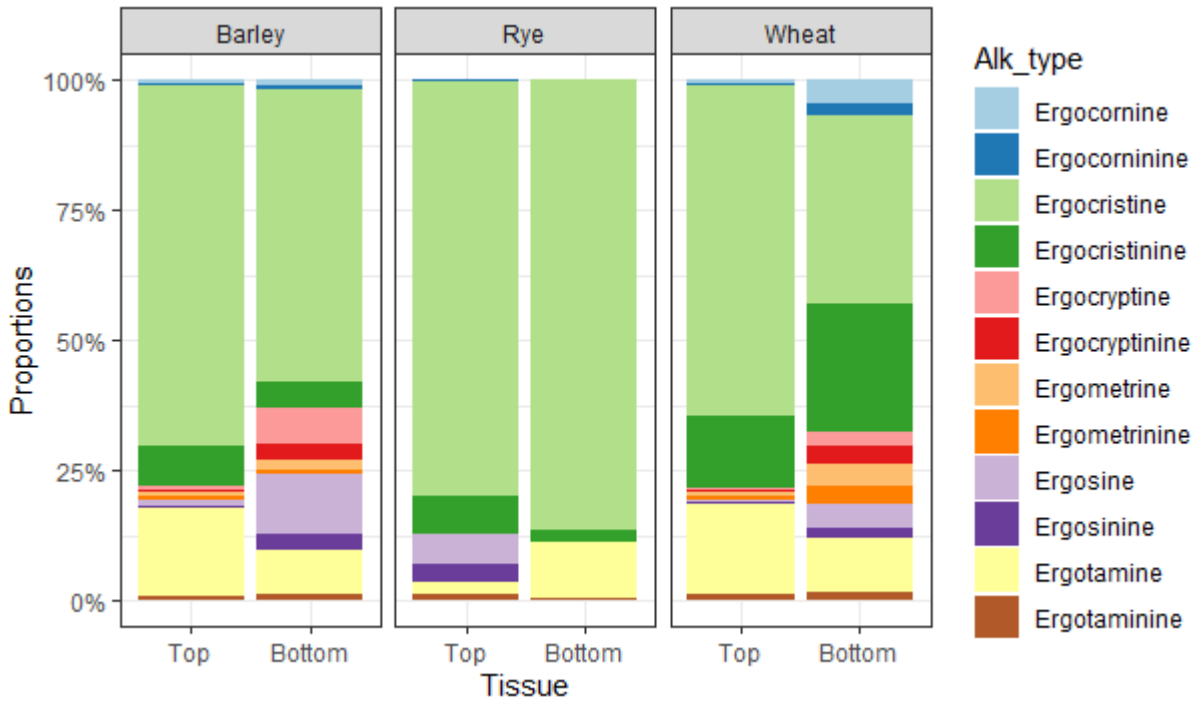

Figure 4.13: The proportion of 12 ergot alkaloids (%) found in grain that developed above (Top) and below (Bottom) flowers inoculated with the *C. purpurea* isolate 04-97.1 grown on the wheat variety Mulika, barley variety Concerto and rye variety Mephisto. The proportions of replicate means are shown.

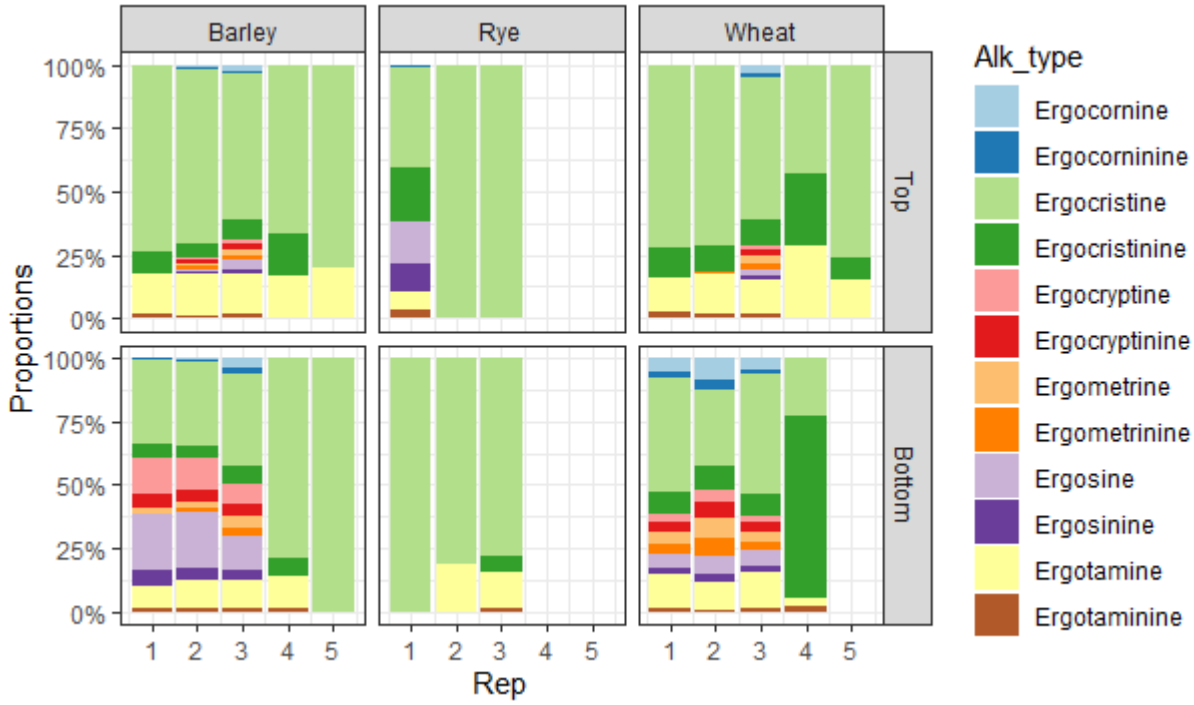

Figure 4.14: The proportion of 12 ergot alkaloids (%) found in grain that developed above (Top) and below (Bottom) flowers inoculated with the *C. purpurea* isolate 04-97.1 grown on the wheat variety Mulika, barley variety Concerto and rye variety Mephisto. The proportions of individual replicate tests are shown.

4.4.4 Comparisons between three *Claviceps purpurea* isolates inoculated on wheat and barley

The above findings, and particularly the detection of alkaloids on healthy grains that developed above and below flowers infected with *C. purpurea*, prompted the repetition of the experiment. In order to confirm the transfer of ergot alkaloids from *C. purpurea* infected flowers to healthy grain within the same ear, middle flowers of wheat and barley were inoculated again using isolate 04-97.1. In addition, two more isolates were included in this experiment in order to determine whether there are differences between isolates with respect to the transfer of ergot alkaloids to healthy grain. The isolates EI4 and Rye 20.1 were chosen for their differing alkaloid profiles compared to isolate 04-97.1, as well as for their diversity of alkaloids (as observed in Figure 4.8).

4.4.4.1 Variation in ergot sclerotia size and weight between three isolates of *Claviceps purpurea* grown on wheat and barley

Statistical analyses revealed no significant differences in mean weight ($F = 0.36$, $p = 0.701$) and mean size ($F = 0.85$, $p = 0.431$) of mature sclerotia produced by the three isolates, either on barley or wheat (Figure 4.15). While isolate 04-97.1 produced heavier and bigger (albeit not significantly) sclerotia than those produced by isolates EI4 and Rye 20.1 on wheat, the same could not be said for the sclerotia it produced on barley. On barley isolate 04-97.1 produced lighter and smallest sclerotia compared with the other two isolates (Figure 4.15). This would suggest a greater adaption of isolate 04-97.1 to wheat.

Comparing cereal hosts, significant differences were detected for both mean weight ($F = 47.15$, $p < 0.001$) and mean size ($F = 46.20$, $p < 0.001$) of ergot sclerotia. Specifically, wheat was found to support the growth of significantly heavier and bigger sclerotia than barley with all three isolates. This was in contrast to the first experiment, where isolate 04-97.1 produced larger sclerotia on barley than wheat, although the sclerotia on barley were significantly lighter, as in this repeat experiment.

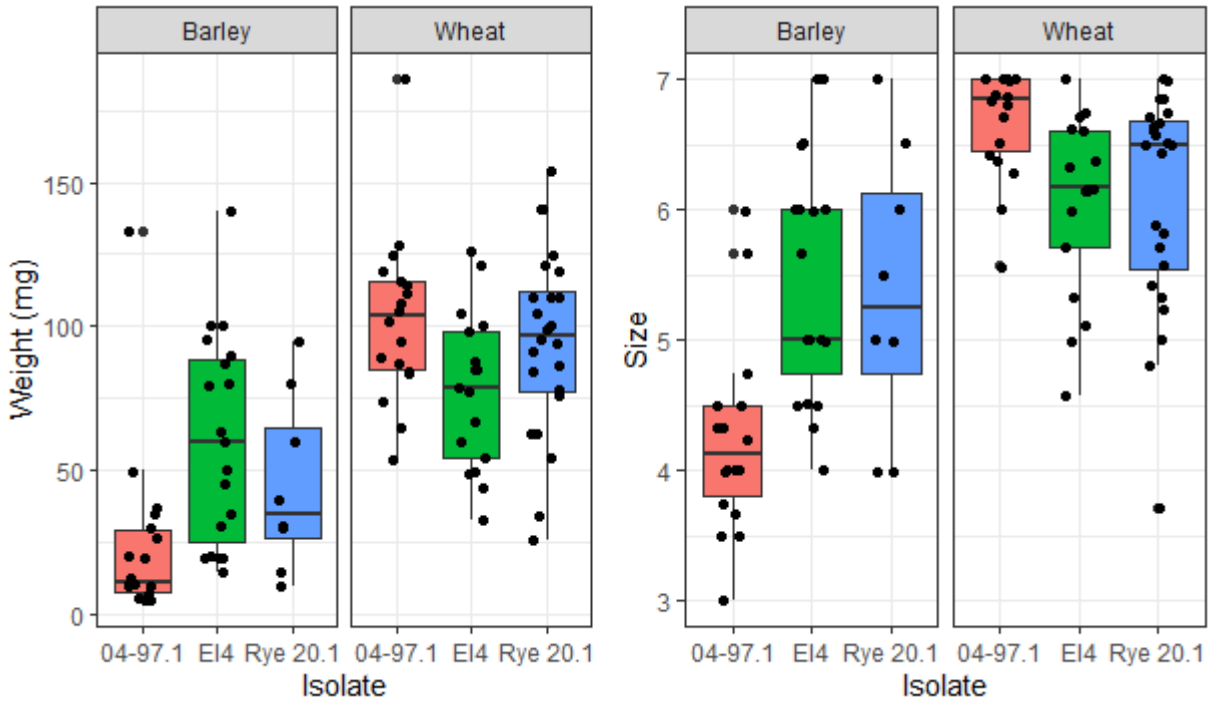

Figure 4.15: Box and whisker plots of mature ergot sclerotia size and weight data from *C. purpurea* isolates 04-97.1, EI4, and Rye 20.1 grown on two cereal hosts. Each data point represents the mean size (length) or weight of sclerotia collected from a single ear. The box defines the upper and lower quartile and shows the median values.

4.4.4.2 Variation in ergot alkaloids in *Claviceps purpurea* isolates 04-97.1, EI4 and Rye 20.1 grown on different cereal species

Mature sclerotia from all three *C. purpurea* isolates produced higher levels of total ergot alkaloids when grown on wheat than on barley (Figure 4.16). Isolate 04-97.1 sclerotia contained the highest levels of alkaloids, followed by isolates EI4 and Rye 20.1. This trend was seen in both wheat and barley (Figure 4.16). Despite these observations, no actual statistically significant differences were found between the cereal species or isolates for total ergot alkaloid levels in sclerotia.

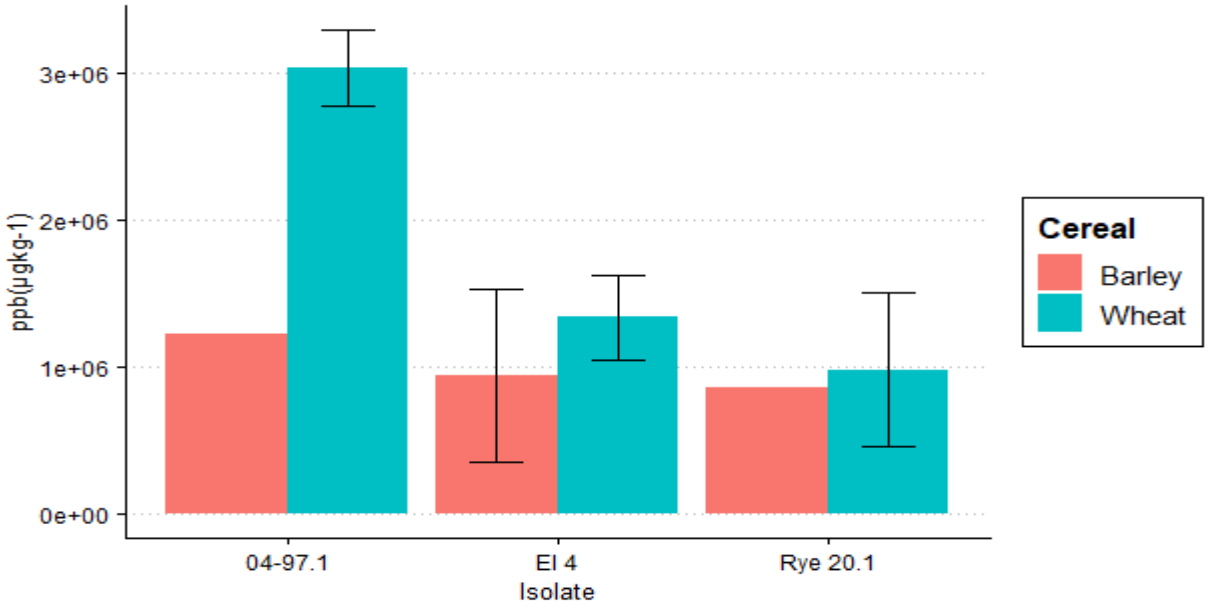

Figure 4.16: The total ergot alkaloid levels (parts per billion) in sclerotia of three *Claviceps purpurea* isolates grown on the wheat variety Mulika and the barley variety Concerto. The error bars show standard errors. Standard errors could not be calculated for the 04-97.1 and Rye 20.1 isolates in barley as there were enough sclerotia for only a single replicate.

Visually, the profiles of EAs in a comparison between wheat and barley, the EI4 isolate was most different between hosts. (Figure 4.17). Specifically, sclerotia from isolate EI4, grown on wheat contained ergocristine and ergocristinine in addition to the individual alkaloids found on sclerotia from barley. Compared to the first experiment (Figure 4.11), where only isolate 04-97.1 was used to inoculate wheat and barley, the profiles of individual alkaloids in sclerotia formed on wheat and barley are very similar. Furthermore, for both cereal species, the alkaloid profiles observed for isolates 04-97.1 and EI4 are similar to those previously found in wheat

(Figure 4.8). In contrast, the isolate Rye.20.1 resulted in a profile that lacked the diversity of alkaloids that was previously observed (Figure 4.8).

Figure 4.17: Proportions of 12 ergot alkaloids (%) found in sclerotia of three *C. purpurea* isolates grown on the wheat variety Mulika and the barley variety Concerto. Alk_type – Individual alkaloids measured.

With regards to individual alkaloid levels, ergotaminine was found to be significantly different between the isolates ($F = 19.77$, $p = 0.001$). Specifically, the isolate EI4 contained significantly less ergotaminine than isolate 04-97.1. No other individual alkaloids exhibited significant differences between isolates, and no significant differences were detected for individual alkaloid levels in sclerotia between wheat and barley (Figure 4.17).

4.4.4.3 Ergot alkaloid profiles on healthy grain formed above and below flowers infected with *Claviceps purpurea*

Alkaloids were detected within healthy grains that had developed above and below the flowers inoculated with *C. purpurea*, with all three isolates, in both wheat and barley (Figure 4.18). However, the alkaloid levels observed were overall much lower than those detected in the first experiment (Figure 4.12). While barley exhibited grain with slightly higher levels of alkaloid than wheat, neither the cereal species nor the position of healthy grain (above and below the infection site) were found to have a significant effect on the total level of alkaloids. Furthermore, no significant differences were found between isolates.

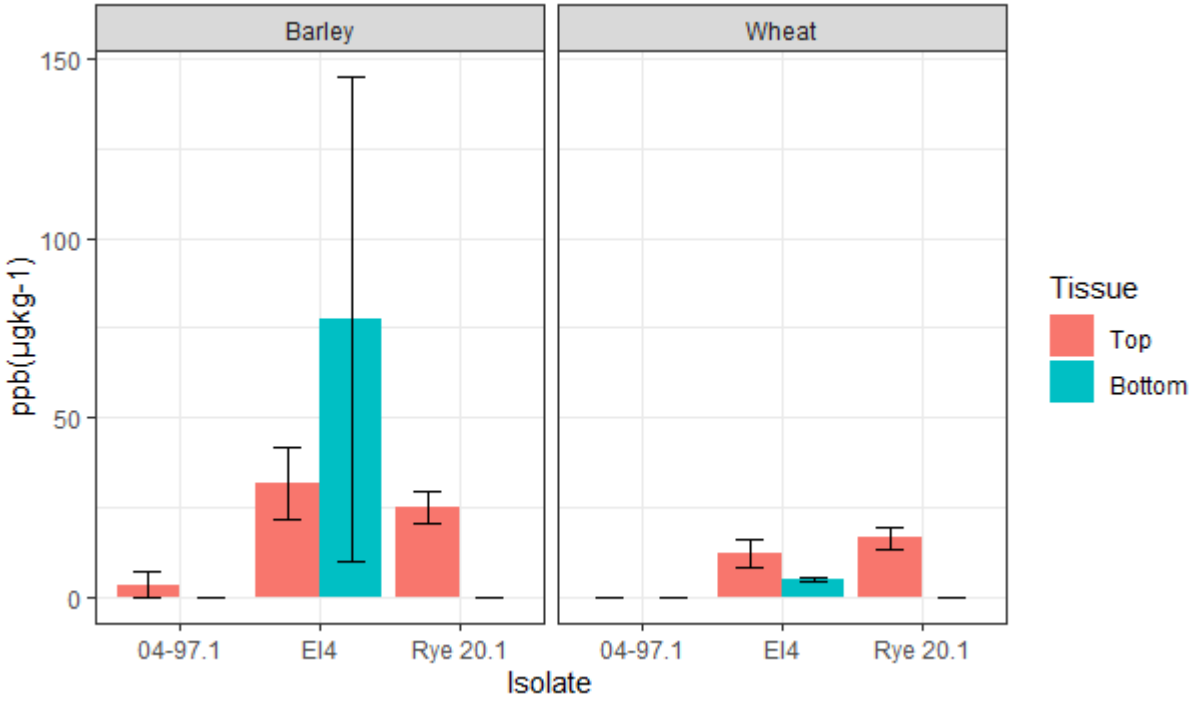

Figure 4.18: The total ergot alkaloid levels (parts per billion) in grain that developed above (top) and below (bottom) flowers inoculated with the *Claviceps purpurea* isolate 04-97.1, EI4, and Rye 20.1 grown on the wheat variety Mulika and barley variety Concerto. Lack of a bar for certain grain positions in certain isolates signifies that no values were found to be above the limit of quantification (LOQ).

Similarly, no significant differences were found when individual alkaloids were analysed. However visual differences were observed between the alkaloid profiles found on the healthy grain in the previous experiment and in this repeat experiment. (Figure 4.13, Figure 4.19). In this experiment alkaloid profiles of healthy grain were far less diverse than detected

previously, and resembled the profiles seen in the mature sclerotia in the first experiment (Figure 4.11).

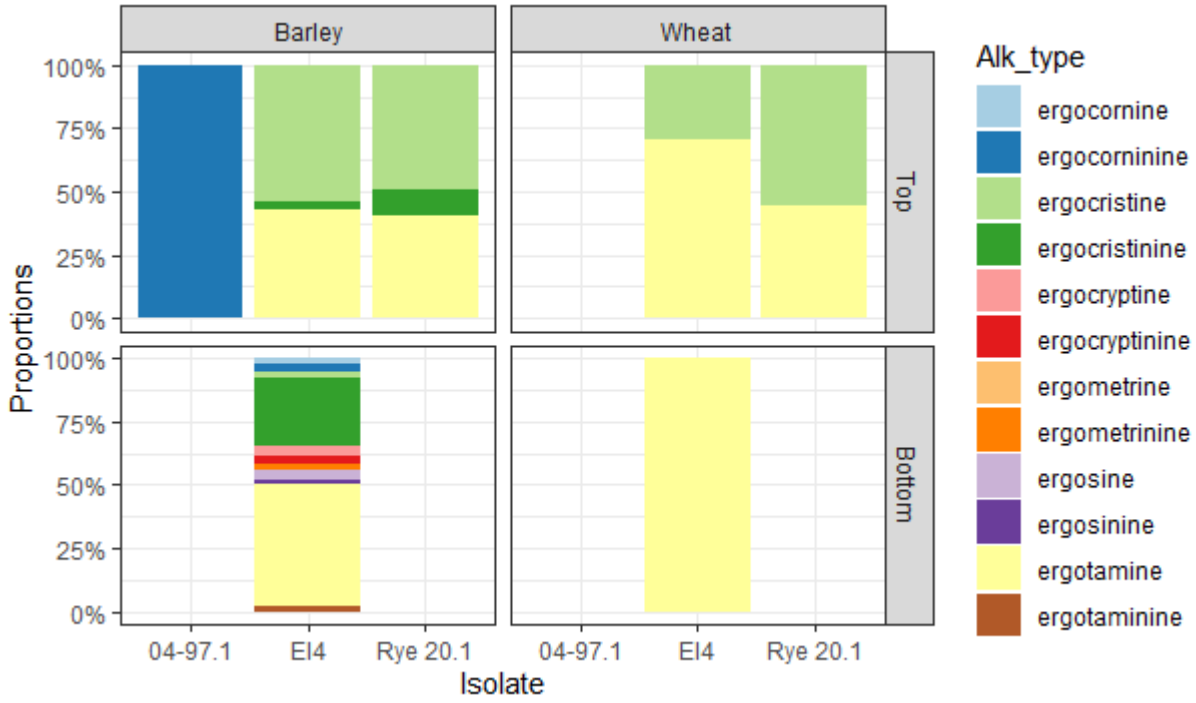

Figure 4.19: The proportion of 12 ergot alkaloids (%) found in grain that developed above (Top) and below (Bottom) flowers inoculated with the *Claviceps purpurea* isolate 04-97.1, EI4 and Rye 20.1 grown on the wheat variety Mulika, and barley variety Concerto. The observed gaps are due to the amounts of alkaloids being below the limit of quantification (LOQ).

4.4.5 Physical transfer of ergot alkaloids to clean grain

In order to determine to what extent ergot alkaloids are transferred to clean, healthy grain during direct, physical contact with whole sclerotia and sclerotia pieces, clean grain of wheat and barley was subjected to physical contact with whole sclerotia and broken sclerotia using a tumbling process. Two ratios of grain to sclerotia were tested, 0.5g and 5g of sclerotia per kilogram of grain. After tumbling the ergot sclerotia were removed by hand, the dust was sieved away, and the grain tested for the presence of ergot alkaloids.

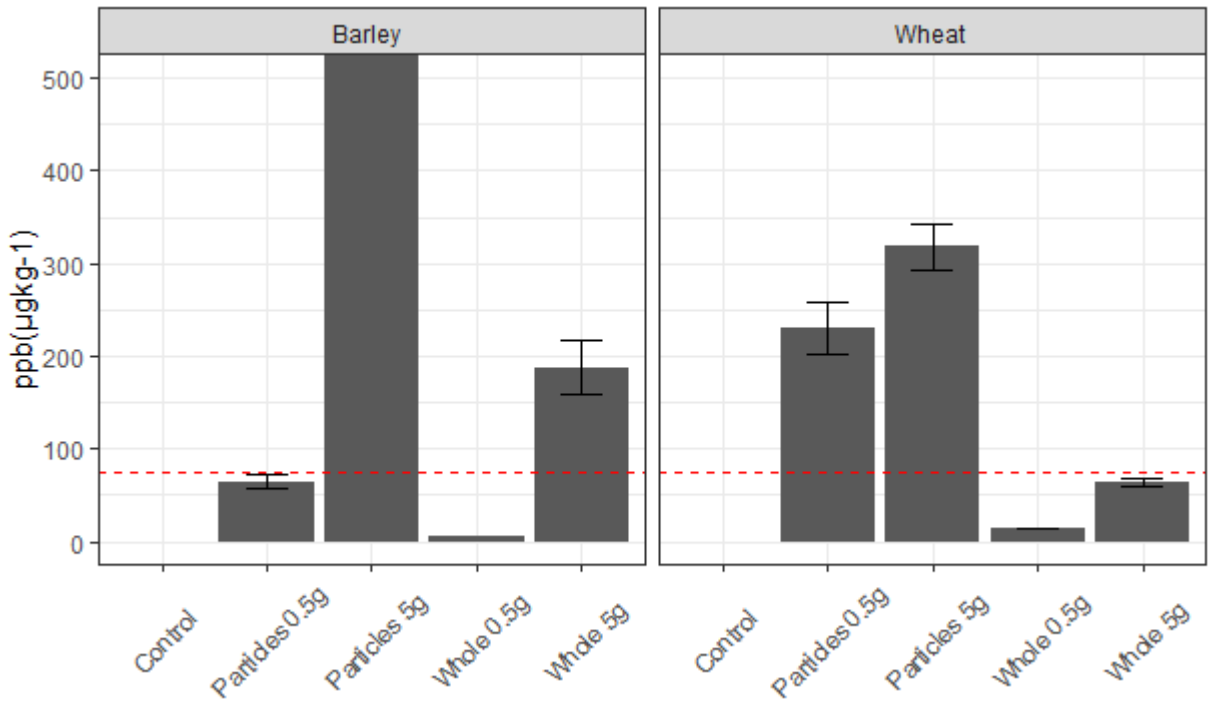

Figure 4.20: Total ergot alkaloid levels found on clean wheat and barley grain that had been in direct physical contact with whole mature ergot sclerotia, or broken particles of sclerotia. Two ratios of grain to sclerotia were tested, 0.5g of sclerotia and 5g of sclerotia per kg of grain. (Axis capped at 500 ppb). The red dashed line intersects the y axis at 75 pbb.

Broken sclerotia transferred significantly higher levels of ergot alkaloids to clean grain of both wheat and barley than whole sclerotia ($F = 595.04$, $p < 0.001$), and the higher the concentration of sclerotia (i.e. 5g per kg of grain) the higher the levels of alkaloids detected on grains of both cereals with barley exhibiting the highest levels at 1462.243 µg/kg (Figure 4.20). However, significant differences were found between the two cereal species ($F = 271.51$, $p < 0.001$). A significant interaction between cereal grain and the nature (whole or broken) and concentration of ergot sclerotia ($F = 315.23$, $p < 0.001$) was also found. The concentration of broken sclerotia had a significant effect on the levels of alkaloids found on clean grain of barley and wheat, with the higher concentration of broken sclerotia transferring more ergot alkaloids to barley grain, compared to wheat. In contrast, the lower concentration of broken sclerotia resulted in higher levels of ergot alkaloids being transferred to wheat grain (Figure 4.20).

With regards to the individual alkaloids, both barley and wheat grains contained primarily ergocristine, ergocristinine, ergotamine and ergotaminine (Figure 4.21). Significant differences were observed between barley and wheat for ergocristine ($F = 150.20$, $p < 0.001$), ergocristinine ($F = 514.04$, $p < 0.001$) and ergotamine ($F = 377.79$, $p < 0.001$) levels, but not for ergotaminine ($F = 6.30$, $p = 0.023$) levels. These alkaloid profiles are consistent with the profiles found in the sclerotia of isolate 04-97.1 (Figure 4.11).

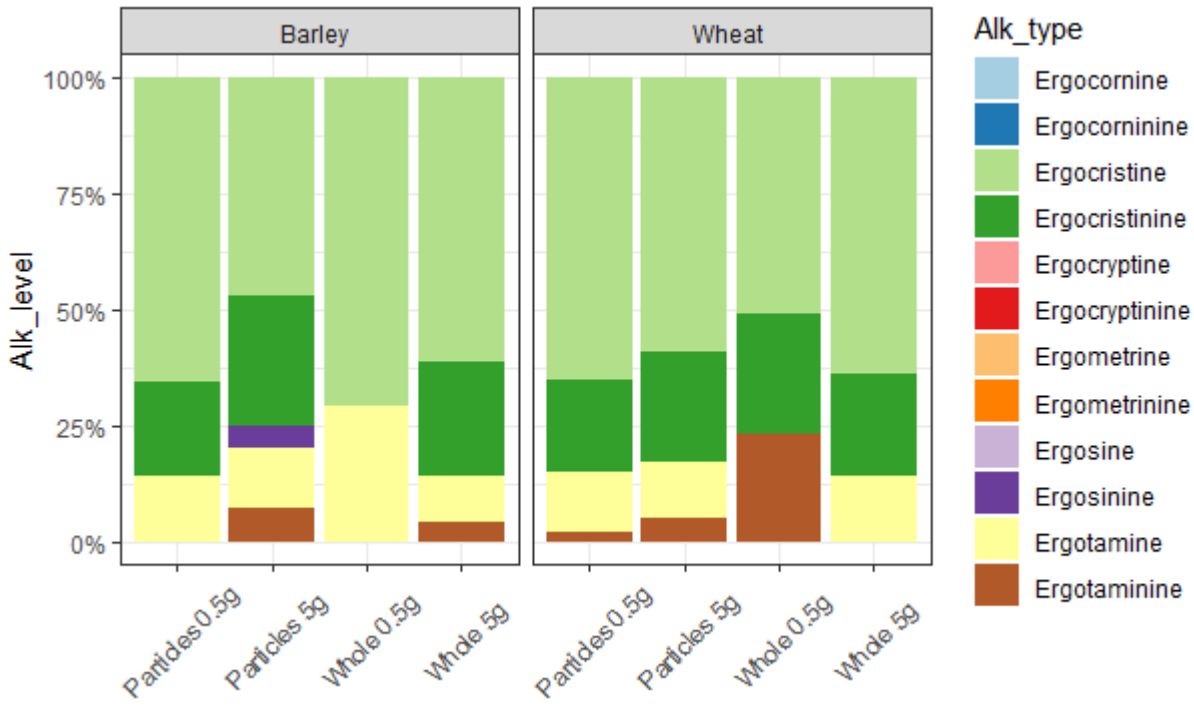

Figure 4.21: Proportions of ergot alkaloids on clean wheat and barley grain that had been in direct physical contact with whole or broken particles of ergot sclerotia of isolate 04-97.1.

4.5 Discussion

The fungal pathogen *C. purpurea* produces sclerotia (sexual overwintering structures) which contain high concentrations of an array of ergot alkaloids that are highly toxic to humans and other animals. The European Union Directorate General for Health and Food safety is proposing introducing changes to the limits of sclerotia found in cereal grain and, unprecedentedly, to impose a threshold of total ergot alkaloids in processed grain, including milling products. For milling products from wheat, spelt, barley and oats, a limit of 75–200 ppb will be set for alkaloids. For rye products, the limit will be higher c.250–500 ppb, while for cereal-based food for infants and young children it will be lower, < 50 ppb. The minimum levels of ergot sclerotia in unprocessed grain lots will be reduced to 0.02% (0.2g/kg), instead of the current 0.05% (0.5g/kg). This chapter therefore aimed to determine whether ergot alkaloids are able to contaminate otherwise clean grain, and whether differences are observed between cereal species and/or pathogen isolates in the total levels of ergot alkaloids, as well as the profiles of individual alkaloids.

The comparison of the seven *C. purpurea* isolates, revealed significant differences in ergot alkaloid levels and profiles, with each isolate having its own distinct ergot alkaloid profile. These isolate specific alkaloid profiles can potentially be attributed to the original host, as well as the location of origin for each isolate. Isolates EI2 and EI4 were found in Canada, but while the alkaloid profile in sclerotia of EI4 differed significantly from isolates 03-20, 04-41 and 04-97 which were found in the UK, EI2 was very similar to the UK isolates. Rye 20.1 differed both in terms of location of origin (Germany) and original host (rye), but had a similar sclerotia alkaloid profile to the Canadian isolate EI4 (Figure 4.8). However, in the repeat experiment, where isolates 04-97.1, EI4 and Rye 20.1 were grown on wheat and barley (Figure 4.17), the alkaloid profile of sclerotia of Rye 20.1 now resembled that of 04-97.1. Young (1981) also observed differences in the types of alkaloids depending on the region, as well as the particular field that sclerotia were harvested from. In addition to the original host and location of origin, the observed differences between isolates could also be due to environmental variations in terms of temperatures and watering regimes between experiments. Even ears that were inoculated a month apart from each other would have been subjected to differences in their environments. Finally, the isolates might be vary significantly at their genetic levels. We are currently not aware of the complete sequence differences that might exist in the ergot

alkaloid gene cluster between these isolates. Additionally, any genetic differences could interact with the environment to produce these observed differences in the alkaloid profiles.

Tittlemier et al., 2016 found that for the isolates EI4 and EI2 alkaloids within honeydew ranged between 16 and 5,459 µg/kg, and that ergometrine and ergosine were the predominant alkaloids. While very low levels of ergot alkaloid were found in honeydew of all seven *C. purpurea* isolates examined, the highest level recorded being 800 ppb, isolates EI4 and EI2 were similarly found to contain higher proportions of ergometrine and ergosine (Figure 4.8). As *C. purpurea* develops within its host's ovule alkaloid levels increase within the fungal tissues. Specifically, ergot alkaloid levels were observed to accumulate in sphacelia and reach their highest levels in mature sclerotia, with isolates 03-20.1 and 04-97.1 having the highest levels (at over 3 million ppb in wheat) (Figure 4.7). Similar total alkaloid levels were observed for sclerotia from isolate 04-97.1 in the repeat experiment (Figure 4.16). Mature sclerotia formed by isolate 04-97.1 were dominated by ergotamine, ergotaminine, ergocristine and ergocristinine. Ergocristine, the major component of mature sclerotia, has been reported as the major alkaloid component found in sclerotia developed on rye (Bryla *et al*., 2015).

Ergot alkaloids can contaminate clean grain either pre- and/or post-harvest, although the extent to which healthy grain may become contaminated with alkaloids pre-harvest is less clear. Ergot alkaloids were first detected is honeydew; the mixture of sugary liquid and asexual conidia produced by the fungus and discharged from infected flowers. However, in the first experiment significantly higher levels of ergot alkaloids were found in the grain of wheat (>162,792 ppb) and barley (>77,589 ppb) compared to honeydew, suggesting that honeydew is unlikely to be the primary source of ergot alkaloid contamination of grain. A broader range of alkaloids was found in the grain that developed above and below flowers infected with *C. purpurea* isolate 04-97.1 than in sclerotia. This would indicate that while the fungus produces a wide range of alkaloids, only a specific subset of those are stored in mature sclerotia. Furthermore, the broader range of alkaloids found on grain, compared to sclerotia, would indicate that the transfer of these alkaloids onto the grain occurred within the ear and was not due to accidental contamination during removal of mature sclerotia from ears. It has been shown in other flower-infecting fungal pathogens, namely *F. culmorum*, that fungal mycotoxins can move within the ear via the xylem vessels and phloem sieve tubes (Kang 1999). The *C. purpurea* sphacelial tissue grows to fill the ovary cavity, surrounding the phloem and xylem tissues that enter the ovule. While there is no evidence that the fungus can grow past the base of the ovary and enter the rachis (allowing the fungus to move between flowers), it is not

known whether the ergot alkaloids can move between flowers via the xylem and phloem. Ergot alkaloids synthesised in the sphacelial tissue could find their way into the xylem and phloem tissues, providing a route for transport of the alkaloids into developing grain above and below the site of *C. purpurea* infection.

In the repeat experiment much lower levels of total alkaloids were detected in grain of wheat and barley, the highest level recorded being 77.34 ppb (Figure 4.18), compared to alkaloid levels found in wheat and barley grain, (of 162,792 ppb and 77,589 ppb respectively), in the first experiment (Figure 4.11). In addition, isolate 04-97.1 could not be compared to the earlier experiment as the levels of the individual ergot alkaloids on wheat grain were below the limits of quantification (LOQ) (Figure 4.19). These lower alkaloids levels seen in the repeat experiment could potentially be due to variation in environmental variables between the two experiments, and the lower number of replicates used in the second experiment. As can be seen in Figure 4.14 (first experiment) there is large variation between replicates in the alkaloid profiles found in grain. On barley, isolate EI4 produced a broad range of ergot alkaloids on grain collected below the site of *C. purpurea* infection (Figure 4.19), much broader than seen in sclerotia (Figure 4.17). In EI4 sclerotia ergocryptine was the major alkaloid, while on barley grain ergotamine and ergocristinine were the dominant alkaloids found. This again supports a genuine result, and not cross contamination from sclerotia to grain during harvest.

The physical contact (tumbling) experiments indicate that ergot alkaloids can be readily transferred to clean grain by both whole, intact ergot sclerotia, as well as broken, particles of sclerotia, post-harvest. This would suggest that the presence of sclerotia during harvest and transport of the grain from the field could lead to the contamination of healthy grain with ergot alkaloids. Thus, despite post-harvest removal of sclerotia by standard cleaning methods, ergot alkaloids have been detected in 'clean' grain samples (Beuerle *et al*., 2012; Byrd *et al*., 2017; MacDonald *et al*., 2017). Tittlemier *et al*., 2015 demonstrated a strong linear relationship between the concentration of ergot alkaloids and the presence of ergot sclerotia. Furthermore, Slaiding and Byrd, 2013 tested wheat, barley and rye grains from harvests rejected due to the presence of sclerotia over three years. The grain was tested before and after sieving to remove sclerotia. Their findings showed higher alkaloid levels on wheat and barley grain after sieving, but not on rye grain.

Significant differences were seen between wheat and barley with regards to the physical transfer of alkaloids to clean grain. Specifically, bigger differences were seen between the two

concentrations of broken sclerotia on barley grain contamination than on wheat grain. It is possible that certain characteristics of the grains have a part to play in the levels of ergot alkaloid contamination found, such as grain size and shape. Indeed, dust from sclerotia has been observed to stick to surfaces such as dried lemma and palea that form the husk remaining on barley seeds (A.Gordon personal communication). Further grain measurements for barley and wheat would have to be measured and correlated with differing alkaloid levels.

In conclusion, cereal grains are at risk of being contaminated with ergot alkaloids, both during grain development, and during harvested and transportation of the grain. With observed levels of alkaloids in sclerotia reaching as high as 3 million ppb (3 million μg of ergot alkaloids per kg of sclerotia), and the average weight of a single sclerotia being 38 mg, a single sclerotia could contain 114 μg of ergot alkaloids. This means that a single ergot sclerotia in a kg of grain would result in an ergot alkaloid contamination of 114 μg/kg (114 ppb), which falls within the limits proposed by the European Commission Containment Working Group of 75 – 200 ppb (75 – 200 ug ergot alkaloid per kg of grain).

4.6 Further work

The experiments described in this chapter raised further questions. Firstly, the variability observed between experiments regarding the alkaloid levels, and profiles found in grain, requires the question regarding the pre-harvest contamination of grain to be further investigated. Is the pre-harvest contamination of grain a result of contamination of developing rain by honeydew, or are ergot alkaloids able to move within the ears of cereals? The route of transfer of ergot alkaloids from infected flowers to healthy grain potentially occurs via the plant's vascular system (xylem and/ or phloem). It is important to determine whether this is indeed the case and if so, how the ergot alkaloids move from the infected flowers to healthy grain, where in the healthy flowers and grain the alkaloids are deposited, when this transfer occurs during the *C. purpurea* infection life cycle and whether there is a difference in the transferability of different ergot alkaloids.

Secondly, the function of ergot alkaloids in *C. purpurea* remains unclear. Potentially, alkaloids could play a role in the pathogenicity of the fungus, its host range, and/or act as a defense against predation of sclerotia. For pathogenicity to be a function of alkaloids, a correlation between infection rates and sclerotia alkaloid levels would need to be determined.

Previous studies have shown isolate 04-97.1 to be highly aggressive isolate and result in high infection rates (Gordon *et al*., 2015). In addition, a comparative sequencing approach to elucidate the differences in the EAS cluster between isolates might could reveal a genetic component for the differences in alkaloid profiles between isolates found in different host species.

While *C. purpurea* isolates can infect a wide range of cereal and grass species, for alkaloids to be implicated in the host range of *C. purpurea*, differences in the alkaloid profiles between fungal tissues, as they develop on different cereal species would have to be observed. In this chapter, the results from both the first and the repeat experiments did not reveal differences in the alkaloid profiles of sclerotia specific to cereal species with any of the isolates used (Figures 4.11 and 4.17). Nor for the other fungal tissues, on different cereal species, were differences in alkaloid profiles observed (Figure 4.11). Nevertheless, the experiments in this chapter focused on a single variety of three cereal crops, spring wheat, spring barley and a winter rye. Further studies should be carried out with increased replication and widened to include more varieties, including winter wheat, winter barley, and other cereal crops such as oats, spelt etc.

Finally, it is very likely that the role of ergot alkaloids is one of defense against predation. Evidence comes from the related fungal genus *Neotyphodium*, a symbiont of grasses, where alkaloids and related compounds are transferred to the grass host, through the vascular system and act as protectants against insect and animal predation, in a process known as 'defensive mutualism' (Panaccione *et al*., 2014). Further work would be needed before any of these hypotheses can be rejected or substantiated.

Chapter 5: General Discussion

The fungal pathogen *C. purpurea* is an economically important disease of cereals and other grasses which has been impacting on human health and agriculture productivity for many centuries. The work in this thesis sheds light on some of the poorly understood molecular mechanisms underlying the complex interaction between the pathogen and its cereal hosts, with a primary focus on the *C. purpurea*- wheat interaction. From the broad transcriptome changes occurring in wheat upon *C. purpurea* infection, to an examination of the role of hormones and Rht DELLA protein mutants in the infection process, and the possible routes ergot alkaloids take to contaminate grain, each set of experiments led to original observations and the formation of new hypotheses for future testing.

Firstly, RNASeq was used to observe the changes in the wheat transcriptome following inoculation with *C. purpurea* over a 7day time period and in defined tissues of the wheat female flower, namely the stigma, transmitting and base tissues. This enabled us to observe the transcriptomic changes occurring as a result of infection at both a temporal and spatial level. The observed host transcriptomic changes of hormone and defence-related genes during the early time-points of the infection suggest that, contrary to what was previously believed, the fungus is not able to avoid recognition by the plant via pollen tube mimicry (Tudzynski & Scheffer, 2004). Until now, it was thought that the ovule tissue did not exhibit any defence reactions, with the fungus growing in a similar manner to pollen tubes, and that defence reactions such as callose deposition could only be observed after the fungal hyphae had abandoned the pollen tube route (Tudzynski *et al*., 1995; Tudzynski & Scheffer, 2004). Instead, our data shows that the plant host is not only able to activate an array of defence responses, but that this occurs long before the fungus diverges from the route normally taken during pollen tube growth. While the pollination process has been found to induce the expression of chitinases in rice (Lan *et al*., 2004) and apple (Dong *et al*., 1998), there is no evidence to show that pollination induces the expression of any of the other early defence-related genes observed in this study, such as NBS-LRR and RPK proteins, and MYB or WRKY transcription factors. In order to further validate our observations, a comparative, time course transcriptomic study between pollinated wheat ovaries and pollen would need to be carried out. It would allow the genes involved in the pollination process in wheat to be directly compared to the data in this study, allowing the identification of pollination-specific genes and *C. purpurea* infection-specific genes.

Moreover, this study revealed for the first time the induction of hormonal and defence-related genes in the base tissue before arrival of *C. purpurea* fungal hyphae. Included in this group of DEG were ethylene responsive transcription factors (ERFs). This observation points towards a possible mobile, ET-like signal that reaches the base tissue, were it primes the activation of defence responses prior to the arrival of the fungus. Ethylene has been found to play an important role in plant defence (van Loon *et al*., 2006), and ethylene signaling has been connected to resistance primarily against a number of necrotrophs (Glazebrook, 2005). A recent comparative transcriptomic analysis showed the accumulation of transcripts related to ethylene signaling in maize infected with the hemibiotrophic fungus *Colletotrichum graminicola* (Miranda *et al*., 2017). However, a study in tobacco infected with tobacco mosaic virus suggested that while ethylene was involved in generating systemic signal molecules, it did not itself function as a long-distance signal (Verberne *et al*., 2003). In order for ethylene to be confirmed as a mobile signal in the wheat-*C. purpurea* interaction, it would have to be quantified at the site of infection, where fungal hyphae are already present, as well as in the base tissue, before the arrival of fungal hyphae. However, the gaseous nature of the hormone, along with the small distance between the stigma and base tissues might prove to be a challenge for the accurate quantification of ethylene. Another approach would be to determine whether the induction of the ERF genes still occurred in the base tissue in the absence of ethylene. This could be achieved by inoculating wheat ears with *C. purpurea* in the presence and absence of a chemical inhibitor of ethylene production, or using wheat transgenic lines where ET biosynthesis had been disrupted by targeted knock-outs. Cyclopropane-1,1-dicarboxylic acid (CDA), a chemical inhibitor of ACC oxidase activity (Dourtoglou *et al*., 2000) could be tried. CDA was previously used to inhibit ethylene production in wheat to show how ethylene can promote resistance of wheat to *Fusarium graminearum* (Foroud *et al*., 2019).

It is known that plants can activate a range of systemic defence mechanisms in response to pathogen infection that lead to an enhancement of resistance in subsequent tissues, a process known as systemic acquired resistance (SAR) (Fu & Dong, 2013; Shah & Zeir, 2013). The existence of mobile signals and their involvement in SAR have been extensively studied (Song & Ryu, 2018). Park *et al*., 2007 showed that methyl salicylate (MeSA) acted as a mobile signal of SAR in tobacco, eliminating SAR by silencing the gene SABP2 (salicylic acid–binding protein 2) and disrupting the MeSA - SA balance. In addition to MeSA a number of other compounds have been implicated as SAR mobile signals, including azelaic acid (AzA), glycerol-3-phosphate (G3P), and abietane diterpenoid dehydroabietinal (DA) (Chandra *et al*.,

2011; Chaturvedi *et al*., 2012; Jung *et al*., 2009). While the above mentioned molecules are related to SA signaling (Song & Ryu, 2018), jasmonates have also been proposed as mobile systemic signals in *Arabidopsis* infected with avirulent strains of *Pseudomonas syringae* (Truman *et al*., 2007). Glycerol-3-phosphate (G3P), along with the lipid transfer protein Defective in Induced Resistance (DIR1), which has been found to be required for G3P induced SAR (Yu *et al*., 2013), were found to both be up-regulated in the base tissue at 72H (Table 7.7, Appendix A). The fact that these genes were only detected at 72H and not earlier in the wheat-*C. purpurea* infection, suggests that G3P and DIR1 may not be part of the mobile signal operating during *C. purpurea* infection, and that the long distance response observed is not strictly a SAR response.

The possibility that the mobile signal could be produced by the fungus to facilitate infection should also be considered. Along with the hormones that *C. purpurea* has been shown to produce (Hinsch *et al*., 2015), fungal effectors are most likely delivered into the host's cells. Indeed, studies on Flax rust (*Melampsora lini*) have shown that biotrophic pathogens are able to deliver effectors through their haustoria which are then transported into the host cytoplasm (Ellis *et al*., 2007). Identifying potential effector candidates for *C. purpurea* would be extremely beneficial in understanding the molecular interactions taking place between the pathogen and wheat. Candidates could first be identified *in silico* by looking for properties that are known to be present in effector proteins from filamentous pathogens (Saunders *et al*., 2012)

Apart from ethylene-related genes, the transcriptomic study revealed the activation of wheat genes related to multiple hormonal pathways. These results, particularly those showing the altered expression of key GA-related genes, along with the observations of Gordon *et al*. (2015) that found partial ergot resistance QTL that co-located with the wheat dwarfing genes *Rht-B1b* and *Rht-D1b*, led us to concentrate on the potential role of GA in *C. purpurea* infection of wheat. In Chapter 3 our results showed partial resistance to *C. purpurea* conferred by GA insensitive lines carrying *Rht* DELLA mutations, further indicating that DELLAs in wheat play a role in the wheat-*C. purpurea* interaction, and that GAs are required for the successful infection of wheat by this fungus. This theory is further supported by our quantification results of endogenous GAs which, for the first time, showed that GA_4 is significantly increased in *C. purpurea* infected tissues. The observed increase could be the result of an auxin mediated induction of the GA biosynthetic pathway, as auxin has been shown to induce the synthesis of bioactive GAs (Wolbang *et al*., 2004), and levels of IAA also increased in response to infection. As *C. purpurea* is also able to synthesis auxins (P. Galuszka, unpubl. data), it is possible that

the observed increase in auxin levels are products of the fungus. It is therefore tempting to speculate that *C. purpurea* acts to enhance susceptibility of wheat by indirectly inducing GA biosynthesis *in planta*, which in turn lead to the degradation of DELLAs. This degradation of DELLAs might ultimately be affecting susceptibility via the roles these proteins play in JA-mediated defences (Hou *et al*. 2010), as well as ROS homeostasis (Achard *et al*., 2008). To answer these questions the origin of the elevated IAA levels, fungal or plant, would need to be determined.

Many pathogens have been found that can manipulate plant hormone biosynthesis and/or signaling pathways (Burger & Chory, 2019), manipulating or hijacking hormone homeostasis by either producing effectors or phytohormones (Chanclud & Morel, 2016; Patkar & Naqvi, 2017; Han & Kahmann, 2019). For instance, the biotrophic fungal pathogen *Ustilago maydis* has been shown to indirectly impede the host's ability to produce SA by secreting chorismate mutase (Cmu1) into the host's cells (Djamei *et al*., 2011). The biotrophic fungus, *Puccinia graminis* f. sp. *tritici*, the causal agent of stem rust in wheat, is able to produce one of the key enzymes of IAA biosynthesis, tryptophan 2-monooxygenase (Pgt-IaaM) in its haustoria, leading to an increase in endogenous IAA levels (Yin *et al*., 2014). Silencing of the *P. graminis*. f. sp. *tritici* gene expressing this precursor using *Barley stripe* mosaic virus (BSMV)-mediated host-induced gene silencing (HIGS) led to fewer pustules being formed (Yin *et al*., 2014). Similarly to *C. purpurea*, the rice-blast fungus *M. oryzae* has also been found to produce multiple phytohormones in order to modulate the host's immunity, namely JA, CKs and ABA (Patkar *et al*., 2015; Chanclud *et al*., 2016; Spence *et al*., 2015).

While we observed activation of a wide array of defence-related genes, *C. purpurea* was still able to successfully infect wheat ovules, such that approximately 2 weeks after inoculation hardened, dark sclerotia formed where a seed would have developed. These sclerotia contain high concentrations of an array of toxic alkaloids. Our results showed that ergot alkaloids were not only found in sclerotia, but could be detected in the honeydew, albeit at much lower levels. Furthermore, when looking at the fungal transcriptome (unpublished data), the genes responsible for alkaloid biosynthesis are found to be expressed 5 days after inoculation through-out the wheat ovule. While this indicates that alkaloid production starts even before honeydew production, a time-course experiment, to quantify ergot alkaloids between 3 and 14 days after inoculation, when honeydew is typically present, could potentially reveal the earliest point of detectable alkaloid levels. The early biosynthesis of ergot alkaloids during *C. purpurea* infection suggests that they play a more complex role than simply acting

as a deterrent for herbivory of sclerotia. Indeed, there are various hypotheses to explain why fungi produce mycotoxins (Reverberi *et al*., 2010). One hypothesis proposes that mycotoxins are a response to the oxidative stress resulting from the production of ROS by the host plant (Reverberi *et al*., 2010). The biosynthesis of toxins was found to be stimulated in the fungal pathogen *F. graminearum* in the presence of H_2O_2, while the addition of catalase, which removes H_2O_2, led to a reduction in mycotoxin accumulation (Ponts *et al*., 2006; Ponts *et al*., 2007). In this study, the expression of alkaloid biosynthesis genes in *C. purpurea* was found to coincide with the up-regulation of ROS-production related genes in wheat (data not shown). It is therefore possible that alkaloid biosynthesis occurs, at least in part, in response to oxidative stress.

Our results also indicated that ergot alkaloids are synthesised in the sphacelial tissue, and could potentially find their way into the xylem and phloem tissues, providing a route for transport of the alkaloids into healthy grain developing above and below the sites of *C. purpurea* infection. Mycotoxins of *F. culmorum* have been found in the xylem vessels and phloem sieve tubes of wheat (Kang, 1999), while plants that had been treated with the *F. verticilliodes* mycotoxin fumonisin B1 as seedlings accumulated the toxin in their aerial parts, thus suggesting the toxin was taken up by roots and transported through the plant vasculature (Zimeri *et al*., 2006). If ergot alkaloids are able to be transported in this manner, this would mean that the absence of sclerotia might not be an adequate indicator for the absence of ergot alkaloids in grain lots. With the current limits on ergot alkaloids proposed by the European Commission Containment Working Group being 75 – 200 ppb (75 – 200 ug ergot alkaloid per kg of grain), the presence of alkaloids found on otherwise clean grain, could potentially become a significant compliance issue for farmers, as well as the milling industry.

The specific role of alkaloids remains unclear. A possible explanation might be that they act in a mutually beneficial way, being of benefit to both the fungus and the host, in a process known as ‘defensive mutualism’. It is very likely that alkaloids benefit the fungus by acting as protectants against insect and animal predation of sclerotia. On the plant side there is a growing number of studies into endophytic fungi, and specifically into *Neotyphodium*, a fungus belonging to the Clavicipitaceae and a symbiont of grasses, which show that alkaloids and related compounds are transferred to the grass host, through the vascular system and have antiherbivore properties (Panaccione *et al*., 2014; Schardl *et al*., 2013; Saikkonen *et al*., 2010). Another way that *C. purpurea* might be acting in a mutually beneficial way could be through oxidative stress protection. White & Torres, (2010) have suggested that endophytic fungi are

able to produce ROS which, in turn, lead the plant host to increase production of antioxidant compounds. Ultimately, the production of these compounds can protect the plant host from oxidative stress. This hypothesis could also apply to the *C. purpurea*- wheat interaction, as *C. purpurea* has been found to significantly contribute to the accumulation of ROS in plants during infection (Giesbert *et al*., 2008).

In the past, this specific pathogen-host relationship has been overlooked. However, the development of new technologies for wheat breeding and improvement, along with certain policy changes regarding food quality and consumer health, make it important for research to revisit this disease. With the European Commission proposing new threshold levels for ergot alkaloids, our discovery of alkaloids in otherwise healthy grain, as well as in grain that had come into contact with sclerotia, could prove to be a significant compliance issue. In addition, the production of hybrid wheat cultivars which, through heterosis, can out-yield commercial line cultivars (Zhao *et al*., 2015) comes with an open-flowering trait which can increase susceptibility to *C. purpurea* and has the potential of exacerbating infection rates. It is therefore imperative to better understand the mechanisms that characterize this unique plant-pathogen system. This research has highlighted the importance of hormones and the roles they play in the successful fungal colonization of wheat, as well as shedding light into the array of defences that get induced in the plant upon infection. Overall, the work presented in this PhD thesis makes a number of contributions to our knowledge regarding the complex biological and molecular interactions that occur between *C. purpurea* and wheat.

6. References

Aach, H., Bode, H., Robinson, D.G. and Graebe, J.E., 1997. ent-Kaurene synthase is located in proplastids of meristematic shoot tissues. *Planta*, *202*(2), pp.211-219.

Aanes H, Winata C, Lars F. Moen, Olga Østrup, Sinnakaruppan Mathavan, Philippe Collas, Torbjørn Rognes, and Peter Aleström. 2014. Normalization of RNA-sequencing data from samples with varying mRNA levels. PLoS One. 9(2):e89158. doi: 10.1371/journal.pone.0089158

Achard, P., Renou, J.P., Berthomé, R., Harberd, N.P. and Genschik, P., 2008. Plant DELLAs restrain growth and promote survival of adversity by reducing the levels of reactive oxygen species. *Current Biology*, *18*(9), pp.656-660.

Achard, P. and Genschik, P., 2009. Releasing the brakes of plant growth: how GAs shutdown DELLA proteins. *Journal of experimental botany*, *60*(4), pp.1085-1092.

Afzal, A.J., Wood, A.J. and Lightfoot, D.A., 2008. Plant receptor-like serine threonine kinases: roles in signaling and plant defense. Molecular Plant-Microbe Interactions, 21(5), pp.507-517.

AHDB 2020, *Ergot in cereals*, viewed August 2020, https://ahdb.org.uk/ergot

Allen, R.L., Bittner-Eddy, P.D., Grenville-Briggs, L.J., Meitz, J.C., Rehmany, A.P., Rose, L.E. and Beynon, J.L., 2004. Host-parasite coevolutionary conflict between Arabidopsis and downy mildew. Science, 306(5703), pp.1957-1960.

Alm, T., 2003. The witch trials of Finnmark, northern Norway, during the 17th century: Evidence for ergotism as a contributing factor. *Economic Botany*, *57*(3), p.403.

Alonge, M., Shumate, A., Puiu, D., Zimin, A. and Salzberg, S.L., 2020. Chromosome-Scale Assembly of the Bread Wheat Genome Reveals Thousands of Additional Gene Copies. *Genetics*.

Ambawat, S., Sharma, P., Yadav, N.R. and Yadav, R.C., 2013. MYB transcription factor genes as regulators for plant responses: an overview. Physiology and Molecular Biology of Plants, 19(3), pp.307-321.

Andrews S. (2010). FastQC: a quality control tool for high throughput sequence data. Available online at: http://www.bioinformatics.babraham.ac.uk/projects/fastqc

Antico, C.J., Colon, C., Banks, T. and Ramonell, K.M., 2012. Insights into the role of jasmonic acid-mediated defenses against necrotrophic and biotrophic fungal pathogens. *Frontiers in Biology*, *7*(1), pp.48-56.

Appels, R., Eversole, K., Stein, N., Feuillet, C., Keller, B., Rogers, J., Pozniak, C.J., Choulet, F., Distelfeld, A., Poland, J. and Ronen, G., 2018. Shifting the limits in wheat research and breeding using a fully annotated reference genome. *Science*, *361*(6403).

Bai, Y., Meng, Y., Huang, D., Qi, Y. and Chen, M., 2011. Origin and evolutionary analysis of the plant-specific TIFY transcription factor family. *Genomics*, *98*(2), pp.128-136.

Bari, R. and Jones, J.D., 2009. Role of plant hormones in plant defence responses. Plant molecular biology, 69(4), pp.473-488.

Bayles, R., Fletcher, M., Gladders, P., Hall, R., Hollins, W., Kenyon, D. and Thomas, J., 2009. Towards a sustainable whole-farm approach to the control of Ergot. *HGCA Project report*, (456).

Bebber, D. P. & Gurr, S. J. 2015. Crop-destroying fungal and oomycete pathogens challenge food security. Fungal Genetics and Biology, 74(62-64.

Bebber, D. P., Holmes, T. & Gurr, S. J. 2014. The global spread of crop pests and pathogens. Global Ecology and Biogeography, 23(12), pp 1398-1407.

Bedő, Z. and Láng, L., 2015. Wheat breeding: current status and bottlenecks. In *Alien Introgression in Wheat* (pp. 77-101). Springer, Cham.

Berrocal-Lobo, M., Molina, A. and Solano, R., 2002. Constitutive expression of ETHYLENE-RESPONSE-FACTOR1 in Arabidopsis confers resistance to several necrotrophic fungi. *The Plant Journal*, *29*(1), pp.23-32.

Beuerle, T., Benford, D., Brimer, L., Cottrill, B., Doerge, D., Dusemund, B., Farmer, P., Fürst, P., Humpf, H. and Mulder, P.P.J., 2012. Scientific Opinion on Ergot alkaloids in food and feed. *EFSA Journal*, *10*(7), p.2798.

Bhattacharya, A., Kourmpetli, S., Ward, D.A., Thomas, S.G., Gong, F., Powers, S.J., Carrera, E., Taylor, B., de Caceres Gonzalez, F.N., Tudzynski, B. and Phillips, A.L., 2012. Characterization of the fungal gibberellin desaturase as a 2-oxoglutarate-dependent

dioxygenase and its utilization for enhancing plant growth. *Plant physiology*, *160*(2), pp.837-845.

Boyd, L. A., Ridout, C., O'Sullivan, D. M., Leach, J. E. & Leung, H. 2013. Plant–pathogen interactions: disease resistance in modern agriculture. Trends in genetics, 29(4), pp 233-240.

Brennan, J, 2020. Ergot alkaloids - avoiding a bad trip on new regulations. *Milling Wheat Conference*, AHDB, 27 February.

Bürger, M. and Chory, J., 2019. Stressed out about hormones: how plants orchestrate immunity. *Cell host & microbe*, *26*(2), pp.163-172.

Bryła, M., Szymczyk, K., Jędrzejczak, R. and Roszko, M., 2015. Application of liquid chromatography/ion trap mass spectrometry technique to determine ergot alkaloids in grain products. *Food technology and biotechnology*, *53*(1), pp.18-28.

Byrd, N., De Alwis, J., Booth, M. and Jewell, K., 2014. Monitoring the Presence of Ergot Alkaloids in Cereals and a Study of the Possible Relationship between Occurrence of Sclerotia Content and Levels of Ergot alkaloids. *Food Standard Agency, Final report, Project number FS516009. Available online: https://www. food. gov. uk/sites/defa ult/files/FS516009% 20Final% 20Ergot% 20Alkaloid% 20report*, *20*(283), p.29.

Byrd N, Slaiding IR. - Final Project Report: Monitoring of mycotoxins and other contaminants in UK cereals used in malting, milling & animal feed. AHDB PR578 (2017) AHDB Website

Catinot, J., Huang, J.B., Huang, P.Y., Tseng, M.Y., Chen, Y.L., Gu, S.Y., Lo, W.S., Wang, L.C., Chen, Y.R. and Zimmerli, L., 2015. ETHYLENE RESPONSE FACTOR 96 positively regulates A rabidopsis resistance to necrotrophic pathogens by direct binding to GCC elements of jasmonate–and ethylene-responsive defence genes. *Plant, cell & environment*, *38*(12), pp.2721-2734.

Chanclud, E. and Morel, J.B., 2016. Plant hormones: a fungal point of view. *Molecular plant pathology*, *17*(8), pp.1289-1297.

Chanclud, E., Kisiala, A., Emery, N.R.J., Chalvon, V., Ducasse, A., Romiti-Michel, C., Gravot, A., Kroj, T. and Morel, J.B., 2016. Cytokinin production by the rice blast fungus is a pivotal requirement for full virulence. *PLoS pathogens*, *12*(2), p.e1005457.

Chanda, B., Xia, Y., Mandal, M.K., Yu, K., Sekine, K.T., Gao, Q.M., Selote, D., Hu, Y., Stromberg, A., Navarre, D. and Kachroo, A., 2011. Glycerol-3-phosphate is a critical mobile inducer of systemic immunity in plants. *Nature genetics*, *43*(5), pp.421-427.

Chaturvedi, R., Venables, B., Petros, R.A., Nalam, V., Li, M., Wang, X., Takemoto, L.J. and Shah, J., 2012. An abietane diterpenoid is a potent activator of systemic acquired resistance. *The Plant Journal*, *71*(1), pp.161-172.

Chen, L., Phillips, A. L., Condon, A. G., Parry, M. A. & Hu, Y.-G. 2013. GA-responsive dwarfing gene Rht12 affects the developmental and agronomic traits in common bread wheat. PLoS One, 8(4), pp e62285.

Cho Won Kyong, Lian Sen, Sang-Min Kim, Bo Yoon Seo, Jin Kyo Jung, and Kook-Hyung Kim. 2015. Time-Course RNA-Seq Analysis Reveals Transcriptional Changes in Rice Plants Triggered by Rice stripe virus Infection. PLoS ONE 10(8): e0136736. doi:10.1371/journal.pone.0136736

Colebrook, E. H., Thomas, S. G., Phillips, A. L. & Hedden, P. 2014. The role of gibberellin signalling in plant responses to abiotic stress. Journal of experimental biology, 217(1), pp 67-75.

Collinge, D.B., Kragh, K.M., Mikkelsen, J.D., Nielsen, K.K., Rasmussen, U. and Vad, K., 1993. Plant chitinases. The Plant Journal, 3(1), pp.31-40.

Collins, N.C., Thordal-Christensen, H., Lipka, V., Bau, S., Kombrink, E., Qiu, J.L., Hückelhoven, R., Stein, M., Freialdenhoven, A., Somerville, S.C. and Schulze-Lefert, P., 2003. SNARE-protein-mediated disease resistance at the plant cell wall. Nature, 425(6961), p.973.

Conesa Ana, Pedro Madrigal,corresponding author Sonia Tarazona, David Gomez-Cabrero, Alejandra Cervera, Andrew McPherson, Michał Wojciech Szcześniak, Daniel J. Gaffney, Laura L. Elo, Xuegong Zhang, and Ali Mortazavi. 2016. A survey of best practices for RNA-seq data analysis. Genome Biol. 2016; 17: 13. doi: 10.1186/s13059-016-0881-8.

Curtis, B., Rajaram, S. & Gomez Macpherson, H. 2002. Wheat in the world.

Dangl, J. L., Horvath, D. M. & Staskawicz, B. J. 2013. Pivoting the plant immune system from dissection to deployment. Science, 341(6147), pp 746-751.

Davière, J.M. and Achard, P., 2013. Gibberellin signaling in plants. *Development*, *140*(6), pp.1147-1151.

De Bruyne, L., Höfte, M. and De Vleesschauwer, D., 2014. Connecting growth and defense: the emerging roles of brassinosteroids and gibberellins in plant innate immunity. *Molecular plant*, *7*(6), pp.943-959.

De Coninck, B., Cammue, B.P. and Thevissen, K., 2013. Modes of antifungal action and in planta functions of plant defensins and defensin-like peptides. Fungal Biology Reviews, 26(4), pp.109-120.

De Costa, C. 2002. St Anthony's fire and living ligatures: a short history of ergometrine. The Lancet, 359(9319), pp 1768-1770.

de Jesus Miranda, V., Porto, W.F., da Rocha Fernandes, G., Pogue, R., Nolasco, D.O., Araujo, A.C.G., Cota, L.V., de Freitas, C.G., Dias, S.C. and Franco, O.L., 2017. Comparative transcriptomic analysis indicates genes associated with local and systemic resistance to Colletotrichum graminicola in maize. *Scientific reports*, *7*(1), pp.1-14.

de Jonge, R., van Esse, H. P., Kombrink, A., Shinya, T., Desaki, Y., Bours, R., van der Krol, S., Shibuya, N., Joosten, M. H. & Thomma, B. P. 2010. Conserved fungal LysM effector Ecp6 prevents chitin-triggered immunity in plants. Science, 329(5994), pp 953-955.

De Lucas, M., Daviere, J.M., Rodríguez-Falcón, M., Pontin, M., Iglesias-Pedraz, J.M., Lorrain, S., Fankhauser, C., Blázquez, M.A., Titarenko, E. and Prat, S., 2008. A molecular framework for light and gibberellin control of cell elongation. *Nature*, *451*(7177), pp.480-484.

DeYoung, B.J. and Innes, R.W., 2006. Plant NBS-LRR proteins in pathogen sensing and host defense. Nature immunology, 7(12), p.1243.

Djamei, A., Schipper, K., Rabe, F., Ghosh, A., Vincon, V., Kahnt, J., Osorio, S., Tohge, T., Fernie, A. R. & Feussner, I. 2011. Metabolic priming by a secreted fungal effector. Nature, 478(7369), pp 395-398.

Dodds, P. N. & Rathjen, J. P. 2010. Plant immunity: towards an integrated view of plant–pathogen interactions. Nature Reviews Genetics, 11(8), pp 539-548.

Dong, Y.H., Kvarnheden, A., Yao, J.L., Sutherland, P.W., Atkinson, R.G., Morris, B.A. and Gardner, R.C., 1998. Identification of pollination-induced genes from the ovary of apple (Malus domestica). *Sexual plant reproduction*, *11*(5), pp.277-283.

Dourtoglou, V., Koussissi, E. and Petritis, K., 2000. Inhibition of wound ethylene in Lycopersicum esculentum fruit discs by 1-amino cyclopropane-1-carboxylic acid oxidase inhibitors. *Plant growth regulation*, *30*(1), pp.79-86.

Dudoit, S., Y. H. Yang, M. J. Callow, and T. P. Speed (2002). Statistical methods for identifying genes with differential expression in replicated cdna microarray experiments. Stat. Sin. 12(1), 111–139.

Eadie, M.J., 2003. Convulsive ergotism: epidemics of the serotonin syndrome?. *The Lancet Neurology*, *2*(7), pp.429-434.

Ellis, J.G., Dodds, P.N. and Lawrence, G.J., 2007. Flax rust resistance gene specificity is based on direct resistance-avirulence protein interactions. *Annu. Rev. Phytopathol.*, *45*, pp.289-306.

Eulgem, T. and Somssich, I.E., 2007. Networks of WRKY transcription factors in defense signaling. Current opinion in plant biology, 10(4), pp.366-371.

European Commission, 2006. Commission Regulation (EC) No 1881/2006 of 19 December 2006 setting maximum levels for certain contaminants in foodstuffs. *Off J Eur Union*, *364*(365–324).

Evans, L.T., Evans, L.T. and Evans, L.T., 1998. *Feeding the ten billion: plants and population growth*. Cambridge University Press.

Ferguson, B.J., Foo, E., Ross, J.J. and Reid, J.B., 2011. Relationship between gibberellin, ethylene and nodulation in Pisum sativum. *New Phytologist*, *189*(3), pp.829-842.

Figueiredo, A., Monteiro, F. and Sebastiana, M., 2014. Subtilisin-like proteases in plant–pathogen recognition and immune priming: a perspective. *Frontiers in plant science*, *5*, p.739.

Faris, J.D., 2014. Wheat domestication: Key to agricultural revolutions past and future. In *Genomics of plant genetic resources* (pp. 439-464). Springer, Dordrecht.

Fisher, M. C., Henk, D. A., Briggs, C. J., Brownstein, J. S., Madoff, L. C., McCraw, S. L. & Gurr, S. J. 2012. Emerging fungal threats to animal, plant and ecosystem health. Nature, 484(7393), pp 186-194.

Fleet, C.M., Yamaguchi, S., Hanada, A., Kawaide, H., David, C.J., Kamiya, Y. and Sun, T.P., 2003. Overexpression of AtCPS and AtKS in Arabidopsis confers increased ent-kaurene production but no increase in bioactive gibberellins. *Plant physiology*, *132*(2), pp.830-839.

Fleet, C.M. and Sun, T.P., 2005. A DELLAcate balance: the role of gibberellin in plant morphogenesis. *Current opinion in plant biology*, *8*(1), pp.77-85.

Flintham, J., Börner, A., Worland, A. & Gale, M. 1997. Optimizing wheat grain yield: effects of Rht (gibberellin-insensitive) dwarfing genes. The Journal of Agricultural Science, 128(1), pp 11-25.

Flood, J. 2010. The importance of plant health to food security. Food Security, 2(3), pp 215-231.

Fones, H. & Gurr, S. 2015. The impact of Septoria tritici Blotch disease on wheat: an EU perspective. Fungal Genetics and Biology, 79(3-7.

Food Agric. U.N. 2015. FAOSTAT database. Rome: FAO. http://faostat.fao.org/site/291/default. Aspx

Food Standards Agency (FSA) 2019, J*une 2019 Stakeholder Update on Rapidly Developing Policy on Food Contaminants*, viewed March 2020, https://www.food.gov.uk/news-alerts/consultations/june-2019-stakeholder-update-on-rapidly-developing-policy-on-food-contaminants

Foroud, N., Ouellet, T., Laroche, A., Oosterveen, B., Jordan, M., Ellis, B. & Eudes, F. 2012. Differential transcriptome analyses of three wheat genotypes reveal different host response pathways associated with Fusarium head blight and trichothecene resistance. Plant Pathology, 61(2), pp 296-314.

Foroud, N.A., Pordel, R., Goyal, R.K., Ryabova, D., Eranthodi, A., Chatterton, S. and Kovalchuk, I., 2019. Chemical Activation of the Ethylene Signaling Pathway Promotes Fusarium graminearum Resistance in Detached Wheat Heads. *Phytopathology*, *109*(5), pp.796-803.

Frigerio, M., Alabadí, D., Pérez-Gómez, J., García-Cárcel, L., Phillips, A.L., Hedden, P. and Blázquez, M.A., 2006. Transcriptional regulation of gibberellin metabolism genes by auxin signaling in Arabidopsis. *Plant physiology*, *142*(2), pp.553-563.

Fu, Y.B. and Somers, D.J., 2009. Genome-wide reduction of genetic diversity in wheat breeding. *Crop Science*, *49*(1), pp.161-168.

Fu, Z.Q., Yan, S., Saleh, A., Wang, W., Ruble, J., Oka, N., Mohan, R., Spoel, S.H., Tada, Y., Zheng, N. and Dong, X., 2012. NPR3 and NPR4 are receptors for the immune signal salicylic acid in plants. Nature, 486(7402), p.228.

Fu, Z.Q. and Dong, X., 2013. Systemic acquired resistance: turning local infection into global defense. *Annual review of plant biology*, *64*, pp.839-863.

Gallego-Bartolomé, J., Minguet, E.G., Grau-Enguix, F., Abbas, M., Locascio, A., Thomas, S.G., Alabadí, D. and Blázquez, M.A., 2012. Molecular mechanism for the interaction between gibberellin and brassinosteroid signaling pathways in Arabidopsis. *Proceedings of the National Academy of Sciences*, *109*(33), pp.13446-13451.

Gao, X.H., Xiao, S.L., Yao, Q.F., Wang, Y.J. and Fu, X.D., 2011. An updated GA signaling 'relief of repression'regulatory model. *Molecular Plant*, *4*(4), pp.601-606.

Garnica, D. P., Upadhyaya, N. M., Dodds, P. N. & Rathjen, J. P. 2013. Strategies for wheat stripe rust pathogenicity identified by transcriptome sequencing. PLoS One, 8(6), pp e67150.

Gasperini, D., Greenland, A., Hedden, P., Dreos, R., Harwood, W. & Griffiths, S. 2012. Genetic and physiological analysis of Rht8 in bread wheat: an alternative source of semi-dwarfism with a reduced sensitivity to brassinosteroids. Journal of experimental botany, 63(12), pp 4419-4436.

Gerhards, N., Neubauer, L., Tudzynski, P. and Li, S.M., 2014. Biosynthetic pathways of ergot alkaloids. *Toxins*, *6*(12), pp.3281-3295.

Giesbert, S., Schuerg, T., Scheele, S. & Tudzynski, P. 2008. The NADPH oxidase Cpnox1 is required for full pathogenicity of the ergot fungus Claviceps purpurea. Molecular plant pathology, 9(3), pp 317-327.

Glazebrook, J., 2005. Contrasting mechanisms of defense against biotrophic and necrotrophic pathogens. Annu. Rev. Phytopathol., 43, pp.205-227.

Goetz, K.E., Coyle, C.M., Cheng, J.Z., O'Connor, S.E. and Panaccione, D.G., 2011. Ergot cluster-encoded catalase is required for synthesis of chanoclavine-I in Aspergillus fumigatus. *Current genetics*, *57*(3), p.201.

Gordon A, 2009. FASTX-Toolkit: FASTQ/A short-reads pre-processing tools. Available online at: http://hannonlab.cshl.edu/fastx_toolkit/

Gordon, A., Basler, R., Bansept-Basler, P., Fanstone, V., Harinarayan, L., Grant, P. K., Birchmore, R., Bayles, R. A., Boyd, L. A. & O'Sullivan, D. M. 2015. The identification of QTL controlling ergot sclerotia size in hexaploid wheat implicates a role for the Rht dwarfing alleles. Theor Appl Genet, 128(12), pp 2447-60.

Gordon, A., Delamare, G., Tente, E., Boyd, L.A 2019 Determining the routes of transmission of ergot alkaloids in cereal grains. AHDB Project Report 603. https://cereals.ahdb.org.uk/media/1479196/pr603-final-project-report.pdf

A Gordon, C McCartney, RE Knox, N Ereful, CW Hiebert, DJ Konkin, Ya-C Hsueh, V Bhadauria, M Sgroi, DM O'Sullivan, C Hadley, LA Boyd, JG Menzies (2020) Genetic and transcriptional dissection of resistance to Claviceps purpurea in the durum wheat cultivar Greenshank. Theoretical and Applied Genetics, 1-14

Grant, M.R. and Jones, J.D., 2009. Hormone (dis) harmony moulds plant health and disease. *Science*, *324*(5928), pp.750-752.

Griffiths, J., Murase, K., Rieu, I., Zentella, R., Zhang, Z.-L., Powers, S. J., Gong, F., Phillips, A. L., Hedden, P. & Sun, T.-p. 2006. Genetic characterization and functional analysis of the GID1 gibberellin receptors in Arabidopsis. The Plant Cell, 18(12), pp 3399-3414.

Haarmann, T., Machado, C., Lübbe, Y., Correia, T., Schardl, C.L., Panaccione, D.G. and Tudzynski, P., 2005. The ergot alkaloid gene cluster in Claviceps purpurea: extension of the cluster sequence and intra species evolution. *Phytochemistry*, *66*(11), pp.1312-1320.

Haarmann, T., Ortel, I., Tudzynski, P. and Keller, U., 2006. Identification of the cytochrome P450 monooxygenase that bridges the clavine and ergoline alkaloid pathways. *ChemBioChem*, *7*(4), pp.645-652.

Haarmann, T., Rolke, Y., Giesbert, S. and Tudzynski, P., 2009. Ergot: from witchcraft to biotechnology. *Molecular Plant Pathology*, *10*(4), pp.563-577.

Haas, M., Schreiber, M. and Mascher, M., 2019. Domestication and crop evolution of wheat and barley: Genes, genomics, and future directions. *Journal of integrative plant biology*, *61*(3), pp.204-225.

Hambrock, A., Peveling, E. and Tudzynski, P., 1992. Lokalisation von Callose in verschiedenen Stadien der Entwicklung von Claviceps purpurea auf Secale cereale. Botanikertagung, p.403.

Han, X. and Kahmann, R., 2019. Manipulation of phytohormone pathways by effectors of filamentous plant pathogens. *Frontiers in plant science*, *10*, p.822.

Hardcastle, T J , Kelly K A. 2010. baySeq: Empirical Bayesian methods for identifying differential expression in sequence count data. BMC Bioinformatics. 11:422

Hardcastle, TJ. 2017a. baySeq: Empirical Bayesian analysis of patterns of differential expression in count data (vignette). https://www.bioconductor.org/

Hardcastle, TJ. 2017b. Advanced analysis using baySeq; generic distribution definitions (vignette). https://www.bioconductor.org

Hedden, P., 1997. The oxidases of gibberellin biosynthesis: their function and mechanism. *Physiologia Plantarum*, *101*(4), pp.709-719.

Hedden, P. and Phillips, A.L., 2000. Gibberellin metabolism: new insights revealed by the genes. *Trends in plant science*, *5*(12), pp.523-530.

Hedden, P., 2003. The genes of the Green Revolution. *TRENDS in Genetics*, *19*(1), pp.5-9.

Hedden, P. and Thomas, S.G., 2012. Gibberellin biosynthesis and its regulation. *Biochemical Journal*, *444*(1), pp.11-25.

Hedden, P., 2018. Gibberellin biosynthesis in higher plants. *Annual Plant Reviews online*, pp.37-71.

Heil, M. and Ton, J., 2008. Long-distance signalling in plant defence. *Trends in plant science*, *13*(6), pp.264-272.

Hinsch, J., Galuszka, P. & Tudzynski, P. 2016. Functional characterization of the first filamentous fungal tRNA-isopentenyltransferase and its role in the virulence of Claviceps purpurea. New Phytologist, 211(3), pp 980-992.

Hinsch, J., Vrabka, J., Oeser, B., Novák, O., Galuszka, P. & Tudzynski, P. 2015. De novo biosynthesis of cytokinins in the biotrophic fungus Claviceps purpurea. Environmental microbiology, 17(8), pp 2935-2951.

Hirano, K., Ueguchi-Tanaka, M. and Matsuoka, M., 2008. GID1-mediated gibberellin signaling in plants. Trends in plant science, 13(4), pp.192-199.

Hou, X., Lee, L. Y. C., Xia, K., Yan, Y. & Yu, H. 2010. DELLAs modulate jasmonate signaling via competitive binding to JAZs. Developmental cell, 19(6), pp 884-894.

Hulvová, H., Galuszka, P., Frébortová, J. and Frébort, I., 2013. Parasitic fungus Claviceps as a source for biotechnological production of ergot alkaloids. *Biotechnology Advances*, *31*(1), pp.79-89.

The International Wheat Genome Sequencing Consortium (IWGSC), et al. 2018. Science, 17 (361) eaar7191 DOI: 10.1126/science.aar7191. Available online at: https://wheat-urgi.versailles.inra.fr/

Iwai, T., Miyasaka, A., Seo, S. and Ohashi, Y., 2006. Contribution of ethylene biosynthesis for resistance to blast fungus infection in young rice plants. *Plant physiology*, *142*(3), pp.1202-1215.

Jasinski, S., Piazza, P., Craft, J., Hay, A., Woolley, L., Rieu, I., Phillips, A., Hedden, P. and Tsiantis, M., 2005. KNOX action in Arabidopsis is mediated by coordinate regulation of cytokinin and gibberellin activities. *Current Biology*, *15*(17), pp.1560-1565.

Jayaswall, K., Mahajan, P., Singh, G., Parmar, R., Seth, R., Raina, A., Swarnkar, M.K., Singh, A.K., Shankar, R. and Sharma, R.K., 2016. Transcriptome analysis reveals candidate genes involved in blister blight defense in tea (Camellia sinensis (L) Kuntze). Scientific reports, 6, p.30412.

Jones, J. D. & Dangl, J. L. 2006. The plant immune system. Nature, 444(7117), pp 323-329.

Jung, H.W., Tschaplinski, T.J., Wang, L., Glazebrook, J. and Greenberg, J.T., 2009. Priming in systemic plant immunity. *Science*, *324*(5923), pp.89-91.

Jupe, J., Stam, R., Howden, A. J., Morris, J. A., Zhang, R., Hedley, P. E. & Huitema, E. 2013. Phytophthora capsici-tomato interaction features dramatic shifts in gene expression associated with a hemi-biotrophic lifestyle. Genome biology, 14(6), pp 1.

Kamoun, S. 2007. Groovy times: filamentous pathogen effectors revealed. Current opinion in plant biology, 10(4), pp 358-365.

Kang, Z. and Buchenauer, H., 1999. Immunocytochemical localization of Fusarium toxins in infected wheat spikes by Fusarium culmorum. *Physiological and Molecular Plant Pathology*, *55*(5), pp.275-288.

Kasahara, H., Hanada, A., Kuzuyama, T., Takagi, M., Kamiya, Y. and Yamaguchi, S., 2002. Contribution of the mevalonate and methylerythritol phosphate pathways to the biosynthesis of gibberellins inArabidopsis. *Journal of Biological Chemistry*, *277*(47), pp.45188-45194.

Katsir, L., Schilmiller, A.L., Staswick, P.E., He, S.Y. and Howe, G.A., 2008. COI1 is a critical component of a receptor for jasmonate and the bacterial virulence factor coronatine. *Proceedings of the National Academy of Sciences*, *105*(19), pp.7100-7105.

Kawaide, H., Imai, R., Sassa, T. and Kamiya, Y., 1997. ent-Kaurene Synthase from the FungusPhaeosphaeria sp. L487 cDNA ISOLATION, CHARACTERIZATION, AND BACTERIAL EXPRESSION OF A BIFUNCTIONAL DITERPENE CYCLASE IN FUNGAL GIBBERELLIN BIOSYNTHESIS. *Journal of Biological Chemistry*, *272*(35), pp.21706-21712.

Kazan, K. & Lyons, R. 2014. Intervention of phytohormone pathways by pathogen effectors. The Plant Cell, 26(6), pp 2285-2309.

Keller, U. and Tudzynski, P., 2002. Ergot alkaloids. In *Industrial Applications* (pp. 157-181). Springer, Berlin, Heidelberg.

Kim, M., Ahn, J.W., Jin, U.H., Choi, D., Paek, K.H. and Pai, H.S., 2003. Activation of the programmed cell death pathway by inhibition of proteasome function in plants. *Journal of Biological Chemistry*, *278*(21), pp.19406-19415.

Kind, S., Hinsch, J., Vrabka, J., Hradilová, M., Majeská-Čudejková, M., Tudzynski, P. and Galuszka, P., 2018. Manipulation of cytokinin level in the ergot fungus Claviceps purpurea emphasizes its contribution to virulence. *Current genetics*, *64*(6), pp.1303-1319.

Kokkonen, M. and Jestoi, M., 2010. Determination of ergot alkaloids from grains with UPLC-MS/MS. *Journal of separation science*, *33*(15), pp.2322-2327.

Komolong, B., Chakraborty, S., Ryley, M. and Yates, D., 2003. Ovary colonization by Claviceps africana is related to ergot resistance in male-sterile sorghum lines. Plant Pathology, 52(5), pp.620-627.

Korzun, V., Röder, M.S., Ganal, M.W., Worland, A.J. and Law, C.N., 1998. Genetic analysis of the dwarfing gene (Rht8) in wheat. Part I. Molecular mapping of Rht8 on the short arm of chromosome 2D of bread wheat (Triticum aestivum L.). *Theoretical and Applied Genetics*, *96*(8), pp.1104-1109.

Lan, L., Chen, W., Lai, Y., Suo, J., Kong, Z., Li, C., Lu, Y., Zhang, Y., Zhao, X., Zhang, X. and Zhang, Y., 2004. Monitoring of gene expression profiles and isolation of candidate genes involved in pollination and fertilization in rice (Oryza sativa L.) with a 10K cDNA microarray. *Plant molecular biology*, *54*(4), pp.471-487.

Langmead B, Salzberg S. Fast gapped-read alignment with Bowtie 2. Nature Methods. 2012, 9:357-359.

Lee, S.L., Floss, H.G. and Heinstein, P., 1976. Purification and properties of dimethylallylpyrophosphate: tryptophan dimethylallyl transferase, the first enzyme of ergot alkaloid biosynthesis in Claviceps. sp. SD 58. *Archives of biochemistry and biophysics*, *177*(1), pp.84-94.

Lee, G.I. and Howe, G.A., 2003. The tomato mutant spr1 is defective in systemin perception and the production of a systemic wound signal for defense gene expression. *The Plant Journal*, *33*(3), pp.567-576.

Leyser, O., 2006. Dynamic integration of auxin transport and signalling. Current Biology, 16(11), pp.R424-R433.

Leyser, O., 2018. Auxin Signaling. Plant Physiology, 176: 465-479.

Li H, Handsaker B, Wysoker A, Fennell T., Ruan J., Homer N., Marth G., Abecasis G., Durbin R. and 1000 Genome Project Data Processing Subgroup (2009) The Sequence alignment/map (SAM) format and SAMtools. Bioinformatics, 25, 2078-9.

Li, Q.F., Wang, C., Jiang, L., Li, S., Sun, S.S. and He, J.X., 2012. An interaction between BZR1 and DELLAs mediates direct signaling crosstalk between brassinosteroids and gibberellins in Arabidopsis. *Science signaling*, *5*(244), pp.ra72-ra72.

Lindig-Cisneros, R., Dirzo, R. & Espinosa-García, F. J. 2002. Effects of domestication and agronomic selection on phytoalexin antifungal defense in Phaseolus beans. Ecological Research, 17(3), pp 315-321.

Liu Y, Zhou J, White KP. RNA-seq differential expression studies: more sequence or more replication? Bioinformatics. 2014;30:301–304. doi: 10.1093/bioinformatics/btt688.

Lorenz, N., Olšovská, J., Šulc, M. and Tudzynski, P., 2010. Alkaloid cluster gene ccsA of the ergot fungus Claviceps purpurea encodes chanoclavine I synthase, a flavin adenine dinucleotide-containing oxidoreductase mediating the transformation of N-methyl-dimethylallyltryptophan to chanoclavine I. *Appl. Environ. Microbiol.*, *76*(6), pp.1822-1830.

Loutre, C., Wicker, T., Travella, S., Galli, P., Scofield, S., Fahima, T., Feuillet, C. and Keller, B., 2009. Two different CC-NBS-LRR genes are required for Lr10-mediated leaf rust resistance in tetraploid and hexaploid wheat. The Plant Journal, 60(6), pp.1043-1054.

Love, Michael I., Anders S, Kim V and Huber W. RNA-seq workflow: gene-level exploratory analysis and differential expression. https://www.bioconductor.org/help/workflows/rnaseqGene/

MacDonald SJ, Anderson WAC. A desk study to review current knowledge on ergot alkaloids and their potential for contamination to cereal grains. AHDB Research Review No. PR575 (2017) AHDB Website

MacMILLAN, J.A.K.E., 1999. Diterpene biosynthesis. *Isoprenoid Including Carotenoids and Steroids*.

Martín, A.C., Castillo, A., Atienza, S.G. and Rodriguez-Suarez, C., 2018. A cytoplasmic male sterility (CMS) system in durum wheat. *Molecular Breeding*, *38*(7), p.90.

Matuschek, M., Wallwey, C., Wollinsky, B., Xie, X. and Li, S.M., 2012. In vitro conversion of chanoclavine-I aldehyde to the stereoisomers festuclavine and pyroclavine controlled by the second reduction step. *RSC advances*, *2*(9), pp.3662-3669.

McKenna A, Hanna M, Banks E, Sivachenko A, Cibulskis K, Kernytsky A, Garimella K, Altshuler D, Gabriel S, Daly M, DePristo MA, 2010. The Genome Analysis Toolkit: a MapReduce framework for analyzing next-generation DNA sequencing data. Genome Research. 20:1297-303. doi: 10.1101/gr.107524.110

Memelink, J., 2009. Regulation of gene expression by jasmonate hormones. Phytochemistry, 70(13-14), pp.1560-1570.

Mette, M. F., Gils, M., Longin, F. H., Reif, J. C. 2015. Hybrid Breeding in Wheat. In: Advances in wheat genetics: From Genome to Field. Ed Ogihara, Y. et al., DOI: 10.1007/978-4-431-55675-6_24

Miedaner, T., Dänicke, S., Schmiedchen, B., Wilde, P., Wortmann, H., Dhillon, B.S., Geiger, H.H. and Mirdita, V., 2010. Genetic variation for ergot (Claviceps purpurea) resistance and alkaloid concentrations in cytoplasmic-male sterile winter rye under pollen isolation. *Euphytica*, *173*(3), pp.299-306.

Miedaner, T. and Geiger, H.H., 2015. Biology, genetics, and management of ergot (Claviceps spp.) in rye, sorghum, and pearl millet. *Toxins*, *7*(3), pp.659-678.

Min, X.J., Butler, G., Storms, R. and Tsang, A. OrfPredictor: predicting protein-coding regions in EST-derived sequences. Nucleic Acids Res., 2005, Web Server Issue W677-W680. http://bioinformatics.ysu.edu/tools/OrfPredictor.html

Misra, R C, Sandeep, Kamthan M, Kumar S and Ghosh S. 2016. A thaumatin-like protein of Ocimum basilicum confers tolerance to fungal pathogen and abiotic stress in transgenic Arabidopsis. Scientific Reports 6, 25340. doi:10.1038/srep25340

Monaghan, J. & Zipfel, C. 2012. Plant pattern recognition receptor complexes at the plasma membrane. Current opinion in plant biology, 15(4), pp 349-357.

Morrone, D., Chen, X., Coates, R.M. and Peters, R.J., 2010. Characterization of the kaurene oxidase CYP701A3, a multifunctional cytochrome P450 from gibberellin biosynthesis. *Biochemical Journal*, *431*(3), pp.337-347.

Mur, L.A., Kenton, P., Atzorn, R., Miersch, O. and Wasternack, C., 2006. The outcomes of concentration-specific interactions between salicylate and jasmonate signaling include synergy, antagonism, and oxidative stress leading to cell death. Plant physiology, 140(1), pp.249-262.

Navarro, L., Bari, R., Achard, P., Lisón, P., Nemri, A., Harberd, N. P. & Jones, J. D. 2008. DELLAs control plant immune responses by modulating the balance of jasmonic acid and salicylic acid signaling. Current Biology, 18(9), pp 650-655.

Nielen, M.W. and van Beek, T.A., 2014. Macroscopic and microscopic spatially-resolved analysis of food contaminants and constituents using laser-ablation electrospray ionization mass spectrometry imaging. *Analytical and bioanalytical chemistry*, *406*(27), pp.6805-6815.

Oerke, E.-C. 2006. Crop losses to pests. The Journal of Agricultural Science, 144(01), pp 31-43.

Oeser, B., Kind, S., Schurack, S., Schmutzer, T., Tudzynski, P. and Hinsch, J., 2017. Cross-talk of the biotrophic pathogen Claviceps purpurea and its host Secale cereale. BMC genomics, 18(1), p.273.

Oh Sunghee, Seongho Song, Gregory Grabowski, Hongyu Zhao, and James P. Noonan. 2013. Methodology Report Time Series Expression Analyses Using RNA-seq: A Statistical Approach. Hindawi Publishing Corporation BioMed Research International. 203681. doi.org/10.1155/2013/203681

Panaccione, D.G., Beaulieu, W.T. and Cook, D., 2014. Bioactive alkaloids in vertically transmitted fungal endophytes. *Functional Ecology*, *28*(2), pp.299-314.

Pandey, S.P. and Somssich, I.E., 2009. The role of WRKY transcription factors in plant immunity. Plant physiology, 150(4), pp.1648-1655.

Patkar, R.N., Benke, P.I., Qu, Z., Chen, Y.Y.C., Yang, F., Swarup, S. and Naqvi, N.I., 2015. A fungal monooxygenase-derived jasmonate attenuates host innate immunity. *Nature chemical biology*, *11*(9), pp.733-740.

Patkar, R.N. and Naqvi, N.I., 2017. Fungal manipulation of hormone-regulated plant defense. *PLoS pathogens*, *13*(6), p.e1006334.

Patro, R, Duggal, G, Love, MI, Irizarry, RA, and Kingsford, C. (2017). Salmon provides fast and bias-aware quantification of transcript expression. Nature Methods. 14(4): 417-419.

Pearce, S., Saville, R., Vaughan, S.P., Chandler, P.M., Wilhelm, E.P., Sparks, C.A., Al-Kaff, N., Korolev, A., Boulton, M.I., Phillips, A.L. and Hedden, P., 2011. Molecular characterization of Rht-1 dwarfing genes in hexaploid wheat. *Plant physiology*, *157*(4), pp.1820-1831.

Pečenková, T., Hála, M., Kulich, I., Kocourková, D., Drdová, E., Fendrych, M., Toupalová, H. and Žárský, V., 2011. The role for the exocyst complex subunits Exo70B2 and Exo70H1 in the plant–pathogen interaction. Journal of experimental botany, 62(6), pp.2107-2116.

Peng, J., Richards, D. E., Hartley, N. M., Murphy, G. P., Devos, K. M., Flintham, J. E., Beales, J., Fish, L. J., Worland, A. J. & Pelica, F. 1999. 'Green revolution'genes encode mutant gibberellin response modulators. Nature, 400(6741), pp 256-261.

Peng, J.H., Sun, D. and Nevo, E., 2011. Domestication evolution, genetics and genomics in wheat. *Molecular Breeding*, *28*(3), p.281.

Phillips, A.L., 2018. Genetic control of gibberellin metabolism and signalling in crop improvement. *Annual Plant Reviews online*, pp.405-429.

Pieterse, C. M., Van der Does, D., Zamioudis, C., Leon-Reyes, A. & Van Wees, S. C. 2012. Hormonal modulation of plant immunity. Annual review of cell and developmental biology, 28(489-521.

Ponts, N., Pinson-Gadais, L., Verdal-Bonnin, M.N., Barreau, C. and Richard-Forget, F., 2006. Accumulation of deoxynivalenol and its 15-acetylated form is significantly modulated by oxidative stress in liquid cultures of Fusarium graminearum. *FEMS Microbiology Letters*, *258*(1), pp.102-107.

Ponts, N., Pinson-Gadais, L., Barreau, C., Richard-Forget, F. and Ouellet, T., 2007. Exogenous H2O2 and catalase treatments interfere with Tri genes expression in liquid cultures of Fusarium graminearum. *FEBS letters*, *581*(3), pp.443-447.

Qin, X., Liu, J. H., Zhao, W. S., Chen, X. J., Guo, Z. J. & Peng, Y. L. 2013. Gibberellin 20-oxidase gene OsGA20ox3 regulates plant stature and disease development in rice. Molecular plant-microbe interactions, 26(2), pp 227-239.

Rapaport F, Khanin R, Liang Y, Pirun M, Krek A, Zumbo P, et al. Comprehensive evalution of differential gene expression analysis methods for RNA-seq data. Genome Biol. 2013;14:261. doi: 10.1186/gb-2013-14-9-r95.

Reed, J.D., Tuinstra, M.R., McLaren, N.W., Kofoid, K.D., Ochanda, N.W. and Claflin, L.E., 2002. Analysis of combining ability for ergot resistance in grain sorghum. Crop science, 42(6), pp.1818-1823.

Rebetzke, G.J. and Richards, R.A., 2000. Gibberellic acid-sensitive dwarfing genes reduce plant height to increase kernel number and grain yield of wheat. *Australian journal of agricultural research*, *51*(2), pp.235-246.

Reverberi, M., Ricelli, A., Zjalic, S., Fabbri, A.A. and Fanelli, C., 2010. Natural functions of mycotoxins and control of their biosynthesis in fungi. *Applied microbiology and biotechnology*, *87*(3), pp.899-911.

Robinson MD and Oshlack A. 2010. A scaling normalization method for differential expression analysis of RNA-seq data. Genome Biology Method. 11:R25. doi.org/10.1186/gb-2010-11-3-r25.

Ross, J.J., Miraghazadeh, A., Beckett, A.H., Quittenden, L.J. and McAdam, E.L., 2018. Interactions between gibberellins and other hormones. *Annual Plant Reviews online*, pp.229-252.

Rudd, J. J., Kanyuka, K., Hassani-Pak, K., Derbyshire, M., Andongabo, A., Devonshire, J., Lysenko, A., Saqi, M., Desai, N. M. & Powers, S. J. 2015. Transcriptome and metabolite profiling of the infection cycle of Zymoseptoria tritici on wheat reveals a biphasic interaction with plant immunity involving differential pathogen chromosomal contributions and a variation on the hemibiotrophic lifestyle definition. Plant physiology, 167(3), pp 1158-1185.

Saikkonen, K., Saari, S. and Helander, M., 2010. Defensive mutualism between plants and endophytic fungi?. *Fungal Diversity*, *41*(1), pp.101-113.

Salazar-Cerezo, S., Martínez-Montiel, N., García-Sánchez, J., Pérez-y-Terrón, R. and Martínez-Contreras, R.D., 2018. Gibberellin biosynthesis and metabolism: A convergent route for plants, fungi and bacteria. *Microbiological research*, *208*, pp.85-98.

Sato, T. and Theologis, A., 1989. Cloning the mRNA encoding 1-aminocyclopropane-1-carboxylate synthase, the key enzyme for ethylene biosynthesis in plants. Proceedings of the National Academy of Sciences, 86(17), pp.6621-6625.

Saunders, D. G., Win, J., Cano, L. M., Szabo, L. J., Kamoun, S. & Raffaele, S. 2012. Using hierarchical clustering of secreted protein families to classify and rank candidate effectors of rust fungi. PLoS One, 7(1), pp e29847.

Saville, R.J., Gosman, N., Burt, C.J., Makepeace, J., Steed, A., Corbitt, M., Chandler, E., Brown, J.K.M., Boulton, M.I. and Nicholson, P., 2012. The 'Green Revolution'dwarfing genes play a role in disease resistance in Triticum aestivum and Hordeum vulgare. *Journal of experimental botany*, *63*(3), pp.1271-1283.

Saunders, D. G., Win, J., Cano, L. M., Szabo, L. J., Kamoun, S. & Raffaele, S. 2012. Using hierarchical clustering of secreted protein families to classify and rank candidate effectors of rust fungi. PLoS One, 7(1), pp e29847.

Schardl, C.L., Panaccione, D.G. and Tudzynski, P., 2006. Ergot alkaloids–biology and molecular biology. *The alkaloids: chemistry and biology*, *63*, pp.45-86.

Schardl, C.L., Young, C.A., Pan, J., Florea, S., Takach, J.E., Panaccione, D.G., Farman, M.L., Webb, J.S., Jaromczyk, J., Charlton, N.D. and Nagabhyru, P., 2013. Currencies of mutualisms: sources of alkaloid genes in vertically transmitted epichloae. *Toxins*, *5*(6), pp.1064-1088.

Schiff Jr, P.L., 2006. Ergot and its alkaloids. *American journal of pharmaceutical education*, *70*(5).

Schmieder R and Edwards R. 2011. Quality control and preprocessing of metagenomic datasets. Bioinformatics. 27:863-864.

Schmülling, T., Werner, T., Riefler, M., Krupková, E. and y Manns, I.B., 2003. Structure and function of cytokinin oxidase/dehydrogenase genes of maize, rice, Arabidopsis and other species. Journal of plant research, 116(3), pp.241-252.

Schwechheimer, C. & Willige, B. C. 2009. Shedding light on gibberellic acid signalling. Current opinion in plant biology, 12(1), pp 57-62.

Selin, C., de Kievit, T. R., Belmonte, M. F. & Fernando, W. D. 2016. Elucidating the role of effectors in plant-fungal interactions: progress and challenges. Frontiers in microbiology, 7(

Seo, M., Jikumaru, Y. and Kamiya, Y., 2011. Profiling of hormones and related metabolites in seed dormancy and germination studies. In *Seed Dormancy* (pp. 99-111). Humana Press.

Shah, J. and Zeier, J., 2013. Long-distance communication and signal amplification in systemic acquired resistance. *Frontiers in Plant Science*, *4*, p.30.

Singh, R.P., Singh, P.K., Rutkoski, J., Hodson, D.P., He, X., Jørgensen, L.N., Hovmøller, M.S. and Huerta-Espino, J., 2016. Disease impact on wheat yield potential and prospects of genetic control. *Annual review of phytopathology*, *54*, pp.303-322.

Slaiding, I.R. and Byrd, N., 2013. *Ensuring that UK cereals used in malting, milling and animal feed achieve food and feed safety standards*. HGCA.

Spanos, N.P. and Gottlieb, J., 1976. *Ergotism and the Salem Village witch trials*. Na

Spence, C.A., Lakshmanan, V., Donofrio, N. and Bais, H.P., 2015. Crucial roles of abscisic acid biogenesis in virulence of rice blast fungus Magnaporthe oryzae. *Frontiers in plant science*, *6*, p.1082.

Sponsel, V.M. and Hedden, P., 2010. Gibberellin biosynthesis and inactivation. In *Plant Hormones* (pp. 63-94). Springer, Dordrecht.

Sponsel, V.M., 2018. Signal achievements in gibberellin research: the second half-century. *Annual Plant Reviews online*, pp.1-36.

Staswick, P.E., Serban, B., Rowe, M., Tiryaki, I., Maldonado, M.T., Maldonado, M.C. and Suza, W., 2005. Characterization of an Arabidopsis enzyme family that conjugates amino acids to indole-3-acetic acid. The Plant Cell, 17(2), pp.616-627.

Stepanova, A.N. and Alonso, J.M., 2005. Ethylene signalling and response pathway: a unique signalling cascade with a multitude of inputs and outputs. *Physiologia Plantarum*, *123*(2), pp.195-206.

Sun, T.-p. & Gubler, F. 2004. Molecular mechanism of gibberellin signaling in plants. Annu. Rev. Plant Biol., 55(197-223.

Swan, D. J. & Mantle, P. G. 1991. Parasitic interactions between Claviceps purpurea strains in wheat and an acute necrotic host response. Mycological Research, 95(7), pp 807-810.

Tanaka, N., Matsuoka, M., Kitano, H., Asano, T., Kaku, H. & Komatsu, S. 2006. gid1, a gibberellin-insensitive dwarf mutant, shows altered regulation of probenazole-inducible protein (PBZ1) in response to cold stress and pathogen attack. Plant Cell Environ, 29(4), pp 619-31.

Tenberge, K. B. 1999. 2. Biology and life strategy of the ergot fungi. Ergot: the genus Claviceps, 25.

Tenberge K, Tudzynski P. Early infection of rye ovaries by Claviceps purpurea is inter-and intracellular. 1994. BioEng Sondernr. 10:22

Thomas, S.G., Phillips, A.L. and Hedden, P., 1999. Molecular cloning and functional expression of gibberellin 2-oxidases, multifunctional enzymes involved in gibberellin deactivation. *Proceedings of the National Academy of Sciences*, *96*(8), pp.4698-4703.

Thornton, C. R. & Wills, O. E. 2015. Immunodetection of fungal and oomycete pathogens: established and emerging threats to human health, animal welfare and global food security. Critical reviews in microbiology, 41(1), pp 27-51.

Tittlemier, S.A., Drul, D., Roscoe, M. and McKendry, T., 2015. Occurrence of ergot and ergot alkaloids in western Canadian wheat and other cereals. *Journal of agricultural and food chemistry*, *63*(29), pp.6644-6650.

Tittlemier, S.A., Drul, D., Roscoe, M. and Menzies, J.G., 2016. The effects of selected factors on measured ergot alkaloid content in Claviceps purpurea-infected hexaploid and durum wheat. *World Mycotoxin Journal*, *9*(4), pp.555-564.

Truman, W., Bennett, M.H., Kubigsteltig, I., Turnbull, C. and Grant, M., 2007. Arabidopsis systemic immunity uses conserved defense signaling pathways and is mediated by jasmonates. *Proceedings of the national academy of sciences*, *104*(3), pp.1075-1080.

Tudzynski, B., Kawaide, H. and Kamiya, Y., 1998. Gibberellin biosynthesis in Gibberella fujikuroi: cloning and characterization of the copalyl diphosphate synthase gene. *Current genetics*, *34*(3), pp.234-240.

Tudzynski, P., Correia, T. & Keller, U. 2001. Biotechnology and genetics of ergot alkaloids. Applied microbiology and biotechnology, 57(5-6), pp 593-605.

Tudzynski, P. & Scheffer, J. 2004. Claviceps purpurea: molecular aspects of a unique pathogenic lifestyle. Mol Plant Pathol, 5(5), pp 377-88.

Tudzynski, B., 2005. Gibberellin biosynthesis in fungi: genes, enzymes, evolution, and impact on biotechnology. *Applied Microbiology and Biotechnology*, *66*(6), pp.597-611.

van Loon, L.C., Geraats, B.P. and Linthorst, H.J., 2006. Ethylene as a modulator of disease resistance in plants. *Trends in plant science*, *11*(4), pp.184-191.

Vartapetian, A.B., Tuzhikov, A.I., Chichkova, N.V., Taliansky, M. and Wolpert, T.J., 2011. A plant alternative to animal caspases: subtilisin-like proteases. *Cell Death & Differentiation*, *18*(8), pp.1289-1297.

Venske, E., dos Santos, R.S., Busanello, C., Gustafson, P. and de Oliveira, A.C., 2019. Bread wheat: a role model for plant domestication and breeding. *Hereditas*, *156*(1), pp.1-11.

Verberne, M.C., Hoekstra, J., Bol, J.F. and Linthorst, H.J., 2003. Signaling of systemic acquired resistance in tobacco depends on ethylene perception. *The Plant Journal*, *35*(1), pp.27-32.

Verstraete, F., 2008. European Union Legislation on mycotoxins in food and feed. Overview of the decision-making process and recent and future developments. *Mycotoxins: Detection methods, management, public health and agricultural trade*, pp.77-99.

Wäli, P.P., Wäli, P.R., Saikkonen, K. and Tuomi, J., 2013. Is the pathogenic ergot fungus a conditional defensive mutualist for its host grass?. PLoS One, 8(7), p.e69249.

Walters, D., Cowley, T. and Mitchell, A., 2002. Methyl jasmonate alters polyamine metabolism and induces systemic protection against powdery mildew infection in barley seedlings. *Journal of Experimental Botany*, *53*(369), pp.747-756.

Wallwey, C. and Li, S.M., 2011. Ergot alkaloids: structure diversity, biosynthetic gene clusters and functional proof of biosynthetic genes. *Natural product reports*, *28*(3), pp.496-510.

Walzel, B., Riederer, B. and Keller, U., 1997. Mechanism of alkaloid cyclopeptide synthesis in the ergot fungus Claviceps purpurea. *Chemistry & biology*, *4*(3), pp.223-230.

Wang, D., Pajerowska-Mukhtar, K., Culler, A.H. and Dong, X., 2007. Salicylic acid inhibits pathogen growth in plants through repression of the auxin signaling pathway. Current Biology, 17(20), pp.1784-1790.

Wang, J., Ma, X.M., Kojima, M., Sakakibara, H. and Hou, B.K., 2011. N-Glucosyltransferase UGT76C2 is involved in cytokinin homeostasis and cytokinin response in Arabidopsis thaliana. *Plant and Cell Physiology*, *52*(12), pp.2200-2213.

White Jr, J.F. and Torres, M.S., 2010. Is plant endophyte-mediated defensive mutualism the result of oxidative stress protection?. *Physiologia Plantarum*, *138*(4), pp.440-446.

Wilhelm, E.P., Boulton, M.I., Al-Kaff, N., Balfourier, F., Bordes, J., Greenland, A.J., Powell, W. and Mackay, I.J., 2013. Rht-1 and Ppd-D1 associations with height, GA sensitivity, and days to heading in a worldwide bread wheat collection. *Theoretical and applied genetics*, *126*(9), pp.2233-2243.

Woodward, A.W. and Bartel, B., 2005. Auxin: regulation, action, and interaction. Annals of botany, 95(5), pp.707-735.

Wolbang, C.M., Chandler, P.M., Smith, J.J. and Ross, J.J., 2004. Auxin from the developing inflorescence is required for the biosynthesis of active gibberellins in barley stems. *Plant Physiology*, *134*(2), pp.769-776.

Wolf, J. B. 2013. Principles of transcriptome analysis and gene expression quantification: an RNA-seq tutorial. Molecular ecology resources, 13(4), pp 559-572.

Yang, S.F. and Hoffman, N.E., 1984. Ethylene biosynthesis and its regulation in higher plants. *Annual review of plant physiology*, *35*(1), pp.155-189

Yang, D.-L., Li, Q., Deng, Y.-W., Lou, Y.-G., Wang, M.-Y., Zhou, G.-X., Zhang, Y.-Y. & He, Z.-H. 2008. Altered disease development in the eui mutants and Eui overexpressors indicates that gibberellins negatively regulate rice basal disease resistance. Molecular plant, 1(3), pp 528-537.

Yang, D.L., Yao, J., Mei, C.S., Tong, X.H., Zeng, L.J., Li, Q., Xiao, L.T., Sun, T.P., Li, J., Deng, X.W. and Lee, C.M., 2012. Plant hormone jasmonate prioritizes defense over growth by interfering with gibberellin signaling cascade. *Proceedings of the National Academy of Sciences*, *109*(19), pp.E1192-E1200.

Yang, F., Li, W. & Jørgensen, H. J. 2013. Transcriptional reprogramming of wheat and the hemibiotrophic pathogen Septoria tritici during two phases of the compatible interaction. PLoS One, 8(11), pp e81606.

Yin, C., Gan, L., Ng, D., Zhou, X. and Xia, K., 2007. Decreased panicle-derived indole-3-acetic acid reduces gibberellin A1 level in the uppermost internode, causing panicle enclosure in male sterile rice Zhenshan 97A. *Journal of Experimental Botany*, *58*(10), pp.2441-2449.

Yin, C., Park, J.J., Gang, D.R. and Hulbert, S.H., 2014. Characterization of a tryptophan 2-monooxygenase gene from Puccinia graminis f. sp. tritici involved in auxin biosynthesis and rust pathogenicity. *Molecular Plant-Microbe Interactions*, *27*(3), pp.227-235.

Young, J.C., 1981. Variability in the content and composition of alkaloids found in Canadian ergot. II. Wheat. *Journal of Environmental Science & Health Part B*, *16*(4), pp.381-393.

Youssefian, S., Kirby, E.J.M. and Gale, M.D., 1992. Pleiotropic effects of the GA-insensitive Rht dwarfing genes in wheat. 2. Effects on leaf, stem, ear and floret growth. *Field Crops Research*, *28*(3), pp.191-210.

Yu, K., Soares, J.M., Mandal, M.K., Wang, C., Chanda, B., Gifford, A.N., Fowler, J.S., Navarre, D., Kachroo, A. and Kachroo, P., 2013. A feedback regulatory loop between G3P and lipid transfer proteins DIR1 and AZI1 mediates azelaic-acid-induced systemic immunity. *Cell Reports*, *3*(4), pp.1266-1278.

Zhang, Z., Li, Q., Li, Z., Staswick, P.E., Wang, M., Zhu, Y. and He, Z., 2007. Dual regulation role of GH3. 5 in salicylic acid and auxin signaling during Arabidopsis-Pseudomonas syringae interaction. Plant Physiology, 145(2), pp.450-464.

Zhang, H., Yang, Y., Wang, C., Liu, M., Li, H., Fu, Y., Wang, Y., Nie, Y., Liu, X. and Ji, W., 2014. Large-scale transcriptome comparison reveals distinct gene activations in wheat responding to stripe rust and powdery mildew. BMC genomics, 15(1), p.89

Zhao, Y., Li, Z., Liu, G., Jiang, Y., Maurer, H.P., Würschum, T., Mock, H.P., Matros, A., Ebmeyer, E., Schachschneider, R. and Kazman, E., 2015. Genome-based establishment of a high-yielding heterotic pattern for hybrid wheat breeding. *Proceedings of the National Academy of Sciences*, *112*(51), pp.15624-15629.

Zhu, Y., Nomura, T., Xu, Y., Zhang, Y., Peng, Y., Mao, B., Hanada, A., Zhou, H., Wang, R., Li, P. and Zhu, X., 2006. ELONGATED UPPERMOST INTERNODE encodes a cytochrome P450 monooxygenase that epoxidizes gibberellins in a novel deactivation reaction in rice. *The Plant Cell*, *18*(2), pp.442-456.

Zimeri, A.S., Williams, L.D., Riley, R.T. and Glenn, A.E., 2006. The mycotoxin fumonisin B 1 is necessary for corn seedling disease development and is translocated from roots to shoot. *Phytopathology*, *96*(6).

7. Appendices

Appendix A: Supplementary Material for Chapter 2

Table 7.1: Percentage alignment rates for 114 libraries using the RefSeq transcriptome.

Library	No. of reads	% alignment using RefSeq	**Average coverage**
EB1T10	8646439	83.08	9.607154444
EB4T10	4110531	68.87	4.567256667
EB5T10	26563767	82.14	29.51529667
ES1T10	8338638	78.12	9.265153333
ES4T10	8140388	80.08	9.044875556
ET1T10	5342892	78.82	5.936546667
ET4T10	10329694	83.5	11.47743778
ET5T10	8266242	83.73	9.184713333
F6B	10349223	82.69	11.49913667
F6S	5282310	78.49	5.869233333
F7T	7402362	82.87	8.224846667
FB1T10	9518508	84.08	10.57612
FB5T10	5570863	83.86	6.189847778
FS1T10	3719359	78.47	4.132621111
FS5T10	2565118	80.02	2.850131111
FT2T10	7106179	84.62	7.895754444
H7B	9038734	82	10.04303778
H7S	958381	77.46	1.064867778
H7T	3991733	80.92	4.435258889
HB1T1H	4039352	81.54	4.488168889
HB5T24H	10455117	84.6	11.61679667
HS1T1H	3005658	77.75	3.33962
HS4T1H	6943134	78.11	7.714593333
HT1T1H	3392286	83.05	3.769206667
HT5T24H	15227496	84.2	16.91944
IB2T1H	14530662	81.46	16.14518
IB3T1H	1698614	83.85	1.887348889
IB5T1H	5722919	82.14	6.358798889
IS2T1H	1471138	78.01	1.634597778
IS3T1H	13566658	81.34	15.07406444
IT2T1H	10616236	67.8	11.79581778
IT3T1H	14022049	84.34	15.58005444
IT5T1H	2801902	81.08	3.113224444
KB4T5H	4144793	80.54	4.605325556
KB5T5H	1181001	78.29	1.312223333

KS4	728409	74.87	0.809343333
KS5T5H	751563	75.17	0.83507
KT4T5H	1068529	80.87	1.187254444
KT5T5H	1274409	81.71	1.41601
LB1T5H	11222147	83.59	12.46905222
LB3T5H	19834227	83.62	22.03803
LB4T5H	2644868	81.83	2.938742222
LS1T5H	581836	77.63	0.646484444
LS4T5H	148791	71.69	0.165323333
LS5T5H	526205	79.66	0.584672222
LT1T5H	5894932	82.41	6.549924444
LT3T5H	6345375	82.29	7.050416667
LT4T5H	1808326	80.71	2.009251111
MB1T24H	8996380	83.46	9.995977778
MB3T24H	13532668	84.26	15.03629778
MB4T24H	10663021	84.14	11.84780111
MS1T24H	12260120	79.1	13.62235556
MS3T24H	11062304	30.37	12.29144889
MS4T24H	7840358	79.24	8.711508889
MT1T24H	14926364	84.52	16.58484889
MT3T24H	3630257	73.83	4.033618889
MT4T24H	1942409	83.12	2.158232222
NB1T24H	20206113	76.82	22.45123667
NB2T24H	12578496	82.87	13.97610667
NB5T1H	6087878	83.95	6.764308889
NS2T24H	14346498	79.38	15.94055333
NS5T1H	2016424	78.79	2.240471111
NT1T24H	9443334	83.24	10.49259333
NT2T24H	6285660	83.19	6.984066667
NT5T1H	2906021	82.51	3.228912222
OB2T48H	12703101	84.76	14.11455667
OB4T48H	5248668	83.65	5.831853333
OB5T48H	5189031	84.11	5.76559
OT2T48H	7569385	84.89	8.410427778
OT4T48H	11137831	83.71	12.37536778
OT5T48H	4312611	83.64	4.79179
PB1T48H	14567310	83.88	16.1859
PB2T48H	10873847	83.26	12.08205222
PB5T48H	7322356	83.59	8.135951111
PT1T48H	10173382	82.79	11.30375778
PT2T48H	4245053	80.79	4.716725556
PT5T48H	8949836	84.1	9.944262222
QB1T72H	2925436	84.73	3.250484444
QB2T72H	9009199	83.58	10.01022111

QB3T72H	3226946	83.89	3.585495556
QT1T72H	8230101	83.24	9.144556667
QT2T72H	9334661	80.54	10.37184556
QT4T72H	11068654	82.04	12.29850444
RB1T72H	13473051	84.21	14.97005667
RB2T72H	10309054	83.62	11.45450444
RB4T72H	9270608	82.79	10.30067556
RT1T72H	8182526	83.47	9.091695556
RT2T72H	5640401	83.6	6.267112222
RT4T72H	2599522	71.53	2.888357778
SB1T120H	5143207	83.23	5.714674444
SB4T120H	5273324	83.92	5.859248889
SS5T120H	489017	64.66	0.543352222
ST1T120H	4083856	81.48	4.537617778
ST4T120H	6065295	82.39	6.739216667
TB1T120H	9874448	53.15	10.97160889
TB2T120H	7576524	56.18	8.41836
TB4	10439653	55.51	11.59961444
TS1T120H	1811030	51.92	2.012255556
TS2T120H	6664702	51.69	7.405224444
TS4T120H	7673838	52.45	8.526486667
TT1T120H	6021216	51.34	6.69024
TT2T120H	7411083	52.28	8.234536667
TT4T120H	12101102	53.75	13.44566889
UB1T7D	8124653	84.67	9.027392222
UB3T7D	5635053	84.01	6.26117
UB5T7D	11842104	84.29	13.15789333
UT3T7D	2935220	79.94	3.261355556
UT5T7D	2410978	81.92	2.678864444
VB1T7D	11398753	43.64	12.66528111
VB2T7D	16517028	52.71	18.35225333
VB3T7D	9605947	36.06	10.67327444
VT1T7D	8740565	46.11	9.711738889
VT2T7D	5550154	50.12	6.166837778
VT3T7D	5232927	39.19	5.814363333

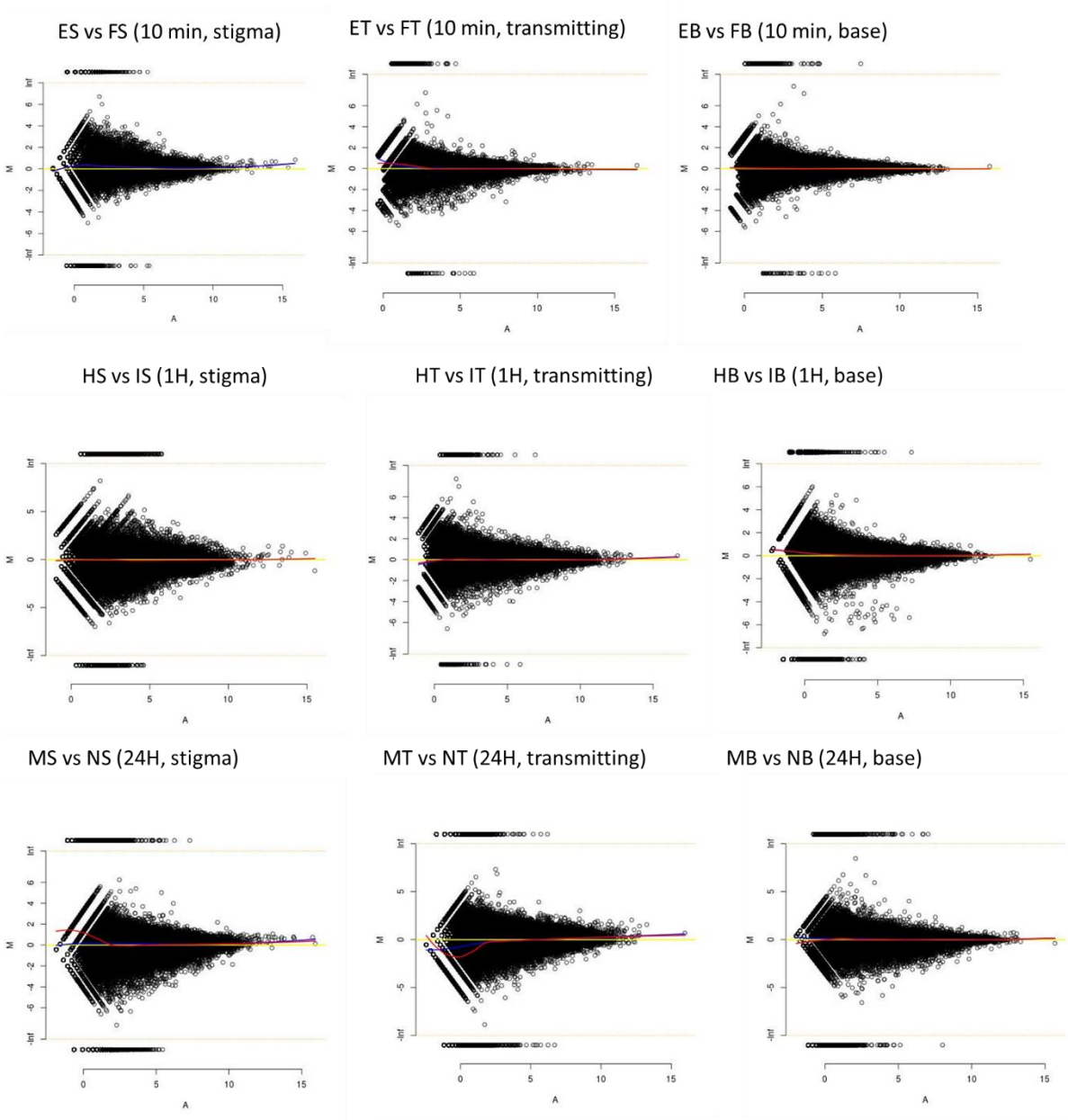

Figure 7.1: MA plots for wheat transcripts at 10 mins, 1 hour and 24 hours. Loess curves (red/blue) were drawn along with the line of symmetry at M=0 (yellow). The blue Loess curve are smoothened curves set at family = "symmetric". The red is a regular Loess curve (M~A). In some figures, only one line is visible since two/all curves may overlap.

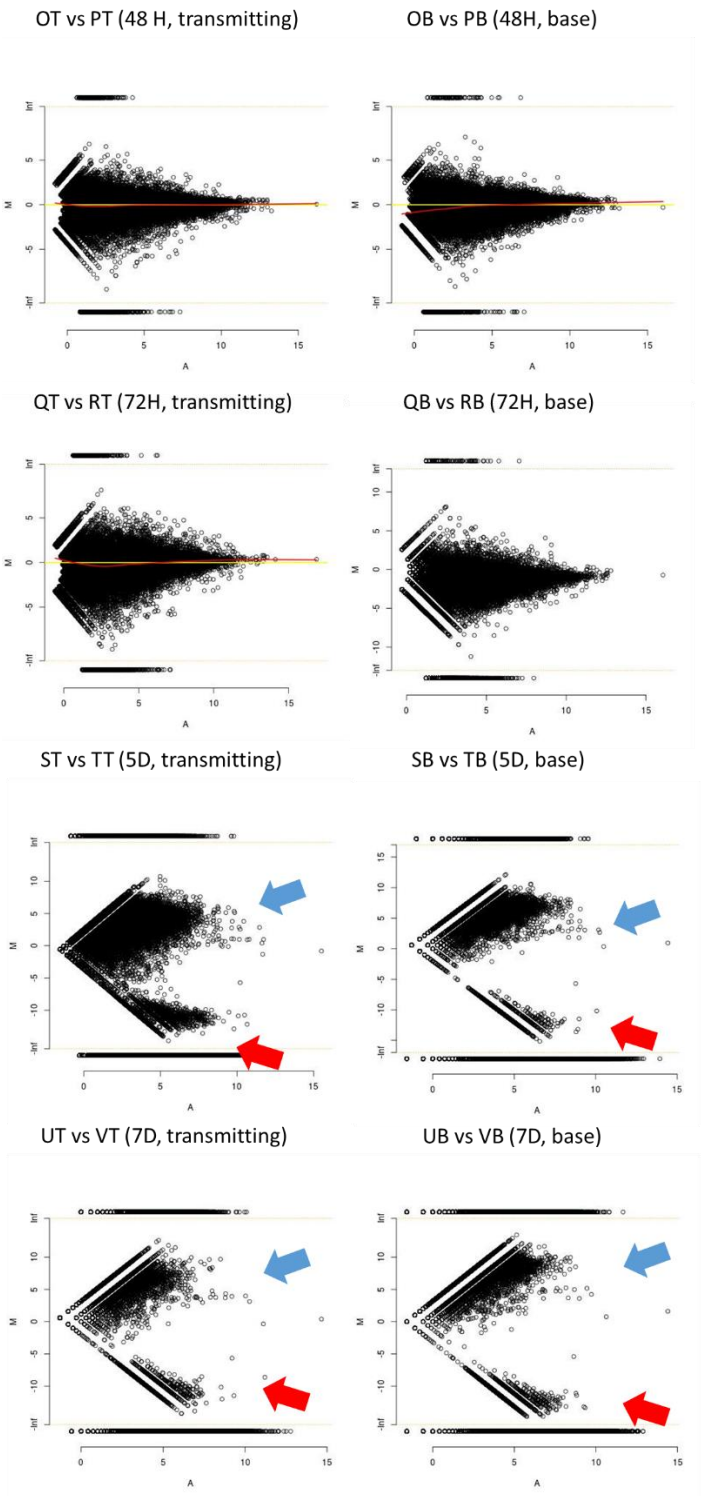

Figure 7.2: MA plots for wheat transcripts at 48 hours, 72 hours, 5 days, and 7 days. Loess curves (red/blue) were drawn along with the line of symmetry at M=0 (yellow). The blue Loess curve are smoothened curves set at family = "symmetric". The red is a regular Loess curve (M~A). In some figures, only one line is visible since two/all curves may overlap. To demonstrate the asymmetric distribution of points, MA plots were generated using both wheat (blue arrow) and *C. purpurea* (red) transcripts.

Table 7.2: Table of all differentially expressed hormone-related genes at the base tissue. The red colour represents up-regulated genes and the green represents down-regulated genes. At the top, a schematic representation of the stage of fungal development in the wheat ovule at each time point is shown.

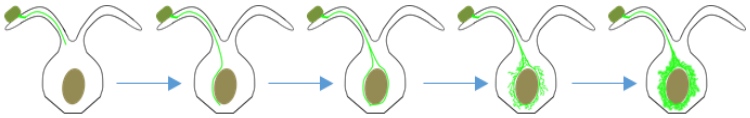

		BASE									
	Type of DE hormone genes	24h		48h		72h		120h		7days	
		UP	DOWN	UP	DOWN	UP	DOWN	UP	DOWN	UP	DOWN
Ethylene	ethylene-responsive transcription factor (ERF)	5	0	19	0	13	5	3	8	0	11
	AP2 domain transcription factor	0	0	1	0	1	1	0	1	0	1
	1-aminocyclopropane-1-carboxylate oxidase (ACO)	0	0	2	0	2	0	0	3	0	2
	1-aminocyclopropane-1-carboxylate synthase (ACS)	0	0	2	0	6	0	3	0	1	0
	5' methylthioadenosine	0	0	0	0	0	0	0	0	0	1
	Ethylene overproduction 1 (ETO1)	0	0	0	0	0	0	0	1	0	0
	Ethylene response sensor 1 (ERS1)	0	0	0	0	0	0	0	2	0	3
	Ethylene receptor	0	0	0	0	0	0	0	1	0	0
	Ethylene Insensitive 3 (EIN3)	0	0	1	0	0	0	0	0	0	1
Auxin	Auxin responsive AUX/IAA	0	0	6	0	27	0	2	2	0	6
	Auxin responsive SAURs	0	0	1	0	1	3	0	0	3	0
	IAA-amido synthetase (GH3)	0	0	7	0	10	0	4	0	0	0
	Indole-3-glycerol phosphate (IGP)	0	0	1	0	0	0	0	0	0	0
	indole-3-acetic acid-induced ARG7	0	0	0	2	0	14	0	3	0	0
	Auxin binding protein (ABP)	0	0	0	0	0	1	0	0	0	1
	Auxin response factor (ARF)	0	0	0	0	2	0	0	2	0	7
	2 oxoglutarate-dependent dioxygenase (DAO)	0	0	1	0	4	1	1	2	0	4
	indole-3-acetate beta glucosyltransferase	0	0	1	0	1	0	0	0	0	0
	probable auxin efflux carrier	0	0	0	0	5	0	0	0	1	1
	PIN-FORMED (PIN)	0	0	0	0	0	1	0	0	0	1
	auxin transporter	0	0	0	0	4	0	0	0	0	0
	auxin induced	0	0	0	0	3	2	0	0	0	0
	PINOID protein kinase	0	0	0	0	2	0	0	0	0	0
	WALLS ARE THIN 1 (WAT1)	0	0	0	0	4	1	0	0	0	1
	SUPPRESOR OF AUXIN RESISTANCE 1 (SAR1)	0	0	0	0	0	0	0	1	0	1
Cytokinin	Cytokinin oxidase dehydrogenase (CKX)	0	0	1	0	1	0	0	0	0	1
	cytokinin 5' monophosphate phosphoribohydrolase	0	0	2	0	4	1	0	1	0	0
	cytokinin glycosyltransferase	0	0	0	0	1	0	1	0	1	0
	Histidine phosphotransfer protein (AHP)	0	0	0	0	0	0	0	2	0	1
Brassinosteroid	BZR1	0	0	0	0	0	3	0	2	0	4
	Interact-With-Spt6 (IWS1)	0	0	0	0	0	0	0	2	0	0
	BRASSINOSTEROID INSENSITIVE 1 (BRI1)	0	0	0	0	0	0	0	2	0	1
	BSL2	0	0	0	0	0	0	0	0	0	0
Gibberellin	Gibberellin receptor GID1	0	0	0	1	1	1	0	1	0	1
	Gibberellin 2-beta-dioxygenase	0	0	0	0	2	0	0	0	0	1
	Gibberellin 3-beta-dioxygenase	0	0	0	0	2	0	0	0	0	0
	Gibberellin 3-hydroxylase	0	0	0	0	1	0	0	0	0	0
	ent-kaurene synthase	0	0	0	0	0	0	0	1	0	0
	ent-kaurene oxidase	0	0	0	0	0	0	0	0	1	0
	Chitin-inducible gibberellin responsive (CIGR)	0	0	5	0	0	0	0	0	0	0
	DELLA	0	0	0	0	0	0	0	2	0	1
	GAST1	0	0	0	0	0	0	0	2	0	3
	Gibberellin regulated	0	0	0	0	0	1	0	2	0	2
Abscisic acid	Abscisic acid receptor PYL4	0	0	0	0	1	0	0	0	0	0
	ABSCISIC ACID INSENSITIVE 5 (ABI5)	0	0	0	0	1	0	0	0	0	0
	Abscisic acid 8' hydroxylase	0	0	0	0	1	0	0	0	0	0
	Abscisic acid inducible kinase	0	0	0	0	0	0	0	1	0	0
	FBW2	0	0	0	0	0	0	0	2	0	1
	SAPK7	0	0	0	0	0	0	0	0	0	1
	SNF kinase	0	0	0	0	1	0	0	2	0	3
Jasmonic Acid	Allene oxide synthase (AOS)	0	0	1	0	0	1	0	0	0	0
	12-oxophytodienoate reductase (OPR)	0	0	0	0	1	0	1	1	0	1
	Chlorophyllase 1 (CLH1)	0	0	0	0	0	1	0	0	0	0
	TIFY transcription factors	2	0	16	0	2	0	0	2	0	7
	Novel interactor of JAZ (NINJA)	0	0	0	0	0	0	0	1	0	2
	Jasmonate induced	0	1	0	0	1	0	0	0	0	0
SA	Salicylic acid binding protein (SABP)	0	0	0	0	0	0	0	0	0	0

Table 7.3: Table of all differentially expressed hormone-related genes at the transmitting tissue. The red colour represents up-regulated genes and the green represents down-regulated genes. At the top, a schematic representation of the stage of fungal development in the wheat ovule at each time point is shown.

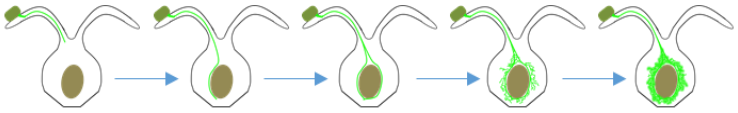

	TRANSMITING TISSUE										
	Type of DE hormone genes	24h		48h		72h		120h		7days	
		UP	DOWN	UP	DOWN	UP	DOWN	UP	DOWN	UP	DOWN
Ethylene	ethylene-responsive transcription factor (ERF)	0	0	1	0	1	0	6	9	0	11
	AP2 domain transcription factor	0	0	0	0	0	0	2	0	0	3
	1-aminocyclopropane-1-carboxylate oxidase (ACO)	0	0	0	0	0	0	0	2	1	3
	1-aminocyclopropane-1-carboxylate synthase (ACS)	0	0	1	0	3	0	3	0	0	0
	5' methylthioadenosine	0	0	0	0	0	0	0	1	0	1
	Ethylene overproduction 1 (ETO1)	0	0	0	0	0	0	0	1	0	0
	Ethylene response sensor 1 (ERS1)	0	0	0	0	0	0	0	0	0	2
	Ethylene receptor	0	0	0	0	0	0	0	1	0	0
	Ethylene Insensitive 3 (EIN3)	0	0	0	0	0	0	0	0	0	3
Auxin	Auxin responsive AUX/IAA	0	0	11	0	10	0	4	3	0	4
	Auxin responsive SAURs	0	0	2	0	1	0	1	0	0	0
	IAA-amido synthetase (GH3)	0	0	6	0	3	0	4	0	0	0
	Indole-3-glycerol phosphate (IGP)	0	0	0	0	1	0	0	0	0	0
	indole-3-acetic acid-induced ARG7	0	0	0	4	0	3	0	4	0	2
	Auxin binding protein (ABP)	0	0	0	1	0	0	0	1	0	1
	Auxin response factor (ARF)	0	0	0	1	1	0	0	1	0	4
	2 oxoglutarate-dependent dioxygenase (DAO)	0	0	1	0	1	1	0	2	0	6
	indole-3-acetate beta glucosyltransferase	0	0	0	0	0	0	1	0	0	0
	probable auxin efflux carrier	0	0	0	0	2	0	1	0	0	2
	PIN-FORMED (PIN)	0	0	0	0	0	0	0	0	0	0
	auxin transporter	0	0	0	0	2	0	0	1	0	2
	auxin induced	0	0	0	0	0	0	0	0	0	0
	PINOID protein kinase	0	0	0	0	0	0	0	0	0	0
	WALLS ARE THIN 1 (WAT1)	0	0	0	0	0	0	0	3	0	3
	SUPPRESOR OF AUXIN RESISTANCE 1 (SAR1)	0	0	0	0	0	0	0	0	0	0
Cytokinin	Cytokinin oxidase dehydrogenase (CKX)	0	0	2	0	0	0	0	4	0	2
	cytokinin 5' monophosphate phosphoribohydrolase	0	0	1	0	0	0	1	0	0	0
	cytokinin glycosyltransferase	0	0	1	0	0	0	1	0	0	0
	Histidine phosphotransfer protein (AHP)	0	0	0	0	0	0	0	0	0	0
Brassinosteroid	BZR1	0	0	0	0	0	0	0	3	0	0
	Interact-With-Spt6 (IWS1)	0	0	0	0	0	0	0	0	0	0
	BRASSINOSTEROID INSENSITIVE 1 (BRI1)	0	0	0	0	0	0	1	2	0	3
	BSL2	0	0	0	0	0	0	0	0	0	0
Gibberellin	Gibberellin receptor GID1	0	0	0	1	0	0	0	1	1	4
	Gibberellin 2-beta-dioxygenase	0	0	1	0	1	0	0	0	0	0
	Gibberellin 3-beta-dioxygenase	0	0	0	0	0	0	0	0	0	1
	Gibberellin 3-hydroxylase	0	0	0	0	0	0	0	0	0	0
	ent-kaurene synthase	0	0	0	0	0	0	0	1	0	0
	ent-kaurene oxidase	0	0	0	0	0	0	0	1	0	0
	Chitin-inducible gibberellin responsive (CIGR)	0	0	0	0	0	0	0	0	0	0
	DELLA	0	0	0	0	0	0	0	2	0	1
	GAST1	0	0	0	0	0	0	0	0	0	2
	Gibberellin regulated	0	0	0	0	1	0	0	0	0	0
Abscisic acid	Abscisic acid receptor PYL4	0	0	0	0	0	0	0	0	0	0
	ABSCISIC ACID INSENSITIVE 5 (ABI5)	0	0	0	0	0	0	0	0	0	1
	Abscisic acid 8' hydroxylase	0	0	0	0	0	0	0	0	0	0
	Abscisic acid inducible kinase	0	0	0	0	0	1	0	0	0	1
	FBW2	0	0	0	0	0	0	0	2	0	0
	SAPK7	0	0	0	0	0	0	0	1	0	0
	SNF kinase	0	0	2	0	3	0	0	1	0	5
Jasmonic Acid	Allene oxide synthase (AOS)	0	0	0	0	0	0	0	3	0	6
	12-oxophytodienoate reductase (OPR)	0	0	0	0	0	0	4	0	1	2
	Chlorophyllase 1 (CLH1)	0	0	0	0	0	2	0	2	0	1
	TIFY transcription factors	0	0	0	0	0	0	1	0	0	8
	Novel interactor of JAZ (NINJA)	0	0	0	0	0	0	0	0	0	0
	Jasmonate induced	0	0	0	0	0	0	0	0	0	0
SA	Salicylic acid binding protein (SABP)	0	0	0	0	0	0	1	0	0	0

Table 7.4: Table of all differentially expressed hormone-related genes at the stigma tissue. The red colour represents up-regulated genes and the green represents down-regulated genes. At the top, a schematic representation of the stage of fungal development in the wheat ovule at each time point is shown.

	STIGMA		
	Type of DE hormone genes	24h	
		UP	DOWN
Ethylene	ethylene-responsive transcription factor (ERF)	0	0
	AP2 domain transcription factor	0	0
	1-aminocyclopropane-1-carboxylate oxidase (ACO)	0	0
	1-aminocyclopropane-1-carboxylate synthase (ACS)	0	0
	5' methylthioadenosine	0	0
	Ethylene overproduction 1 (ETO1)	0	0
	Ethylene response sensor 1 (ERS1)	0	0
	Ethylene receptor	0	0
	Ethylene Insensitive 3 (EIN3)	0	0
Auxin	Auxin responsive AUX/IAA	0	0
	Auxin responsive SAURs	0	0
	IAA-amido synthetase (GH3)	0	0
	Indole-3-glycerol phosphate (IGP)	0	0
	indole-3-acetic acid-induced ARG7	0	0
	Auxin binding protein (ABP)	0	0
	Auxin response factor (ARF)	0	0
	2 oxoglutarate-dependent dioxygenase (DAO)	0	0
	indole-3-acetate beta glucosyltransferase	0	0
	probable auxin efflux carrier	0	0
	PIN-FORMED (PIN)	0	0
	auxin transporter	0	0
	auxin induced	0	0
	PINOID protein kinase	0	0
	WALLS ARE THIN 1 (WAT1)	0	0
	SUPPRESOR OF AUXIN RESISTANCE 1 (SAR1)	0	0
Cytokinin	Cytokinin oxidase dehydrogenase (CKX)	0	0
	cytokinin 5' monophosphate phosphoribohydrolase	0	0
	cytokinin glycosyltransferase	0	0
	Histidine phosphotransfer protein (AHP)	0	0
Brassinoster	BZR1	0	0
	Interact-With-Spt6 (IWS1)	0	0
	BRASSINOSTEROID INSENSITIVE 1 (BRI1)	0	0
	BSL2	0	0
Gibberellin	Gibberellin receptor GID1	1	0
	Gibberellin 2-beta-dioxygenase	0	0
	Gibberellin 3-beta-dioxygenase	0	0
	Gibberellin 3-hydroxylase	0	0
	ent-kaurene synthase	0	0
	ent-kaurene oxidase	0	0
	Chitin-inducible gibberellin responsive (CIGR)	0	0
	DELLA	0	0
	GAST1	0	0
	Gibberellin regulated	0	0
Abscisic acid	Abscisic acid receptor PYL4	0	0
	ABSCISIC ACID INSENSITIVE 5 (ABI5)	0	0
	Abscisic acid 8' hydroxylase	0	0
	Abscisic acid inducible kinase	0	0
	FBW2	0	0
	SAPK7	0	0
	SNF kinase	0	0
Jasmonic Acid	Allene oxide synthase (AOS)	1	0
	12-oxophytodienoate reductase (OPR)	0	0
	Chlorophyllase 1 (CLH1)	0	0
	TIFY transcription factors	2	0
	Novel interactor of JAZ (NINJA)	0	0
	Jasmonate induced	0	0
	Coronatine insensitive (COI1)	0	0
SA	Salicylic acid binding protein (SABP)	0	0
	NPR1		
	NPR3		

Table 7.5: Table of all differentially expressed defence-related genes at the stigma tissue. The red colour represents up-regulated genes and the green represents down-regulated genes. At the top, a schematic representation of the stage of fungal development in the wheat ovule at each time point is shown.

STIGMA			
	Type of DE Defence genes	24H	
		UP	DOWN
NBS-LRR class proteins	NBS-LRR		
	disease resistance RPM1		
	disease resistance RPS2		
	disease resistance RPP13	2	1
	disease resistance RPP8		
	disease resistance RGA1		
	disease resistance RGA2		
	disease resistance RGA3		
Transcription factors	WRKY transcription factors	5	
	MYB transcription sactors		
Antifungal proteins	plant-pathogenesis (PR) proteins		
	Cytochrome P450		
	chitinase		
	chitin elicitor-binding		
	Defensins	2	
	non-specific lipid transfer proteins (nsLTPs)		
	Glycine-rich proteins (GRPs)		
	polygalacturonase inhibiting protein (PGIP)		
	beta purothionins		
	Bowman-Birk type trypsin inhibitor		
Exocytosis/Endocytosis related proteins	SNARE proteins		
	syntaxins		
	exocyst complex component EXO70B1-like		
	Clathrin		
Receptor protein kinases	serine/threonine kinases (STKs)		
	Cysteine-rich receptor-like kinases (CRKs)		
	CBL-interacting protein kinases (CIPK)		
	Lectin receptor kinases (LecRK)	9	1
	FLAGELLIN-SENSING 2 (FLS2)		
	Mitogen-activated kinase (MAPK)		
	GTPase activating 1		
Calcium signalling	cyclic nucleotide-gated channels (CNGCs)		
	calreticulin-3 (CRT3)		
	calmodulin	1	
	Glutamate receptor		
	glutamate decarboxylase (GAD)		
	calmodulin binding proteins (CaMBPs)		
ROS regulation/signalling	Thioredoxins (TRX)		
	Glutaredoxins (GRX)		
	manganese superoxide dismutase (Mn SOD)		
	Monodehydroascorbate reductase		
	dehydroascorbate reductase		
	peroxidases		
	catalase (CAT)		
	ferredoxin		
	metallothionein		
	phosphatase inhibitor	3	
	isocitrate dehydrogenase [NADP]		
	NADP dehydrogenase		
	Fructose-bisphosphate aldolase		
	aldehyde dehydrogenase		
	aldo-keto reductase		
	aldose reductase		
	aldehyde oxidase		
	glutathione S-transferase (GST)		
RNS regulation/signalling	glutamine synthetase (GS)		
	digalactosyldiacylglycerol synthase		
Ubiquitination	E3 ubiquitin-ligases (RING type)		
	E2 ubiquitin-conjugating enzyme	1	1
	COP9 signalosome		
	Tetratricopeptide repeat (TPR)-like superfamily		
	suppressor of the G2 allele of SKP1 (SGT1)		
Programmed cell death	subtilisin-like proteases		
	metacaspase		
	Potassium transporter		
	polyphenol oxidase (PPO)	4	1
	Harpin induced protein (HIN1)		
	Accellerated Cell Death 11 (ACD11)		
	hexokinase (HXK)		
	polyamine oxidase (PAO)		
Circadian clock	REVEILLE (RVE)	3	
	PHYTOCLOCK1 (PCL1)		
Carbohydrate metabolism	Glycosyl hydrolase family 10 (xylanase)		
	beta glucosidase		
	fructan 6-exohydrolase (FEHs)		
	endoglucanases		
	xylanase inhibitor (XIP)		
	Callose synthase (CalS)		
	xyloglucan endotransglucosylase hydrolase	1	1
	cell wall invertase		
	chemocyanin		
	pectinesterase		
	hydroxyproline-rich glycoprotein (HRGP) [extensin]		
	annexins		
	expansins		
Chromatin modification	histone H4		1
	histone deacetylase		
Lipid transfer/metabolism	lipid-transfer defective in induced resistance (DIR1)		
	GDSL esterase lipase		
	remorins		
Fatty-acid metabolism	9-lipoxygenase (9-LOX)	1	
	bifunctional epoxide hydrolases		
	Phospholipase A1 (PLDa1)		
Phenylpropanoid metabolism	Phenylalanine ammonia-lyase (PAL1)		
	dirigent proteins		
	isoflavone reductase		
	cinnamoyl-CoA reductase 2 (CCR2)	1	
	light-inducible CPRF2-like		
	scopoletin glucosyltransferase		
	glycosyltransferase family (GSTs)		
Sulfur Metabolism	serine acetyltransferase (SAT)		
	disulfide isomerase		
	phytosulfokines		
	cytosolic sulfotransferase		
Proteolysis Regulation	cathepsin B-like		
	aspartyl protease (AED)		
	Cysteine protease inhibitor		
Sugar Metabolism/Transport	galactinol synthase (GolS)		
	glycerol-3-phosphate (G3P)		
	phosphoenolpyruvate carboxylase (PEPC)		
	sugar transporter		
entose-phosphate Metabolism	transaldolase	1	
	glucose-6-phosphate		
Alkaloid biosynthesis	berberine bridge enzyme		
	STRICTOSIDINE SYNTHASE-LIKE		
Nuclear pore complex	nucleoporin NUP		
	nucleoporin SEH1		

Table 7.6: Table of all differentially expressed defence-related genes at the transmitting tissue. The red colour represents up-regulated genes and the green represents down-regulated genes. At the top, a schematic representation of the stage of fungal development in the wheat ovule at each time point is shown.

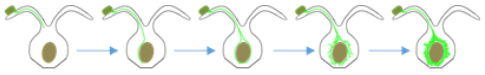

		Transmitting Tissue									
	Type of DE Defence genes	24H		48H		72H		120H		7D	
		UP	DOWN	UP	DOWN	UP	DOWN	UP	DOWN	UP	DOWN
NBS-LRR class proteins	NBS-LRR										
	disease resistance RPM1										
	disease resistance RPS2										
	disease resistance RPP13	3		19	1	6	1	5	25		31
	disease resistance RPP8										
	disease resistance RGA1										
	disease resistance RGA2										
	disease resistance RGA3										
Transcription factors	WRKY transcription factors			21	6	13	4	6	12		13
	MYB transcription sactors										
Antifungal proteins	plant-pathogenesis (PR) proteins										
	Cytochrome P450										
	chitinase										
	chitin elicitor-binding										
	Defensins			17		3		23	37	12	53
	non-specific lipid transfer proteins (nsLTPs)										
	Glycine-rich proteins (GRPs)										
	polygalacturonase inhibiting protein (PGIP)										
	beta-purothionins										
	Bowman-Birk type trypsin inhibitor										
Exocytosis/Endocytosis related proteins	SNARE proteins										
	syntaxins	1		7					7		21
	exocyst complex component EXO70B1-like										
	Clathrin										
Receptor protein kinases	serine/threonine kinases (STKs)										
	Cysteine-rich receptor-like kinases (CRKs)										
	CBL-interacting protein kinases (CIPK)										
	Lectin receptor kinases (LecRK)			37	1	12		18	47	1	58
	FLAGELLIN-SENSING 2 (FLS2)										
	Mitogen-activated kinase (MAPK)										
	GTPase activating 1										
Calcium signalling	cyclic nucleotide-gated channels (CNGCs)										
	calreticulin-3 (CRT3)										
	calmodulin	1		8		3		4	3		12
	Glutamate receptor										
	glutamate decarboxylase (GAD)										
	calmodulin binding proteins (CaMBPs)										
ROS regulation/signalling	Thioredoxins (TRX)										
	Glutaredoxins (GRX)										
	manganese superoxide dismutase (Mn SOD)										
	Monodehydroascorbate reductase										
	dehydroascorbate reductase										
	peroxidases										
	catalase (CAT)										
	ferredoxin										
	metallothionein			11	1	10		35	49	13	78
	phosphatase inhibitor										
	isocitrate dehydrogenase (NADP)										
	NADP dehydrogenase										
	Fructose-bisphosphate aldolase										
	aldehyde dehydrogenase										
	aldo-keto reductase										
	aldose reductase										
	aldehyde oxidase										
	glutathione S-transferase (GST)										
RNS regulation/signalling	glutamine synthetase (GS)					1			5		5
	digalactosyldiacylglycerol synthase										
Ubiquitination	E3 ubiquitin-ligases (RING type)										
	E2 ubiquitin-conjugating enzyme			4	1		4	3	40	1	56
	COP9 signalosome										
	Tetratricopeptide repeat (TPR)-like superfamily										
	suppressor of the G2 allele of SKP1 (SGT1)										
Programmed cell death	subtilisin-like proteases										
	metacaspase										
	Potassium transporter										
	polyphenol oxidase (PPO)			5		1	4	1	12	2	27
	Harpin induced protein (HIN1)										
	Accellerated Cell Death 11 (ACD11)										
	hexokinase (HXK)										
	polyamine oxidase (PAO)										
Circadian clock	REVEILLE (RVE)			1	1				3		3
	PHYTOCLOCK1 (PCL1)										
Carbohydrate metabolism	Glycosyl hydrolase family 10 (xylanase)										
	beta-glucosidase										
	fructan 6-exohydrolase (FEHs)										
	endoglucanases										
	xylanase inhibitor (XIP)										
	Callose synthase (CalS)										
	xyloglucan endotransglucosylase-hydrolase		1	2	1	1	1	2	29	4	47
	cell wall invertase										
	chemocyanin										
	pectinesterase										
	hydroxyproline-rich glycoprotein (HRGP) [extensin]										
	annexins										
	expansins										
Chromatin modification	histone H4								14		20
	histone deacetylase										
Lipid transfer/metabolism	lipid-transfer-defective in induced resistance (DIR1)										
	GDSL-esterase-lipase			1	1	6	2	2	12		25
	remorins										
Fatty-acid metabolism	9-lipoxygenase (9-LOX)										
	bifunctional epoxide hydrolases							1	7		20
	Phospholipase A1 (PLDa1)										
Phenylpropanoid metabolism	Phenylalanine ammonia-lyase (PAL1)										
	dirigent proteins										
	isoflavone reductase										
	cinnamoyl-CoA reductase 2 (CCR2)	1		4	2	3		11	19		30
	light-inducible CPRF2-like										
	scopoletin glucosyltransferase										
	glycosyltransferase family (GSTs)										
Sulfur Metabolism	serine acetyltransferase (SAT)										
	disulfide isomerase				1	2		2	7		12
	phytosulfokines										
	cytosolic sulfotransferase										
Proteolysis Regulation	cathepsin B-like										
	aspartyl protease (AED)					1					7
	Cysteine protease inhibitor										
Sugar Metabolism/Transport	galactinol synthase (GolS)										
	glycerol-3-phosphate (G3P)			2	1	1	5	10	13		22
	phosphoenolpyruvate carboxylase (PEPC)										
	sugar transporter										
ntose-phosphate Metabolism	transaldolase								1		11
	glucose-6-phosphate										
Alkaloid biosynthesis	berberine bridge enzyme			1		1			2		6
	STRICTOSIDINE SYNTHASE-LIKE										
Nuclear pore complex	nucleoporin NUP										
	nucleoporin SEH1										1

Table 7.7: Table of all differentially expressed defence-related genes at the Base tissue. The red colour represents up-regulated genes and the green represents down-regulated genes. At the top, a schematic representation of the stage of fungal development in the wheat ovule at each time point is shown.

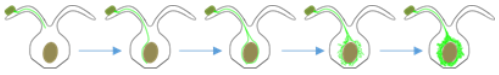

		Base									
	Type of DE Defence genes	24H		48H		72H		120H		7D	
		UP	DOWN	UP	DOWN	UP	DOWN	UP	DOWN	UP	DOWN
NBS-LRR class proteins	NBS-LRR										
	disease resistance RPM1										
	disease resistance RPS2										
	disease resistance RPP13		1	33		46	7	3	37	8	34
	disease resistance RPP8										
	disease resistance RGA1										
	disease resistance RGA2										
	disease resistance RGA3										
Transcription factors	WRKY transcription factors	3		48	1	39	9	2	11	1	8
	MYB transcription factors										
Antifungal proteins	plant-pathogenesis (PR) proteins										
	Cytochrome P450										
	chitinase										
	chitin elicitor-binding										
	Defensins										
	non-specific lipid transfer proteins (nsLTPs)			16		32	15	20	22	23	43
	Glycine-rich proteins (GRPs)										
	polygalacturonase inhibiting protein (PGIP)										
	beta purothionins										
	Bowman-Birk type trypsin inhibitor										
Exocytosis/Endocytosis related proteins	SNARE proteins										
	syntaxins										
	exocyst complex component EXO70B1-like	1		13		5			11		21
	Clathrin										
Receptor protein kinases	serine/threonine kinases (STKs)										
	Cysteine-rich receptor-like kinases (CRKs)										
	CBL-interacting protein kinases (CIPK)										
	Lectin receptor kinases (LecRK)	3		76		101	10	6	65	25	65
	FLAGELLIN-SENSING 2 (FLS2)										
	Mitogen-activated kinase (MAPK)										
	GTPase activating 1										
Calcium signalling	cyclic nucleotide-gated channels (CNGCs)										
	calreticulin-3 (CRT3)										
	calmodulin										
	Glutamate receptor			11	2	20	2	2	11	3	8
	glutamate decarboxylase (GAD)										
	calmodulin binding proteins (CaMBPs)										
ROS regulation/signalling	Thioredoxins (TRX)										
	Glutaredoxins (GRX)										
	manganese superoxide dismutase (Mn SOD)										
	Monodehydroascorbate reductase										
	dehydroascorbate reductase										
	peroxidases										
	catalase (CAT)										
	ferredoxin										
	metallothionein	2		12	6	42	18	26	56	11	78
	phosphatase inhibitor										
	isocitrate dehydrogenase (NADP)										
	NADP dehydrogenase										
	Fructose-bisphosphate aldolase										
	aldehyde dehydrogenase										
	aldo-keto reductase										
	aldose reductase										
	aldehyde oxidase										
	glutathione S-transferase (GST)										
RNS regulation/signalling	glutamine synthetase (GS)					4	4		5		4
	digalactosyldiacylglycerol synthase										
Ubiquitination	E3 ubiquitin-ligases (RING type)										
	E2 ubiquitin-conjugating enzyme										
	COP9 signalosome	3	1	7	1	17	8	1	41		65
	Tetratricopeptide repeat (TPR)-like superfamily										
	suppressor of the G2 allele of SKP1 (SGT1)										
Programmed cell death	subtilisin-like proteases										
	metacaspase										
	Potassium transporter										
	polyphenol oxidase (PPO)			9		23	4		19	2	20
	Harpin induced protein (HIN1)										
	Accellerated Cell Death 11 (ACD11)										
	hexokinase (HXK)										
	polyamine oxidase (PAO)										
Circadian clock	REVEILLE (RVE)										
	PHYTOCLOCK1 (PCL1)			3	1				3		4
Carbohydrate metabolism	Glycosyl hydrolase family 10 (xylanase)										
	beta glucosidase										
	fructan 6-exohydrolase (FEHs)										
	endoglucanases										
	xylanase inhibitor (XIP)										
	Callose synthase (CalS)										
	xyloglucan endotransglucosylase hydrolase		1	1	1	19	13	5	44	1	52
	cell wall invertase										
	chemocyanin										
	pectinesterase										
	hydroxyproline-rich glycoprotein (HRGP) (extensin)										
	annexins										
	expansins										
Chromatin modification	histone H4		1		1		4		205		146
	histone deacetylase										
Lipid transfer/metabolism	lipid-transfer defective in induced resistance (DIR1)										
	GDSL esterase lipase				1	20	5	2	16		21
	remorins										
Fatty acid metabolism	9-lipoxygenase (9-LOX)										
	bifunctional epoxide hydrolases			1		4	5		13		18
	Phospholipase A1 (PLDa1)										
Phenylpropanoid metabolism	Phenylalanine ammonia-lyase (PAL1)										
	dirigent proteins										
	isoflavone reductase										
	cinnamoyl-CoA reductase 2 (CCR2)	1	1	16	3	10	9	5	10	1	23
	light-inducible CPRF2-like										
	scopoletin glucosyltransferase										
	glycosyltransferase family (GSTs)										
Sulfur Metabolism	serine acetyltransferase (SAT)										
	disulfide isomerase										
	phytosulfokines			1		2	5	1	3		12
	cytosolic sulfotransferase										
Proteolysis Regulation	cathepsin B-like										
	aspartyl protease (AED)			4		5			4		5
	Cysteine protease inhibitor										
Sugar Metabolism/Transport	galactinol synthase (GolS)										
	glycerol-3-phosphate (G3P)			2	1	3	3	4	7		8
	phosphoenolpyruvate carboxylase (PEPC)										
	sugar transporter										
entose-phosphate Metabolism	transaldolase				1				9		8
	glucose-6-phosphate										
Alkaloid biosynthesis	berberine bridge enzyme								1		3
	STRICTOSIDINE SYNTHASE-LIKE										
Nuclear pore complex	nucleoporin NUP								8		7
	nucleoporin SEH1										

Appendix B: Supplementary Material for Chapter 4

Table 7.8: Levels of individual ergot alkaloids in Claviceps purpurea Honeydew. The ergot alkaloid levels (parts per billion) of 12 alkaloid types found in honeydew of seven *C. purpurea* isolates grown on the wheat variety Mulika. The brackets below each alkaloid type contain the p-value used to determine significant differences between isolates. Blank spaces contained values below the limit of quantification.

Isolate	Rep	Ergocornine	Ergocorninine	Ergocristine **(p = 0.013)**	Ergocristinine **(p = 0.037)**	Ergocryptine **(p = 0.138)**	Ergocryptinine **(p = 0.381)**	Ergometrine **(p = 0.039)**	Ergometrinine **(p = 0.500)**	Ergosine **(p < 0.001)**	Ergosinine **(p = 0.125)**	Ergotamine **(p = 0.071)**	Ergotaminine **(p = 0.203)**
EI2	1			132	103	11	6	98	21	11	5	145	79
EI2	2			25	23			31	7			27	15
EI2	3			58	61	8	6	89	29	7	4	64	38
EI4	1			10		8	4	14	3	12	5	4	
EI4	2			4				4					
EI4	3					4	4	16		10	6		
03-48.1	1	4		40	55					189	78	37	14
03-48.1	2			11	6					157	66	22	8
03-48.1	3	6		20	11					202	10	44	16
03-20.1	1			40	57							13	6
03-20.1	2			73	40							28	11
03-20.1	3			102	63							4	16

Rye 20.1	1			6	5			7		17	7	4	
Rye 20.1	2							16		36	16	7	
Rye 20.1	3				5			3		11	4		
04-41.1	1			170	124						6	78	33
04-41.1	2			95	225	6	6			32	15	120	51
04-41.1	3			133	99					31	15	63	28
04-97.1	1			287	249	6	6			5		179	70
04-97.1	2			233	158	5	4					93	35
04-97.1	3			91	57							34	13

Table 7.9: Levels of individual ergot alkaloids in Claviceps purpurea Sphacelia. The ergot alkaloid levels (parts per billion) of 12 alkaloid types found in sphacelia of seven *C. purpurea* isolates grown on the wheat variety Mulika. The brackets below each alkaloid type contain the p-value used to determine significant differences between isolates. Blank spaces contained values below the limit of quantification.

Isolate	Rep	Ergocornine **(p < 0.001)**	Ergocorninine **(p = 0.001)**	Ergocristine **(p = 0.001)**	Ergocristinine **(p < 0.001)**	Ergocryptine **(p = 0.182)**	Ergocryptinine **(p < 0.001)**	Ergometrine **(p = 0.015)**	Ergometrinine **(p = 0.008)**	Ergosine **(p < 0.001)**	Ergosinine **(p = 0.499)**	Ergotamine **(p < 0.001)**	Ergotaminine **(p = 0.001)**
04-97.1	1	6		34721	5329	219	43			98	14	8584	1474
04-97.1	2	6	4	44223	6892	211	40			95	13	12024	2038
04-97.1	3	10	5	65543	9400	421	79			178	24	15523	2460
03-20.1	1	7	5	47996	7867	318	60			191	30	11267	2013
03-20.1	2	6	5	44791	7695	292	57			148	20	10757	189
03-20.1	3	6	4	40798	6779	263	52			115	17	9677	1806
03-48.1	1		255	20323	3747	72	17			15992	360	10142	198
03-48.1	2		456	36909	6889	195	37			28990	6374	14822	313
03-48.1	3		503	44453	8442	217	40			35588	7437	17195	3321
04-41.1	1	9	39	36961	6672	194	47			1532	313	9000	1734
04-41.1	2	11	55	38835	7798	187	45			1502	355	10268	2289
04-41.1	3		35	31247	6019	155	35			128	307	824	1531
Rye 20.1	1	6	131	5481	1291	7166	2379	682	12	5372	1512	1893	525

Rye 20.1	2		93	3990	846	3750	1233	469	9	3506	999	1447	384
Rye 20.1	3	12	191	8637	2367	7894	3592	453	10	6442	2062	2675	680
EI2	1	14	5	177134	18098	1493	305	1959	31	680	177134	40066	5860
EI2	2	9		137115	14264	1093	215	1590	25	521	63	34723	4822
EI2	3	7	4	130345	13449	864	164	1040	14	350	43	27225	3922
EI4	1	751	204	9042	1625	279297	9523	1960	36	9350	2323	1751	365
EI4	2	399	211	12170	2048	36298	9896	2982	39	12678	2868	3030	509
EI4	3	640	11	8799	982	22890	4394	2474	39	9162	1549	21336	286

Table 7.10: Levels of individual ergot alkaloids in Claviceps purpurea Sclerotia. The ergot alkaloid levels (parts per billion) of 12 alkaloid types found in sclerotia of seven *C. purpurea* isolates grown on the wheat variety Mulika. The brackets below each alkaloid type contain the p-value used to determine significant differences between isolates. Blank spaces contained values below the limit of quantification.

Isolate	Rep	Ergocornine **(p < 0.001)**	Ergocorninine **(p < 0.001)**	Ergocristine **(p < 0.001)**	Ergocristinine **(p < 0.001)**	Ergocryptine **(p < 0.001)**	Ergocryptinine **(p < 0.001)**	Ergometrine **(p < 0.001)**	Ergometrinine **(p < 0.001)**	Ergosine **(p < 0.001)**	Ergosinine **(p < 0.001)**	Ergotamine **(p < 0.001)**	Ergotaminine **(p < 0.001)**
04-97.1	1	60	67	1537951	395247	2708	780	35	26	756	214	275061	84869
04-97.1	2	58	60	1725594	421312	2073	658	35	26	693	188	316273	96353
04-97.1	3	51	45	904662	239209	1172	383	33	25	409	117	177474	60086
04-41.1	1	70	606	1791374	362640	3551	687	38	27	53961	12639	366128	99671
04-41.1	2	76	1087	1346734	280868	2063	650	36	26	46650	13055	301575	83035
04-41.1	3	75	1895	1577317	332252	2665	636	35	26	97799	28156	381167	92389
03-48.1	1	78	10371	664967	110985	2074	517	29	25	429477	95335	207417	44061
03-48.1	2	57	13178	705000	112937	1870	453	29	26	542098	127031	238057	54647
03-48.1	3	80	15985	926747	151239	3785	594	29	26	687127	160992	278347	63405
03-20.1	1	78	593	1748251	363411	4030	714	35	26	43933	11583	382406	98783
03-20.1	2	73	126	1961953	349331	4205	613	34	25	6276	779	414125	94720
03-20.1	3	72	83	2541155	496879	5913	818	36	25	2718	310	489868	125702
Rye 20.1	1	159	7924	475125	91484	179625	87368	36941	4591	288996	87949	125229	31885

Rye 20.1	2	174	9023	517641	125833	223633	113086	34774	5232	276686	96663	132859	36426
Rye 20.1	3	239	7454	357150	80819	224829	93979	44655	6474	294217	105977	117380	27229
EI2	1	55	88	596276	181567	5019	2111	26495	4128	3483	1010	217941	70007
EI2	2	56	81	695086	196130	5897	2122	25341	3810	3534	946	228938	69892
EI2	3	56	84	654377	195762	4612	1999	30492	5050	2870	882	224358	71752
EI4	1	156	2563	135053	41318	324412	155053	57736	5991	114295	42649	32326	9976
EI4	2	192	3066	362625	102087	414519	173881	64435	6377	136529	49340	86958	29309
EI4	3	172	2745	241162	71711	310274	155592	59016	5862	111097	41454	56864	17091